Universität für Bodenkultur Wien

Department für Chemie

Vorstand: Univ. Prof. Dr.techn. Dipl.-Ing. Paul Kosma

Betreuer:
Univ. Prof. Dr.rer.nat. Dipl.-Chem. Thomas Rosenau

STUDIES INTO FUNDAMENTALS OF *ORTHO*-QUINONE METHIDE CHEMISTRY

Dissertation
zur Erlangung des Doktorgrades
an der Universität für Bodenkultur Wien

Eingereicht von
Dipl.-Ing. Stefan Böhmdorfer

Wien, November 2009

The world is a thing of utter inordinate complexity and richness and strangeness that is absolutely awesome.

Douglas Adams

Acknowledgment

Of course there are many people I would like to express my gratefulness to. I will try my best, but I fear that it is impossible to not forget somebody. I sincerely hope the unlucky reader that feels forgotten remembers that it will be a very memorable experience when I realize what has happened.

First of all, I want to express my gratitude to Professor Thomas Rosenau: he supervised the work on my PhD-thesis, gave important advice in chemistry and non-chemistry matters, made me realize that simple experiments can be very enlightening, has the unrivalled ability to realize his visions, almost always allowed me to interrupt his train of thoughts and became a friend as well. The same holds true for Professor Antje Potthast, with the exception that she did not supervise my thesis. To become a member of your research group and learn from you was an improbable stroke of luck!

The people I spent the most time with during the past three years are my colleagues. Some of you have been accompanying me for several years now, others I have to come to know for a much shorter time. I am happy that going to work meant also going to meet some friends, who had the added value of being inspiring and extremely competent colleagues. That it did not matter which research group people were working for definitely improved entertainment during the not-strictly-chemistry times. I know that this close contact opened up possibilities that otherwise would just have passed by unnoticed, and I am convinced that occasional distraction is actually beneficial for work. So to all people whose company I was privileged to enjoy during work (and after hours): Thank you very much!

It is too easy to forget the people who keep our department operational, and we are very lucky that our lab-technicians and secretaries can bear this responsibility. I am also indebted to FWF, who gave me more than sufficient amounts of money every month without even knowing what they were paying for. And thanks to Thomas Netscher and the friendly people at DSM Kaiseraugst who allowed me to learn from their experience.

Some of my friends actually don´t work with me, and they too influenced me to become who I am. This is strictly speaking not directly linked to my thesis, but I still enjoy your company and should try harder to do so more often. Thanks a lot!

Like everybody else I have a family. Unlike anybody else, I have my family. I am grateful to my parents, who facilitated my ambition to become a chemist and nourished my interests from early times on, and also to my brainy sisters for inspiration and support.

And finally I am very happy to share my life with the marvellous Tini and the amazing Finn, who are both one-of-a-kind.

Table of Contents

Kurzfassung

Das für den Menschen essentielle Vitamin E ist ein Gemisch mehrerer Tocopherole und Tocotrienole, die hochwirksame Antioxidantien darstellen. Durch Oxidation entstehen aus den Tocopherolen komplexe Substanzgemische, deren Zusammensetzung stark von den konkreten Oxidationsbedingungen bestimmt wird. Von den dabei vorkommenden primären Intermediaten hat sich das *ortho*-Chinonmethid als besonders wichtig und interessant herausgestellt, da es zu einer Vielzahl unerwarteter Produkte führt. Außerdem kann es auch gut als Modell für andere in der Natur vorkommende Prozesse, z.B. die Ligninsynthese, herangezogen werden.

Schon länger wird vermutet, daß die Entstehung des *ortho*-Chinonmethids über einen zwitterionischen Übergangszustand erfolgt. Dabei sollte der Übergang vom intermediären aromatischen Zwitterion zum olefinischen *ortho*-Chinonmethid lediglich an eine Drehung um eine Einfachbindung gekoppelt sein. Anhand spezieller Tocopherolderivate konnte nun die zwitterionischen Stufe spektroskopisch eingehend untersucht werden. Eine Erschwerung der Drehung um die Bindung zur exozyklischen Methylengruppe führt dabei zu einer verzögerten Entstehung des *ortho*-Chinonmethids. Somit gelang es erstmals, das Zwitterion mittels NMR-Spektroskopie und Isotopenmarkierung direkt nachzuweisen. Durch dieses Ergebnis müssen bisherige Lehrmeinungen zur Entstehung und Chemie von *ortho*-Chinonmethiden revidiert werden. Abgesehen von der Bedeutung für die Grundlagenforschung ist im weiteren auch die Nutzung dieses „Drehschalters“ zwischen Aromatizität und Antiaromatizität in der Nanotechnologie denkbar.

Erst kürzlich wurde durch mögliche chemotherapeutische Anwendungen großes Interesse an der Stoffklasse der Tocopheramine – die phenolische OH-Gruppe der Tocopherole ist hierbei durch eine Aminogruppe ersetzt – geweckt. Das Wissen um das Reaktionsverhalten und um die Reaktionsprodukte dieser Verbindungen ist eine Vorraussetzung für jede Art von Anwendung. Daher wurde erstmal systematisch das Reaktionsverhalten der Tocopheramine in Einelektronen- und Zweielektronen-Oxidationsprozessen erforscht, wobei methodisch Elektronenspinresonanz und chemische Abfangreaktionen zur Anwendung kamen. Dabei stellten sich Ähnlichkeiten zum Verhalten von Tocopherolen heraus, die Unterschiede im Detail waren allerdings erheblich.

Die Bromierung von Tocopherolen kann nach zwei unterschiedlichen Mechanismen erfolgen: entweder es erfolgt eine klassische elektrophile Substitution am Aromaten, oder das Tocopherol wird über ein *ortho*-Chinonmethid in einer Oxidations-Additions-Sequenz zur Bromomethylverbindung oxidiert. Anhand der Produktverhältnisse und durch quantenchemische Berechnungen wurden die Aktivierungsenergien bestimmt und der jeweils bevorzugte Reaktionsmechanismus erklärt. Die Bromierungsprodukte aller vier Tocopherole wurden synthetisiert und vollständig charakterisiert, um eine verlässliche Grundlage für zukünftige Studien zu bilden.

In den letzten Jahren hat sich herausgestellt, daß die traditionellen Lehrmeinungen zur Oxidationschemie der Tocopherole teilweise falsch und mißverständlich sind. Einige Oxidationsprodukte, die mit Reaktionen des Tocopherylradikals erklärt wurden, entstehen in Wirklichkeit aus dem *ortho*-Chinonmethid. Ebenso wurde (s.o.) der detaillierte Bildungsmechanismus der ortho-Chinonmethide revidiert. Um den derzeitigen Stand des Wissens darzustellen und die neuen Entwicklungen einzubinden, wurde ein umfassender Review verfasst.

Abstract

Vitamin E is an essential nutrient which actually comprises several tocopherols and tocotrienols. These compounds are highly potent antioxidants and show complex and multifaceted oxidation behaviour. Among the intermediate oxidation products, the *ortho*-quinone methide has proven to be the most interesting and crucial one, yielding a great variety of unexpected products. Additionally, it serves as a model for other important *ortho*-quinone methide based processes in nature, for example lignifications and lignin synthesis.

ortho-Quinone methide formation has been suspected to include a short-lived zwitterionic intermediate, the conversion of this aromatic zwitterion to the olefinic *ortho*-quinone methide being simply controlled by bond rotation. In the present work, special tocopherol derivatives were synthesized that allowed detailed spectroscopic studies on the zwitterionic intermediate. A hindered rotation around the bond to the exocyclic methylene group effectively retarded *ortho*-quinone methide formation. This way, for the first time a direct spectroscopic proof of the zwitterion was achieved by NMR and isotopic labelling methodology. Conventional, decade-old teaching on formation and chemistry of ortho-quinone methides will now have to be revised. Apart from the impact of this result on the fundamental understanding of that particular chemistry, also applications of this “swith” between aromaticity and antiaromaticity in nano-engineering are imminent.

Most recently the almost completely neglected class of tocopheramines – tocopherols that bear an amino group instead of the phenolic hydroxyl group – have undergone a surge of interest due to their potential in chemotherapy. A comprehensive knowledge about their chemistry, reactivity and products is a prerequisite to any (and first of all a medical) application. Making heavy use of electron spin resonance spectroscopy and chemical trapping, for the first time the one-electron and two-electron oxidation chemistry of tocopheramines was established, revealing an oxidation behaviour that showed general similarity to that of tocopherols, but offering some essential differences in the detail.

The bromination of different tocopherols can proceed, in principle, according to two different mechanisms, either by a classical electrophilic substitution at the aromatic core or by an oxidation-addition sequence leading to a bromomethyl derivative. The bromination behaviour of all four tocopherols was thoroughly studied. Based on the product ratios and computational studies, activation energies were calculated and the preferred pathways were identified. All bromination products were synthesized and fully analytically characterized, clarifying contradictory data in the pertinent literature and providing a reliable set of standard compounds for future studies.

Over the past several years, some traditional teaching on the oxidation chemistry of tocopherols has proved to be erroneous. Oxidation products that so far have been explained based on tocopheroxyl radical chemistry are actually formed involving the *ortho*-quinone methide as key intermediate. The general mechanism of *ortho*-chinone methide formation was revised as well. To update the current knowledge of ortho-quinone methide chemistry related to tocopherols, also considering the new results of the present thesis, this topic was comprehensively reviewed.

Schematic Abstract

Bromination of Tocopherols in Apolar Media

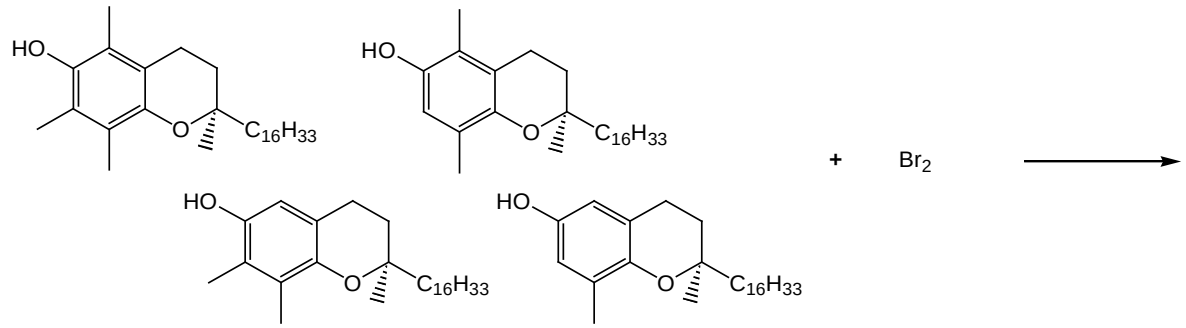

Oxidation Chemistry of Tocopheramines

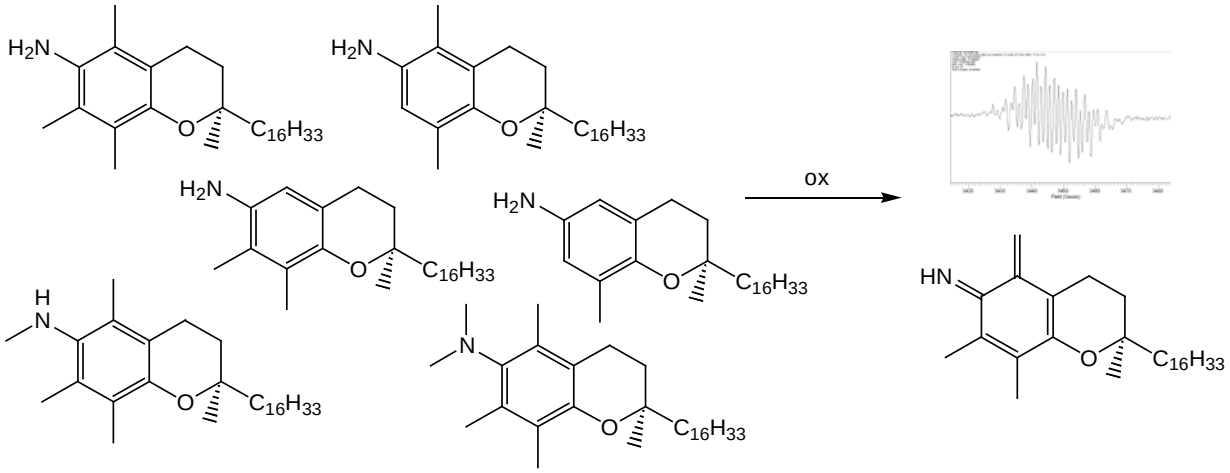

Detailed Mechanism of *ortho*-Quinone Methide Formation

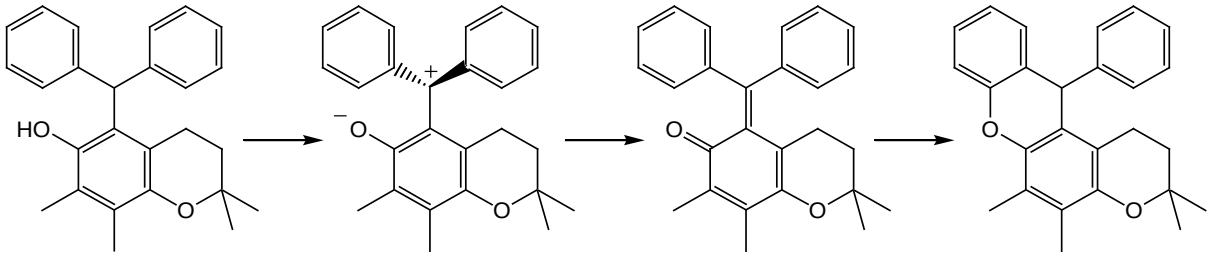

Introduction

A Short History of Vitamin E

When Casimir Funk coined the term "vitamin" in 1912,[1] it was an expression of the then new abilities of science. The available research tools were developed to an extend that allowed a more detailed analysis of food and natural products and to draw a direct connection between the isolated compounds and their effect on the human body. One could say today's Life Sciences are born in the word *vitamin* since *vita* is Latin for life and *amin* denotes the scientific perspective.

Funk´s goal was to find the substance the lack of which was responsible for the emergence of Beriberi, a commonplace neural disease in Asian countries that is triggered by insufficient uptake of vitamin B_1. Doves that were fed diets of purified carbohydrates, fats and proteins or only polished rice developed polyneuritis, that could or couldn't be cured by different food additives.[2] After several chemical separations and feeding experiments, Funk had finally extracted a highly potent agent. Over the years it became obvious that this agent actually consisted of several individual substances, including vitamin B_1, an amine that cures Beriberi.

As mentioned, he called the isolated compound vitamin, an expression not everybody was satisfied with at that time. McCollum, then a highly regarded expert on nutrition, criticized it openly, since *vita* suggested a paramount importance of the compound for the existence of life, and the evidence for the presence of an amine was not definite.[3] Instead he suggested the terms *Fat-soluble A* and *Water-soluble B* for the two groups of essential nutrients known at that time.[4] This is also the reason why the B vitamins are known for a longer time than vitamin A, although one would expect otherwise. Moreover it was still not definite whether diseases like beriberi or scurvy were a sign of malnutrition or had an altogether different cause.

Three years later Drummond added to the two established accessory food factors *Fat-soluble A* and *Water-soluble B* (or antineuritic factor) the *Water-soluble C* (or antiscorbutic factor) and thus started the alphabetic designation of the vitamins.[5]

In 1925 Evans and Burr changed the name of their provisional *vitamin X* to *vitamin E*[6] (it was preceded by *antirachitic factor D*) and after Evans, Emerson and Emerson had identified it as an alcohol and had been inspired by Calhoun, they gave it the epithet *tocopherol* (bearing [the responsibility of] childbirth).[7]

When Olcott *et al.* realized in 1937 that the antioxidant extracted from natural oils - "inhibitol" - consisted mainly or exclusively of tocopherols, they started the long-lasting research on the antioxidative properties of tocopherols.[8] A fundamental step forward was taken when E. Fernholz

identified the structure of tocopherol accurately. He could deduce partial structures from the properties of the pyrolysis products of vitamin E and connected them the correctly.[9,10] After just one year two research groups independently reported a total synthesis of racemic α-tocopherol.[11-13] It would still take several years, until the absolute configuration of α-tocopherol was assigned[14] and a synthesis for (*R*,*R*,*R*)-α-tocopherol had been published.[15]

Figure 1: Although pure tocopherol is colorless, commercial tocopherol is usually stained by oxidation products (left). Tocopherol esters are protected against oxidation and thus retain their colorlessness (right).

Eight substances are known today that can cure the effects of vitamin E deficiency (Figure 2).[16] According to the isoprenoid side chains, they are classified either as tocopherols (saturated side chain) or tocotrienols (unsaturated side chain). In natural tocopherols and tocotrienols only one stereochemical configuration can be found, the RRR-configuration. The second attribute that is used for classification is the methylation pattern at the aromatic ring. α-tocopherols and tocotrienols are permethylated, β and γ lack one and δ two methyl groups. α-Tocopherol is the most active and most common of these four substances and has been subject of numerous studies in diverse fields of science. Furthermore it is frequently used as preservative in the food and cosmetics industry.

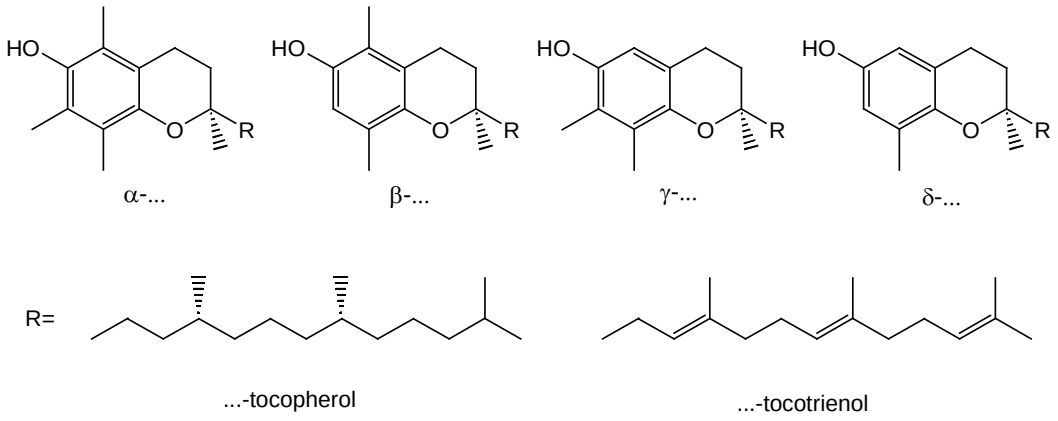

Figure 2: Classification of the four constituents of vitamin E. α-, β-, γ- or δ-tocopherol or –tocotrienol are distinguished by the methylation pattern at the aromat and the nature of the side chain.

Vitamins[17]

The complex processes of a human organism need a constant supply of substances that it cannot produce itself. Some of these substances are required in comparatively large amounts (e.g. water or digestible carbohydrates and fats as a source of energy), of some others a few grams are sufficient (e.g. essential amino acids, essential fatty acids or salts) and of some a few hundred milligram are all that is needed. In this case, inorganic salts are called trace elements (Cr, Cu, Co, I,…) and organic substances are called vitamins. By definition, if a typical human body needs not more than 100-200 mg of a certain substance per day, it is arbitrarily considered a vitamin or trace element.

Today, 13 substances are classified as vitamins (Table 1). Since an insufficient uptake of vitamins results in typical diseases, public health services have a legitimate interest in supplying the population with adequate sources of vitamins. Since almost all the vitamins are produced by plants (vitamin A is synthesized in animals, vitamin B_{12} is made by microorganisms), a significant amount of the daily diet should consist of fruits and vegetables. Nowadays robust, industrial scale syntheses are established for all the vitamins, which allow the food industry to enhance its products inexpensively.

	Typical Name Fragment	*Effect of Deficiency*	*Effect of Hypervitaminosis*	*Representative Structure*
Vitamin A	Retinol, Retinal, Carotene	night blindness, blindness, immunodefficiency	birth defects, osteoporosis, skin defects	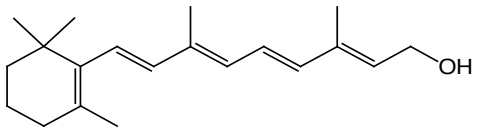
Vitamin D	Calciferol, Lumisterol	Rachitis, osteomalacia osteoporosis	hypercalcemia	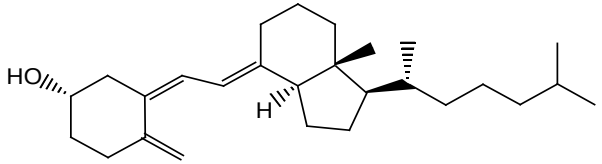
Vitamin E	Tocopherol, Tocotrienol	miscarriages, ataxia	not observed	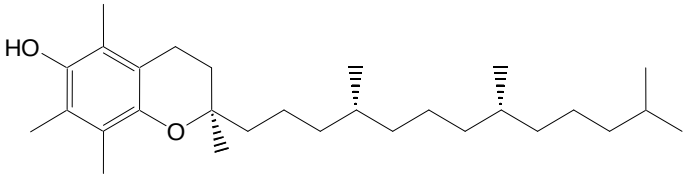
Vitamin K	Phylloquinone, Menaquinone, Menadione	hematomas, birth defects	not observed	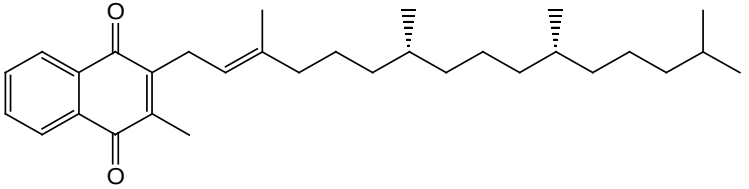
Vitamin C	Ascorbic Acid	Scurvy	indigestion	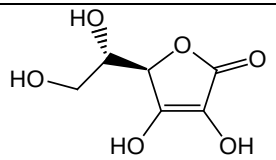

	Typical Name Fragment	*Effect of Deficiency*	*Effect of Hypervitaminosis*	*Representative Structure*
Vitamin B_1	Thiamine	Beriberi Wernicke's encephalopathy	not observed	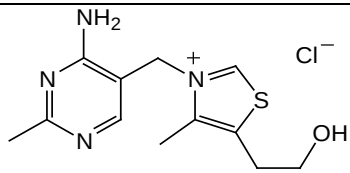
Vitamin B_2	Riboflavin	Ariboflavinosis: swollen and inflamed mouth and throat, dermatitis, anemia	not observed	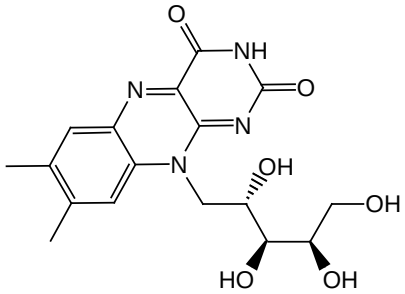
Vitamin B_3	Niacin	Pellagra	not observed	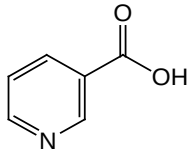
Vitamin B_5	Pantothenic acid	Weakness, neurological symptoms, hypoglycemia	not observed	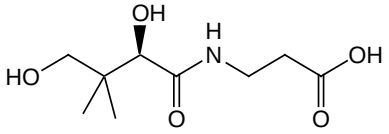
Vitamin B_6	Pyridoxine, Pyridoxal, Pyridoxamine	Pyridoxine Deficiency: cheilitis, conjunctivitis, neural symptoms	not observed	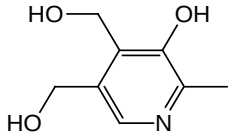

	Typical Name Fragment	*Effect of Deficiency*	*Effect of Hypervitaminosis*	*Representative Structure*
Vitamin $B_{7,}$ Vitamin H	Biotin	Biotin Deficiency: skin and hair problems	not observed	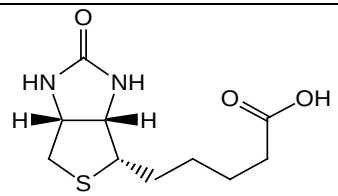
Vitamin B_9	Folic Acid	Folate Deficiency: weakness, loss of appetite, birth defects	not observed	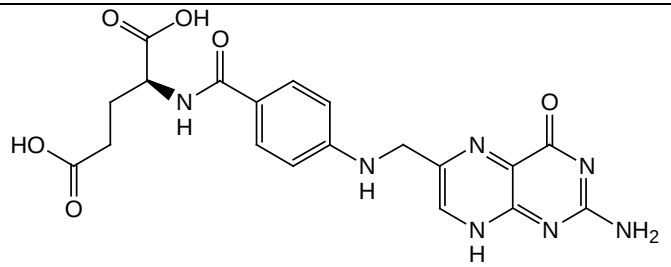
Vitamin B_{12}	Cobalamin	asymptomatic anemia	not observed	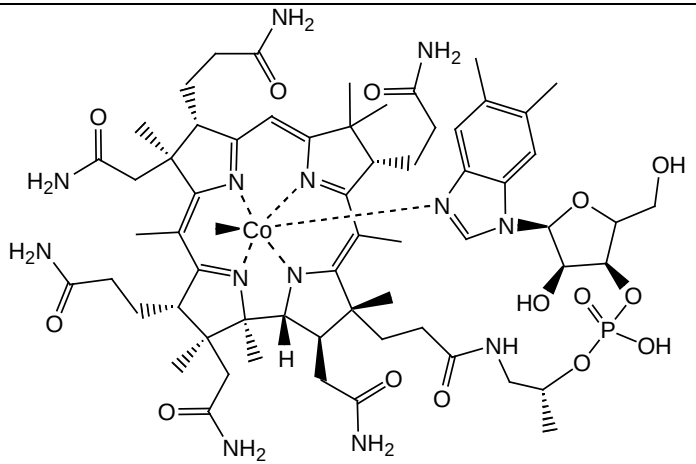

Table 1: List of vitamins

Physiological Importance of Vitamin E[18-25]

Today vitamin E is in a unique position: of all the vitamins it is the only one whose physiological mechanism of action is not known. The effects of tocopherol deficiency are evidently known, but why they occur, why they are prevented by vitamin E and whether the tocopherols and tocotrienols have different functions is still subject to research.

Two properties of vitamin E are obvious *in vitro*: the tocopherols and tocotrienols are extremely efficient radical scavengers and by their lipophilic tail predestined to be located in lipid membranes. It is therefore reasonable to assume that vitamin E´s main function should lie in the protection of the membrane against radical oxygen species. But a comparison of the rate constants of typical lipid oxidation reactions and the corresponding chain-breaking reactions of the tocopherols suggests that the reactions with oxygen are either too fast in any case, or that the physiological concentration of tocopherol is too small to be effective. An exception could be the scavenging of peroxidized fatty acid radicals, and it is still possible that certain domains in the cell could have exceptionally high concentrations of tocopherols. Additionally, clinical studies that tried to correlate the administration of high doses of vitamin E and a decrease of currently available markers of oxidative damage very often failed. Excreted tocopherol metabolites also do not give definite evidence of whether they are derived from oxidized precursors or were oxidized during analysis, and whether the assumed oxidation is the result of its physiological function or of the excretive metabolism. Also, if tocopherols are oxidized regularly in the body, an efficient mechanism should exist to recycle the tocopheryl radical to active tocopherol. Most often ascorbate is discussed as an important factor in tocopherol recovery, but *in vivo* evidence for this reaction is limited. Another probable redox partner could ubiquinol, but ubiquinol concentrations in cells can vary between almost nonexistent and sufficient for tocopherol recycling. This makes it an improbable cofactor for a ubiquitous molecule like tocopherol.

Even if there is no direct chemical function of vitamin E, it is still affecting enzyme and gene activity. Typically these genes are involved in uptake and degradation of vitamin E, lipid uptake and atherosclerosis, modification of extracellular proteins, inflammatory processes and cellular signaling and cell cycle control. Until now, these regulatory effects could only be observed in complex systems, a direct interaction between the affected enzymes and tocopherol could not be detected. A common regulator for all tocopherol related enzyme expressions and gene activities could not be found. Possibly the triggering mechanism is not a direct molecule/enzyme interaction but an indirect effect of the presence of tocopherol or oxidized tocopherol. The fluidity and structure of cell membranes is connected to the concentration of vitamin E, and it is likely that this has a regulating effect on certain membrane bound molecules or lipid rafts. As an alternative the ratio of oxidized/unchanged tocopherols could act as a sensor for oxidative stress, triggering an adequate response in the cell. All in all vitamin E seems to be a crucial factor in processes that require membrane fusion, as the uptake into

the cell and excretion of compounds and particles, fusion of cells and organelles, cell adhesion, vesicular transport and the recycling of vesicles. In particular these processes include the release of transmitters in the nervous system, cell fusion and feto-maternal trafficking. These effects would be a possible plausible explanation for the ataxia that α-tocopherol deficiency patient experience and the abort that is happening with vitamin E-depleted mammals at placentation.

Additionally, unnaturally high levels of tocopherol induce the enzymes that are responsible for its degradation. Since the tocopherols are metabolized unspecifically, this also results in an increased excretion of xenobiotics. This would not only help the body to remove unwanted substances, but would also increase the degradation of voluntarily taken drugs, thereby changing their therapeutic efficacy. Since too high levels of tocopherols trigger tocopherol metabolism, extreme supplementation with vitamin E does not reach the exceedingly raised tocopherol plasma levels that would be necessary to achieve the positive effects predicted by *in vitro* experiments. Instead, intake of large supplementary amounts of vitamin E only results in increased secretion, a process that seems to be very intensive anyway, since it is estimated that the whole circulating amount of tocopherols is removed by the liver from plasma and recycled at least once a day.[26] β-, γ-, and δ-tocopherol levels also never constitute more than a small fraction of the total tocopherol level, γ-tocopherol having the highest proportion with about 10% of the α-tocopherol content irrespective of the α/γ-ratio in the diet.

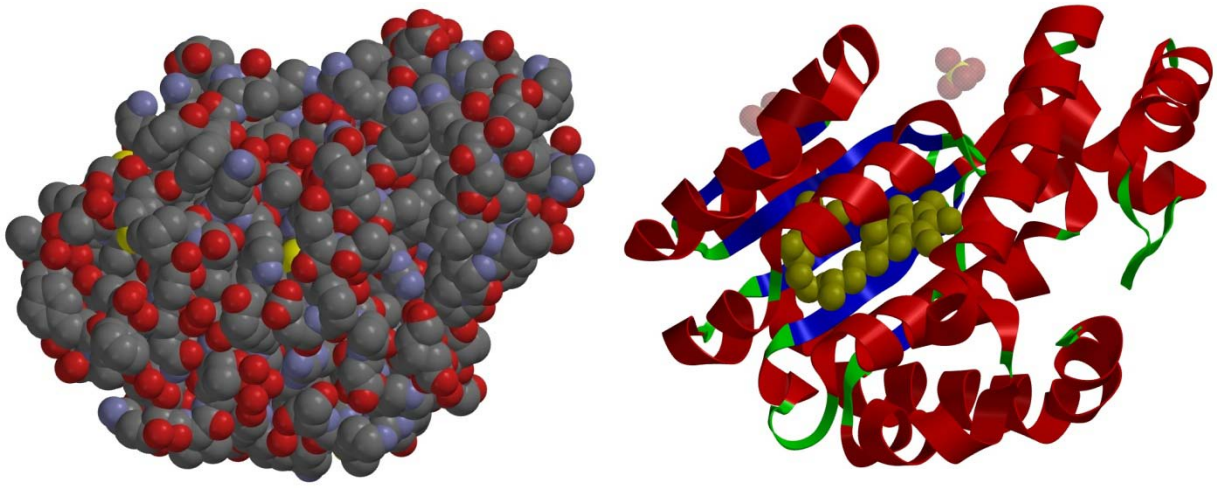

Figure 3: α-TTP as space filling model and as ribbon model. α-Tocopherol is completely enclosed by the protein during transport.

Upon intestinal absorption from food, the body does not distinguish between the different types of tocopherols and tocotrienols. The compounds are transported to the liver either in chylomicrons or by high-density lipoprotein, where it seems to be passed on to the α-Tocopherol Transfer Protein (α-TTP, Figure 3). This protein´s major function is to distribute tocopherol throughout the human body, since the highly lipophilic tocopherol needs a carrier protein to be transported in the aqueous environment of

the body. There are three additional Tocopherol-Associated Proteins (TAPs), whose specific function has yet to be elucidated. α-Tocopherol deficiency patients, who miss the gene for α-TTP, and α-TTP knockout mice both have extremely low plasma α-tocopherol levels and have similar symptoms of their genetic deficiency, particularly ataxia with progressing age. Moreover, α-TTP binds tocopherols with different selectivity, the affinity for β-, γ- and δ-tocopherol compared to α-tocopherol is only 38%, 9% and 2%, respectively. Bound to the enzyme, the tocopherols are protected against degradation, one of the reasons why α-tocopherol is the dominant form in the human body regardless of the tocopherol content of the diet. Why the body has such a strong preference for *R,R,R*-α-tocopherol is still unknown. γ-Tocopherol could for instance function as a scavenger for aggressive nucleophiles as peroxynitrite or nitrogen dioxide, as it has a reactive aromatic hydrogen. Unfortunately, this reaction might also happen with protein thiols with toxic effects, but evidence for this reaction is very scarce. β-Tocopherol is *in vitro* an antioxidant with an efficiency comparable to α-tocopherol, but its *in vivo* effect is severely reduced or totally absent. δ-tocopherol seems to have an even lower biological activity, which is combined with unfavourable plasma levels of about 1% of that of α-tocopherol.

Concluding, a lot of questions remain unanswered: Why is α-tocopherol so strongly favored? Is it the only relevant tocopherol? Do the other tocopherols and tocotrienols have any special function? How does the uptake and distribution of vitamin E work? Why and how do the tocopherols help against ataxia and female reproductive failure? And why does the body need vitamin E at all? Recent progress in research on the physiological action of tocopherols has been impressive, justifying hopes for a soon breakthrough in understanding the essentiality of vitamin E.

Biosynthesis of Vitamin E[27]

Although animal products can be a significant part of a vitamin E-rich diet, the main sources of tocopherols are plants. This is hardly a surprise, since vitamin E is metabolized in plants only. The primary photosynthetic tissues of plans contain reasonable amount of tocopherols, but seeds and the oils have tocopherol contents that are orders of magnitude larger. Interestingly, the portion of each tocopherol in the produced vegetable oil varies according to the plant. So the major tocopherol in a typical american diet is γ-tocopherol due to the predominant use of soybean seed oil, that contains about 70% γ-tocopherol and just 7% α-tocopherol. In Europe oils rich in α-tocopherol are used (e.g. sunflower seed containing about 96% α-tocopherol), resulting in lower γ-tocopherol blood levels.

Today's possibilities in genome sequencing, gene expression and metabolite profiling have rendered it possible to elucidate the biosynthetic pathway of the tocopherols, including the enzymes responsible for each step (Figure 4). The biosynthetic enzymes participating in the synthesis of tocopherols are

very similar in plant and cyanobacteria. This not only emphasizes their common heritage, but also facilitates research on this topic. As usual Arabidopsis Thaliana has served as model plant.

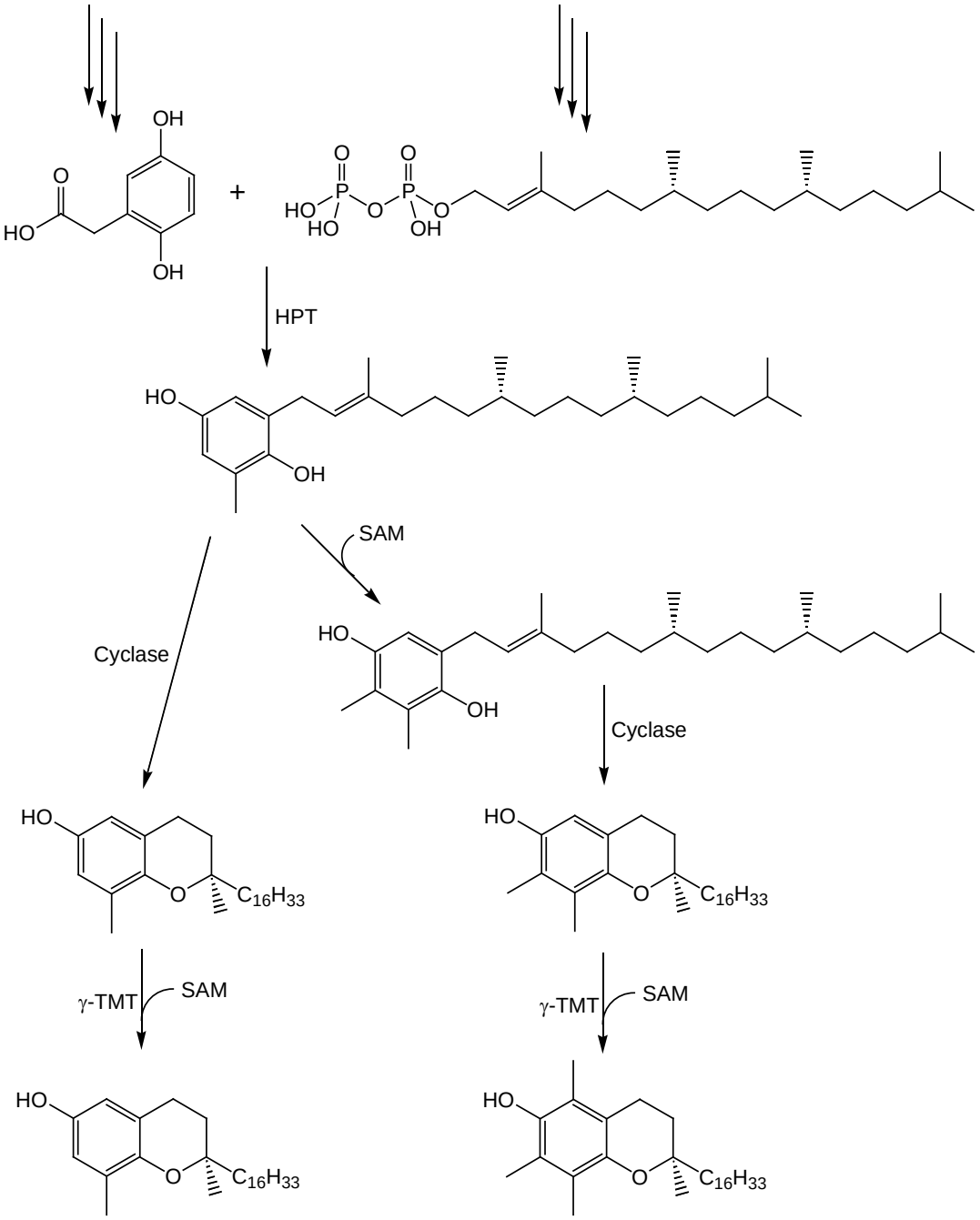

Figure 4: Biosynthetic pathway of tocopherols. HPT: homogentisate phytyltransferase; cyclase: tocopherol cyclase; SAM: S-adenosyl methionine; γ-TMT: γ -tocopherol methyltransferase.

The starting substances are homogentisic acid and phytyl-diphosphate for the tocopherols and homogentisic acid geranylgeranyl-diphosphate for the tocotrienols (not shown), which are derived from the cytosolic aromatic amino acid metabolism and the plastidic deoxyxylulose 5-phosphate pathway, respectively.

The step that yields the first intermediates exclusive to the tocopherol biosynthesis is the attachment of the phytyl side chain to the aromatic system. Here the pathway forks: either the aromat is methylated at the future C7-position, or the fused ring of the chromanol is closed. The former case will yield either α- or γ-tocopherol, the latter δ-tocopherol and after methylation β-tocopherol. The γ-tocopherol precursor will also undergo enzymatic cyclization, to yield γ-tocopherol, and one further methylation finally gives α-tocopherol.

Catabolism of Vitamin E[20]

Regardless of the essentiality of vitamin E, the organism seems to have a highly efficient system to metabolise and remove excessive amounts of it. Interestingly, the method of degradation and the utilized enzymes correspond to the pathway that is typical for xenobiotic substances. This seems also to be the reason why highly elevated levels of vitamin E, which increase the catabolism of tocopherols, also increase the catabolism of xenobiotics.

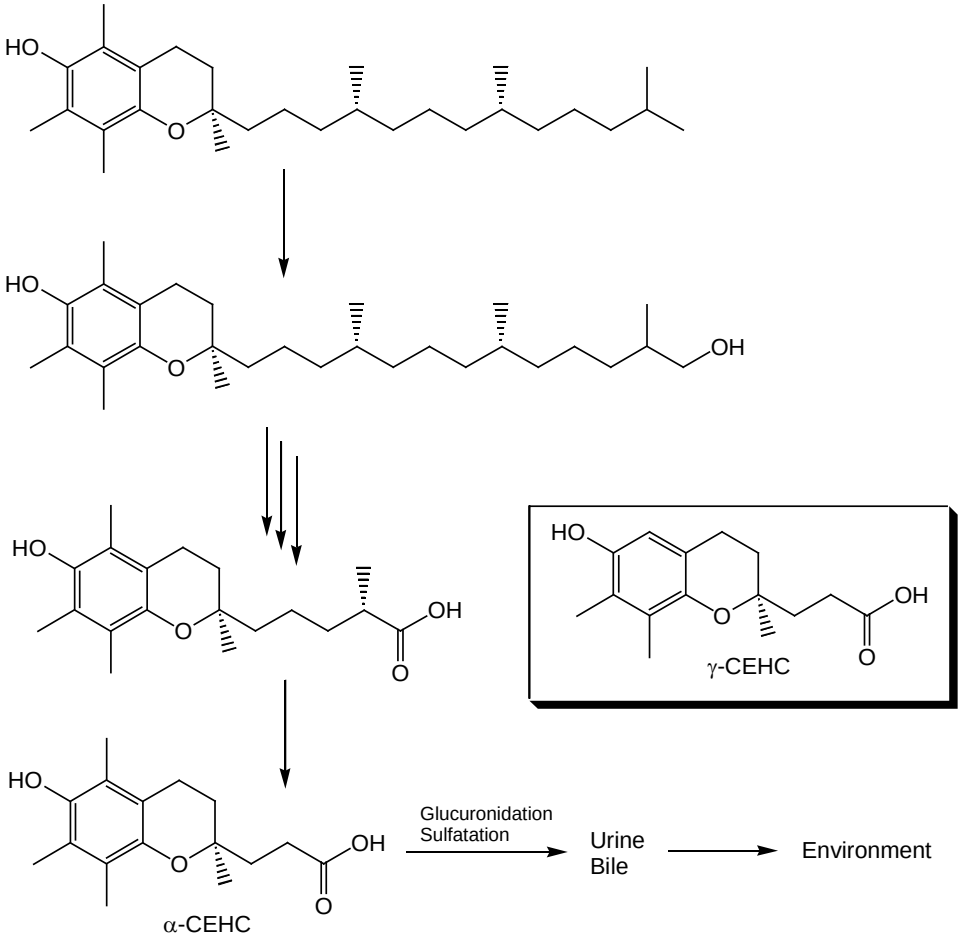

Figure 5: Catabolic pathway of α-tocopherol.

Both the tocopherols and the tocotrienols are oxidized several times by cytochrome P450 enzymes, esterified with glucuronic acid or sulfuric acid and finally excreted (Figure 5). The oxidation is not

unspecific, but consist of an ω-hydroxylation, followed by a β-oxidation and a finally decomposition to the respective carboxyethyl hydroxychroman (CEHC). After glucuronidation or sulfatation the degraded vitamin is excreted *via* bile or urine. Notably this metabolite is not oxidized to a benzoquinone but retains the original aromatic chromane, suggesting that not only oxidized tocopherols are removed but unused ones as well. Again, this seems to be the effect of the body´s protection against excessive amounts of tocopherols. The well-known Simon-metabolites (Figure 6) seem to be mainly the artifacts of oxidation during sample preparation since they are not obtained if oxidants are carefully avoided during work-up.

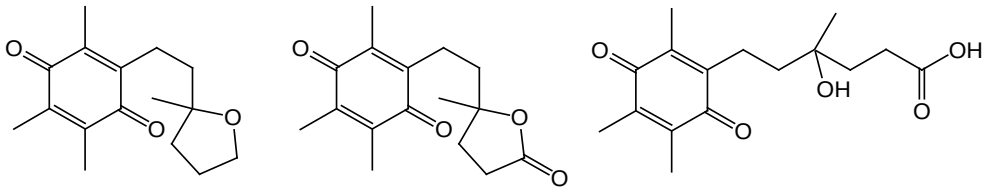

Figure 6: The Simon-metabolites of α-tocopherol.

Being derivatives of highly bioactive substances it is not surprising that the metabolites of tocopherols can have an influence on the body as well. γ-CEHC can increase natriuresis and diuresis at nanomolar concentrations, if the administration is combined with previous depletion of vitamin E and a sodium-rich diet, circumstances that limit the therapeutic usefulness. To be able to exploit the *in vitro* effects of high plasma levels of tocopherols and tocotrienols, concentrations have to be reached that usually are prohibited by metabolism. To reduce the effectivity of the degradation by CYP450, the addition of sesame seeds or sesame oil, which contain substances that inhibit CYP450, to the diet has been proven to be successful. The resulting plasma levels where higher than the ones obtained by a tenfold higher dosage of tocopherol.

Industrial Synthesis of Vitamin E[28]

In terms of price and production capacity most vitamins can be considered fine chemicals, costing more than 10 $ per kg at an annual production in amounts of 1,000-10,000 t (for tocopheryl acetate ~35,000 t/a). For reasons of competitiveness the use of stoichiometric amounts of catalysts, exotic solvents and conditions or even toxic reagents are not viable for a process on an industrial scale, since the costs for reagents, waste disposal or detoxification would result in a prohibitively expensive product. Laborious methods of purification, that might be useful at lab-scale, are usually to costly at large scale. For all this reasons industrial processes are constantly revised and improved. Especially the use of the right catalyst system can improve yields and throughput and can reduce the amounts of byproducts that have to be separated later, making a process more economic, environmentally friendlier, safer, sustainable and resulting in products of higher quality.

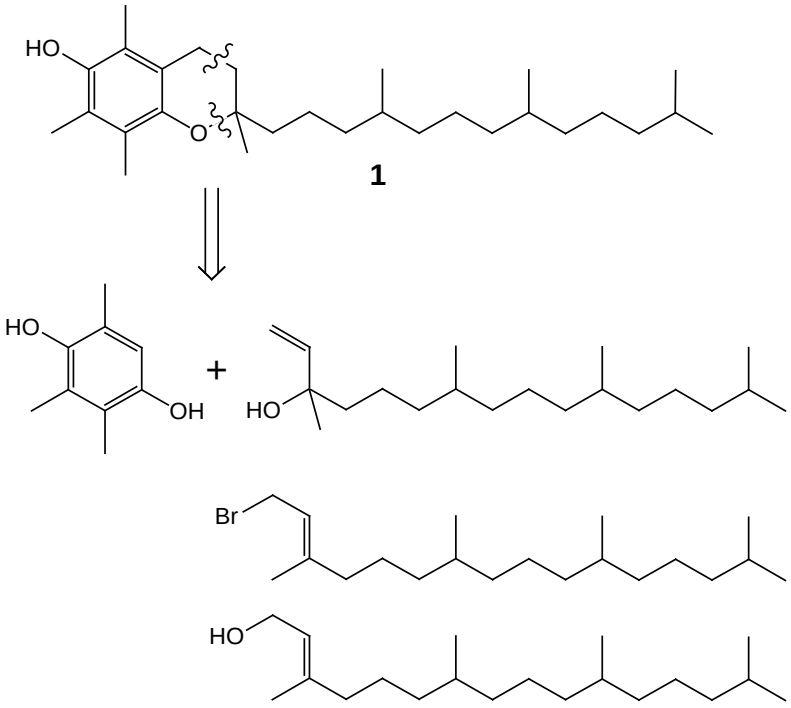

Figure 7: Most commonly applied retrosynthetic breakdown of α-tocopherol.

In the case of α-tocopherol (**1**), the generally applied synthetic pathway has not changed since the first patented industrial method (Figure 7).[29-32] Still the chromanol skeleton is established as the final step by a *Friedel-Crafts* reaction of trimethylhydroquinone with a phytol derivative followed by condensation. In 1946 Karrer and Isler still had to rely on stoichiometric catalysts, such as anhydrous zinc chloride, anhydrous formic acid or saturated solutions of hydrochloric acid in organic solvents. Extractive workup procedures that employed acidic and basic aqueous solutions and alcoholates lead to tremendous amounts of waste. Finally, the use of hydrocarbon solvents as reaction media and the generation of hydrogen bromide if phytyl bromide was used as starting material did not indicate an environmentally friendly process. Today the extensive application of catalysts permits the use of favorable starting materials, processes that are solvent free or utilize water as solvent and processes with rather mild temperature and pressure conditions.

As already mentioned, the key step in the synthesis of tocopherols is the *Friedel-Crafts* alkylation of trimethylhydroquinone with an excess of isophytol, phytol or a phytyl halide. A lot of classical Brønsted or Lewis acids catalyze this reaction, but the necessary amounts of acid, waste water contamination with halides and metal ions and corrosion issues limit their usefulness. Modern catalysts like zeolithes, ion exchange resins, rare earth metal triflates, or special polyfluorinated compounds[33] usually increase yield and selectivity, can be used in real catalytic concentrations and are in some cases recyclable. Reactions in multi-phase-solvent systems and supercritical solvents are feasible as well.

Synthesis of Trimethylhydroquinone[16,28,34]

Three synthetic pathways are useful to afford trimethylhydroquinone (Figure 8). *m*-Cresol can be methylated to a trimethylphenol, which yields the hydroquinone upon oxidation and reduction. Methanol can be used as methylating agent in this gas-phase reaction. The temperature is usually above 350°C, and oxides of transition metals are commonly used catalysts.

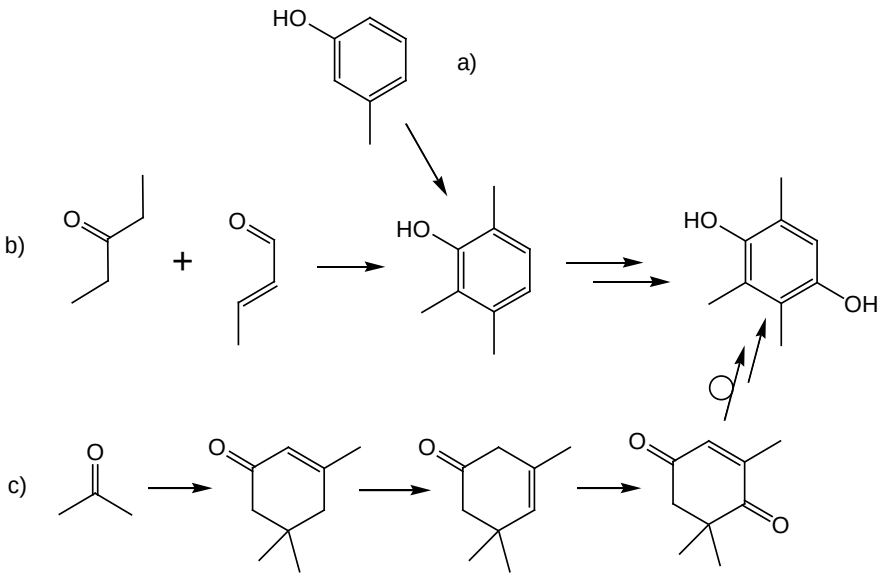

Figure 8: Exemplary industrial syntheses of trimethylhydroquinone. a) Methylation of *m*-cresol. b) Condensation of 3-pentanone and crotonaldehyde. c) From acetone.

A different approach uses a condensation of 3-pentanone and crotonaldehyde which is followed by dehydration on platinum catalysts. The resulting phenol can be oxidized in various solvents to the quinone by air or an oxygen-containing gas at 60-110°C and with copper chloride as a catalyst, or by peroxides and silica-based catalysts. Homogenous phase oxidation can be achieved with heteropolyacids like $H_7PMo_8V_4O_{40}$. Reduction is usually achieved heterogeneously by hydrogenation with classical catalysts such as Pd/C, Raney-nickel and platinum group elements or nobel metals on zeolites, silica or aluminium oxide carriers.

Another synthetic option is to convert three acetone molecules to α-isophorone and to its isomer β-isophorone with the help of Lewis acids (indium triflate). The oxidation to ketoisophorone is achieved by several catalysts, for example lead acetate in pyridine, molybdic acids or complexes of transition metals. After an acid catalyzed Wagner-Meerwein rearrangement and rearomatization in acetic acid anhydride at room temperature, the obtained acetate can be saponified to the desired hydroquinone.

Synthesis of Isophytol[28,35]

Apart from the option of using natural products as starting materials for the synthesis of the alkyl part of tocopherol, various syntheses based on cheap bulk chemicals have been developed. For vitamin E

synthesis, two pathways are of special significance, since they use cheap starting materials, are extremely efficient and produce little amounts of byproducts and waste (Figure 9).

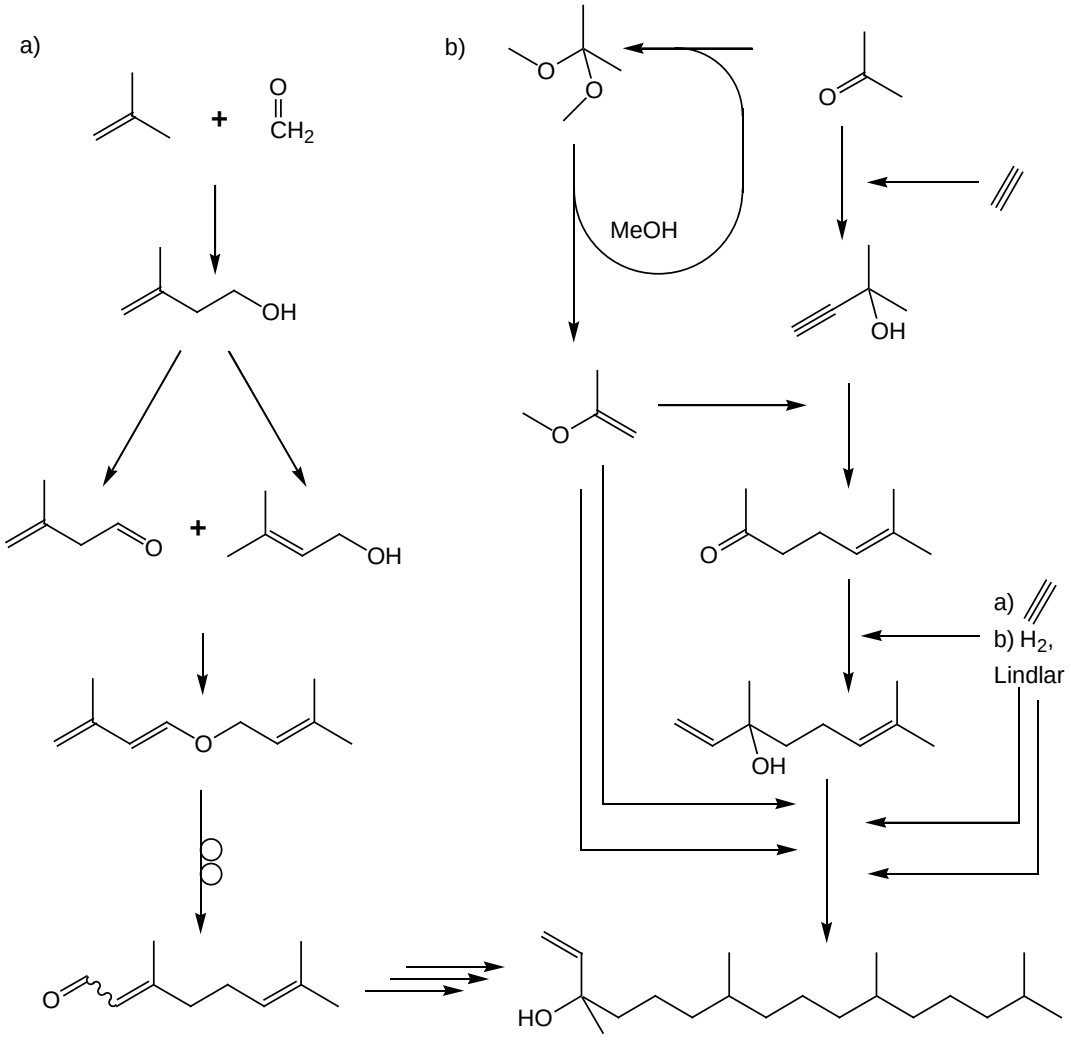

Figure 9: Exemplary industrial syntheses of isophytol. a) From isobutene and formaldehyde. b) From acetone and ethyne.

Using isobutene and formaldehyde as starting material, isoprenol can be obtained under acidic conditions by a *Prins*-reaction. Isoprenol is then both oxidized to isoprenal by a supported silver catalyst in the gas phase at 500°C and isomerized to prenol by a palladium catalyst. After condensation – the only step that yields a byproduct, namely water – two Claisen-rearrangements take place that result in the highly useful intermediate citral, that can easily be converted to isophytol.

The second pathway uses one reaction sequence repeatedly to finally yield isophytol. Acetone is converted with ethyne and the resulting alkyne reacts with 2-methoxypropene, accounting for a chain elongation by 5 carbon atoms. 2-Methoxypropene is made from a ketal that is produced from acetone and methanol and cleaved again to 2-methoxypropene. The methanol can be recycled to be reacted again with acetone. After this the reaction with ethyne and methoxypropene is repeated, with the

variation that the intermediary alkyne is reduced to the alkene with a deactivated Lindlar-catalyst. In the end acetone has been converted to isophytol by the addition of four ethyne and three modified acetone molecules. Both the reaction with the alkyne under basic conditions and with the methoxypropene under acidic conditions can be catalyzed by ion exchange resins at high temperatures and pressures, the catalysts for the hydrogenations are palladium on calcium carbonate for the Lindlar reduction or palladium on activated charcoal for the final reduction. Both this and the previous process are highly advantageous with regard to starting material, atom efficiency and waste production.

(*R*,*R*,*R*)-α-Tocopherol[28]

While synthetic all rac-α-tocopherol is primarily used for animal feed, *R*,*R*,*R*-α-tocopherol is preferred for food, pharmaceutics and cosmetics. At the moment no industrial synthesis has been established to produce this enantiomerically pure form at a large scale, although highly selective processes to synthesize the isoprenoid side-chain are in development.[33] Still it is more efficient to extract natural fats and oils as soybean oil to obtain *R*,*R*,*R*-α-tocopherol. However the α-tocopherol content of some important plant oils is small compared to the content of other forms of tocopherol. Therefore the non-α-tocopherols are industrially methylated to give the permethylated α-form. Current processes that apply halo-, hydroxyl- or amino-methylation followed by reductive cleavage suffer from the generation of large amounts of waste and the use of corrosive substances as hydrochloric acid, zinc chloride, tin chloride or phosphorous oxychloride. The reaction can also be done at supercritical or near-supercritical conditions in methanol, carbon dioxide or hydrogen with a non-polar organic co-solvent such as hexane or toluene. Under these conditions corrosive catalysts can be replaced by hydrotalcites.

Synthesis of Tocopheryl Acetate[28,36]

Very often tocopheryl esters are used commercially instead of tocopherol. Derivatizing the phenol has the important advantage that the thus protected tocopherol is not as readily oxidized as the original compound and can therefore be stored and handled more easily. Usually the esters of nicotinic acid (**1a**), succinic acid (**1b**) and most importantly acetic acid (**1c**) are used (Figure 10).

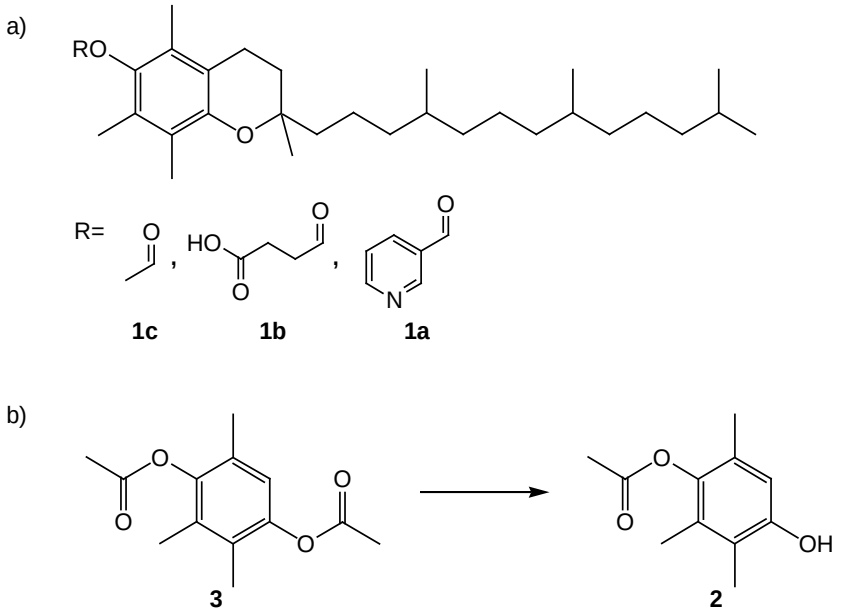

Figure 10: a) Commercial tocopheryl esters. b) Selective cleavage of the trimethylhydroquinone diacetate as α-tocopherol precursor.

For the production of the protected tocopherol there are two options: esterification of the completed tocopherol or using the ester of a precursor compound for tocopherol synthesis. In the former case, acetic anhydride is used together with an acid or base catalyst (e.g. sulfuric acid, pyridine, respectively) in a continuous or discontinuous process. Alternatively, catalyst-free processes that utilize microwave radiation are feasible. In the latter case, a monoacetylated hydroquinone (**2**) has to be synthesized as starting material for the final *Friedel-Crafts* reaction with isophytol. The challenge in that case is to acetylate only one of the available two phenols selectively. Immobilized *Thermomyces lanoginosus* lipase, a very cheap enzyme that is used at large scale in cleaning agents, is able to selectively cleave the right ester of trimethylhydroquinone diacetate (**3**) at temperatures up to 55°C in a mixture of water and *tert*-butyl methyl ether (Figure 10).

Chemical Properties of Vitamin E[16,37,38]

General

From a chemist´s perspective, tocopherols and tocotrienols can be considered to consist of two parts (Figure 11). On the one hand, the chromanol moiety, that is mainly responsible for hydrophilic interaction and the antioxidative behavior of the molecule. On the other hand, the isoprenoid chain that acts as a lipophilic anchor that connects the molecule to lipid membranes. Since the side chain is basically a linear alkane, it has little to no chemical reactivity. In contrast to that, the molecules´ annulated hydrophilic part contains a variety of chemically interesting structures: a phenol that is part of a hidden hydroquinone system, benzylic methyl groups and in some cases aromatic hydrogens.

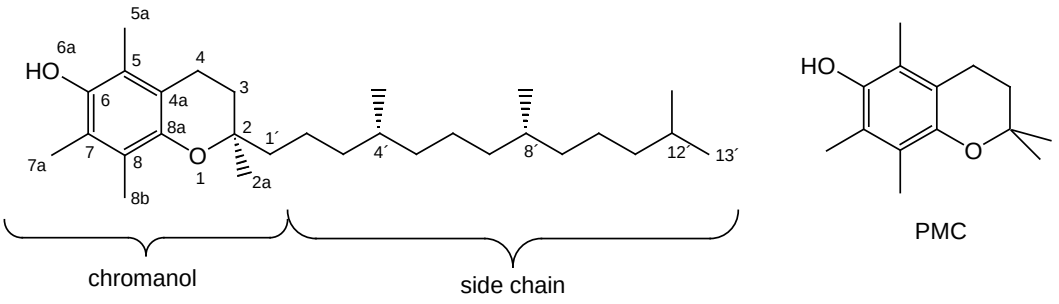

Figure 11: General description of α-tocopherol. The numbering and nomenclature of tocopherols and tocotrienols have been regulated by IUPAC.[39]

It is therefore common to use "truncated" model compounds for *in vitro* studies on the reactivity of tocopherols. These models are identical to their parent compound apart from the exchange of the long isoprenoid side chain with a short methyl group. Of course this changes the lipophilicity of the molecule, but it does not alter the behavior towards chemical reagents, since the reactive positions of tocopherols are located at the annelated core. Using these model compounds has multiple benefits: Handling solid models is much easier than oily tocopherols; spectra are considerably simplified, since the signals of the side chain are removed; special derivatives are accessible more easily, because the extensive and stereoselective synthesis of the side chain can be omitted and cheap commercial chemicals can be used instead; after removing the highly lipophilic side chain, small changes at the chroman system make a bigger difference in terms of lipophilicity, this extends the usefulness of chromatographic techniques; the models and their reaction products can often be crystallized; the smaller lipophilicity of the models allows it to be dissolved in more polar solvents, this permits reactions with reactants that would not be soluble in apolar solvents. Today the α-tocopherol model PMC (2,2,5,7,8-pentamethyl-6-chromanol, **4**) is commercially available, and simple syntheses for the other models exist. The atom numbering and the nomenclature of the tocopherols and tocotrienols have been regulated by IUPAC, and the same system is used for the model compounds as well.[39]

Oxidation Chemistry

Over the years many studies on the reactivity and oxidative behavior of vitamin E were conducted, and the topic proved to be rather complex. Although different oxidants and different solvents result in very different oxidation products, the initial oxidation phase is rather simple, and only 3 primary intermediates can be distinguished (Figure 12). Depending on the chosen conditions, only one of these three major intermediates forms, while the other two don´t occur at all. The type of solvent has such a strong influence on the preferred reaction pathway, that this factor determines the structure of the resulting product almost on its own. The three main intermediates in tocopherol oxidation are briefly covered in the following.

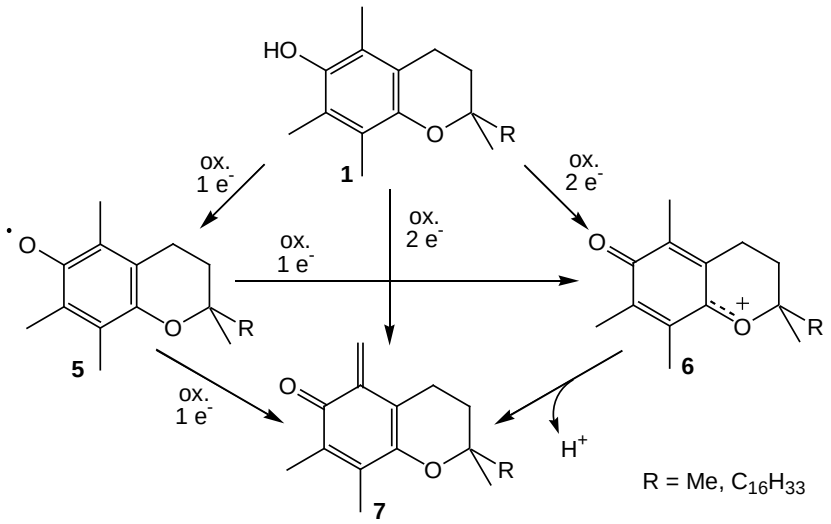

Figure 12: Primary oxidation pathways of α-tocopherol.

Chromanoxyl Radical (**5**)

Homolytic (one-electron) oxidations of chromanols yield a chromanoxyl radical. The unpaired electron is mainly located at oxygen O-6, but spin density is increased in the *ortho*- and *para*-positions of the aromatic ring as well. Carbon centered radicals react primarily with O-6 to give chromanyl ethers, while other radicals react preferably with C-8a resulting in 8a-substituted chromanones. Of course the reaction partner can be another chromanyl radical, giving an intermediary 8a-chromanyl-chromanone that readily fragments ("disproportionates") by 1,4-elimination into starting chromanol **1** and *ortho*-quinone methide (**6**). Alternatively, one chromanoxyl is regenerated by the abstraction of a hydrogen from C-5a of another chromanoxyl, turning it into an oQM. Further oxidation of chromanoxyl radicals yield chromanoxylium cation (**7**) and oQM, respectively.

Many reaction products of oxidized tocopherol have earlier been explained by reactions of the C-5a centered tautomer of chromanoxyl, but it has been shown that this tautomer does not exist and that these substances are actually products of reactions that involve the corresponding *ortho*-quinone methide (oQM).[40] Compared to chromanoxyl, the C-5a centered radical is energetically much less stable and highly unlikely to occur.

Chromanoxylium Cation **7**

Heterolytic (two-electron) oxidations of chromanols and one-electron oxidations of the chromanoxyl radical in aqueous or polar solvents result in a chromanoxylium cation. The charge is mainly localized at C-8a,[41] and because of resonance stabilization a positive partial charge is also present at C-5 and C-7. The primary reaction of the chromanoxylium cation is the addition of nucleophiles at C-8a, resulting in 8a-substituted tocopherones that might further react to the corresponding *para*-quinones.

ortho-Quinone Methide **6**[42]

In apolar, aprotic or dry solvents, an *ortho*-quinone methide (oQM) is the main two-elextron oxidation product of vitamin E-type chromanols. It can be obtained by direct two-electron oxidation, one-electron oxidation of the chromanoxyl or proton loss from C-5a of the chromanoxylium cation. Reactions of the oQM include the reduction to chromanol, 1,4-addition of nucleophiles at C-5a and O-6 and hetero-*Diels-Alder* reactions with inverse electron demand. Typically these reactions restore the aromaticity of the molecule and are thus energetically strongly favored. Addition to C-5a is a reliable and often applied method to synthesize C-5a-substituted tocopherol derivatives that are used as starting points for complex reaction sequences. Interestingly, the oQM can serve both as electron deficient diene and as electron rich dienophil in the *Diels-Alder* reaction, permitting a reaction between two oQMs to form a spiro dimer (**8**), that can even continue to react to a spiro trimer (**9**).[43] The reduction of spiro-dimer to an ethano-dimer and its reoxidation to spiro-dimer can be accomplished repeatedly without yield penalty, therefore the two compounds can be considered a reversible redox pair.

Amazingly the oQM´s double bond system almost exclusively includes C-5a ("up"-oQM), and only traces of the C-7a comprising "down"-oQM can be detected. This is caused by the strain-induced bond localization (SIBL) effect in the aromatic chromanol.[44] In an ideally relaxed benzene ring the C-C and the C-H bonds draw an angle of 120°. If this angle is changed for some reason (Figure 13), for example by replacing the hydrogens with bulky substituents or rigid annelated structures, the aromatic frame is affected. Instead of six C-C bonds of equal length, as it would be the case in completely relaxed, highly symmetric benzene, the aromatic scaffold now consists of bonds of different lengths. This corresponds to a strain-induced adjustments of electron densities that reflect the rearragement of the aromatic system towards a system of three localized, conjugated double bonds.[45,46] In the case of chromanols, the strain of the tetrahydropyran moiety leads to angles that are larger than 120°. This results in a double bond placement that anticipates the double bond pattern of "up"-oQM, which is the dominant species accordingly. Substitution that results in smaller angles as for example in vitamin E-type benzofuranols enforces the alternative double bond pattern on the aromatic ring and therefore mostly yields "down"-oQM.[44] Substitution patterns that mimic chromanol electronically but allow unrestricted alignment of the substituents (the angles are therefore very close to 120°) result in 1:1 mixtures of "up"-oQM and "down"-oQM.[44]

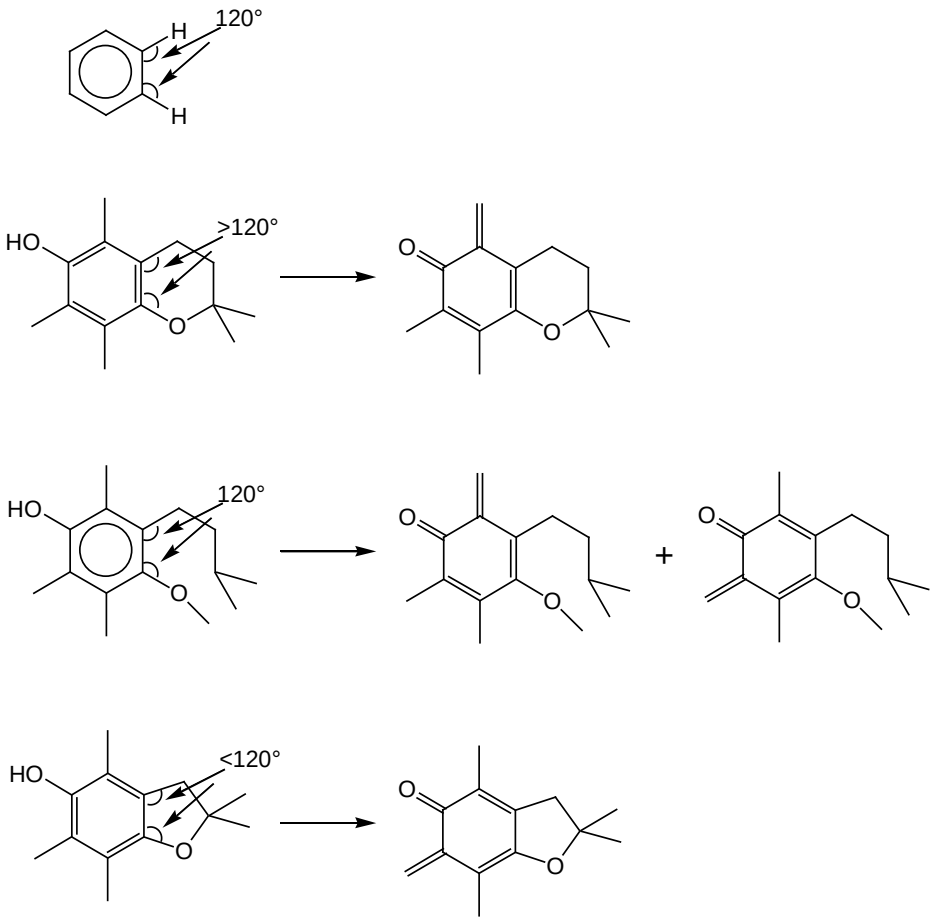

Figure 13: The strain imposed by the substituents on the aromatic ring controls the formation of either "up"- or "down"-oQM.

Schematic Overview on Tocopherol Oxidation

Depending on the oxidation conditions α-Tocopherol can undergo a variety of possible oxidation pathways. The three main oxidation intermediates presented above are just the starting point for a multitide of different reaction products that can be obtained. Figure 14 and Figure 15 give a rough overview on the rich oxidation chemistry of tocopherol.

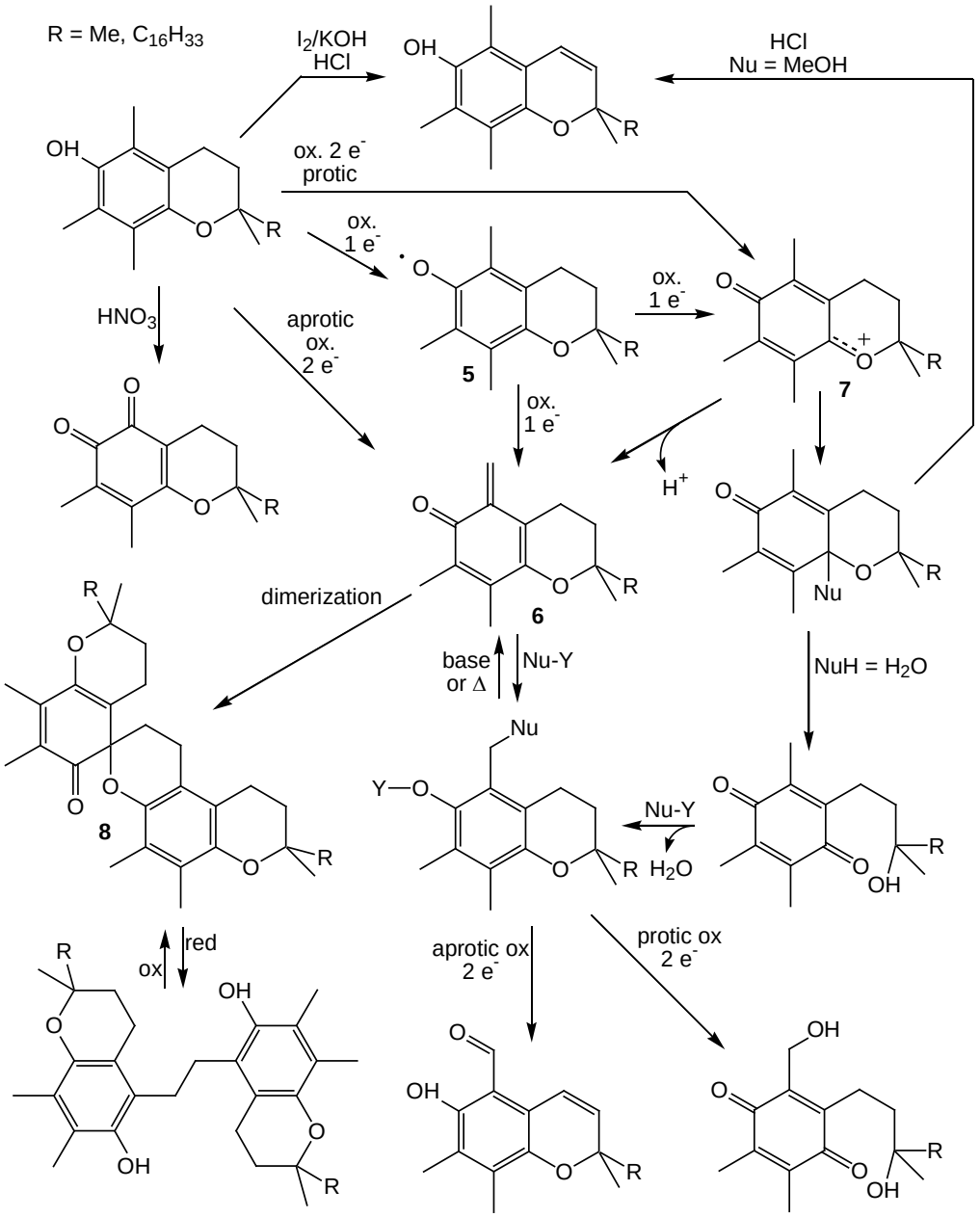

Figure 14: Overview on tocopherol oxidation in protic media.

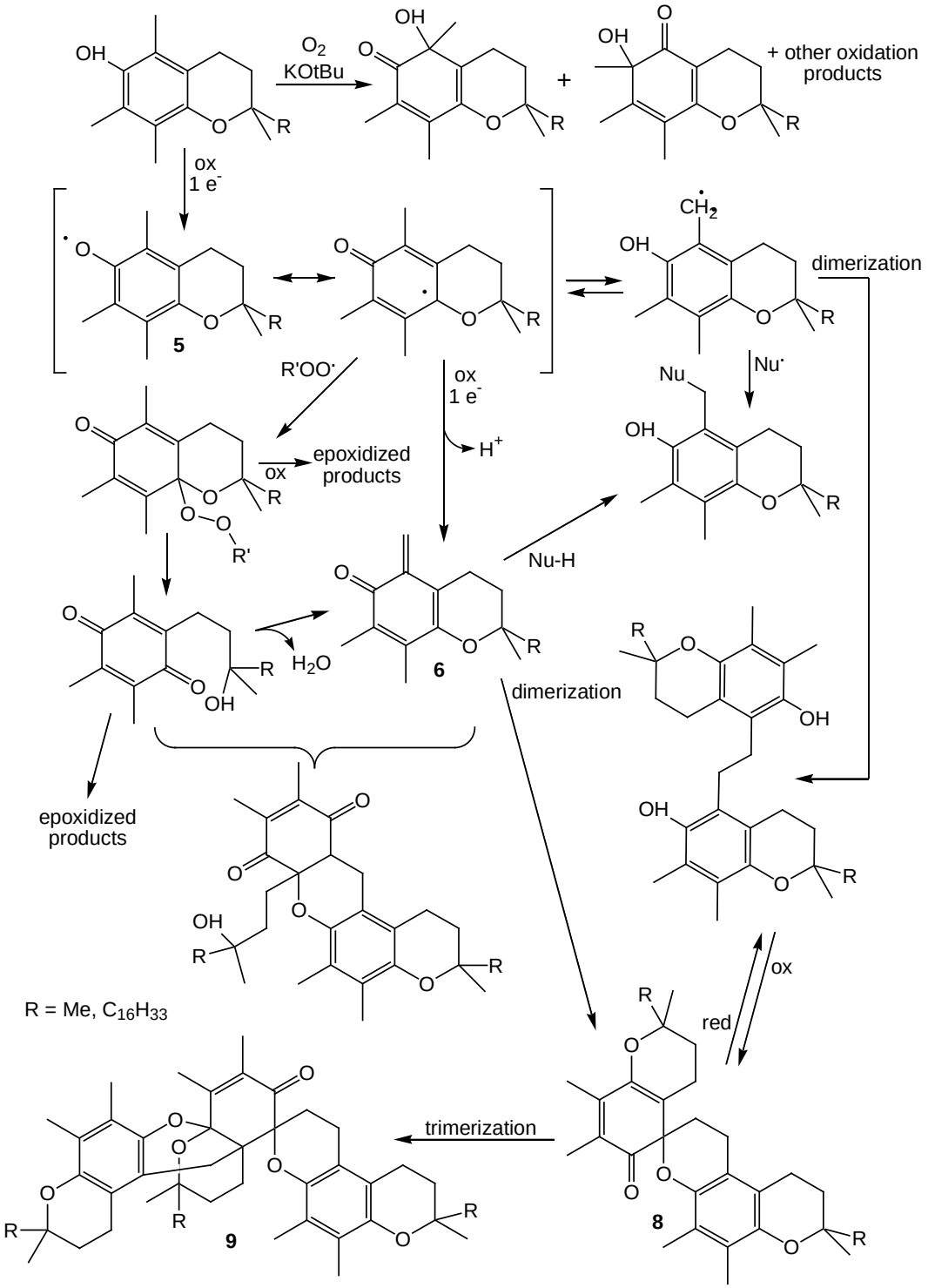

Figure 15: Overview on tocopherol oxidation in aprotic media.

Aim of Work

The *ortho*-quinone methide derived from α-tocopherol has not only proved to be a crucial and ubiquitous intermediate in the chemistry of the vitamin, it has also been used increasingly as a model and standard for *ortho*-quinone methides in general.

It was the general aim of this work to address and clarify the role of the oQM in the oxidation chemistry of tocopherols. In this effort, four topics had to be considered in particular:

Detailed mechanism of oQM formation.

Previous computational studies in our group have indicated that *ortho*-quinone methide formation might be a stepwise process involving an aromatic, zwitterionic compound which is an intermediate but not a resonance structure. Clarification of this issue would have a major impact on the understanding of a general oxidation procedure, and confirmation of such intermediates – if indeed existing – would revise decade-old teaching on *ortho*-quinone methides. New ways to scrutinize the oQM system and the details of oQM formation would be needed.

oQM-formation *vs.* electrophilic substitution in non-α-tocopherols.

While α-tocopherol with its persubstituted aromatic core is unable to undergo electrophilic aromatic substitution, all other forms – the so-called non-α-tocopherols – have free aromatic positions. In these compounds, oxidation and S_E reactions would be competitive processes in the presence of suitable coreactants that combine oxidative and electrophilic character. Bromination – and the action of bromonium ion Br^+ on the different tocopherols – would be a primary example here. So far no data on the respective reactivities of non-α-tocopherols are known.

Oxidation chemistry of α-tocopheramine: *ortho*-quinone methide chemistry *vs.* *ortho*-quinonimine methide chemistry.

Tocopheramines, in which the phenolic hydroxyl group is replaced by a free or substituted amino group, are a class of tocopherol derivatives that is largely uninvestigated and not understood. Especially the oxidation chemistry of these compounds – both in homolytic and heterolytic processes – is a completely new field for scientific endeavors. The structure of the primary one-electron and two-electron oxidation products, which would correspond to the three primary oxidation products in α-tocopherol oxidation, is of particular interest. The analogue to the α-tocopherol-derived chromanoxyl radical would be an aminyl radical, the analogue to the oQM an *ortho*-quinonimine methide, of which existence, structure and reactivity are completely unknown.

Generalization of the *ortho*-quinone methide chemistry of α-tocopherol.

A comprehensive account of the chemistry of the α-tocopherol-derived oQM, combining own results with previous ones of the work group and considering the manifold and sometimes contradictory views in the literature, appeared to be overdue. A thorough and authoritative treatise of the tocopherol-derived oQM was the concluding task of the present work.

Results and Discussion

Bromination of Tocopherols in Apolar Media[47]

Introduction

α-Tocopherol **1** offers rich oxidation chemistry but little possibility for derivatization at the aromatic ring, as has already been presented in the introduction. The non-α-tocopherols (**10**, **11**, **12**) possess free aromatic positions, and so they are readily susceptible to electrophilic aromatic substitution. It is known today that the γ-homologue – in contrast with the α-form[48,49] – is a good trap of electrophiles under physiological conditions, and such trapping products have been detected in human plasma and tissue samples.[50-52] No analogous studies for the β- and δ-homologues exist.

We were interested in the interactions of tocopherols with oxidizing enzymes, which are sources of potent electrophiles or electrophile precursors, such as hypohalites, peroxynitrite, cyanate, or thiocyanate. Non-α-tocopherols seem to be ideal candidates as molecular probes of the reaction modes of such enzymes. In previous studies the nitrosation[53] and nitration[54] chemistry of non-α-tocopherols have already been addressed, both to provide the different nitroso- and nitrotocopherols as standard compounds and to establish their analytical data reliably. This was necessary because a review of the pertinent literature had revealed largely contradictory analytical data (UV, NMR) for the reaction products of γ-tocopherol with nitrating/nitrosating species,[55-61] as well as a nearly complete lack of data for the reaction products of β- and δ-tocopherol. When we started to work on the interplay of non-α-tocopherols with hypohalites and halogenating enzyme systems we faced a similar problem. Apart from data on 5-bromo-γ-tocopherol[62] and rearrangement products from the action of hypochlorite on α- and γ-tocopherol,[63,64] the pertinent literature did not provide relevant information. For practical reasons we focused first on bromine as the halogen (to avoid the difficult-to-handle and difficult-to-dose gaseous chlorine), and this lack of data left us with the task either of establishing (for β- and δ-tocopherol) or reinvestigating (for γ-tocopherol) the structures of the corresponding bromination products, so that standard compounds and a reliable reference set of analytical data would then be available. This was done in all cases both for the tocopherols themselves and for the corresponding truncated model compounds (**4**, **13**, **14**, **15**), each bearing a methyl group instead of the tocopherols' isoprenoid side chain. Replacement of this chain is known to have no effect on the UV data and the aromatic NMR resonances.[65,66] The α- form has been included in the following report for reasons of comparability and completeness.

The results of our synthetic work on the bromination chemistry of non-α-tocopherols in apolar media (also in comparison with that of the α-congener) are presented, together with the products' analytical

data. The more complex reaction systems of β-tocopherol and δ-tocopherol (reaction at C-5/C-5a vs. reaction at C-7) were studied kinetically and computationally as well. Purely brominating conditions (elemental bromine in *n*-hexane) were chosen for this work, in contrast to halogenations in protic or aqueous solvents that allow oxidatively halogenating conditions (hypobromite) as well. The presence of such solvents is expected to change both the types of products formed and the product distributions. The isolation, purification, and unambiguous identification of the in vitro reaction products and intermediates provide a firm basis on which studies on the in vivo reactions with electrophiles can build.

Results and Discussion

Bromination of α-tocopherol **1** in aprotic media has been shown to proceed by a non-radical, two-step oxidation/ addition mechanism *via* the intermediate *o*-quinone methide (*o*QM) **6**, which combines with the hydrogen bromide produced in the first step (Figure 16).[67] The involvement of **6** has been comprehensively confirmed by trapping reactions, addition of competing nucleophiles, and spirodimerization in the absence of co-reactants.

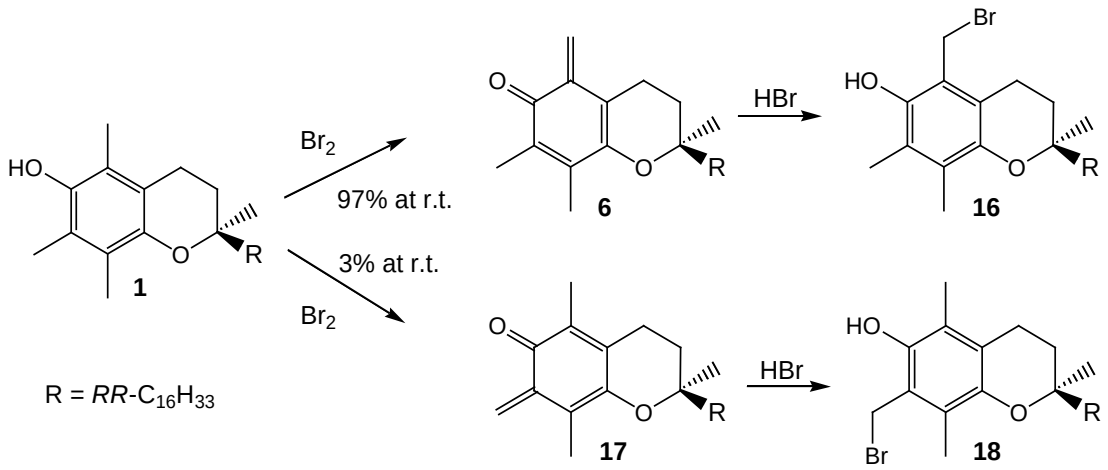

Figure 16: Bromination of α-tocopherol leading to 5a-bromo-α-tocopherol (16) as the main product, by a two-step oxidation/addition mechanism involving *o*QM (6).

The bromination product 5a-bromo-α-tocopherol (**16**) is a key starting material in tocopherol chemistry, being used, for instance, to introduce the Toc (5a-α-tocopherol) protecting group[68] or to produce a variety of 5a-substituted tocopherols. The bromination reaction provides 5a-*o*QM **6** and 7a-*o*QM **7** in an approximate 97:3 ratio at room temp. – and thus also the subsequent bromination products 5a-bromo-α-tocopherol (**16)** and 7a-bromo-α-tocopherol (**18**), respectively. The unusual regioselectivity has been explained by the theory of strain-induced bond localization (SIBL),[44] which predicts the ratio of the two *o*QM intermediates as a function of the annulation angle sum of the heterocyclic ring adjacent to the trimethylaromatic core. By and large, the bromination chemistry of α-

tocopherol and its mechanistic facets can be regarded as reasonably well established, and so shall not be discussed further here. A brief mechanistic summary is given in Figure 16.

Unlike that of the α-congener, bromination of the non- α-tocopherols had remained largely unstudied with regard both to mechanisms and to products, as mentioned above. In the case of β-tocopherol **10**, bromination is more complex than one would think at first glance. β-Tocopherol **10** and its truncated model compound **13** are each characterized by an unsubstituted aromatic carbon (C-7), which is also the position at which bromination predominantly occurs. The aromatic proton in **10** and **13** resonates at δ = 6.47 ppm in the ^{1}H NMR ($CDCl_3$).[54,69]

Two competitive initial reactions took place: bromination at the only available aromatic ring position C-7 to afford 7-bromo-β-tocopherol (**19**), together with bromination at C-5a analogously to the reaction of α-tocopherol, providing 5a-bromo-β-tocopherol (**20**). At –78°C, the former reaction dominated over the latter, with the product ratio of **19** and **20** being 85:15. At 333 K, the ratio had decreased to 72:28. However, as soon as the two primary oxidation products have formed and excess bromine is still present, two subsequent reactions set in: bromination of 7-bromo-β-tocopherol at C-5a, and bromination of 5a-bromo-β-tocopherol at C-7. Both reactions lead to the same dibromide product (Figure 17): 5a,7-dibromo-β-tocopherol (**21**). There are therefore four parallel bromination reactions going on, which renders the product formation kinetics rather complex.

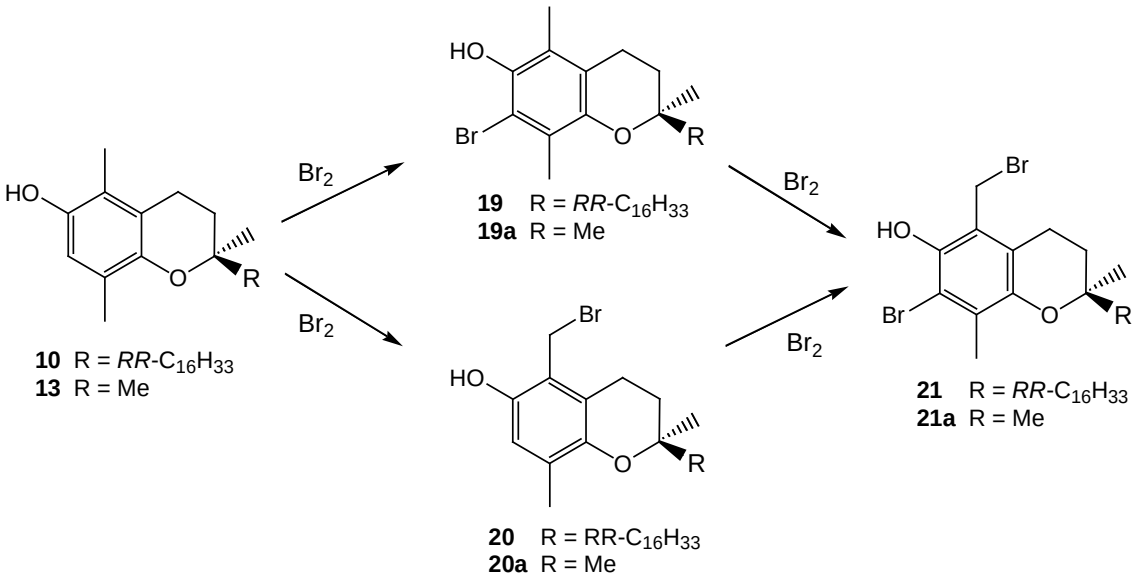

Figure 17: Bromination of β-tocopherol (10), leading to 5a-bromo-β-tocopherol (20) and 7-bromo-β-tocopherol (19) and further to 5a,7-dibromo-β-tocopherol (21). The reactions proceed analogously with the truncated model compound 13.

The two mechanisms leading to either monobromination product are quite different: bromination at C-7 is an electrophilic aromatic substitution, whereas the reaction at C-5a proceeds by a two-step oxidation/addition mechanism, analogously to the bromination of α-tocopherol. The ratio (*r*) between the two bromination products is determined by the activation energy difference (ΔE_A) between the two

rate determining steps of the corresponding pathways, according to Equation (1). For the bromination at C-5a this is the formation of the intermediate *o*-quinone methide – or more precisely the hydride abstraction from C-5a leading to that *o*-quinone methide.[44] For bromination at C-7, the rate-determining step is the formation of the intermediate σ complex with a cyclohexadienol structure. Although the activation energy difference between the two reactions is readily but rather approximately provided by the product ratio (*r*) of the two possible products N_1 and N_2 at a certain temperature as in Equation (1), it can more reliably be obtained by regression analysis of temperature dependence versus product ratio: that is, from the slope ($-\Delta E_A/R$) in a plot of ratio *r* against $1/T$. With a ΔE_A value of 2.61 kJ mol^{-1} (Figure 18) it was evident that the electrophilic substitution to form 7-bromo-β-tocopherol **19** was the preferred process over the competitive formation of monobromide **20**.

$$r = N_1/N_2 = \exp(-\Delta E_A/RT) \qquad (1)$$

Equation (1) and the regression plot can be analogously applied to calculate the activation energy difference between the two bromination reactions leading to dibromide **21**, by subjecting an equimolar mixture of the two monobromides **19** and **20** to bromination treatment. No product ratio can be determined, of course, because both processes form the same final product **21**, but it can be derived from the ratio of remaining starting materials, because both bromination reactions proceeded quantitatively and without formation of byproducts. In this way, the activation energy difference between the brominations of **19** and **20** to form the dibromide **21** was determined to be 28.18 kJ mol^{-1} (Figure 18). The activation energy difference this time was significantly larger, indicating either that the presence of the Br substituent at C-7 retarded further bromination at C-5a or that the presence of the bromine substituent at C-5a facilitated further bromination at C-7 (or both effects at the same time). It seemed reasonable to assume the first case: bromination directly on the aromatic ring could easily influence the electron density and thus the oxidation potential of the phenolic system in a way that oxidation to the corresponding *o*quinone methide – the intermediate en route to the 5a-bromide – would be more difficult, whereas bromination at C- 5a should have only a small influence on the electron density of the aromatic system and thus the bromination rate at C-7. However, acquiring a definitive answer was only possible by experiment.

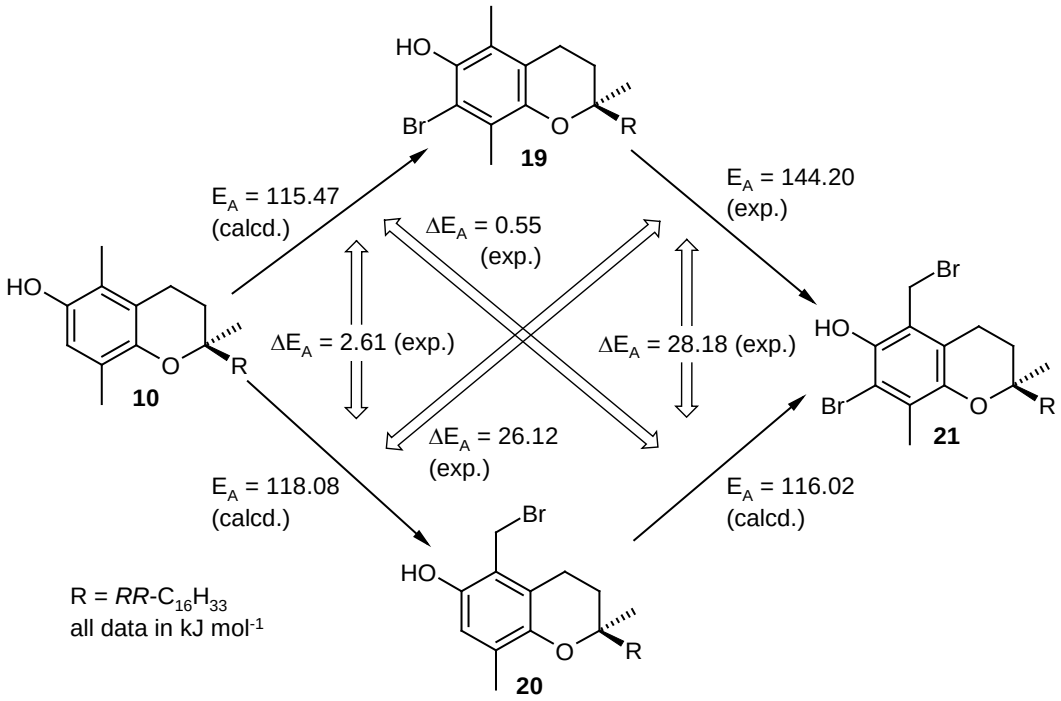

Figure 18: Bromination system of β-tocopherol (10): activation energy differences (ΔE_A) taken from kinetic measurements [temperature dependence of the product ratio, according to Equation (1)].

Activation energies (E_A) have either been determined kinetically (bromination of **9** to **11**) or have been calculated from the ΔE_A values.

We thus used an equimolar mixture of β-tocopherol **104**) and 7-bromo-β-tocopherol **19**, which both undergo bromination at their respective C-5a atoms, in the bromination reaction, and the overall conversion was kept below 5%. At those low degrees of conversion, the two starting compounds are always present in large excess over the reaction products so that it can be approximated that bromine is only reacting with starting **10** and **19**, but not with the newly formed monobromides to afford the dibromide. At higher degrees of conversion the consumption of bromine by the just generated monobromides can no longer be neglected without introducing significant errors. The amounts of consumed β-tocopherol **10** and consumed 7-bromo-β-tocopherol **19**, again determined at different temperatures, correspond to the amounts of the bromination products 5a-bromo- β-tocopherol **20** and 5a,7-dibromo-β-tocopherol **21** – if it is kept in mind that the 7-bromo derivative **19** is not only consumed by bromination, but is also newly generated from **10**. The ratio of the formation of **19** or **20** from **10** as determined above can readily be used to correct the consumption value of β-tocopherol for the part that is converted into the 7-bromo derivative. From the large activation energy difference obtained – 26.12 kJ mol^{-1} (Figure 18) – it was evident that bromination of β-tocopherol to afford the 5a-bromo compound **20** proceeds much more readily than the analogous 5a-bromination of **19** to give **21**. The introduction of the bromo substituent at C-7 of the aromatic ring thus evidently altered the electron density and oxidation potential of the phenol in such a way that the formation of the

corresponding *o*QM and further reaction to provide the 5a-bromo compound **21** was disfavored, verifying the first of the two alternative assumptions above.

In a similar way, bromination of an equimolar mixture of β-tocopherol **10** and 5a-bromo-β-tocopherol **20** at different temperatures was used to determine the activation energy difference for the electrophilic substitution at C-7. Calculation of the formation of **19** (from **10**) and **21** from **20** from the consumption of **10** and **20** provided the activation energy difference (0.55 kJ mol^{-1}; see Figure 18), which was rather small in relation to the values obtained above. Again, the consumption value for β-tocopherol was corrected for the competitive parallel reaction to afford the 5a-bromo derivative. This outcome demonstrated that the introduction of a 5a-bromo substituent as in **20** had only a negligible effect on the electron density and bromination rate of the aromatic core. The four activation energy differences (ΔE_A) as obtained from the kinetics are summarized in Figure 18. From the experimentally determined activation energy of 144.20 kJ mol^{-1} for the bromination of **19** to **21**,[(a)] simple arithmetic allowed the actual activation energies (E_A) to be calculated from those differences. These values are also given in Figure 18, and provide an interesting overview of the kinetics of this system of bromination reactions.

Bromination of γ-tocopherol **11** is a straightforward reaction that affords the 5-bromide **22** quantitatively (Figure 19).[62] γ-Tocopherol **11** and its model compound **14** each possess one free aromatic ring position, like the β- isomer, but this time it is located at C-5. The NMR resonance of the aromatic proton is found at δ = 6.37 ppm ($CDCl_3$).[54,69] In the case of the truncated model compound **14**, bromination provided product **22a** as colorless crystals suitable for X-ray structure determination (Figure 19). In crystalline **22a**, four chemically equivalent but crystallographically different molecules are contained per monoclinic unit cell (space group *P*21/*c*). All OH hydrogens form intramolecular H-bonds to the bromine, and two OH hydrogens exhibit bifurcated H-bonds to neighboring hydroxy groups.

It was interesting to see that the bromination product **22** was completely inert towards further bromination at C-7a. Whereas in the case of α-tocopherol C-7a showed some minor reactivity (cf. Figure 16), in the case of γ-tocopherol this position was completely inert, giving no sign of the hypothetical 7a-bromo-γ-tocopherol (**23)** or 5,7a-dibromo- γ-tocopherol (**24)**. The absence of 5,7a-dibromo-γ-tocopherol can be explained by the electronic effects of the bromo substituents directly on the aromatic ring on *o*QM formation, as seen already in the case of the bromination of 7-bromo-β-tocopherol **19** to afford 5a,7-dibromo-β-tocopherol **21** (*cf.* Figure 18). Although in the β-tocopherol case the 7-bromo substituent was not completely deactivating with regard to *o*QM formation and subsequent bromination at C-5a, the 5-bromo substituent in the γ-tocopherol case had an even more rigorous effect and apparently caused complete inertness of C-7a.

[(a)] The kinetic rate constants (k) were determined at -78, -40, -20, 0 and 22°C, and the activation energy E_A was calculated from the temperature dependence according to the Arrhenius equation

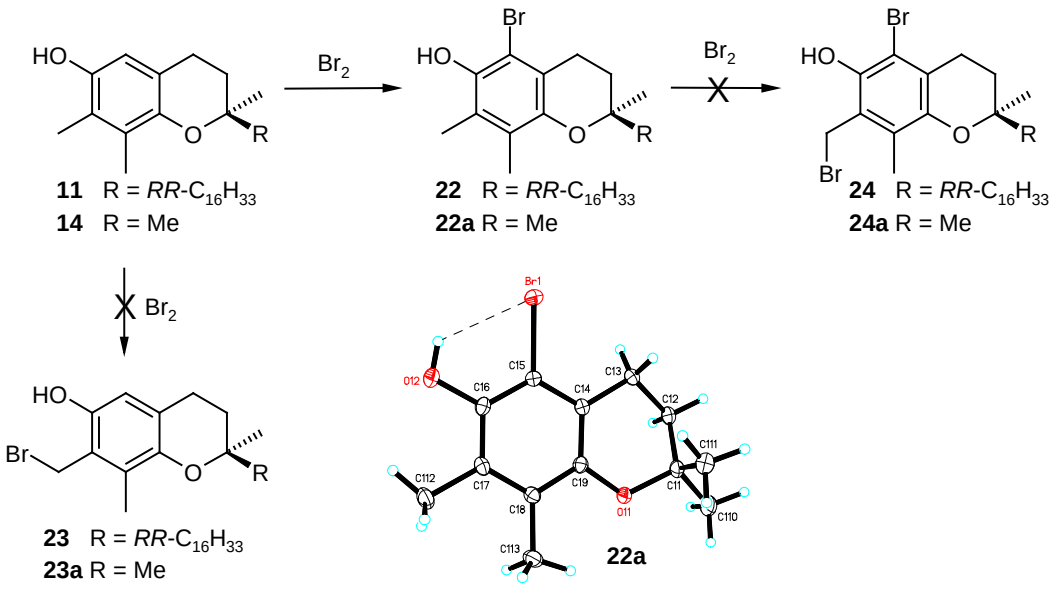

Figure 19: Bromination of γ-tocopherol (11), affording 5-bromo-γ-tocopherol (22) as the only product. The hypothetical species 7a-bromo-γ-tocopherol (23) or 5,7a-dibromo-γ-tocopherol (24), formation of which could be imagined by analogy to the bromination chemistry of α-tocopherol (Figure 16) and β-tocopherol (Figure 17), are not observed. The reactions proceed analogously with the truncated model compound 14, giving the bromination product 22a, a crystal structure of which (thermal ellipsoid plot, 40% ellipsoids) and crystallographic atom labeling are given.

The deactivating effects of aromatic bromine substituents cannot, however, explain why no 7a-bromo-γ-tocopherol **23** was observed, because in **11** no deactivating Br is present. The only structural difference between γ-tocopherol **11** and α-tocopherol **1** is the "missing" methyl group at the C-5 position in the former compound. One can therefore hardly evoke strong electronic effects to explain why the latter compound is (at least moderately) reactive at C-7a whereas the former is not reactive at all at this position. Furthermore, because *o*-quinone methide formation in tocopherol-type antioxidants is dependent on the annulation angle of the heterocyclic ring,[69] it was logical also to assume that reason for the differing oxidation/bromination behavior. However, the annulation angles of **3** and **1** are identical to the second decimal according to computations on the DFT level, so different strains imposed by the substituents and annulated heterocycle also had to be excluded as a rationale. Moreover, no differences in the zwitterionic transition states that lead from **11** or **1** to the corresponding C-7a-*o*-quinone methides could be found. At present, no satisfactory explanatory statement for the difference in the reactivities at C-7a of α-tocopherol **1** and γ-tocopherol **11** can be given.

Bromination of δ-tocopherol **12** – carried out as for the other tocopherols under aprotic apolar conditions – was somewhat more complex than that of the γ-congener, and thus comparable with the non-trivial β-tocopherol case (Figure 18). δ-Tocopherol **12** is the only tocopherol with more than one free aromatic position: both positions *ortho* to the phenolic hydroxy group, C-5 and C-7, are

unsubstituted.[70] The aromatic protons resonate at δ = 6.30 and 6.38 ppm in the ^{1}H NMR ($CDCl_3$) with a coupling constant of 2.9 Hz.[54]

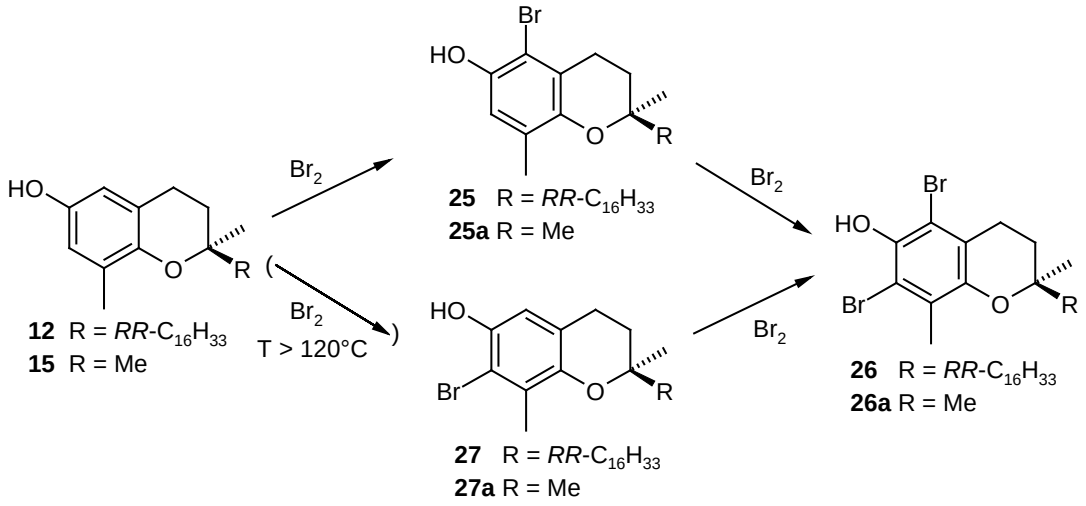

Figure 20: Bromination of δ-tocopherol (12), leading to 5-bromo-δ-tocopherol (25) and 5,7-dibromo-δ-tocopherol (26). 7-Bromo-δ-tocopherol (27) can only be obtained in small amounts at elevated temperatures. With the truncated model compound 15 the reactions proceed analogously.

At –78°C, bromination of δ-tocopherol provided quantitative yields of 5-bromo-δ-tocopherol (**25**, Figure 20). This outcome was independent of the amount of bromination agent used: even with a large excess of bromine only this monobromination product was obtained. At room temperature and with one equivalent of bromine, yields of **25** were still well above 80%, but in addition the dibromination product 5,7-dibromo-δ-tocopherol (**26**) was formed along with some 7-bromo-δ-tocopherol (**27**). With two or more equivalents of bromine, quantitative formation of **26** was achieved either after prolonged reaction times (12 h) or within 2 hours at elevated temperatures (60°C and above). Independently of the amount of bromine present, the yields of **27** – if found at all – were always very low (<3%), indicating that its further bromination to dibromide **26** was preferred over the bromination reaction leading to it. As soon as it was formed it would be immediately consumed again in the second bromination process.

Apparently, C-5-monosubstitution had not a deactivating, but rather a weak activating effect on the second substitution at C-7, although the difference was not very large. With equimolar mixtures of 5-bromo-δ-tocopherol **25** and δ-tocopherol **12**, the former was consumed with slight preference. With 1 equiv. of bromine at room temp., for instance, 53% of **25** and 47% of **12** were converted into the corresponding bromides.

Kinetic measurements for the δ-tocopherol bromination system were carried out similarly to the β-tocopherol scenario, by measuring the product ratios or the corresponding consumption of starting materials as functions of the reaction temperature. The resulting activation energy differences (ΔE_A) are shown in Figure 21. From those values and from the experimentally determined activation energy

for the bromination of **25** to afford **26** (E_A = 164.3 kJ mol^{-1}), the activation energies for the other bromination steps in the system were derived.

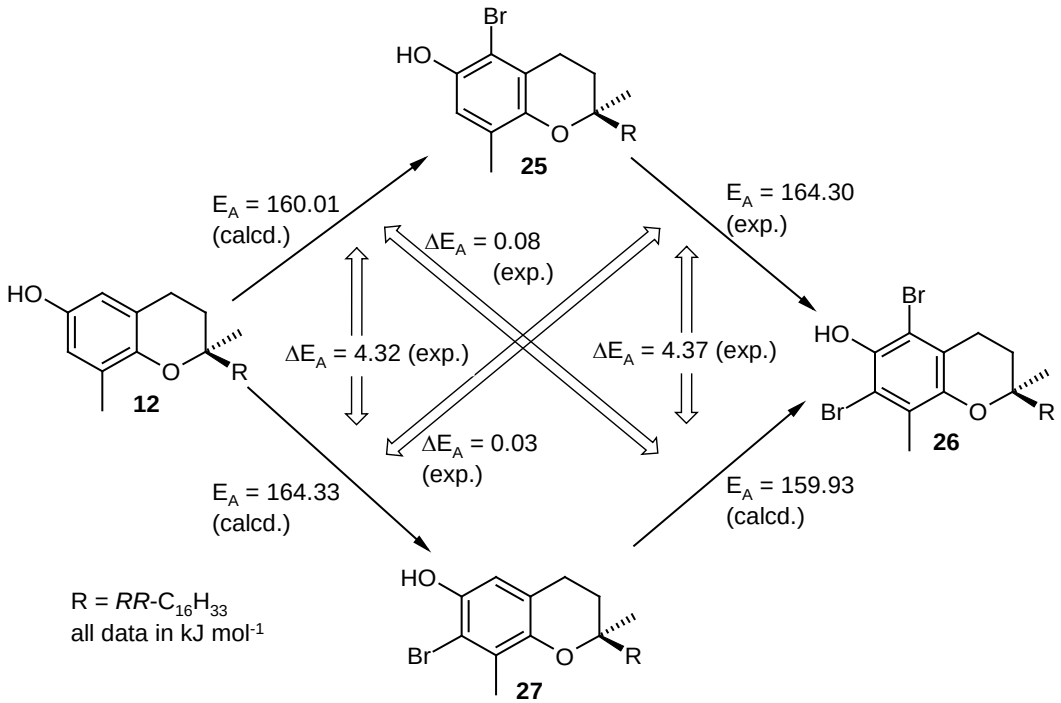

Figure 21: δ-Tocopherol (12) bromination system: activation energy differences (ΔE_A) taken from kinetic measurements [temperature dependence of the product ratio, according to Equation (1)]. Activation energies (E_A) were either determined kinetically (bromination of 25 to afford 26) or calculated from the ΔE_A values.

It was intriguing to see that below temperatures of about –20°C there was a clear preference with regard to bromination at C-5 versus at C-7: monobromination of δ-tocopherol occurred predominantly at C-5 and much less so at C-7, with only a 7% yield of **27** being formed at –40°C and a 13% yield at –20°C. Formation of the C-7 bromination product **27** could only be enforced by applying rather drastic reaction conditions (120°C), but yields were still as low as 22% and compounds **25** and **26** dominated (Figure 20). At a first glance, there was no obvious reason for such regioselectivity: the two *o*-positions in **12** have no obvious differences with regard to electronic effects, spatial conditions, or steric hindrance. The C-7 position, with a neighboring rotating methyl group (C-8b), would even appear slightly more easily accessible than the C-5 position, with its inflexible heterocyclic methylene neighbor (C-4). Neither can thermodynamic reasons be evoked to explain the selectivity: the ZPE-corrected total energies of the 5-bromo derivative **25a** and the 7-bromo derivative **27a**, computed at the MP-2/6–31G(d,p)//B3LYP/6–31G(d,p) level of theory, differ only by 0.5 kJ mol^{-1}, which is almost within the computational error limit and would not translate into any experimentally noticeable preference of one position [cf. Equation (1)].

However, the observed preference for the C-5 position can be explained in terms of the stabilities of the primary bromination intermediates: the bromocyclohexadienyl cations or σ complexes (**28**, **29**,

Figure 22). The 5-bromo intermediate **28** was calculated to be 4.1 kJ mol^{-1} more stable than the corresponding 7-bromo counterpart **29**, a result that agreed well with the observed dominance of the 5-bromo product and the experimentally determined value of ΔE_A = 4.32 kJ mol^{-1}.[(b)] The theory of strain-induced bond localization (SIBL) can readily clarify the preference for **28** over **29**. Recently applied to the case of the frequently observed preference for the α-tocopherol-derived 5-*o*-quinone methide (the "up"-*o*QM) over the isomeric 7-*o*-quinone methide (the "down"-*o*QM),[44] the theory can be analogously applied to the bromination intermediates. Both **28** and **29** can be regarded as quinoid systems, so the same argument as used for those *o*-quinone methides can be applied to these bromocyclohexadienyl cations. In short, the stabilities of the intermediates (no matter whether they are *o*QMs or the bromination intermediates **28** and **29**) are governed by the sums of the annulation angles of the heterocyclic rings. For tocopherols and other 2,2-dialkyl-substituted chroman-6-ol derivatives, these annulation angle sums are approx. 242°. This translates into a theoretical ratio of 97:3 between the two possible *o*QMs of α-tocopherol (at C-5a and C-7a) at room temperature, and exactly this ratio was found experimentally. For the bromination of δ-tocopherol (**12**), the computationally predicted ratios of the two isomeric bromination intermediates **28** and **29** were 92.6:7.4 in favor of the 5-bromo compound at –78°C and 77.8:22.2 at 120°C. Experimentally, the yields of 7-bromo compound were <3% at –78°C and 20% at 120°C, which seem to represent a satisfying overall agreement between computation and experiment.

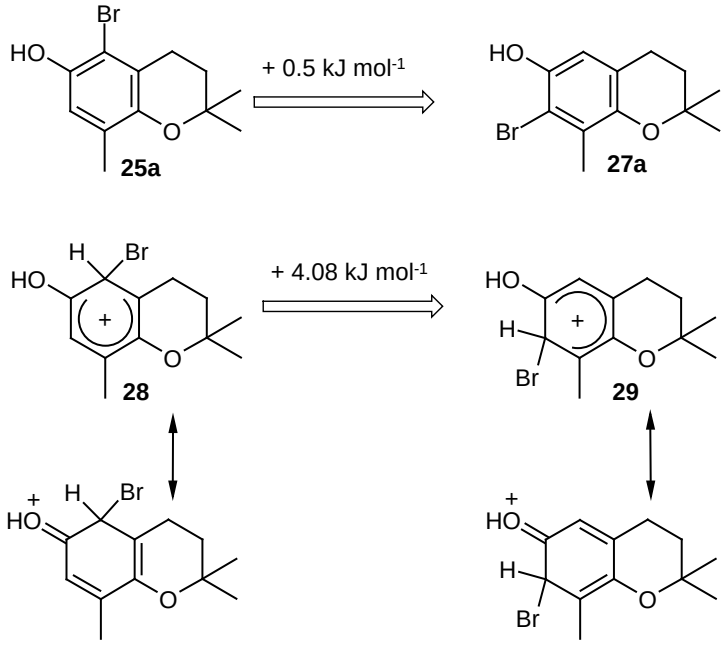

Figure 22: Calculated ZPE-corrected energy differences between 5-bromo-δ-tocopherol model 25a and 7-bromo-δ-tocopherol model 27a, and between the two σ complexes (28, 29) leading to them.

[(b)] It should be noted that whereas absolute computational values for E_A can show relatively large deviations from the experiment even at higher levels of theory, the relative values ΔE_A are quite reliable because systematic errors are largely cancelled out

Conclusions

The bromination chemistry of the three non-α-tocopherols in polar media has been established and compared to that of α-tocopherol. β-Tocopherol and δ-tocopherol each afforded three different bromination products depending on the conditions, whereas γ-tocopherol formed only a single bromination product. All products were fully purified and comprehensively characterized, not only for the tocopherols themselves, but also for the truncated model compounds carrying a methyl group instead of the isoprenoid side chain. A complete set of reference compounds and analytical standards for the bromination products of the tocopherols is now available.

Oxidation Chemistry of Tocopheramines

Introduction

One of the most prominent features of tocopherol is its phenolic hydroxy group. It is the molecule´s most reactive position and crucial for its antioxidative power. Removal or blocking of this group virtually eliminates the antioxidative properties of the molecule, since none of the oxidation intermediates (hydroxyl radical, chromanoxylium cation and *ortho*-quinon methide) can be formed (Figure 23).

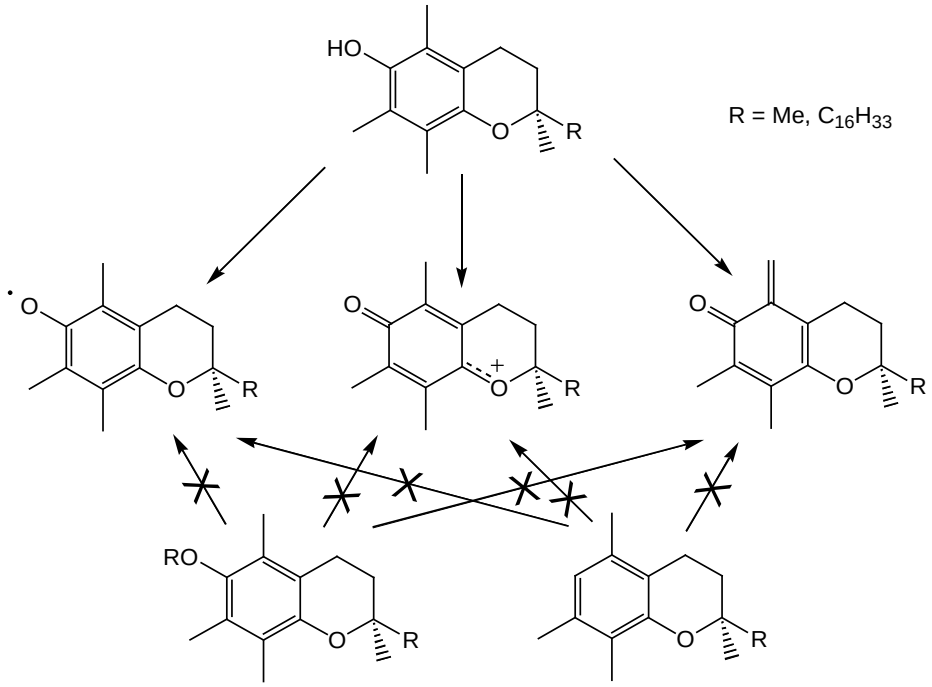

Figure 23: Unsubstituted Tocopherol can generally be oxidized to the chromanoxyl radical, chromanoxylium cation or *ortho*-quinone methide. Blocking the phenolic hydroxyl group by esterification or etherification or completely removing it prohibits these reactions.

Obviously, the electron-rich – and thus readily oxidizable – phenolic system is a prerequisite for the typical oxidation reactions of tocopherol. Equally important for the common oxidation chemistry of tocopherols is the possibility to remove the hydrogen of the phenol group. This is mostly done in the form of a proton, but also a hydrogen atom transfer can be seen as a consecutive transfer of a proton and an electron. If there is no hydrogen that can be separated by an oxidant, oxidation to the three main oxidation intermediates simply does not occur.

But how would the characteristics of tocopherols change, if the oxygen was replaced by a different atom that has an altered electronegativity and more hydrogens to release? An atom that could therefore be substituted and still had a hydrogen to spare? The examination of tocopheramines (Figure 24), a

rather old and severely neglected class of tocopherol analoga that has regained increased attention only recently, might answer some of these questions.

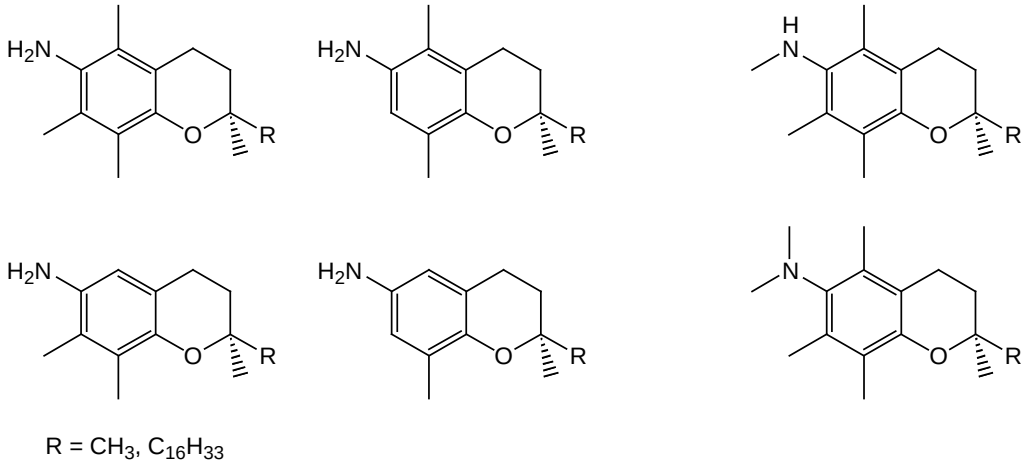

Figure 24: Tocopheramines studied in the course of this project.

Previous Research on Tocopheramines

The first synthesis of α-tocopheramine was done with an intention altogether different from mechanistic studies. Dissatisfied with the inability to obtain crystalline or at least solid tocopherols, Smith *et al.* synthesized the hydrochloride of α-tocopheramine by condensation of a formylated aminophenol prepared by diazotation and phytol derivatives (Figure 25).[71] Although this hydrochloride was still not crystalline, it could be decomposed to tocopherol and tocopheryl quinone and – most importantly – proved to be able to cure vitamin E-depleted rats. Twenty years later Schwieter *et al.* investigated the biological activity in more detail.[72-76] They found out that the activity of α-, β- and γ-tcopheramine was equal to that of the original tocopherols. Surprisingly, *N*-methylation of the amine gave five times more potent β-, and γ-derivatives and virtually deactivated α-tocopheramine. Inactivation was also observed after ethylation and dimethylation of the tocopheramines, the latter case being equivalent to etherification of a regular tocopherol. Since both tocopheryl ethers and dialkylated tocopheramines lack an abstractable hydrogen, they cannot be oxidized easily any more to quinoid intermediates or products. Because Schwieter *et al.* were actually searching for more potent vitamin E derivatives that could be used commercially, they filed patents for the industrial synthesis of tocopheramines as well.[77,78]

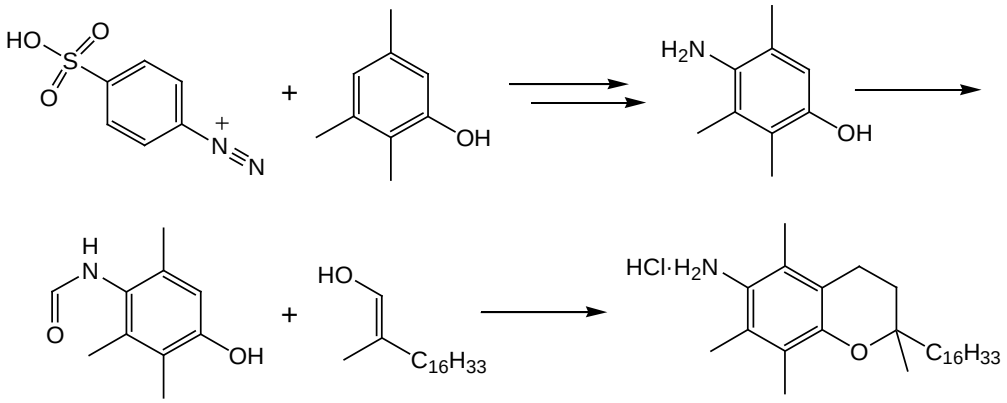

Figure 25: The classical synthesis of tocopheramines: 2,3,5-Trimethylphenol is aminated with the diazonium salt of sulfanilic acid, *N*-formylated, and eventually joined with isophytol to give α-tocopheramine.

During the following decades, the focus of research was generally directed on tocopheramines as *in vitro* antioxidants.[79] Tocopheramines remained a specialized but intriguing field of research. Their outstanding vitamin E activity was unique to all tested antioxidants, and analyses of the metabolites gave sufficient proof that the tocopheramines were not converted to the tocopherols *in vivo* but were the active compounds themselves.[73] Additionally, the high potency of *N*-methyl-β-tocopheramine and *N*-methyl-γ-tocopheramine showed for the first time that permethylation of the aromatic ring was not a prerequisite for full vitamin E activity. Of course the researches suspected the shape and the size to be an important factor,[72] but evidently the precise action of tocopherol and tocopheramines is still not understood.

Research on tocopheramines faded during the following decades, until suddenly the chemotherapeutic potential of tocopheramides was discovered.[80-84] Esters of tocopherol were already known to have high anti-proliferative activity against several cancer cell lines and to display limited toxicity against healthy cells. This knowledge was of limited use, since tocopheryl esters are readily cleaved during digestion, an effect that allows the use of the oxidatively stable tocopheryl acetate as food additive. In contrast to the ester, amide bonds are usually very stable against enzymatic cleavage and could be absorbed unaltered in the intestinal tract. Of course this problem would have been solved by intravenous administration or the use of tocopheryl ethers or alkylated deoxytocopherols as well, but the amides displayed in general higher potency.

A survey of tested tocopherol derivatives (Figure 26) reveals following structure-activity relationships: The lipophilic tail of the molecule is essential. Replacing it with more polar moieties to increase hydrophilicity to obtain a more soluble drug completely eliminates the apoptotic effect. Shortening the tail by one isoprene-unit increases potency a little, and application of the unsaturated chain of tocotrienols also results in a useful drug. The methylation pattern of the chromane has also some influence on the effect. α-Tocopheryl esters and amines are the most potent, followed by β-, γ- and δ-

derivatives. Surprisingly this order is reversed for the tocotrienols. The most important factor is the kind of acid that is used for the substitution of the tocopherol moiety. The introduction of a structure that can sustain a charge is definitely a prerequisite. Esters and amides of dicarboxylic acids are usually employed and show the greatest effect, but lysine derivatives that can stabilize an ammonium ion work as well. The oxalates, malonates and most prominent succinates all show high activity, although derivatives of unsaturated diacids as maleic acid or fumaric acid have even increased potency. Increased chain lengths (eg pimelic acid derivatives) and omission or blocking of the charge carrying moiety as in tocopheryl acetate or succinic acid methyl ester results in inactive compounds.

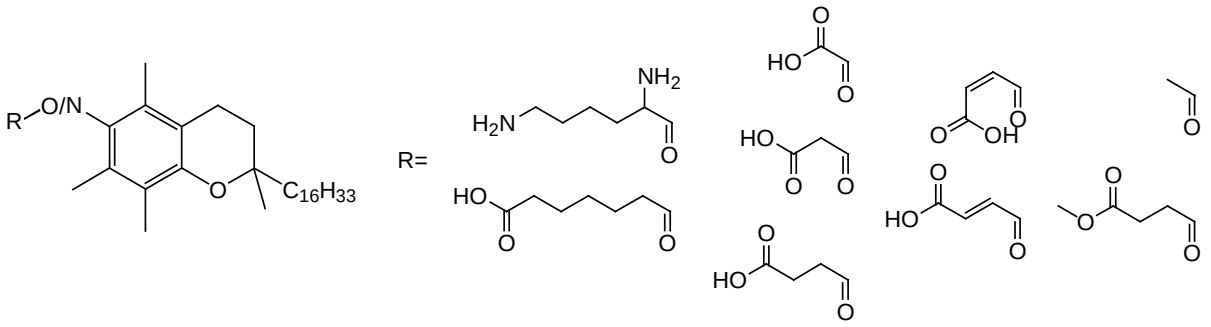

Figure 26: Tocopheryl esters and amides that have been examined for proapoptotic activity.

Why tocopheryl derivatives selectively trigger the suicide of cancer cells is not yet understood, but tocopheryl esters and amides change the conditions in mitochondria in a way that amplifies mitochondrial pathways that finally trigger the controlled apoptosis of the cancer cell. Effects in the mitochondria include direct molecule-enzyme interaction, change of membrane properties that result in relocalization of apoptotic mediators and changes in membrane potential.

Synthesis of Tocopheramines

In 2009 two modern syntheses of tocopheramines starting from tocopherols and tocotrienols were published almost simultaneously (Figure 27): Mahdavian *et al.*[85] and Mazzini *et al.*[86] both developed a palladium-catalyzed Buchwald-Hartwig[87,88] aryl amination, applying benzophenone imine or benzylamine as nitrogen source. The new methods feature not just higher yields of tocopheramines and are significantly shorter, but it became also possible to start from commercially available tocopherols and tocotrienols and obtain tocopheramines that retain the stereochemistry of the starting material.

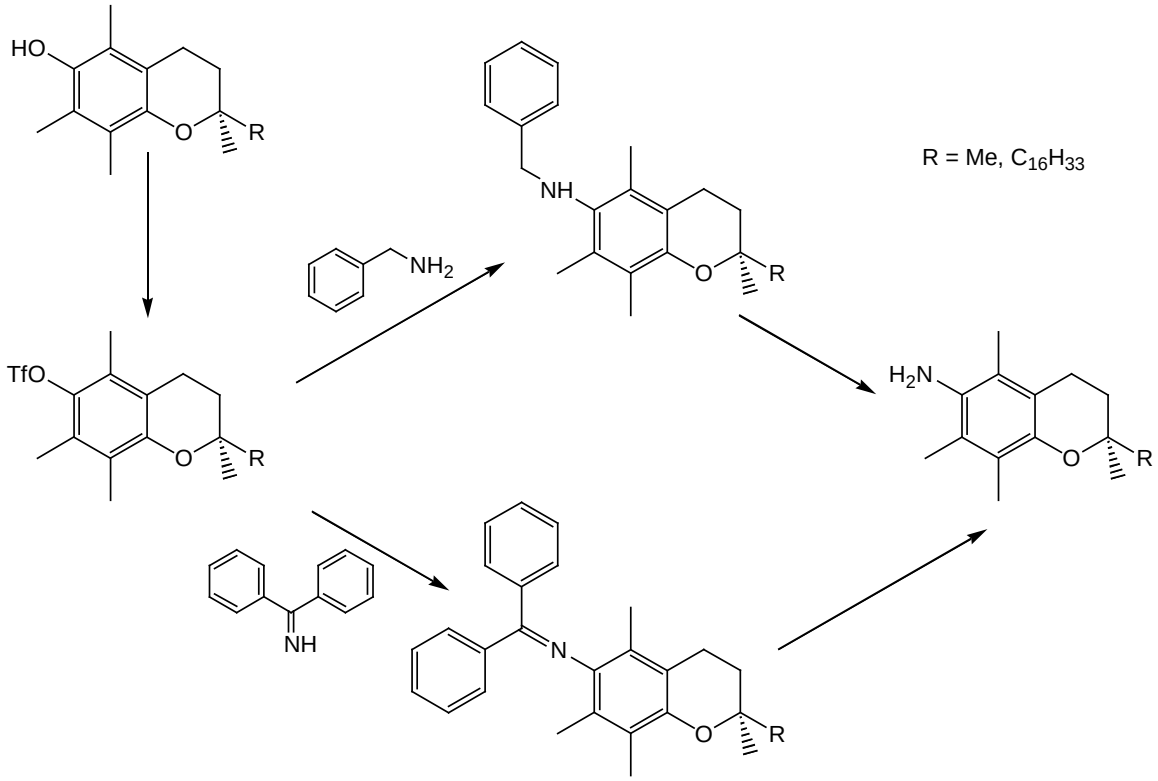

Figure 27: The modern synthesis of tocopheramines: Triflated tocopherols are coupled with either benzylamine or benzophenone imine as nitrogen source. Acidic hydrolysis yields the desired amine.

Synthesis of Tocopheramine Model Compounds

To better understand the behaviour of the rediscovered tocopheramines extensive knowledge on their physicochemical properties is fundamental. As with tocopherols, the application of truncated model compounds was considered to be benefitial. Additionally, special derivatives had to be prepared to study certain effects in greater detail. All in all a library of useful model compounds had to be established synthetically.

The most basic models are those of α-, β-, γ- and δ-tocopheramine having a truncated side chain (**30**-**33)**. Luckily the syntheses of the four tocopherol model compounds **4**, **13**, **14** and **15** have been well established in this research group, setting an excellent starting point for the synthesis of tocopheramine models according to the procedure by Mazzini *et al.* (Figure 28). Especially the challenging synthesis of δ-model has been devised very cleverly. Because of the low degree of methylation of the aromatic ring, application of the standard reaction with 2-methyl-3-buten-2-ol **34** would give great amounts of byproducts as a complex mixture. To avoid this inefficient step a different starting material was chosen to allow a more selective reaction, so that δ-model could be obtained after a final rearrangement step.[54]

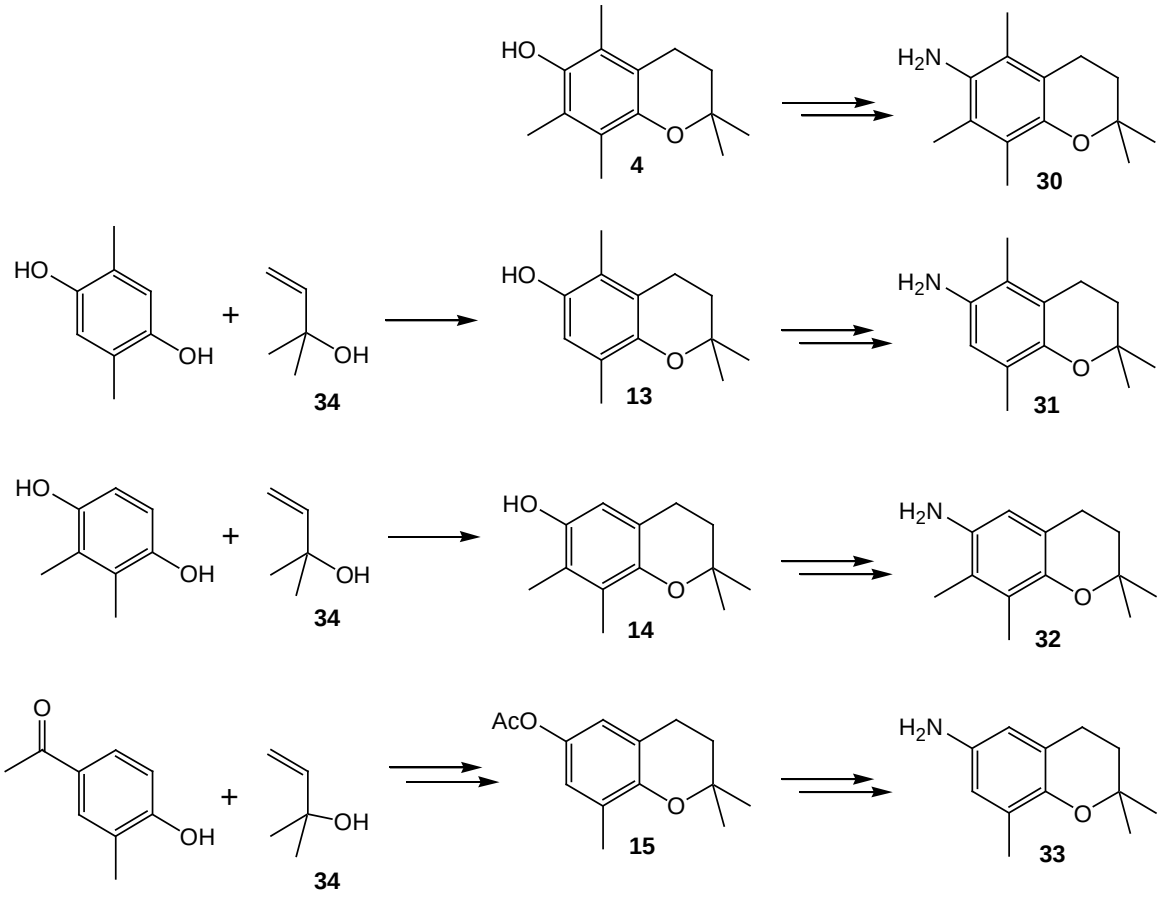

Figure 28: Starting from commercially available PMC or easily accesible model compounds all four tocopheramine models are readily available.

In the first stage of this three step synthesis (Figure 29) the hydroxy group was turned into a more convenient leaving group by triflatation. Quantitative conversion was achieved by a standard procedure. The next step consisted of the Buchwald-Hartwig amination developed by Mazzini *et al.* A racemic palladium-BINAP catalyst was used to exchange the triflic acid against benzophenone imine. Acidic hydrolysis yielded the desired tocopheramine model. The same general approach was applied to the synthesis of the corresponding non-α-tocopheroamine model compounds.

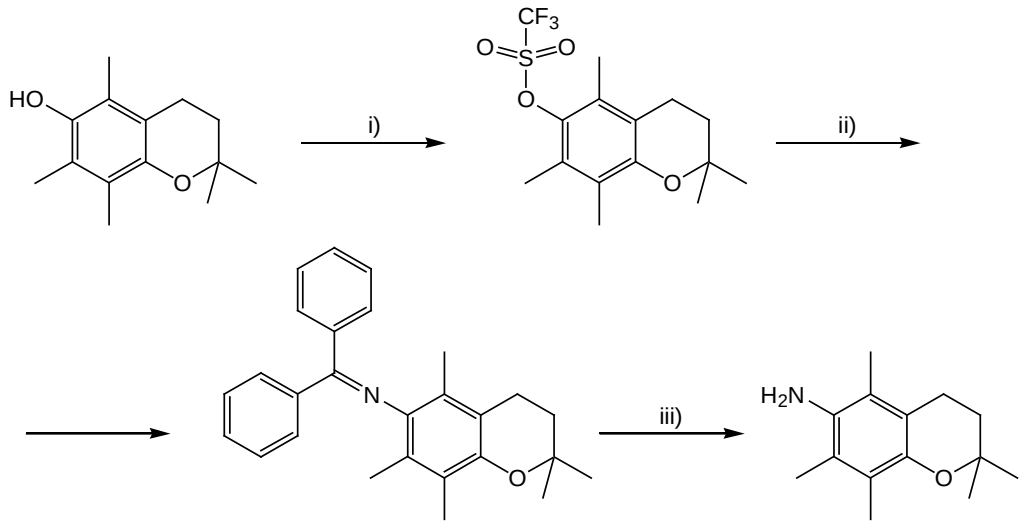

Figure 29: Synthesis of tocopheramine model compounds: i) Tf_2O, pyridine, DCM. ii) $Pd(OAc)_2$, BINAP, benzophenone imine, NaOtBu, toluene. iii) HCl, THF.

Synthesis of ^{15}N-Labeled α-Tocopheramine Model

ESR-spectroscopy was used to observe the behaviour of tocopheraminyl radicals. With this method the shape and pattern of the received signal is depending on the localization of the unpaired electron. The electron is interacting with the spins of the nuclei. Replacing the naturally dominant ^{14}N (S = 1) with ^{15}N (S = 1/2) would give an altered ESR-signal and thus allow deeper insight into the nature of the derived radicals. For this purpose the synthesis of the respective ^{15}N-labeled model compound was required.

For the synthesis of labeled ^{15}N-α-tocopheramine model (**35**) the aryl amination could not be employed, since neither ^{15}N-benzophenone imine nor ^{15}N-benzyl amine were readily available. After several experiments with diazotation corresponding approaches were abandoned due to dissatisfactory yields and tedious procedures. Eventually, ^{15}N-labeled nitric acid was chosen as the source of the nitrogen label, since it was not only rather cheap and readily available, but also offered a way for a straightforward and high-yielding synthesis (Figure 30). Generally the nitration of aromatic compounds might not be a method of choice, since it might proceed unselectively and nitric acid is a strong oxidant in itself, possibly causing plenty of side reactions. On the one hand, the danger of non-selective nitration is not posed in the present case, as 2,2,5,7,8-pentamethylchroman (**36**) has only one free position to offer. On the other hand, carrying out the reaction with acetic acid as co-solvent allows the formation of acetyl nitrate as an intermediate that is the actually active, but much more selective nitration reagent. It has to be noted, however, that acetyl nitrate is highly explosive and great caution has to be exercised during preparation, reaction, and workup. Unselective oxidation of the molecule could not be avoided however.

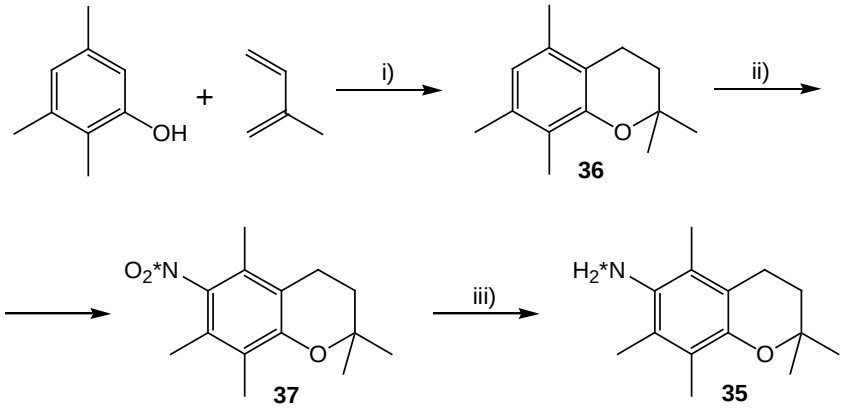

Figure 30: Synthesis of ^{15}N-labeled α-tocopheramine model (35). i) $ZnCl_2$, AcOH, Δ. ii) HNO_3, AcOH. iii) LAH, THF.

The synthesis of **36** was more demanding than expected: At first glance the reaction of trimethylphenol and isoprene seemed to be a straightforward variation of the established protocol, but only after several unsuccessful attempts gram-scale synthesis succeeded. The strict exclusion of humidity and the use of absolutely dry zinc chloride as catalyst proved to be crucial. Bulb-to-bulb distillation was sufficient to afford reasonably pure chroman, higher purities could be achieved by recrystallization from ethanol.

As mentioned before, nitration with nitric acid is not necessarily a selective reaction. For this reason, the reaction temperature was chosen to be as low as possible. Acetic acid was used as a co-solvent, and its freezing point is rather high (16°C). Naturally the reaction mixture started to freeze a few degrees below that temperature, but still the use of ice cooling was not an option. A cold water bath was used instead. Performing the nitration was quite simple: Stirring of the dissolved chromane in acetic acid and 10 M nitric acid for two hours gave 2,2,5,7,8-pentamethyl-6-nitrochroman (**37**). During the reaction the color changed from green to brown to finally black. Excessive acid was destroyed with sodium bicarbonate solution, and the crude product could be obtained by simple extraction.

To finally afford the target amine, reduction of **37** was necessary. After the use of diisobutylaluminium hydride, sodium hydrosulfite, sodium sulfite and hydration with different catalysts (palladium chloride, palladium acetate, palladium on activated carbon, Raney-nickel) and different hydrogen sources (hydrogen, hydrazine, triethylsilane, ammonium formate) had proven to be without effect, fresh lithium aluminium hydride (LAH) gave the desired result. The crude intermediate was dissolved in THF (dried over sodium), LAH was added and the mixture stirred over night. Aqueous workup and precipitation with hydrochloric acid solution in diethyl ether gave the salt of **35**.

Synthesis of *N*-Methyl- and *N*,*N*-Dimethyltocopheramine and their Model Compounds

To examine the oxidation behavior of mono- and disubstituted tocopheramines, *N*-methyl- and *N*,*N*-dimethyltocopheramine models were synthesized (**38**, **39**, Figure 31). If the phenolic group of tocopherol is blocked (e.g. by etherification), it loses its ability to be oxidized. To be able to test whether this holds true for the amino group of a tocopheramine as well, it is necessary to add two substituents to the amino group, thus removing all hydrogens from the nitrogen. Substitution of only one hydrogen atom and retention of the second hydrogen results in an interesting intermediate that is electronically less flexible than the free amine but still has some reaction potential – with regard to proton donation or abstraction – left. Methyl groups were chosen as substituents, since they are the simplest alkyl substituents and impose hardly any electronic and steric effects on the molecule,.

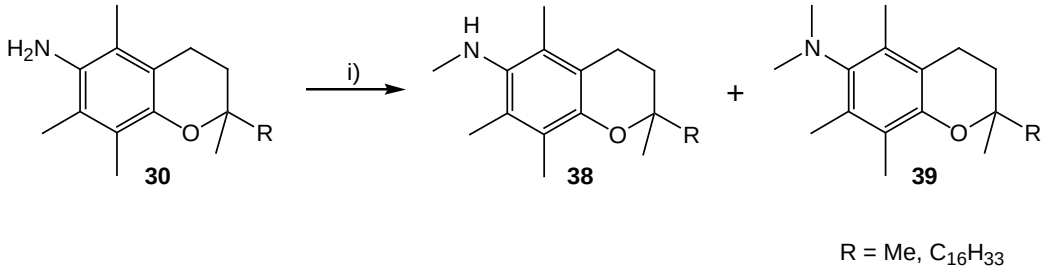

Figure 31:The reaction of tocopheramine (30) with 1.5 equivalents of methylating agent yields equal amounts of monomethylated (38) and bimethylated amine (39). i) MeI, NaOH, DMSO.

At first, selective monomethylation by reductive alkylation with formaldehyde was attempted. Due to the more facile procedure, a simple, unselective one-pot reaction was carried out in the end, that afforded both **38** and **39** simultaneously. The addition of 1.5 equivalents of iodomethane and sodium hydroxide as a base resulted in full conversion of the starting amine to give equal amounts of both derivatives. DMSO was used as solvent and could easily be removed by repeated washing with water. The retention times of the two products and the remaining traces of starting material were so different on a silica column (Figure 32), that purification was extremely simple. All in all, the unselective methylation of tocopheramine with 1.5 equivalents of iodomethane proved to be an excellent choice for the derivatization of both tocopheramines and tocopheramine models.

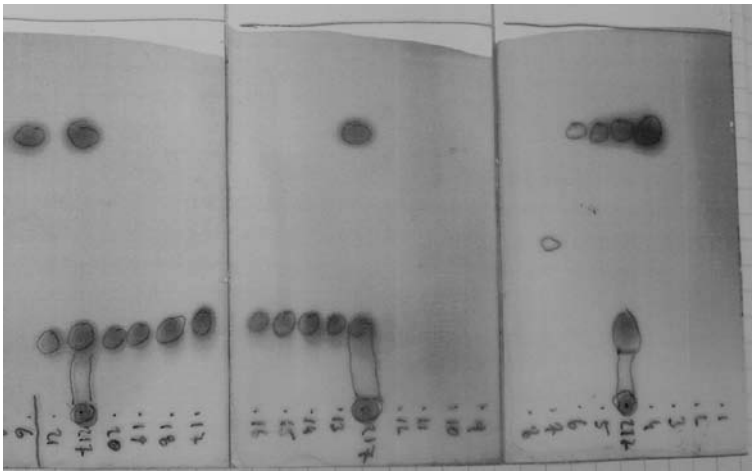

Figure 32: Chromatographic separation of *N,N*-dimethyl-α-tocopheramine model (39, lane 4-6) and *N*-methyl-α-tocopheramine (38, lane 13-21). 217 denotes the unpurified reaction mixture.

Electronic Spin Resonance (ESR) Spectroscopy[(c)]

Nuclear Magnetic Resonance (NMR) spectroscopy is a widely employed and extremely useful tool in organic synthesis. In principle, the magnetic nuclear spins of the nuclei of interest are first aligned by a magnetic field. Then electromagnetic radiation is used to reverse this alignment (excitation), and information about the sample is gained by observing which frequency triggered this reversal. But magnetic spin is not a property unique to nuclei, electron have magnetic spin as well. Therefore it was an obvious idea to measure the resonance frequency of electron magnetic spin as well, a spectroscopic method that is called ESR.[(d)]

ESR and NMR share a common principle: align nuclear magnetic spin to a magnetic field, irradiate it with the right wavelength, measure the frequency-dependent loss of intensity and learn something from that information. Both methods have developed to highly sophisticated techniques that make use of complex pulse sequences and can give multi-dimensional spectra. Despite the shared principle and seemingly similar information, ESR and NMR are fundamentally different in other areas. In contrast to NMR that can measure any substance as long as it contains the right kind of nucleus, with ESR the actual sample has to have an unpaired electron. This usually corresponds to a radical, if organic molecules are to be characterized. Radicals are usually highly reactive molecules with a very short life-span, making it a challenge in itself to generate a concentration of radical species sufficient for measurement. Also the number of signals greatly differs: an organic molecule is usually comprised of plenty of NMR-active nuclei, resulting in spectra with a corresponding amount of signals. On the other hand, organic radicals contain usually just one unpaired electron that gives just one signal in the ESR spectrum. And while in NMR most of the information is gained from the precise frequency of the signals (shift) and coupling patterns are of secondary value, the resonance frequency of different

[(c)] Quite a few introductory textbooks have been written about ESR. The most accessible for chemist without additional training in physics seems to be: Gerson, F., Huber, W. "Electron Spin Resonance Spectroscopy of Organic Radicals", Wiley-VCH, 2003.
[(d)] Because this method can be used for any paramagnetic substance, it is sometimes referred to as EPR, electron paramegnetic resonance.

organic radicals is almost always the same in ESR. The coupling pattern is abundant with information instead. For NMR strong static magnetic fields are used, and variation of the radiation frequency reveals the resonance conditions. ESR spectrometers operate at a set microwave frequency instead, and the strength of the magnetic field has to be varied while looking for resonance. For this reason, the appearance of the spectra is very different for both respective methods. NMR spectra give the positions of resonances as peaks rising from the baseline. ESR spectra usually display the first derivative of the absorption signal (Figure 33). And while NMR spectra can be simulated and explained reasonably well, the analysis of complex EPR spectra is still a challenge that requires skill, experience and involvement of computational chemistry.

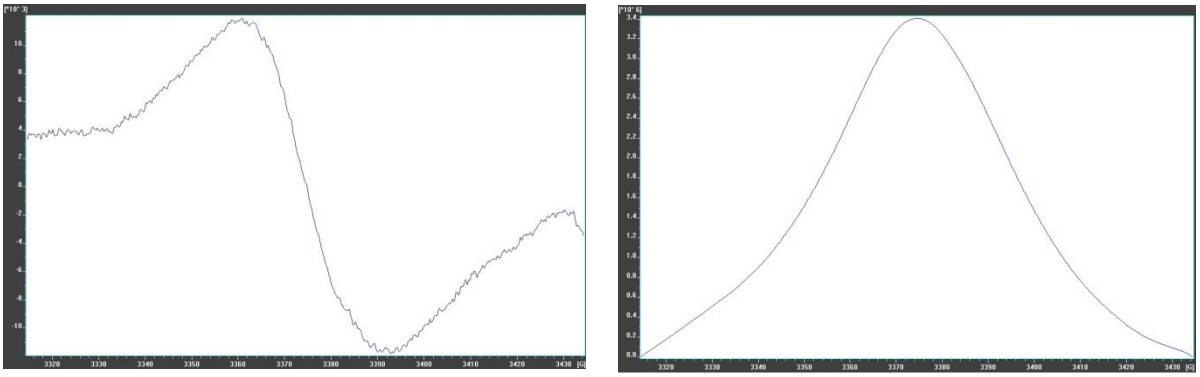

Figure 33: ESR results are typically presented as the first derivative of the recorded spectrum. The integral of the ESR-spectrum on the left gives the more familiar peak shape on the right.

To be a useful sample for ESR a substance has to be paramagnetic. Some metals (alkali metals and most of the rare earth metals) are innately paramagnetic. Organic molecules are usually diamagnetic – they are paramagnetic only if they have unpaired electrons. For some molecules a quantum state with two unpaired electrons might be favourable (for instance oxygen is a diradical in the ground state), other molecules have to have an electron removed or added to become radicals. The distribution of this single electron over the whole molecule is an important factor (Figure 34). Delocalized electrons that are spread over a large portion of the molecule give as a rule much more stable radicals than very localized electrons that reside at one defined atom.

Because the EPR-shift of different organic radicals is almost the same, the interesting information is contained in the coupling pattern of the signal. Coupling happens mainly when the magnetic moment of the unpaired electron is influenced by the magnetic moment of a nucleus. So it stands to reason that following factors govern the extent of the interaction (to be precise: the hyperfine coupling constant): the magnitude of the magnetic moment of the electron (which is alway the same), the magnitude of the magnetic moment of the nucleus (this depends on the nucleus) and the electron´s spin density at the nucleus (the more likely it is to locate the electron at the nucleus, the more likely is its interaction with the nucleus). The factors governing the magnetic moments are characteristics of the particles, while the spin density depends on the molecule and its environment. The most important information that is

usually obtained from an EPR experiment is about the distribution of the electron density in the molecule. Every nucleus that is part of the delocalized electron´s orbital contributes to the coupling pattern of the measured signal. Simple signals correspond to localized radicals, complex patterns are evidence of a highly delocalized electron.

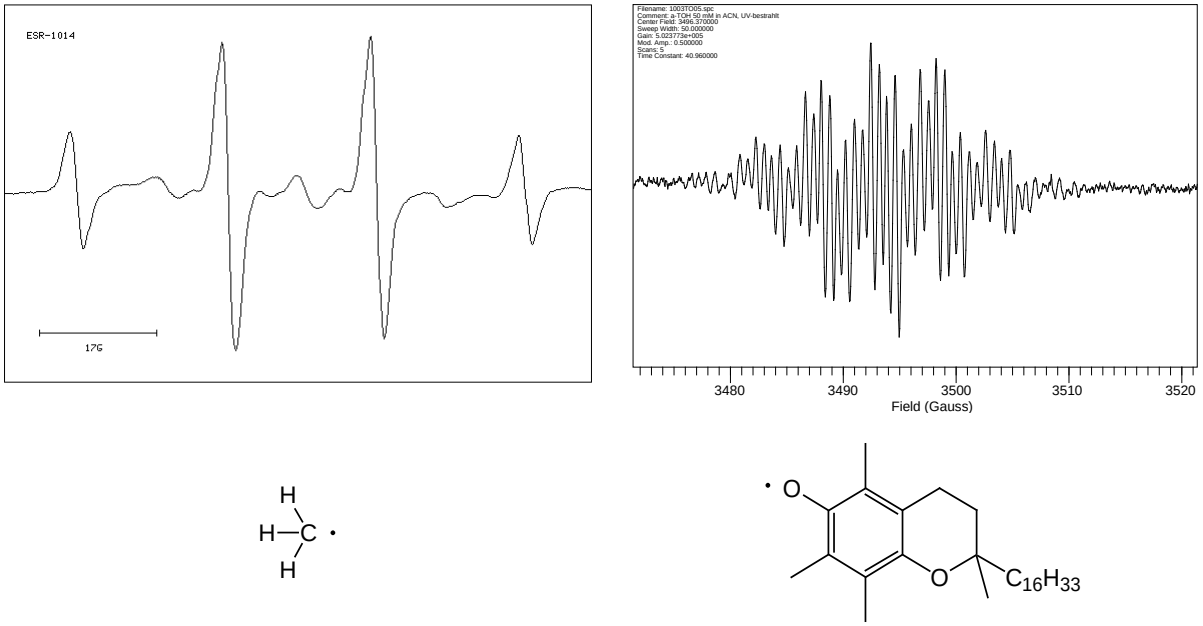

Figure 34: ESR-spectra can quickly become quite complex. On the left a spectrum of a methyl radical[89] is shown, on the right the spectrum of tocopheroxyl is presented. Interaction of the delocalized electron with various hydrogens results in a complicated but still symmetric coupling pattern.

The reason why the prediction of ESR-spectra is so difficult is simple: the electron density at the nuclei is the variable that has the greatest influence on the spectrum. The only experimental way to determine the electron density at the nucleus are X-ray diffraction (XRD) experiments on the crystalline radical. This is only possible in very rare cases. The other option is to use computational chemistry to calculate the spin density at the nucleus and to convert it into coupling constants. This is experimentally much less demanding, but suffers from the restrictions of the applied model.

The spin density and the magnetic moment of the electron cannot be changed, but the magnetic moment of the nucleus can: Isotopes of the same element usually have different magnetic moments and different nuclear spins. If an atom of the examined molecule is replaced by an isomer that naturally has different properties, the ESR signal will change. If it does not, the spin density of the electron at this nucleus is zero, which means that the unpaired electron is not located at this atom. If it is located at this specific atom, the coupling pattern of the signal changes. It is depending on the nucleus´ spin, and different isotopes have different spin. Thus the method of isotopic labelling allows more precise conclusions about the unpaired electron´s localization.

Results and Discussion

Oxidation Reactions of Tocopheramines

Since α-tocopherol shows a remarkably varied oxidation behavior depending on the chosen solvent, oxidation of tocopheramine was examined under both protic and aprotic conditions. In protic solvents as methanol or water, the α-tocopheramine model compound was quantitatively oxidized by iron chloride (Figure 35). The product was the same as the one that would have been obtained from PMC under these conditions: *para*-tocopheryl quinone. The first step of the oxidation was formation of the *para*-quinone imine, from which the amine component was released by a conventional hydrolysis process. NMR kinetic studies confirmed this mechanism. The corresponding byproduct of the unsubstituted tocopheramine was ammonia, the alkylated amines gave a primary and secondary amine, respectively. If unsubstituted tocopheramines were oxidized, the deeply red azotocopherol was found as a minor product as well.

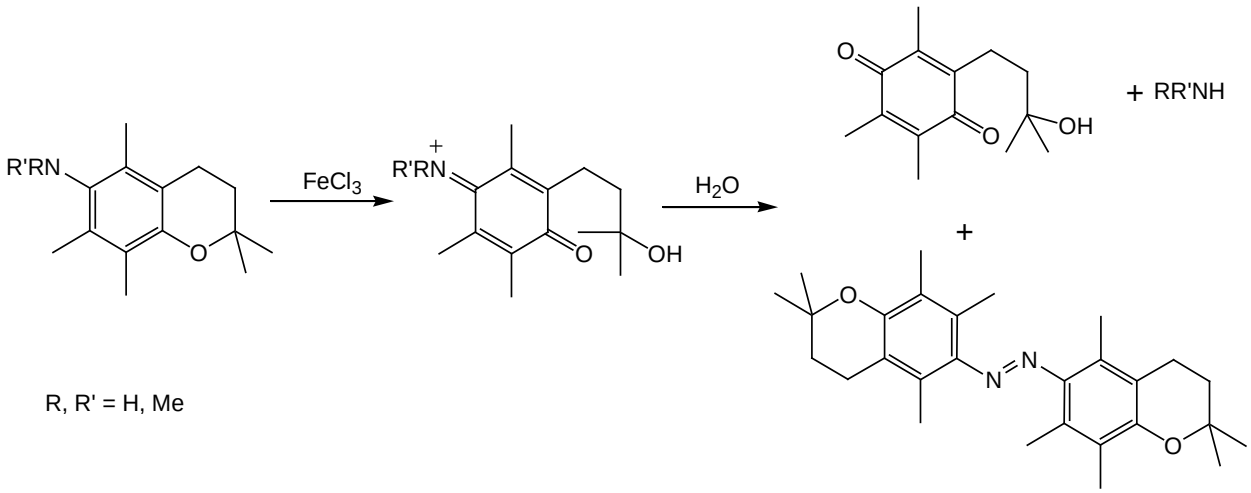

Figure 35: Oxidation of tocopheramines in protic media.

Oxidation in aprotic solvents yielded an *ortho*-quinoneimine methide (oQIM, **40**), the aza-analogue of the oQM (Figure 36). This was the first observation of such an intermediate in the chemistry of tocopherol-derived substances, and also in general quinone methide chemistry such derivatives are rather rare. Unlike the oQM, that can be trapped quantitatively in a hetero-*Diels Alder* reaction with ethylvinyl ether, the oQIM of unsubstituted tocopheramine model gives only 22% yield in this reaction. Trapping of the monomethylated tocopheramine model gives 77% yield, which is still quite far away from the quantitative yields obtained with oQM.

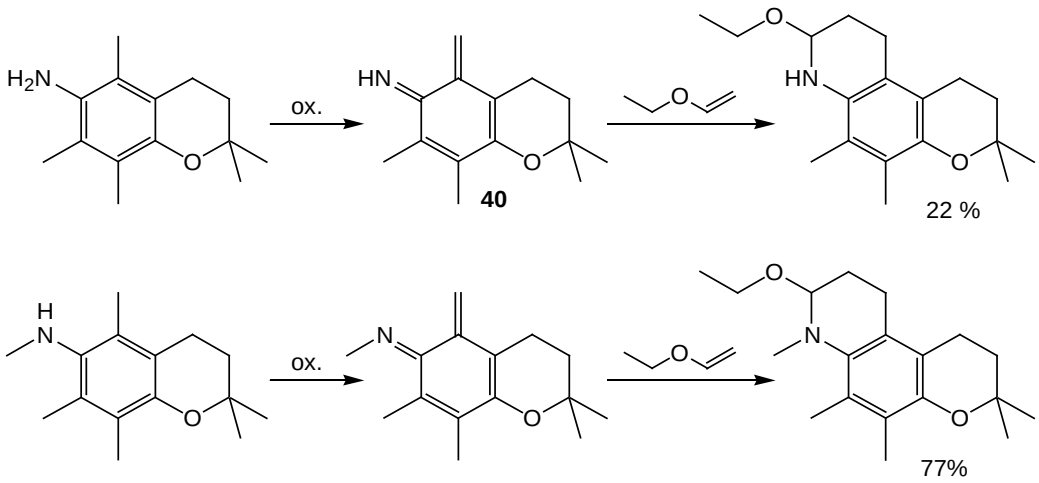

Figure 36:Aprotic oxidation of tocopheramine to oQIM. The oQIM is trapped with etyhlvinyl ether in significantly lower yields than the oQM of tocopherol.

Just as the oQM the oQIM is preceded by a zwitterion. It has been shown that in the case of tocopherols this intermediate can be stabilized by addition of another zwitterion, e.g. NMMO.[90] This stabilizing effect could not be observed with tocopheramine zwitterions (Figure 37).

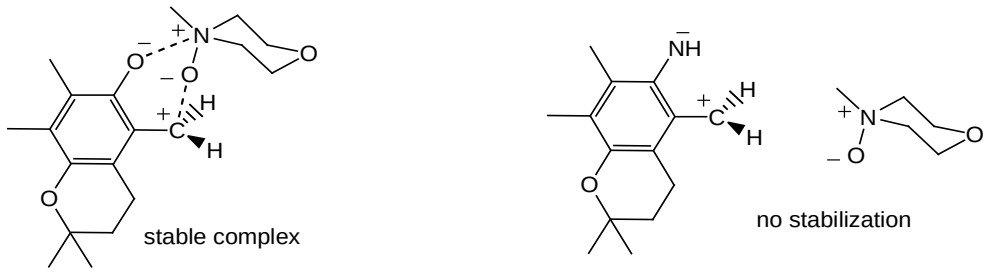

Figure 37: Stabilization of the intermediary zwitterion by NMMO. The stabilizing effect could not be observed starting from tocopheramines.

Analogous to the dimerization reaction of the oQM the oQIM **40** can react with another oQIM in a spiro-dimerization (Figure 38), which actually is a hetero-analogous *Diels-Alder* reaction with inverse electron demand. Apparently, the electronic conditions are less favorable for the amine case as compared to the case of "conventional" tocopherols since the reaction rate is lower for the former, and more byproducts are formed in addition. Although the spiro-dimer (**41**) resulting from the tocopheramine is very similar to the spiro-dimer of the oQM **8** with regard to its general chemical structure, its chemical behaviour is somewhat different. Reduction of **41** to the ethano dimer (**42**) is possible, but the re-oxidation to **41** does not proceed quantitatively but gives several byproducts. This means that these two substances can not be used as a reversible redox pair, as it is possible with the spiro-dimer of the oQM.

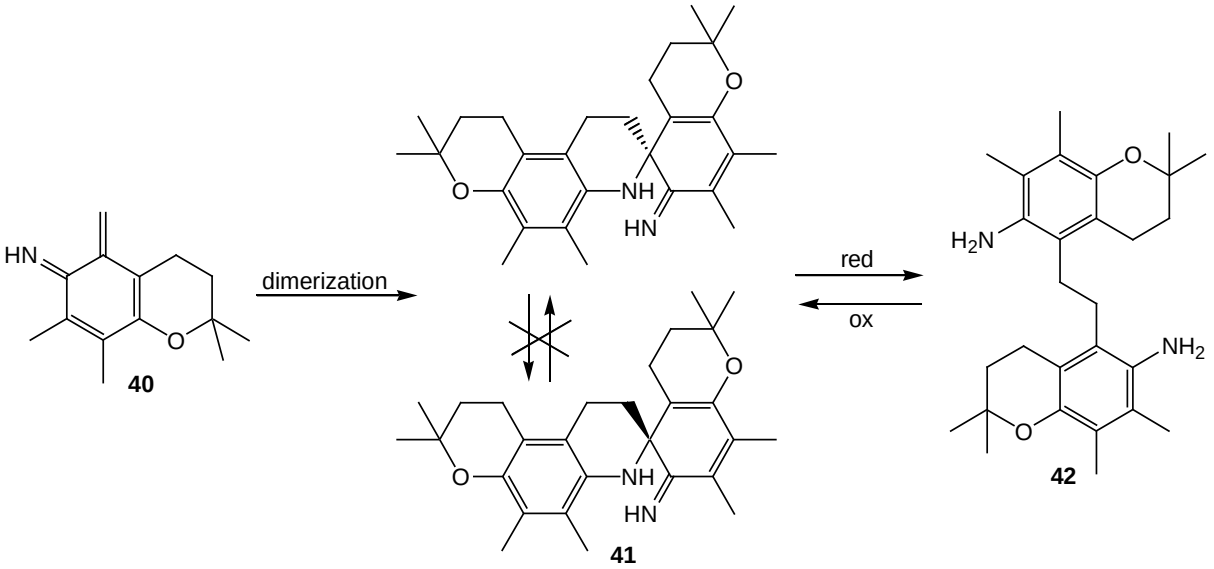

Figure 38: oQIM can be dimerized to a spiro-dimer (41). In contrast to the oQM-derived spiro-dimer (8) reduction to the ethano-dimer (42) and re-oxidation to the spiro-dimer do not proceed quantitatively, and the dimer´s enantiomers do not equilibrate by fluxional interconversion.

The hetero-*Diels Alder* reaction results in a mixture of the two diastereomers of the spiro-dimer (enantiomers in the case of the model compound). While the oQM-derived dimer displays a fluxional interconversion between the two compounds, the oQIM-derived dimer does not show this equilibration. However, the oQIM dimer is readily susceptible to hydrolysis, which replaces the nitrogen function with an oxygen in a stepwise process (Figure 39). The resulting compound is identical to the spiro-dimer of α-tocopherol and thus equilibrates between the two diastereomers. The dimer of the monomethylated oQIM is more stable against hydrolysis than its underivatized counterpart.

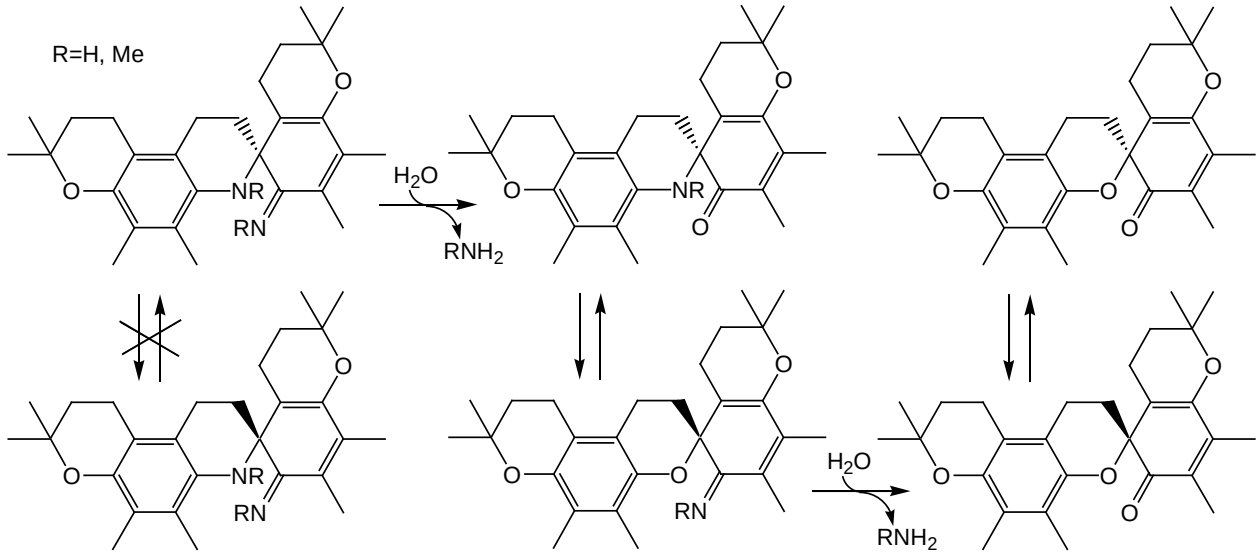

Figure 39: The enantiomers of the spiro-dimer derived from the oQIM (tocopheramine model compound) do not show spontaneous fluxional interconversion. Partial hydrolysis of the imine allows conversion between the two stereoisomers. Not only does the chirality of the molecule change, the endocyclic nitrogen is becoming exocyclic as well, making it accessible for hydrolysis. Upon complete hydrolysis, the spiro-dimer is obstained and thus full equilibration of the enantiomers is possible.

In the case of *N*-methyl tocopheramine two isomers of the oQIM are possible, since the methyl group can be either in *cis*- or *trans*-position ((*E*) or (*Z*) respectively). The ratio of (*E*)-oQIM to (*Z*)-oQIM is solvent dependent and can be determined by a small difference of the ^{1}H NMR-shift of the methyl group (Figure 40). In *n*-hexane the (*E*):(*Z*)-ratio is 8:1, in the ionic liquid BMIM chloride it drops to 1.8:1. Both isomers can be trapped with ethylvinyl ether in a hetero-*Diels-Alder* reaction.

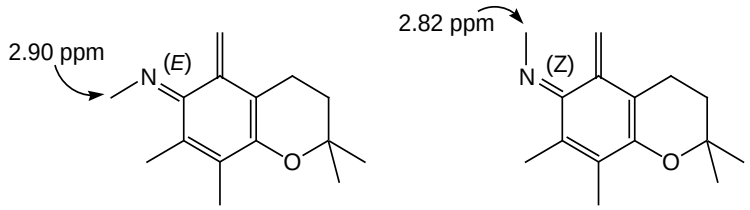

Figure 40: The oQIM of N-Methyl tocopheramine has two possible isomers, since the methyl group can be attached to the imine in either *trans* or *cis* position. *Trans* or (*E*) is usually found in excess.

It should be mentioned that the two-electron oxidation chemistry of α-tocopheramine and its *N*-methyl and *N*,*N*-dimethyl derivatives has been studied for the first time in the present work. Similarly, the primary oxidation products and their subsequent chemistry has been clarified and compared to the well-established chemistry of the α-tocopherol parent compound. These studies lay ground for any utilization of α-tocopheramines – no matter in which field – since its oxidation and follow-up chemistry, its side reactions, its main products and byproducts will be crucial factors regardless of the respective application.

ESR Measurements of Tocopheramines and Related Compounds.

To gain direct insight into the properties of tocopheraminyl radicals, the primary one-electron oxidation product of tocopheramines, an extensive ESR-study was started. The first and foremost task was to establish a reliable method to generate sufficient concentrations of tocopheraminyl radicals that would work with all substances that were to be studied. Additionally, the use of molecular radical starters was to be avoided, since we wanted to make sure that we were recording the signal of tocopheramines and not of an additive.

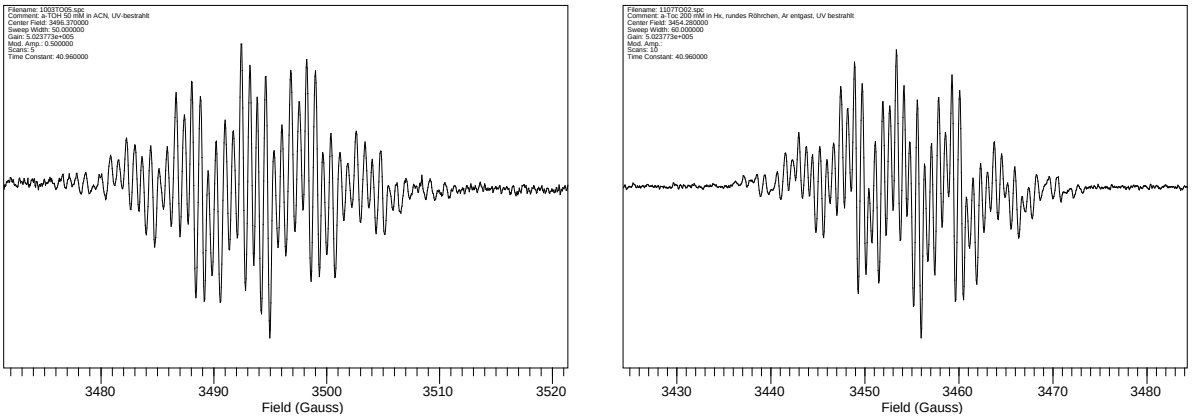

Figure 41: ESR-Spectra of α-tocopherol radical in acetonitrile (left) and in hexane (right).

Very detailed and intense spectra of the α-tocopheryl radical can be obtained if tocopherol **1** dissolved in degassed hexane or acetonitrile is exposed to UV-radiation (Figure 41). First attempts to transfer this straightforward method on the tocopheramines were undertaken with α-tocopheramine (**43**). Acetonitrile was replaced with apolar alkanes as solvents, since they readily dissolve tocopheramines and attenuate microwaves less due to their smaller electric dipole moment. Again it was tried to generate the radicals by photolysis with UV-irradiation or repeated illumination from a flashtube. Although the sample solutions were degassed by cyclic freezing and thawing of the sample in vacuum and inert atmosphere, respectively, and different sample tubes (cylindrical cells with different diameters, cylindrical quartz cells, flat cells) were used, it was not possible to reproducibly obtain useful spectra (Figure 42).

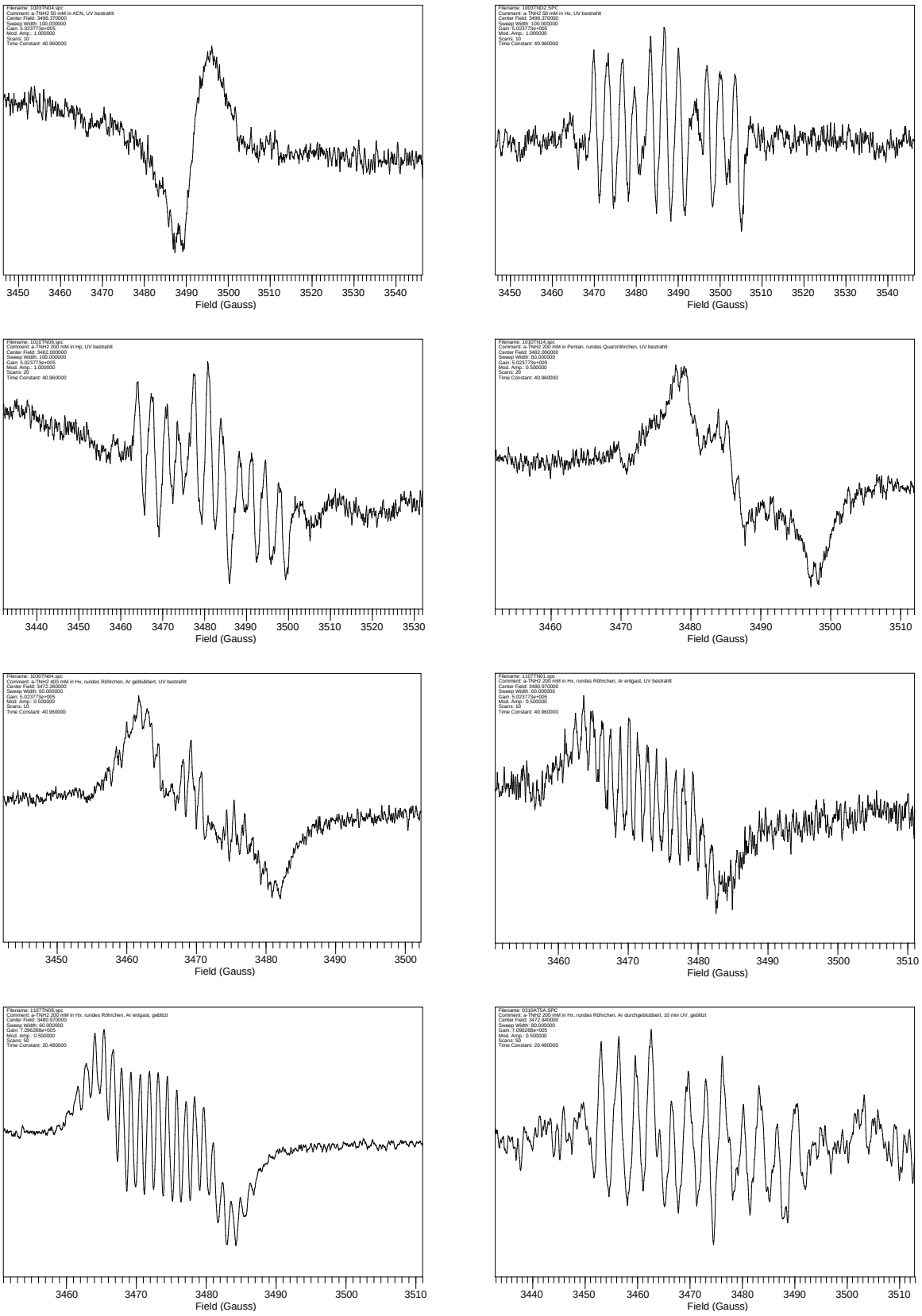

Figure 42: ESR-spectra of α-tocopheramine radical after UV-irradiation in different solvents: (top left to bottom right) acetonitrile, hexane, heptane, pentane, hexane (degassed), hexane (degassed), hexane (degassed, UV-lamp replaced by a flash tube), hexane (degassed, UV and VIS-illumination).

The final choice of the organic solvent was benzene, which is known to facilitate photolytic radical generation. After this last unsuccessful attempt, the solvent was omitted and neat tocopheramine was used. This, too, did not give the desired result (Figure 43).

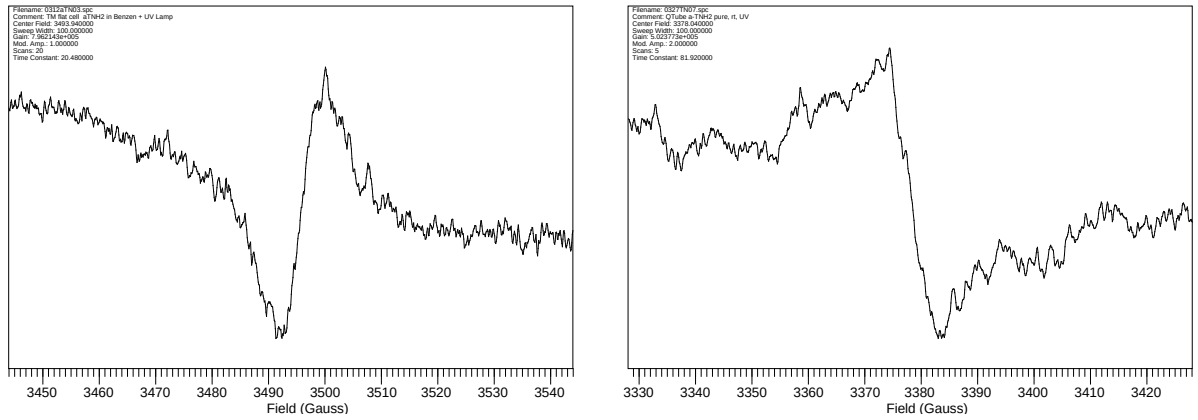

Figure 43: ESR-spectra of α-tocopheramine radical dissolved in benzene (left) and of neat α-tocopheramine (right).

After these inconclusive efforts the idea of radical generation by photolysis was discarded. Instead, radicals produced from hydroperoxide with UV-light should yield the desired tocopheraminyl radicals. This new approach had the drawback that aqueous hydroperoxide solutions had to be employed. To solubilize the highly hydrophobic tocopheramine, high concentrations of the common detergent SDS had to be used. This method reproducibly gave sufficiently detailed spectra of α-tocopheramine (Figure 44).

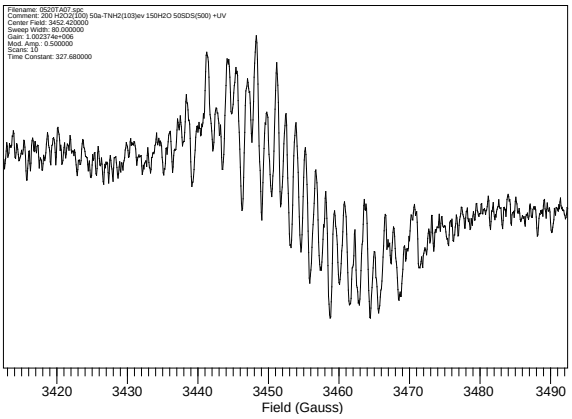

Figure 44: ESR spectrum after UV-irradiation of a 0.103 M solution of α-tocopheramine in 150 µL of water, 200µL of 100 mM H_2O_2-solution and 50 µL of 500 mM SDS-solution.

The standard method for sample preparation was as follows:

Dissolving the sample (25 or 50 µmol) in acetonitrile and evaporation in a stream of argon.
Addition of 375 µL of 500 mM SDS solution and vortexing until the sample was dissolved
Addition of 125 µL of 200 mM H_2O_2 solution
Transfer into a flat cell, UV-illumination and measurement of the spectrum

During the measurements it was observed that acidifying the sample not only changed its colour and viscosity but the observed signal as well. Therefore some of the samples were measured both under neutral and acidic conditions. Unfortunately due to the SDS the acidic samples were highly viscous, which made the sample handling quite difficult.

Aniline

Aniline is the most basic of all aromatic amines, and was thus the obvious choice for a model compound. The signal obtained by the standard procedure is basically a triplet with small coupling patterns (Figure 45). The triplet and the magnitude of the coupling constant indicate that the unpaired electron is localized at the nitrogen to a large extent. The additional fine structure suggests that some of the electron´s spin density is distributed over the aromatic ring where it can interact with hydrogen atoms.

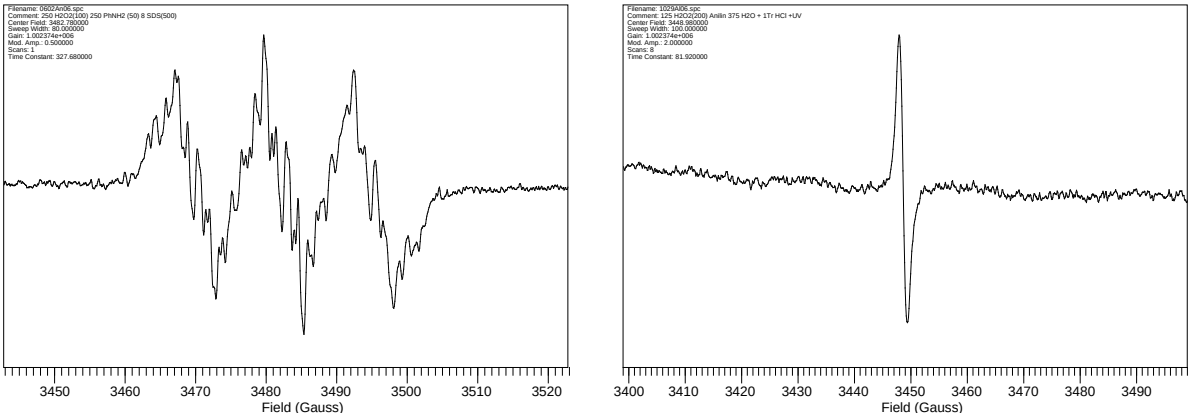

Figure 45: ESR-Spectra of aniline radical in SDS-solution (left) and water (right). Both radicals were generated with H_2O_2 and UV-illumination.

Since aniline is to some extent soluble in water, we tried to omit the SDS-solution and record a spectrum in H_2O_2-solution only. Most unexpectedly a singlet was observed both in neutral and in acidic conditions (Figure 45). No explanation for this result can be offered yet.

As a control experiment and to get an impression of the isotope-effect, ^{14}N-aniline was replaced with ^{15}N-aniline. The measurement in SDS-solution gave the expected duplet, which confirmed that the observed signal really was a nitrogen-centered radical (Figure 46). Replacing the SDS-solution with H_2O_2-solution did not give the unusual singlet, but an excellent signal with high resolution (Figure 46). The absence of the strong nitrogen duplet indicated that the unpaired electron was now much more

distributed over the aromatic system. Obviously, the extent of localization and pattern of radical distribution is highly dependent on the chosen medium.

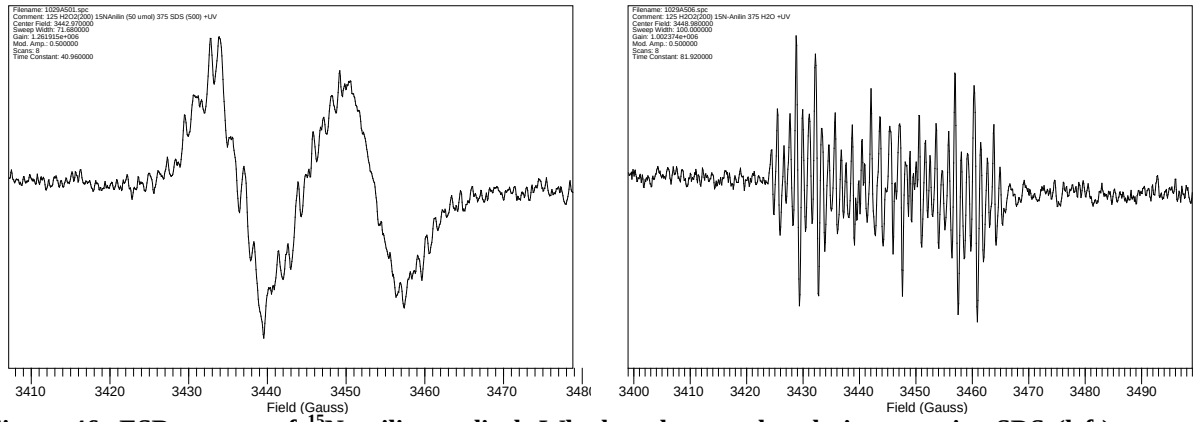

Figure 46: ESR-spectra of ^{15}N-aniline radical. Whether the sample solution contains SDS (left) or not (right) has a dramatic influence on the recorded signal.

p-Anisidine

4-Methoxyaniline was an interesting model compound as well, since its methoxy group reflects the endocyclic oxygen of the tocopheramine´s chroman core. It basically is an aniline complemented with a highly electronegative oxygen. By using anisidine we aimed at investigating tocopheramine-like systems without the complex coupling patterns generated by tocopheramine´s methyl groups.

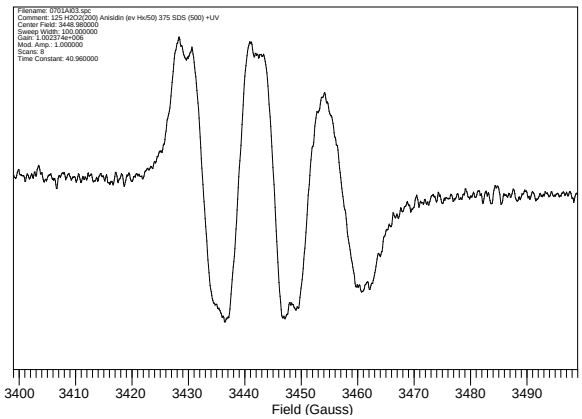

Figure 47: ESR-spectrum of anisidine radical. The triplet is strong evidence for a nitrogen-centered radical.

The recorded signal consisted of three very broad peaks (Figure 47). This triplet was again a strong indication that a nitrogen centered radical had been generated. This radical was surprisingly stable because even after 1.5 h after UV-illumination a strong signal could be observed. Unfortunately, the details that could be found in the aniline spectrum were lacking, and after the addition of acid no radical could be detected at all.

N-Methylaniline

N-Methylaniline was chosen as a model to represent monoalkylated tocopheramines. Intense spectra with excellent resolution were recorded in sample solutions that contained SDS (Figure 48). Interestingly, the effect the concentration of SDS had on the spectrum was clearly visible. Higher concentrations gave less defined signals whose shape was stronger influenced by the nitrogen-derived triplet. The extra methyl group close to the nitrogen visibly adds complexity to the spectrum compared to aniline.

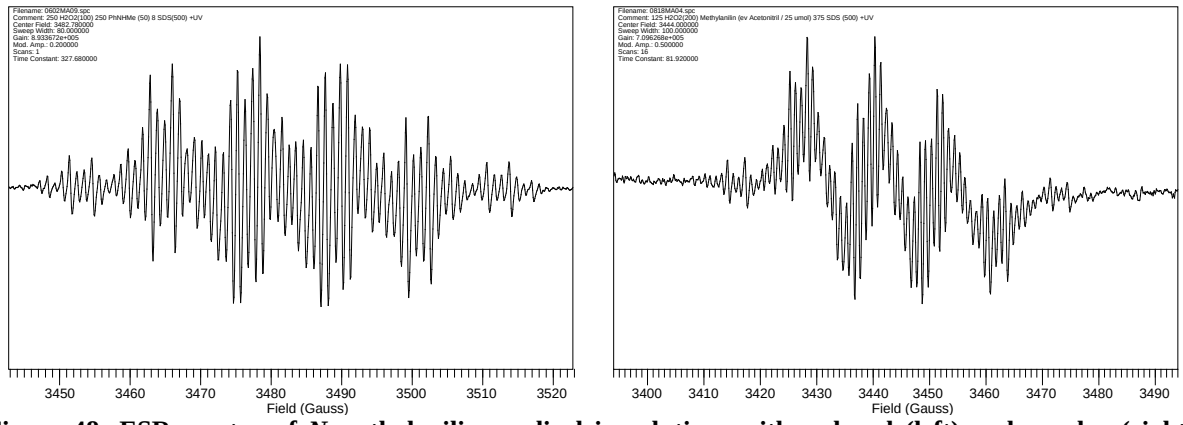

Figure 48: ESR-spectra of *N*-methylaniline radical in solutions with reduced (left) and regular (right) SDS-content.

Tocopheramine Model Compounds

Spectra of all four tocopheramine models **30**-**33** were recorded in either neutral or in acidic medium after dissolving the sample in SDS solution (Figure 49). In general, the obtained spectra displayed a dominant triplet in neutral conditions, indicating highly localized aminyl radicals. However, after acidification the spectra consisted of several small lines with complex coupling patterns. This suggested that the unpaired electron now had additional coupling partners or was now distributed over a larger part of the molecule, where it could interact with several atoms. The neutral spectrum of α-tocopheramine model **30** did not consist of a pure triplet, but of a sextet (possibly a triplet-dublet).

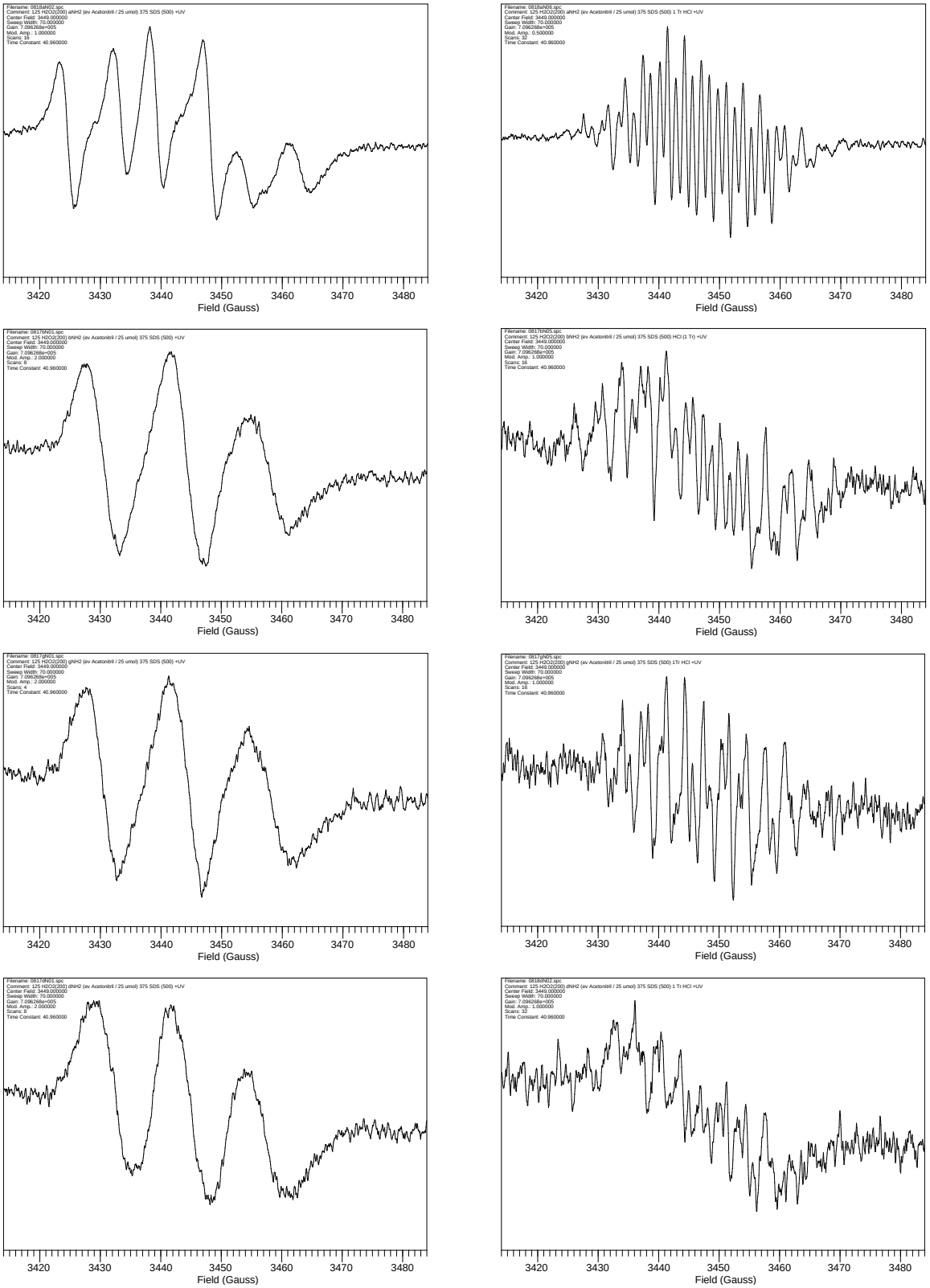

Figure 49 ESR-Spectra of the radicals of tocopheramine model compounds (top to bottom: α (30), β (31), γ (32), δ (33)) under neutral (left) and acidic conditions (right). The signal turns clearly more complex upon acidification, indicating additional coupling of the unpaired electron.

^{15}N-labeled α-tocopheramine model **35** was used to prove that the triplet was actually originating from the interaction with nitrogen. The recorded spectra definitely showed a doublet pattern instead of a triplet, which verifies the presence of a nitrogen-centered radical (Figure 50).

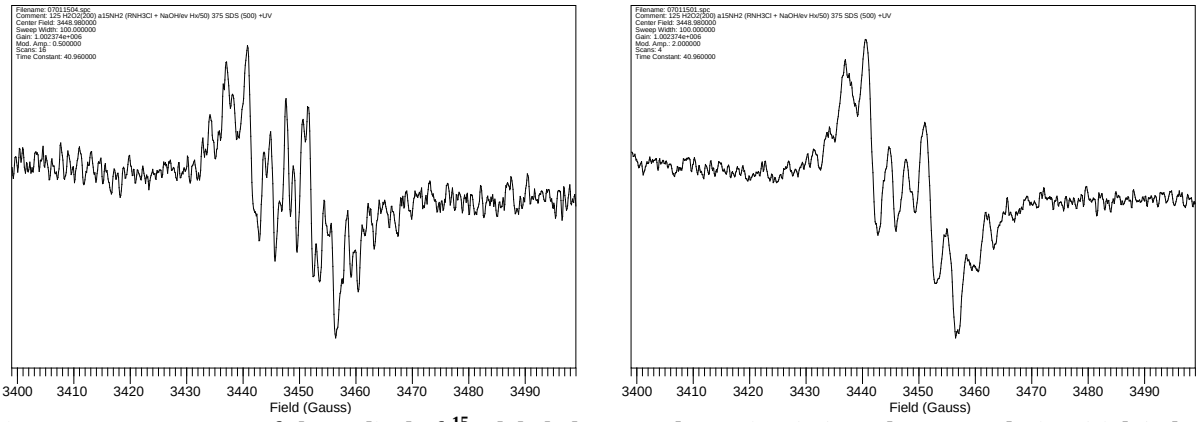

Figure 50 ESR-spectra of the radical of ^{15}N-labeled α-tocopheramine (35). At lower resolution (right) the doublet character is more obvious. The sample was obtained from tocopheramine hydrochloride (addition of NaOH and extraction with hexane), this direct sample preparation had a detrimental effect on the resulting signal.

Prediction of ESR Spectra by Computational Chemistry

The main information that can be derived from an EPR-spectrum is its coupling pattern. Every single coupling is defined by its multiplicity and its hyperfine coupling constant. The multiplicity depends on the number of chemically equal atoms that interact as well as on their spin according to the formula:

$$L = 2 \cdot I \cdot n + 1^{(e)} \qquad (2)$$

Nuclei with I = 0 do not add to the coupling pattern and can not be detected by ESR. Since this is the case for ^{12}C, the delocalization of radicals over a carbon skeleton can not be measured by ESR alone. This is also the reason why naturally abundant ^{14}N with I = 1 gives a triplet and ^{15}N with I = ½ gives a doublet.

The coupling constant displays a different property of the radical: the localization of the unpaired electron. Again a simple formula is used:

$$a_x = (2/3) \cdot \mu_0 \cdot \mu_N \cdot g_n \cdot \rho_S(0)^{(f)} \qquad (3)$$

μ_0 is a natural constant, and μ_N and g_n are characteristic for each nucleus. Thus $\rho_S(0)$ is the crucial factor that determines the value of a_x. A high spin density at a nucleus will give a large value for the corresponding coupling constant, which means that the peaks of the multiplet are further apart. All that is necessary to simulate an ESR spectrum is to know the spin density at each core. This, however, is not a trivial task at all. The only experimental way to determine electron densities is by X-ray

(e) L = multiplicity, I = spin quantum number of the nucleus, n = number of chemically equivalent nuclei
(f) μ_0 = permeability of vacuum, μ_N = nuclear magneton, g_n = g-factor of the nucleus, $\rho_S(0)$ = spin density at the nucleus

diffraction, and stable and solid radicals are exceptionally rare.[91] The other option is to make use of quantum chemical calculations.

We used dedicated software[92] to compute the spin densities of the model compounds that were studied by ESR to simplify the interpretation of the spectra. For the computation a base set that was specially designed for ESR calculations[93] was used and each molecule was entered both as neutral radical (abstraction of a hydrogen) and as cationic radical (abstraction of an electron). The calculated spin densities were directly converted to coupling constants by the software (Figure 51, Figure 52).

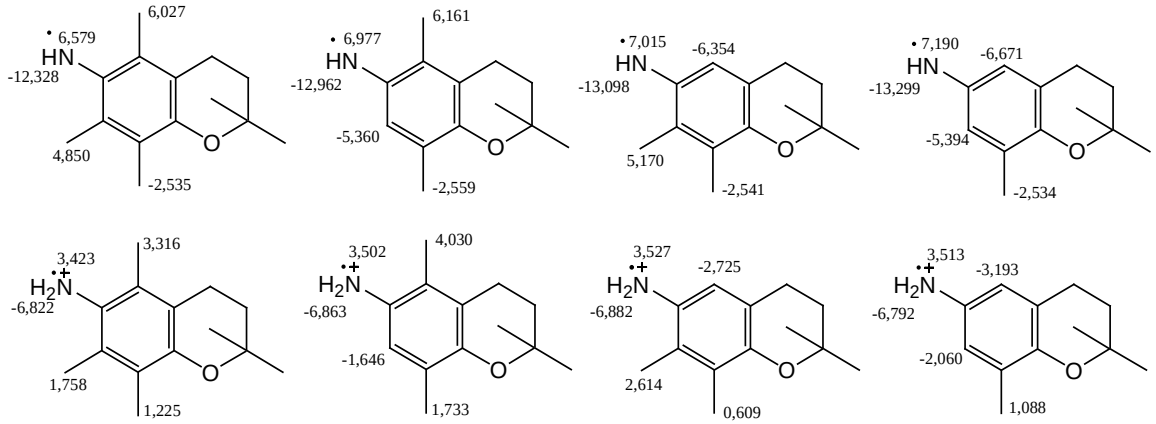

Figure 51: Hyperfine coupling constants in Gauss of thte cationic and neutral radicals of (30) – (33) as calculated by Gaussian 03. Note the very pronounced coupling with the amino hydrogens and the comparably modest coupling with the nitrogen itself.

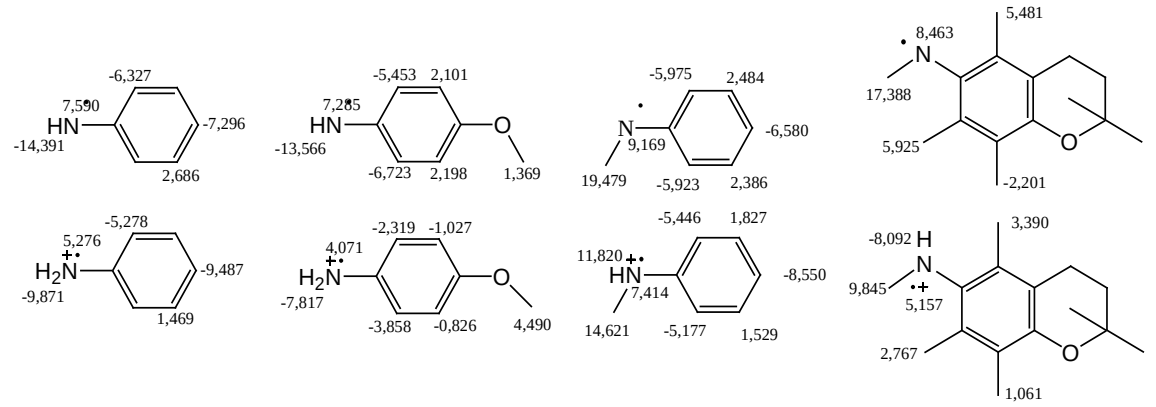

Figure 52: Hyperfine coupling constants in Gauss for the cationic and neutral radicals of aniline, p-anisidine, *N*-methylaniline and (38) as calculated by Gaussian 03.

The results of the computations gave a conclusive pattern for the model compounds: For the neutral radical the hydrogen attached to the nitrogen has a coupling constant of about 14 Gauss and the nitrogen of about 7 Gauss. The coupling becomes weaker from C5 to C7 to C8. For the cationic radical the constants are smaller, the largest is again appointed to the amino hydrogen with about 7 Gauss, the order in which they decrease is the same. Unfortunately these results can only be used as a rough guideline at most, since none of the measured spectra showed a hydrogen derived dublet or triplet with such an enormous coupling constant. On the contrary, the most obvious signal was a triplet

from the nitrogen with coupling constants of 12-14 Gauss. This meant that reliable predictions of the ESR spectra of tocopheramines were evidently not available (Figure 53).

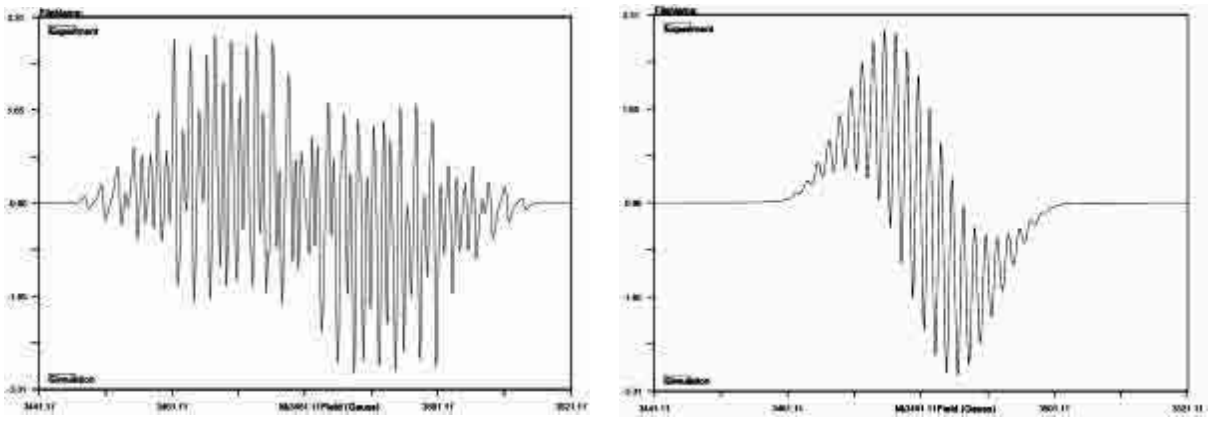

Figure 53: ESR-spectra simulated using the coupling constants predicted by Gaussian 03W. Neither the neutral α-tocopheraminyl radical (left) nor the cationic α-tocopheraminyl radical (right) does resemble any of the recorded spectra.

Conclusions

Radicals of tocopheramines and related compounds were successfully generated by aqueous hydrogen peroxide and UV-irradiation. The recorded spectra were highly dependent on the measuring conditions, which indicates that the nature of the radicals changes. With increasing concentrations of the detergent SDS the resolution and intensity of the recorded signal deteriorated. The triplets with coupling constants of 12 – 14 Gauss that were usually observed for the tocopheramine models under these conditions indicate that the unpaired electron is localized at the nitrogen to a large extent. The very broad peak shape suggests fast spin-spin relaxation, possibly by close arrangement of radicals in SDS-micelles. The asymmetry of the signal with decreasing peak intensities can be a sign of reduced mobility of the observed radicals. Apparently SDS is not the detergent of choice, especially not in high concentrations.

The addition of acid changed the shape of the signals tremendously. The simple coupling patterns with broad peak shapes and large coupling constants were replaced by complex signals with smaller coupling constants. Omission of the detergent, as it was possible with aniline, gave even more detailed spectra. This again strongly indicates that the concentration of detergent should be as low as possible. Moreover acidifying the sample solution drastically increased its viscosity, an effect that can also be observed in pure SDS solutions. The addition of protons seems to remove the amphiphilic properties of the SDS, probably because the anionic sulphate is protonated and loses much of its amphiphilicity and micelle-forming properties.

Preliminary efforts to match simulated to the recorded spectra were not satisfactory. However, the correlation between simulation and experiment was considerably improved if two radical species were assumed to be present simultaneously: a neutral and a cationic one. Whether this is because both are

generated simultaneously by a complex and unselective mechanism or one radical species is formed and then is changed by the medium, maybe by SDS, is not yet known.

It could be determined that tocopheramines form radicals that are sufficiently stable to be observed by ESR. Depending on the conditions the unpaired electron can be highly localized at the nitrogen or be distributed over the aromatic system. Hydrogen peroxide can generate tocopheraminyl radicals after activation by UV-light, the resulting radical could either be a cationic and a neutral species. With the observation of tocopheramine-derived radical species the studies on the one-electron oxidation chemistry of this intriguing compound class stepped on novel ground. The differences to the the relatively simple case of tocopherol were evidently larger than expected, and further studies can be expected to provide more intriguing results and novel facets of that particular chemistry.

The present study is the first on the one-electron oxidation of tocopheramines and the chemical nature of the products. The results allow a deeper understanding of the radical species derived from tocopheramines (and phenolic amines in general) and their reactivity. The knowledge about these reactive intermediates will be of great value in future applications, especially in an already conceivable therapeutic context, and when addressing similarities and differences to the tocopherol counterparts.

Detailed Mechanism of *ortho*-Quinone Methide Formation

Introduction

para-Quinones and *ortho*-quinones are common structures in today´s chemistry that are used in plenty of applications and reactions. However, their cousins *para*-quinone methide (QM) and *ortho*-quinone methide (oQM) (Figure 54) are widely neglected in synthetic chemistry, although they are an important part in natural processes, such as lignification, and are often biologically active. This ignorance is possibly due to the extraordinarily high reactivities of *para*-QMs and *ortho*-QMs that make studies of these intermediary compounds highly demanding. For example, direct spectroscopic studies of unsubstituted oQMs could only be done in an argon matrix at a temperature of 10 K or by laser flash photolysis.[94]

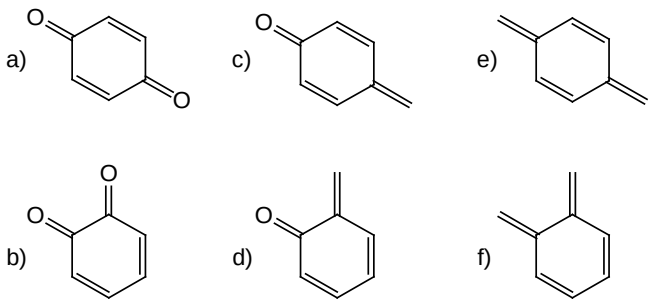

Figure 54: Basic structure of *para*-quinones (a), *ortho*-quinones (b), *para*-quinone methides (c), *ortho*-quinone methides (d), *para*-quinodimethanes (e) and *ortho*-quinodimethanes (f).

Detailed Formation Pathway and Stabilization of the Tocopherol Derived oQM and other oQMs

Fortunately, the general reactivity of the oQM of interest **6** is already well explored.[42] Formation of oQM **6** from α-tocopherol **1** means an overall loss of H_2, i.e. two electrons and two protons are lost or transferred to the oxidant, respectively. The electrons and protons need not be transferred as individual species, but for instance also as hydrogen atoms (one electron “and” one proton) or as hydride anion (two electrons “and” one proton). For the detailed, stepwise mechanism several sequences are thus conceivable. The respective mechanism is obviously not only dependent on the substrate tocopherol, but also on the oxidant and the reaction conditions. So far, only one specific case has been studied in detail and clarified, the oxidation of α-tocopherol – and *ortho*-methylphenols in general – by silver oxide, Ag_2O. Computational treatment by DFT methods predicted the formation of the oQM to proceed in three steps (Figure 55). First, a proton is released forming the corresponding phenolate anion. Second, a hydride ion is released from the *ortho*-methyl group and transferred to the oxidant. In this process, two equivalents of elemental silver and one molecule of water are generated. The hydride is transferred in a way, that the two remaining hydrogens at the resulting methylene group are located

at both sides of the aromatic plane, so that a perpendicular benzyl cation is formed which at the same time is also a phenolate anion. The intermediate is thus a zwitterions carrying both a positive (benzylic position) and a negative (phenolic oxygen) charge. It should be noted that the latter structure is *not* a resonance structure of the oQM. Such canonic structures differ *only* in the arrangement of multiple bonds. However, the zwitterionic intermediate and the oQM are additionally distinguished by a different conformation of the exocyclic methylene group. Only the third step in the overall formation pathway, the rotation of the methylene group into the ring plane, eventually generates the oQM and is coupled to the immediate aromatic-to-quinone conversion. While the intermediate is stabilized by through-space interaction of the two oppositely charged centers, the oQM is stabilized by resonance and is the by far more stable species so that an experimental proof of the occurrence of the zwitterionic intermediate seemed to be rather unlikely.

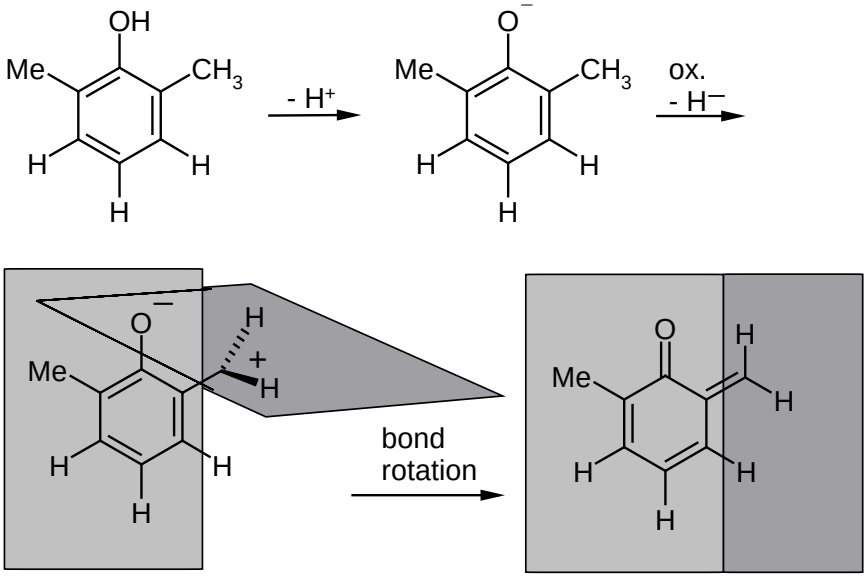

Figure 55. Detailed mechanism of the oxidation of *ortho*-methylphenols to *ortho*-quinone methides by Ag_2O according to DFT computations.[95]

The first indication[90] that a verification of its occurrence might be indeed possible was provided with the observation that oxidation of α-tocopherol by excess Ag_2O at -78°C caused immediate formation of the spiro-dimer *via* the oQM **6** within less than 10s, whereas in the presence of an amine *N*-oxide the tocopherol was consumed equally fast, but the generation of the spiro-dimer was considerable retarded. It was likely that the zwitterionic amine *N*-oxide stabilized the zwitterionic oxidation intermediate by electrostatic interactions in a way that rotation of the exocyclic methylene group into the ring plane was prevented and thus oQM formation (and its dimerization) were retarded. By using *N*-methylmorpholine-*N*-oxide (NMMO), for the first time direct spectroscopic evidence for the zwitterionic intermediate in the formation of oQM **6** was provided (Figure 56) .[90] At low temperatures, a complex (**44**) with *N*-methylmorpholine-*N*-oxide (NMMO) was formed which slowly decomposed into oQM **6** and unchanged NMMO. This degradation was immediate at temperatures above -30°C.[90]

The formation of spiro-dimer **8** from complex **44** was significantly retarded as compared to non-complexed oQM **3**. Oxidation of α-tocopherol **1** in the presence of one equivalent of NMMO at –78°C gave complete spiro-dimer formation only after about 20 min, as compared to about 10 seconds in the absence of the amine *N*-oxide. NMR spectroscopy at low temperature confirmed an interaction between oQM **6** and NMMO. The prominent signal of the proton spectrum was a singlet (2H) at 5.71 ppm, corresponding to the exocyclic methylene group. Its ^{13}C resonance at 182 ppm was indicative of a cationic species.[96] Furthermore, the proton resonances of the 7a-C and 8b-C methyl groups and the 4-C methylene group indicated the presence of an aromatic system, as did the ^{13}C NMR data for C-4a (118 ppm), C-5 (129 ppm) and C-6 (163 ppm), of which the latter strongly disagreed with a quinoid carbonyl carbon. Also the NMMO moiety was influenced by the interaction with oQM **6**.

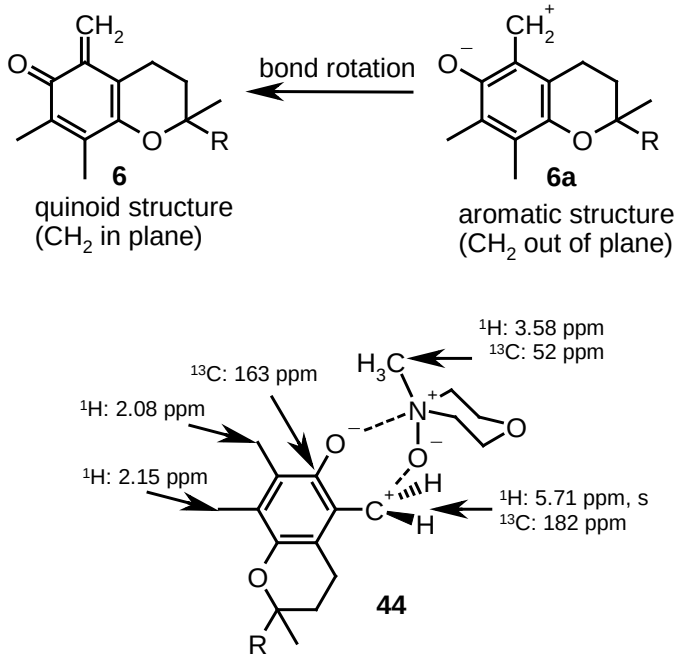

Figure 56. *ortho*-Quinone methide 3: stabilization of the zwitterionic rotamer in a complex with *N*-methylmorpholine *N*-oxide (44). The zwitterionic, aromatic precursor 6a affords the "common" quinoid form of the oQM 6 by in-plane rotation of the exocyclic methylene group.

Thus, in complex **44** the stabilized *ortho*-quinone methide **6** was evidently not present in its "traditional" quinoid form, but in the form of a zwitterionic, aromatic structure with an exocyclic methylene group rotated out of the aromatic plane. With the 5a-CH_2 group standing out-of-plane or even perpendicular to the plane, the positive charge is localized at C-5a and cannot dissipate into the aromatic ring by resonance. It was proposed that the primary stabilization effect was an increase in the rotational barrier of the exocyclic, cationic methylene group by electrostatic interactions with the negative charge of NMMO. This stabilized the aromatic structure, and resulted in a restricted rotation into the in-plane form, which impeded the formation of the quinoid resonance form of oQM **6**, so that the dimerization to spiro-dimer **8** was retarded as observed. The activation parameters for the

formation of free oQM **6** from the complex **44** were estimated to a $\Delta H^{\neq}$ of 47 kJ mol^{-1}, a value which is comparable to the cleavage of a strong hydrogen bond.

The geometry of the zwitterions with its exocylic out-of-plane methylene group was quasi preserved in the recently reported dibenzodioxocine derivative (**45**) that was formed in rather small amounts by rapidly degrading the NMMO complex at elevated temperatures (Figure 57).[97] Strictly speaking, dibenzodioxocine dimer **45** is actually not a dimer of *ortho*-quinone methide **6**, but of its zwitterionic precursor or rotamer **6a** (Figure 57). As soon as the out-of-plane methylene group in this intermediate rotates into the ring plane, the oQM **6** is formed irreversibly, and the spiro-dimer **8** results inevitably. The formation of the dibenzodioxocine dimer from NMMO-complex **44**, which consists actually of two simultaneous etherification reactions driven by charge recombination, is thus competing with this bond rotation and must occur faster for the dioxocine dimer to form. Bond rotations have kinetic rate constants k_{rot} of 10^{-12} s^{-1} to 10^{-14} s^{-1}, the recombination rate of the two zwitterions ions in solution k_{rec} cannot be faster than diffusion-controlled and is limited to about 10^{-7} l mol^{-1} s^{-1} to 10^{-9} l mol^{-1} s^{-1}. The faster rate of the bond rotation accounted for the fact that the yields in the dioxocine dimer were naturally limited, ranging below 5%.

Treatment of dioxocine dimer **45** with acid at 50°C caused its decomposition and neat formation of spiro-dimer **8** (Figure 57). Evidently, the two benzyl ether functions were cleaved, the resulting methylene groups immediately rotated into the plane forming oQM **6**, and this intermediate dimerizes according to the "conventional" pathway into the spiro-dimer **8**. A similar reaction, although accompanied by formation of several minor byproducts was effected by heating compound **45** in neat form above 155°C. Interestingly, the conversion of dioxocine dimer to spiro-dimer proceeded in neat substance, i.e. also in solid state for the truncated model compounds, e.g. by exposing the dioxocine dimers to an atmosphere of HCl or TFA. Within minutes, the dioxocine dimer **45** was converted neatly without any side reactions into the spiro-dimer, as was followed by IR spectroscopy, which was the first report of solid state processes involving *ortho*-quinone methides.

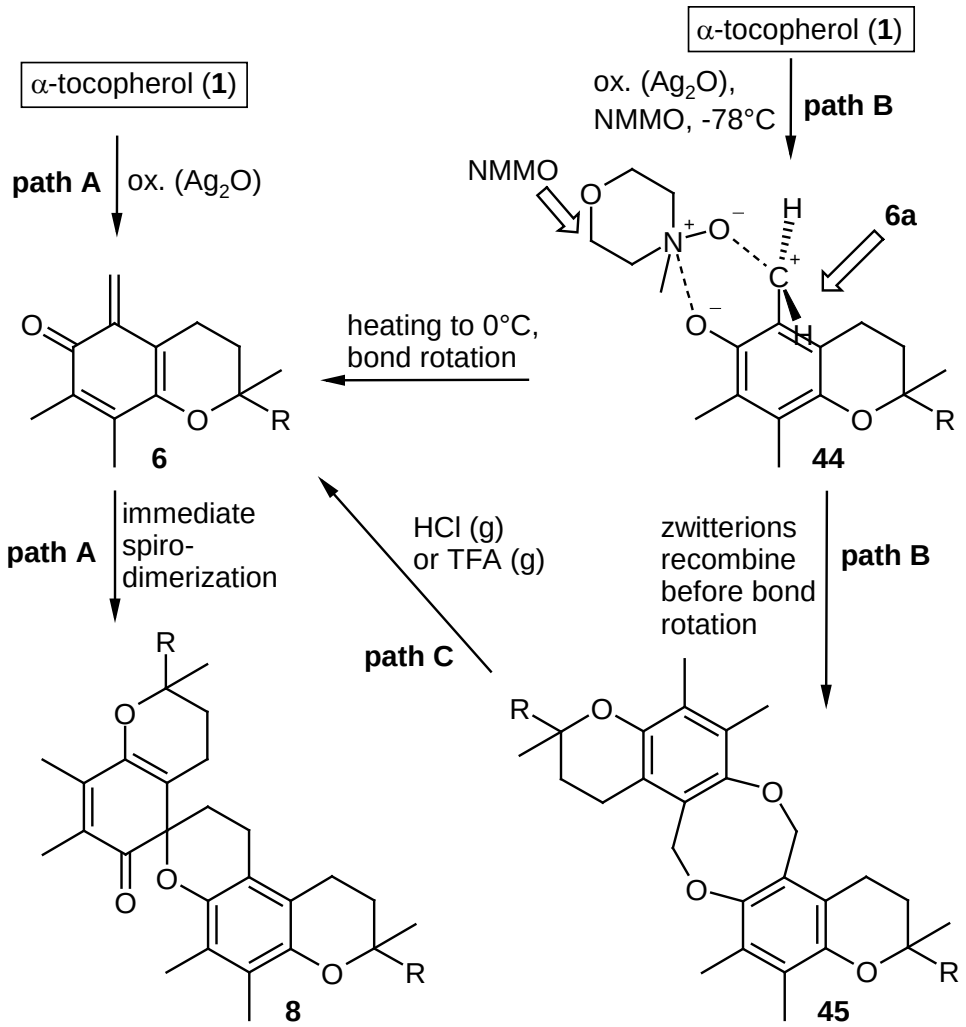

Figure 57. Oxidation of α-tocopherol (1) conventionally leads to its spiro-dimer (8) *via ortho*-quinone methide 6 (path A). The zwitterionic oQM precursor 6a is stabilized by NMMO in complex 44, which upon rapid heating produces small amounts of the new dioxocine dimer 45 (path B). Acid treatment of 45 causes quantitative conversion into spiro-dimer 8, *via* oQM 6 (path C).

It was shown that complexes **46** between the zwitterionic precursors of *ortho*-quinone methides with a bis(sulfonium ylide) derived from 2,5-dihydroxy[1,4]benzoquinone[98] were even more stable than those with amine *N*-oxides (Figure 58). The bis(sulfonium ylide) complexes were formed in a strict 2:1 ratio (oQM / ylide) and were unaltered at −78°C for 10 h and stable at room temperature under inert conditions for as long as 15–30 min (Figure 58).[97] The oQM precursor was produced from α-tocopherol (**1**), its truncated model compound (**4**) or a respective *ortho*-methylphenol in general by Ag_2O oxidation in a solution containing 0.50 to 0.55 equivalents of bis(sulfonium ylide) at -78°C. Although the species interacting with the ylide was actually the zwitterionic oxidation intermediate **6a** and not the oQM itself, the term "stabilized oQM" was introduced for the complexes, since these reacted similar to the oQMs themselves but without dimerization reactions in a well-defined way.

In the 2:1 complexes formed, both oQMs adopt a zwitterionic, aromatic structure with the exocyclic methylene group in perpendicular arrangement to the ring plane, stabilized by the negatively charged

phenolic oxygen. Simultaneously, the negatively charged oxygens in the oQM parts interact with the positively charged sulfur to provide additional stabilization.

The electrostatic interactions in the complexes **46** were obviously sufficient to "favor" the zwitterionic structure in a manner that formation of the usual oQM was "suspended", so that all reactions typical of oQMs in their quinoid form (such as [4+2]-cycloadditions) were suppressed or at least slowed down. Decomposition of the complex of α-tocopherol was immediate by fast heating to 40°C or above. This caused disintegration of the complex **46**, immediate rotation of the methylene group into the ring plane and thus formation of the oQM which then shows the "classical" chemistry of such compounds.

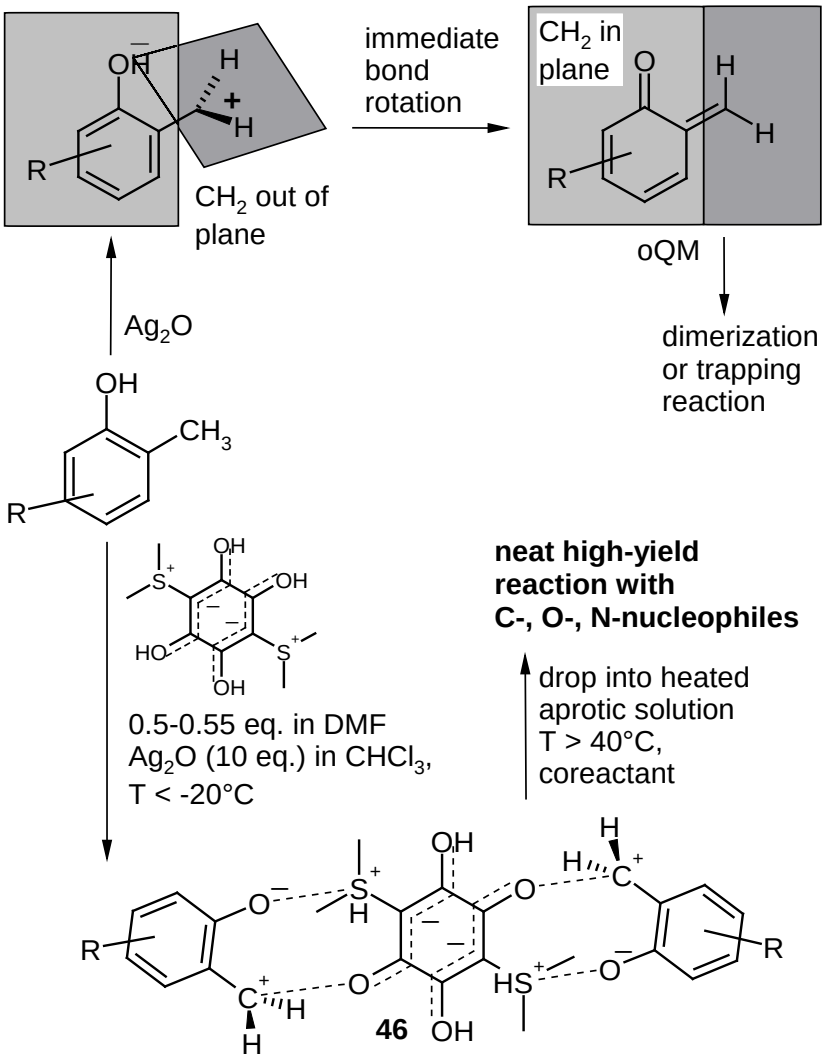

Figure 58. Oxidation of *ortho*-methylphenols to the corresponding *ortho*-quinone methide *via* transient zwitterionic intermediates that are stabilized by forming a complex 46 with the 2,5-dihydroxy[1,4]benzoquinone-derived bis(sulfonium ylide).

The complex **47 (**Figure 59**)** obtained from the truncated α-tocopherol model compound (**4**) by Ag_2O oxidation in the presence of the sulfonium ylide, was isolated at -30°C as an amorphous addition product, and was comprehensively characterized. It showed the exact ratio of 2:1, and a structural

image was obtained by refining a quantum-chemical prediction (DFT) of the crystal structure according to X-ray powder diffraction data. Proton NMR spectroscopy of the complex showed a singlet (2H) at 5.85 ppm, corresponding to the exocyclic methylene group. This peak showed a heteronuclear correlation to a carbon at 191.8 ppm (C-5a), and HMBC cross peaks at 129.9 ppm (C-5, $^{2}J_{H\text{-}C}$), 117.2 ppm (C-4a, $^{3}J_{H\text{-}C}$) and 154.1 ppm (C-6, $^{3}J_{H\text{-}C}$). The proton resonances of the 7a-CH_3, 8b-CH_3 methyl groups and the 4-CH_2 methylene group at 11.8, 12.0 and 20.4 ppm indicated the presence of an aromatic system: due to the ring current effect, the resonances of the protons at C-7a, C-8b, and C-4 experience a down-field shift in tocopherol (**1**) and related derivatives, which evidently seems to be still operative in complex **47**. The high down-field shift of the carbon resonance at 191.8 ppm for the exocyclic methylene group is especially indicative of a cationic species (the ^{13}C resonances of carbocations can range between 100 to above 300 ppm),[96] and the peak at 154 ppm for C-5 agrees with a phenolic carbon, but not with a quinoid carbonyl carbon, as ^{13}C resonances of quinoid carbons are usually found between 180 and 195 ppm. Also the bis(sulfonium ylide) moiety was influenced, albeit rather weakly. The four magnetically equivalent methyl groups in bis(sulfonium ylide) resonating at 3.02 ppm in DMSO-d_6[98] appeared as singlet at 2.94 ppm in complex **47**. The carbon resonances changed from 94.0 (C-S) and 176.2 (C-O) ppm in neat 3 to 88.4 (C-S), 172.2 (C-O) and 193.2 (C=O) ppm, respectively, in the complex. The stabilized zwitterions **6a** actually represent conformers of the oQM **6**, with the conformational change – rotation of the exocyclic methylene group – being coupled to a fundamental change in the electronic structure, the transition from an aromatic into a quinoid system.

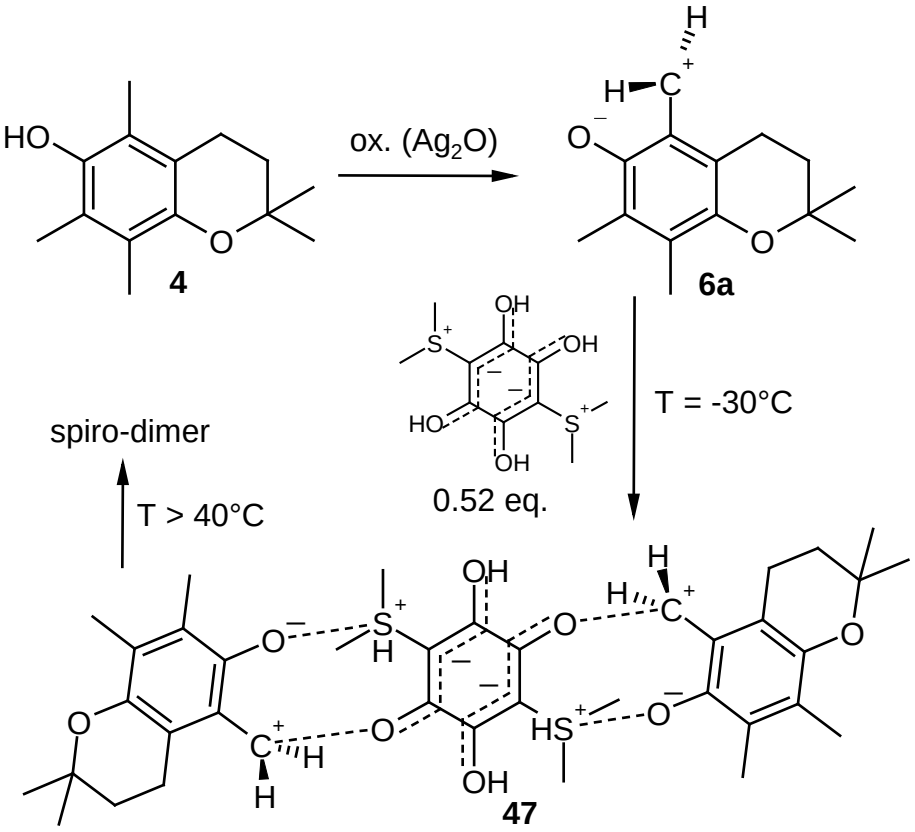

Figure 59. Formula and molecular structure of the 2:1 complex 47, formed between the zwitterionic oQM precursor derived from PMC (4) and bis(sulfonium ylide).

The stabilization of oQMs as in Figure 56 and Figure 59 had two implications. At first, the zwitterionic intermediate in oQM formation mechanism – albeit strictly speaking only for the oxidation by Ag_2O – was confirmed. The stabilization approach might thus be useful also for other oQM as those occurring in tocopherol chemistry and might allow detecting hitherto elusive oQMs by trapping them and converting them into their more stable and better analyzable complexes. The second application of the stabilization approach lies in organic synthesis. The general advantage is that oQMs in the form of their ylide complexes can be used and handled like stable, stoichiometrically usable, dosable reagents. They can be reacted in a controlled way without the danger of immediate self-dimerization or other uncontrolled side reactions.

The stabilization of the zwitterionic oQM precursors is due to electrostatic interactions. It was reasonable to assume that also other methods of stabilizing the zwitterions might be viable, and indeed it was confirmed that both steric and electronic effects are able to stabilize such intermediates.

Stabilization of the zwitterionic intermediate in oQM formation can also occur intramolecularly (Figure 60). In this case, the stabilizing moieties must be able to dissipate the positive charge at the benzylic group by a resonance effect and prevent rotation of the exocyclic methylene group by a steric blocking. One example for such a temporary stabilization is the nitration of α-tocopheryl acetate (**1c**) by concentrated HNO_3, which produced 6-*O*-acetyl-5-nitro-α-tocopherol (**48**) in quite good yields,[99]

the acetyl group not being cleaved during the reaction. The mechanism of the unusual formation reaction was studied in more detail,[100] and was shown to proceed *via* a 1,3,8-trioxa-phenanthrylium cation intermediate (**49**), which eventually added nitrite to afford **48** according to a non-radical, heterolytic course (Figure 60). A deacetylation – oxidation – reacylation mechanism was ruled out by performing the reaction in propionic acid as the solvent and confirming the presence of an acetyl group – but not a propionyl moiety – in the product. In intermediate **49**, an effective charge delocalization over four atoms was effected through spatial interaction of the partially negative acyl oxygen with the positive benzylic position, resulting in strong resonance stabilization (Figure 60). The 1,3,8-trioxa-phenanthrylium cation can be imagined as *O*-acylated zwitterionic precursor of the oQM **6**. The benzylic methylene group is arranged perpendicular to the aromatic plane, so that the compound possesses four aromatic resonance hybrids involving the acetyl group, but no quinoid canonic forms. Generally, *O*-acyl substituent were shown to be crucial for the nitration reaction to proceed as they stabilize the cationic intermediate by resonance.

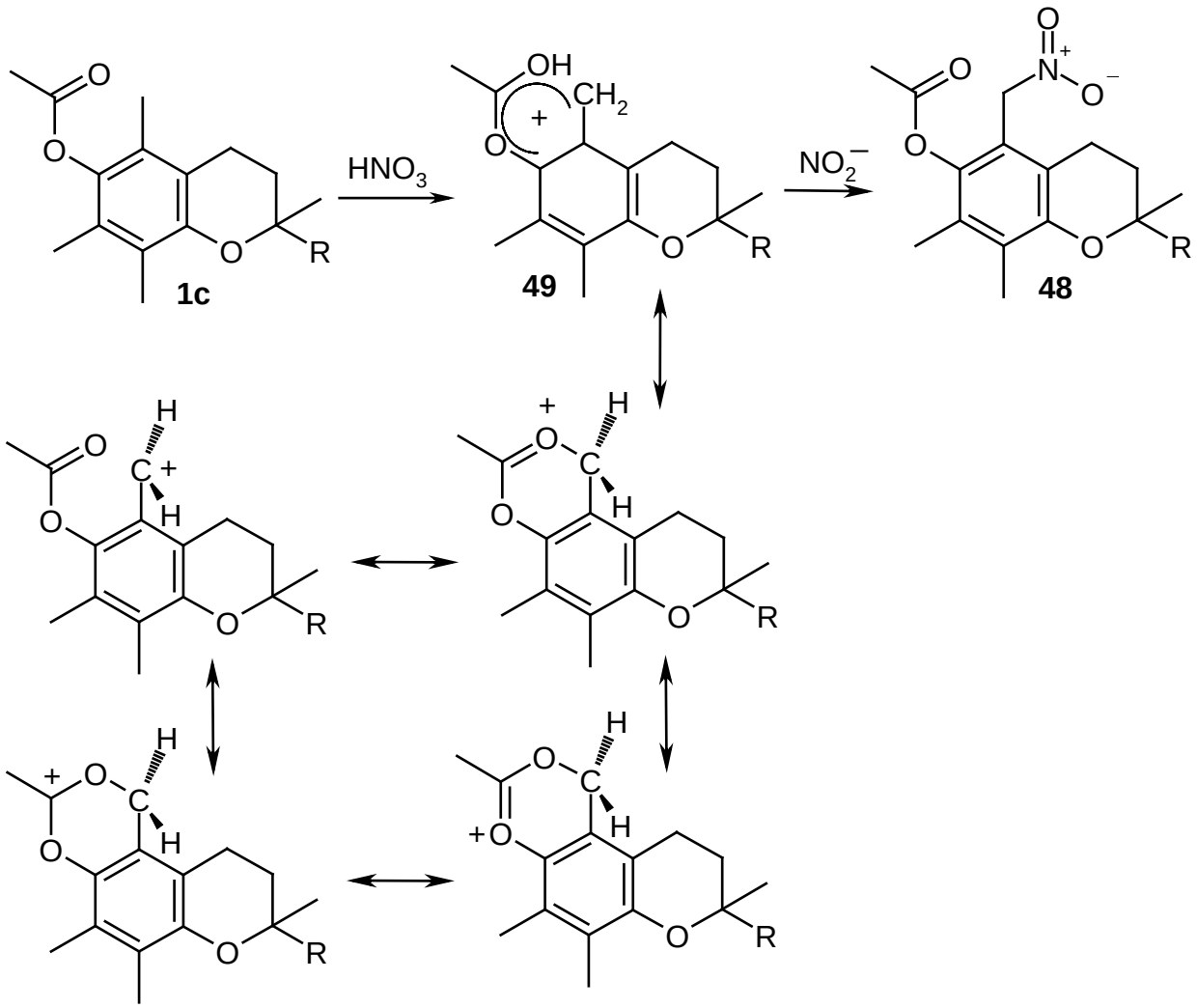

Figure 60. Synthesis of 6-*O*-acetyl-5-nitro-α-tocopherol (48) and four resonance forms of the cationic intermediate (49).

The reactions and compound presented in this chapter support the notion that the formation of oQMs from the parent phenols is a quite complex process. In the case of the oxidation by Ag_2O but also likely in other oxidations, a zwitterionic intermediate is involved that can be stabilized intermolecularly, e.g. by electrostatic interaction with other suitable zwitterions, or intramolecularly by neighboring groups or inductive / mesomeric effects. By stabilizing the zwitterionic intermediate and destabilizing the oQM, the energetic gap between these two intermediates is lowered and both become observable at the same time. The stabilized zwitterionic precursors can be regarded as "stabilized oQMs", as they are converted into oQMs just by a bond rotation. This stabilization might have interesting applications in the identification of transient oQMs and in organic synthesis. A direct spectroscopic proof of the occurrence of the intermediate zwitterion was still to be provided. To provide this proof succeeded by means of derivatives especially synthesized for the purpose of the detailed mechanistic studies, which are presented in the following chapter.

Aim of the Project

As has been shown, α-Tocopherol can be oxidized to an intermediary oQM that has multiple options for further reactions (see Figure 14 and Figure 15). In an attempt to proof the existence of tocopherol-derived zwitterions the oxidation mixture was treated with zwitterions, namely bis-sulfonium ylides[97] and *N*-methylmorpholine-*N*-oxide,[90] completely impeding further reactions of the oQM intermediate at temperatures up to -30°C. This was not a stabilization of the oQM but of the zwitterionic precursor, decomposition of the complexes resulted in the generation of the oQM and the occurrence of its typical reactions. This procedure allows convenient handling and dosage of oQMs as reagents in organic synthesis.

This previously collected data strongly suggested the existence of a zwitterionic intermediate. Simulations of the oxidation reaction also supported a reaction pathway that included a zwitterionic intermediate. The proposed mechanism starts with the removal of a proton from the phenol group and of a hydride from the methyl at C-5a. This means that an anionic phenolate and a benzylic carbocation remain attached to the aromatic core. These two charges exist remotely and in a separated way in the zwitterionic molecule, until the aromatic system can transform itself to the quinoid double bond system. This connects the two ionic groups and neutralizes the charges, resulting in a neutral oQM system. The now quinoid ring contains four conjugated double bonds, which means, that the overall shape of that moiety is planar. This also affects the two hydrogens at C-5a. They are now part of a double bond and therefore have to be arranged in plane with the oQM´s ring. Before the formation of the oQM the ring was aromatic and the hydrogens could be arranged periplanar to the ring (Figure 61).

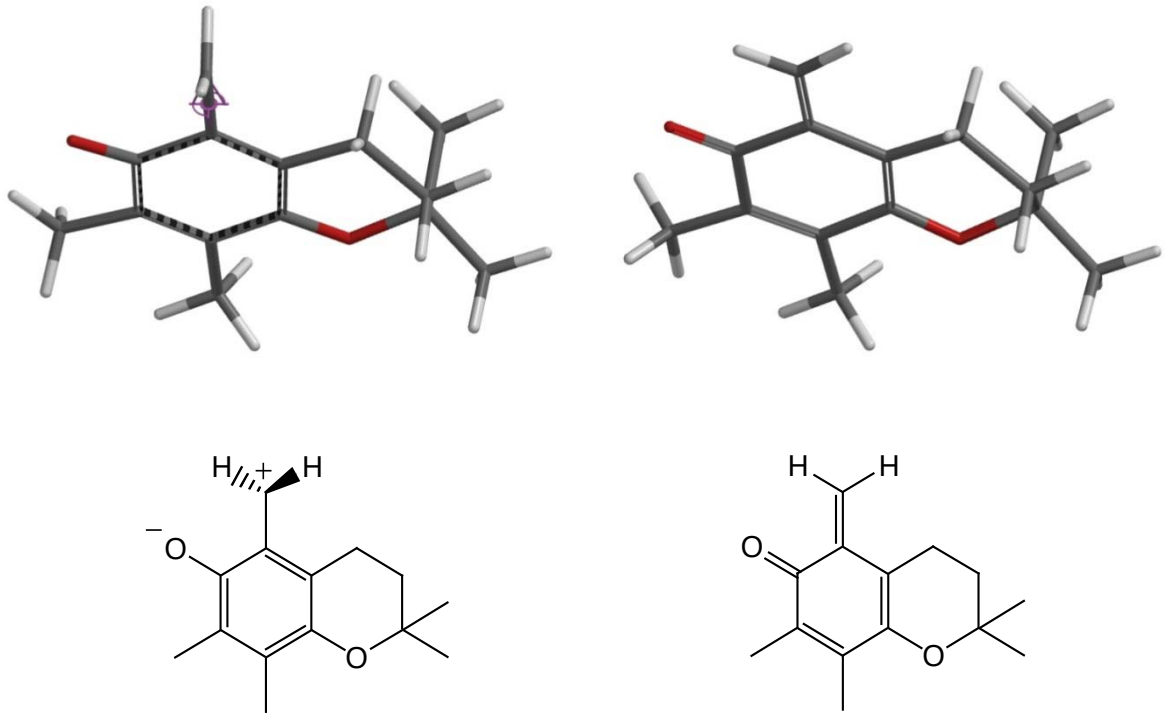

Figure 61: Rotation of the exocyclic hydrogens at C-5a switches between the aromatic zwitterion and the olefinic oQM. On the left, the hydrogens are arranged perpendicular to the plane of the aromatic ring. The actually unfavourable zwitterion is stabilized by the energetically advantegeous aromatic core. On the right, the hydrogens have turned into the plane of the ring, allowing the formation of the roughly planar double bond system of the oQM.

An indirect proof of the zwitterionic intermediate had already been produced by the stabilization experiments. But the verification of the actual existence of the zwitterions by a direct spectroscopic observation was still missing. The unambiguous confirmation would shed new light on the current understanding of oQM-formation: some decade-old teaching in this seemingly well-established chemistry would have to be revised. Moreover, to proof that the change from the zwitterion´s aromatic system to the olefinic oQM is linked to a simple bond rotation would allow a novel perspective on the use of aromatic systems both in synthesis and in nano-scale engineering.

The starting point for this project was the theory that a simple bond rotation which brings the exocyclic methylene group in plane with the aromatic ring system is triggering the change from an aromatic to a quinoid system. Hindering this rotation by steric and/or electronic effects should have a stabilizing effect on the zwitterion and delay the formation of the oQM. If indeed provable, this oQM structure would be the first chemical system where such a fundamental property change as the transition aromat-to-quinone (and back) is coupled to and governed by a very simple process, the rotation around a single bond. Studies of such a system will not only shed new light on the tocopherol system in particular, but fundamentally contribute to our understanding of aromaticity / antiaromaticity as one of the basic concepts in organic chemistry. To find out more about this system, dedicated derivatives of tocopherol were synthesized.

Synthesis of the Required Model Compounds

Alkyl Substitution of α-Tocopherol Model

To examine sterical effects (with the exclusion of electronic ones) on oQM-formation, C-5a was substituted with two unbranched alkyl chains. The initial synthetic concept was to attach an alkane equipped with an electronegative leaving group by *Friedel-Crafts* alkylation to the γ-tocopherol model (Figure 62). First attempts with commercially available 5-nonanol and different organic and inorganic Lewis and Brønsted acids (aluminum chloride, sulphuric acid, formic acid, phosphoric acid, trifluoromethanesulfonic acid) failed to yield the desired product. As an alternative synthetic pathway, the alkylation of dimethylbenzoquinone was attempted, since this substance could have easily been converted to a chromanol precursor. This method also proved to be rather ineffective, so enhancing the properties of the leaving group was tried instead. The hydroxyl group was replaced by chloride with thionyl chloride, but the resulting derivative did not show the desired reactivity. Attempts to tosylate the alcohol failed likewise. To use an olefinic reagent for the alkylation was another option. Commercially available *trans*-4-octene was reacted with the usual selection of acidic catalysts but failed to give satisfactory outcomes.

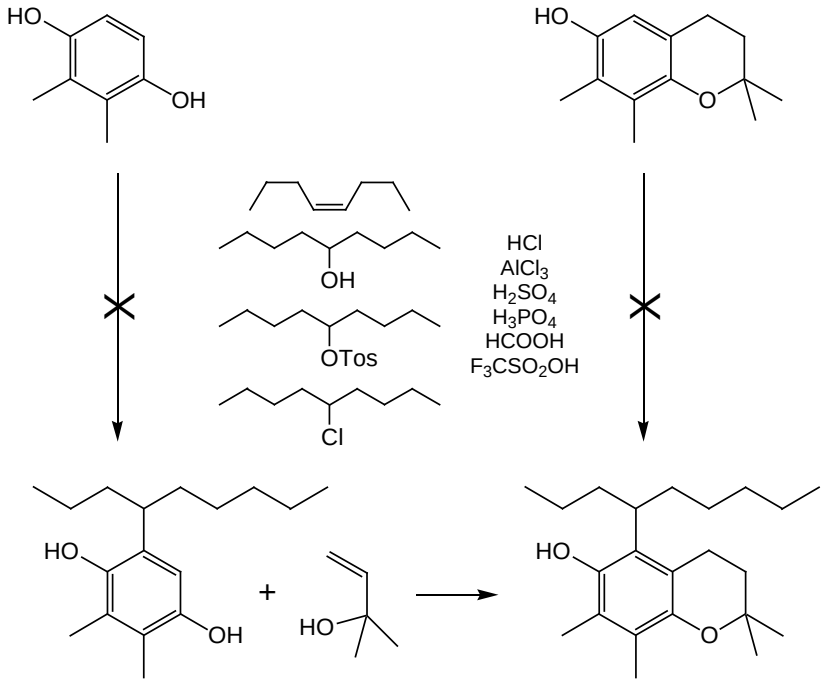

Figure 62: Direct alkylation of tocopherol model compound and their precursor was not possible under classical reaction conditions.

Intensive literature studies suggested that a radical alkylation of a quinone precursor could be possible (Figure 63).[101] The olefinic precursor is boronated in the presence of DMAc, and a radical is generated by the addition of air and DMPU. The action of the amide in this process is not clear, but it greatly

improves the yield of the reactions.[102-104] The precise reaction mechanism has also not been elucidated yet. But the reaction allowed the successful alkylation of dimethylbenzoquinone **50**. After purification and reduction to the hydroquinone the target octyl-tocopherol derivative **51** could be obtained.

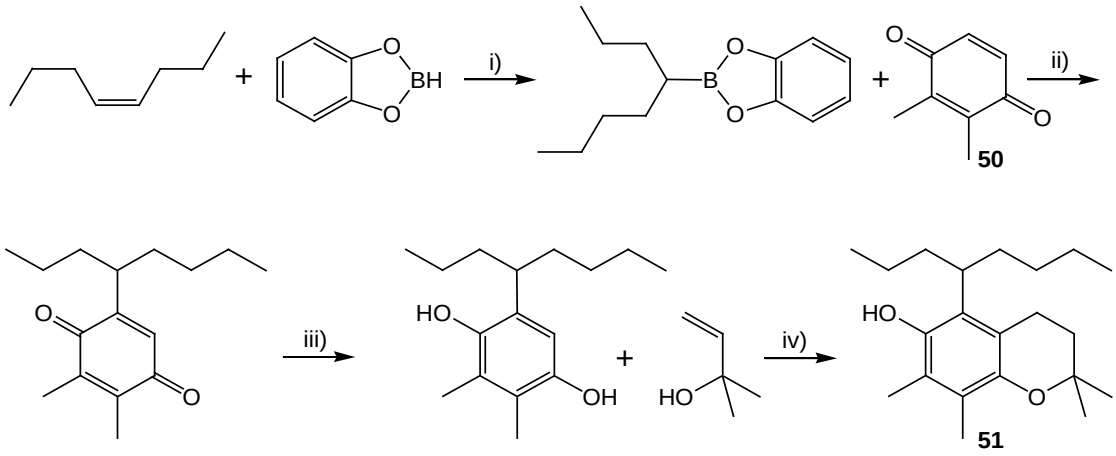

Figure 63: Alkylated α-tocopherol 51 was obtained by radical alkylation of the precursor substance 50. i) DMAc, H_2O, DCM, Δ. ii) DMPU, O_2, DCM. iii) $NaBH_4$, THF. iv) a: HCOOH, Δ. b: HCl, MeOH.

Aromatic Substitution of α-Tocopherol Model

The biphenyl-α-tocopherol model was expected to show extreme stabilization of the intermediate zwitterion both sterically and electronically, since it makes use of both a rotational barrier and of electronic stabilization of the positive charge. γ-Tocopherol model was treated with benzhydrol and aluminium chloride under exclusion of water. This rather simple approach already provided the desired compound **52** in fair yields (Figure 64).

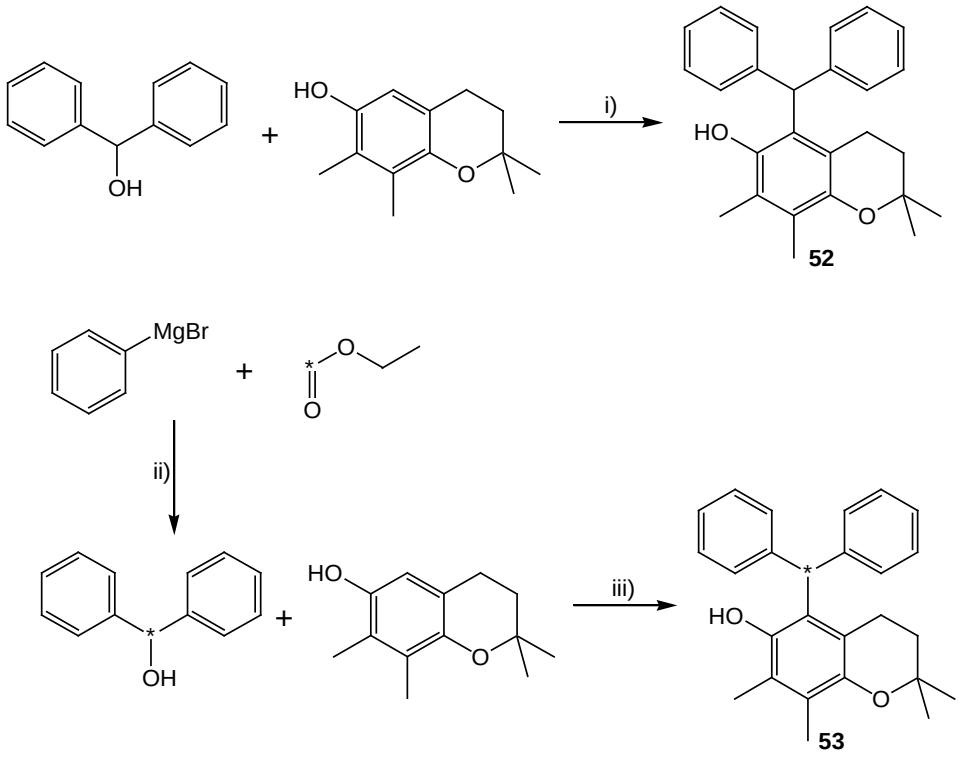

Figure 64: Synthesis of unlabeled (52) and labeled (53) biphenyl-α-tocopherol model. i) $AlCl_3$, THF. ii) THF. iii) $AlCl_3$, THF.

To allow a detailed description of the oxidation process by NMR-spectroscopy – or even a kinetic description – a ^{13}C-labeling at position C-5a was planned (Figure 65). Apart from C-6 which changes from a phenolic group to a quinoid carbonyl group upon oxidation of α-tocopherol to oQM, C-5a is the position which undergoes the most dramatic changes in this process: from an aromatic methyl group to an exocyclic methylene group. If indeed, a cationic intermediate was involved, the change from the methyl moiety to the cation and further to the methylene would be even greater. To introduce the label at position C-5a ^{13}C-labelled benzhydrol was obtained from the reaction of phenyl magnesium bromide and labelled ethyl formate. This special benzhydrol was then reacted with γ-tocopherol model as presented above.

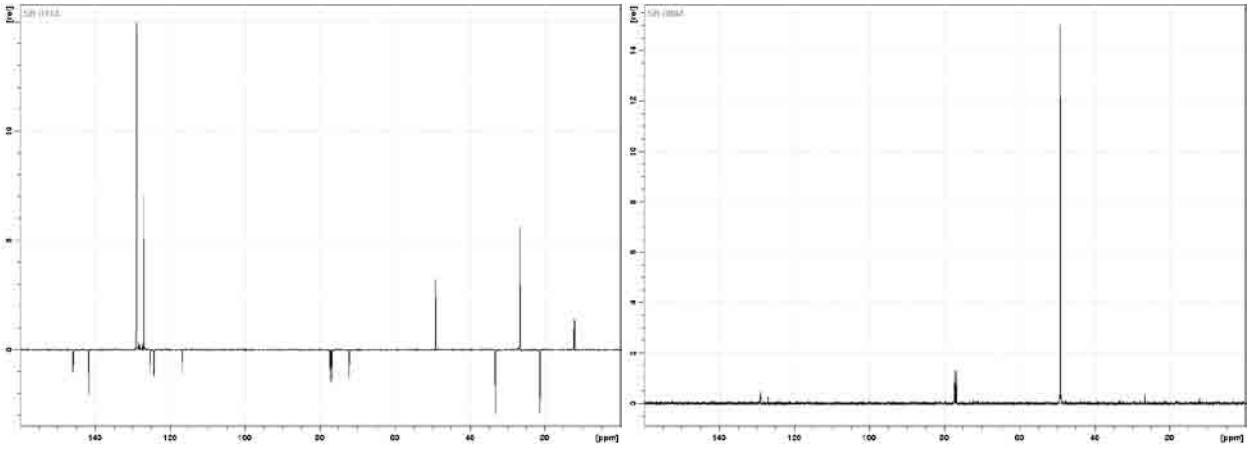

Figure 65: Exemplary NMR spectra of unlabeled 52 (left, APT) and labeled 53 (right, ^{13}C). The intensity gain of C-5a is evident: The spectrum on the left was obtained by accumulating 10240 scans, the spectrum on the right by only 4 scans. The peak of C-5a at 49 ppm is by roughly two orders of magnitude more intensive than the peaks of the other carbon atoms.

The oxidation of **52** resulted in an unknown compound of which the xanthene structure **54** was suggested by NMR spectroscopic experiments. This compound would have basically the same structure as biphenyl-α-tocopherol model but with an additional diaryl ether bond. To prove the suspected structure and to have reference material for characterization, synthesis of an authentic sample was performed.

Since the reaction pathway that leads to the parent compound biphenyl-α-tocopherol model had already been identified, it was plausible to establish the diaryl ether bond first, construct a benzhydrol moiety and then connect it to the tocopherol moiety (Figure 66). For ether formation an arylation reaction that is promoted by copper and a tertiary base like triethylamine was chosen.[105] The crude product obtained after aqueous workup was directly reacted with phenylmagnesium bromide. Purification by column chromatography yielded **55**, a compound that contains both the benzhydrol and the γ-tocopherol model to be reacted in the next step. **55** was dissolved in dry THF, a small amount of sulphuric acid was added and the solution was evaporated *in vacuo*. This facile treatment gave the target xanthene **54** derivative quantitatively.

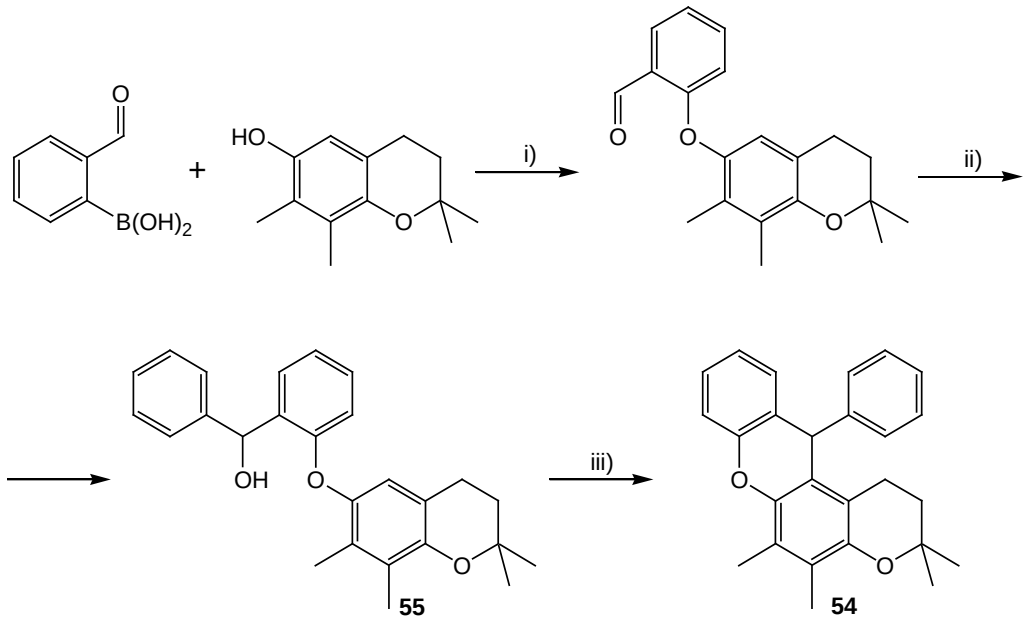

Figure 66: Synthesis of xanthene derivative 54. i) NEt_3, $Cu(OAc)_2$, 4 Å molsieve, DCM. ii) PhMgBr, THF. iii) H_2SO_4, THF.

The comparison of the spectroscopic data of both the authentic sample from the oxidation of 52 and the synthesized standard proved unambiguously that both structures were identical.

Results and Discussion

For the actual experimental studies on the detailed mechanisms of oQM formation, the tocopherol derivatives were oxidized with silver oxide in $CDCl_3$ at low temperatures while NMR spectra were recorded continuously. The change of shift of the labeled C-5a of **53** was most valuable, since this atom is at first an sp^3-hybridized alkyl carbon (49 ppm), then a highly deshielded carbocation of the suspected twitterionic intermediate (205 ppm), then part of the olefinic, exocyclic bond in the oQM-structure (128 ppm) and finally alkylic again in the stable product xanthene (43 ppm). At each stage the electronic environment of C-5a is fundamentally changed, and these changes are exemplarily reflected along all intermediate compounds by the NMR-shift of the ^{13}C-labeled C-5a.

Stabilization by Mechanical Effects only

Every bond rotation is hindered by sterical, mechanical and electronical factors. The steric hindrance of the C5-C5a bond rotation (as required during oxidation to the oQM) of α-tocopherol derivatives depends primarily on the nature of the substituents at C-5a (Figure 67). PMC bears the smallest possible substituents at this position: hydrogen atoms. These can smoothly pass the obstacles of the methylene at C-4 and the hydroxy group at O-6. Bigger substituents as alkyl chains or cyclic structures would have more difficulties to get past these moieties and would require a harder push to make

rotation possible. This push is most often provided by thermal energy, which means that at low temperature a hindered rotation might substantially slow down or even stop.

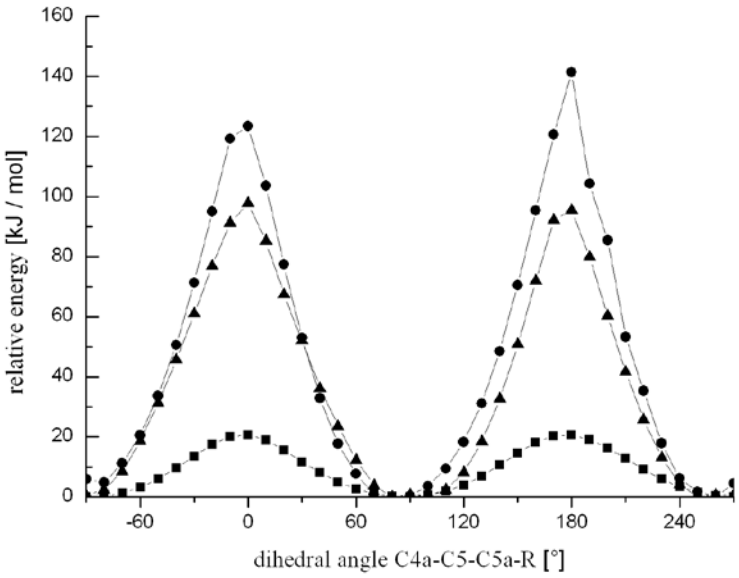

Figure 67: Exemplary rotational barriers of the zwitterions / oQMs of 4 (■) , 52 (▼) and 51 (●). For the calculation a pure molecular mechanics method that does not consider electronic effects was chosen to illustrate the mechanical barrier only. Both the alkyl chain of 51 and the phenyl rings of 52 clearly increase the steric hindrance. The flat phenyl rings can avoid collision with the chromanol skeleton more easily than the tetrahedral methylenes of the alkyl chains.

The formation of oQM is directly linked to the rotation of the substituents at C-5 into the plane of the aromatic ring, therefore a significant deceleration of oQM-formation from sterically hindered zwitterions as the ones derived from **51** and **52** was expected.

In 5-(4-octyl)-γ-tocopherol (5a-butyl-5a-propyl-α-tocopherol, **51**) the octyl group acts as a flywheel which impedes the rotation of the C-5a moiety into the ring plane as compared to the parent zwitterions with the unsubstituted exocyclic methylene group. The situation is comparable with a platform diver performing a somersault (Figure 68). In straight position the rotation will be much slower than in pike position. And concentrating the mass at the center by folding up completely in tuck position will give the fasted rotation due to a minimized torsional moment. Similarly, an exocyclic methylene group will undergo rotation much faster than the propyl-butyl substituted C-5a in the zwitterion derived from **51**.

Figure 68: Three platform divers in different dive positions and rotating at different speeds: straight (slowest), pike, tuck (fastet).

Following Ag_2O oxidation at -78°C, these steric and mechanical effects caused the formation of the oQM to be about 18 times slower from **51** than from **4** as evidenced by NMR. Also in the presence of the bisylide as stabilizing agent, the complexes derived from octyl derivative **51** degraded about 10 times slower than complex **47**.

Stabilization by Additional Electronic Effects

A most illustrative example for the stabilization of the zwitterionic intermediate by electronic and steric effects in the formation of oQMs is the 5a,5a-diphenyl-α-tocopherol derivative **52**. In the zwitterionic intermediate **52a** derived from this compound both steric and electronic effects are active, which stabilize the out-of-plane zwitterions and destabilize the in-plane oQM **56**. The C-5–C-5a bond in **52a** cannot freely rotate unless the two phenyl rings are concomitantly moved into a position perpendicular to the chroman plane which allows their passage over the chroman system. In this orientation the phenyl ring cannot add to a conjugative stabilization of the oQM. The oQM **56** is thus destabilized by combination of disfavorable effects on the bond rotation – the steric demand of the phenyl substituents and the flywheel effect of large substituents that was also active in the case of the octyl derivative **51** discussed above – and also by electronic effects, such as the missing conjugative stabilization of the in-plane (oQM) geometry.

However, the most decisive influence on the reactivity of this compound is the electronic effect of the two phenyl rings which is strongly stabilizing the positive charge. In principle the compound is a derivative of triphenyl methane, in which the positive charge usually experiences strong stabilization by the phenyl substituents. The zwitterionic intermediate is thus favored by both impeded rotation and by strong resonance stabilization of the positive charge. This favoring of the zwitterions **52a** and the disfavoring of the oQM **56** are so strong that the usually wide energetic gap between the two forms, corresponding to the gap between aromaticity and quinoid structure, is diminished and the zwitterion even becomes energetically equal. This was also demonstrated by means of NMR kinetics in combination with isotopic labeling at C-5a.

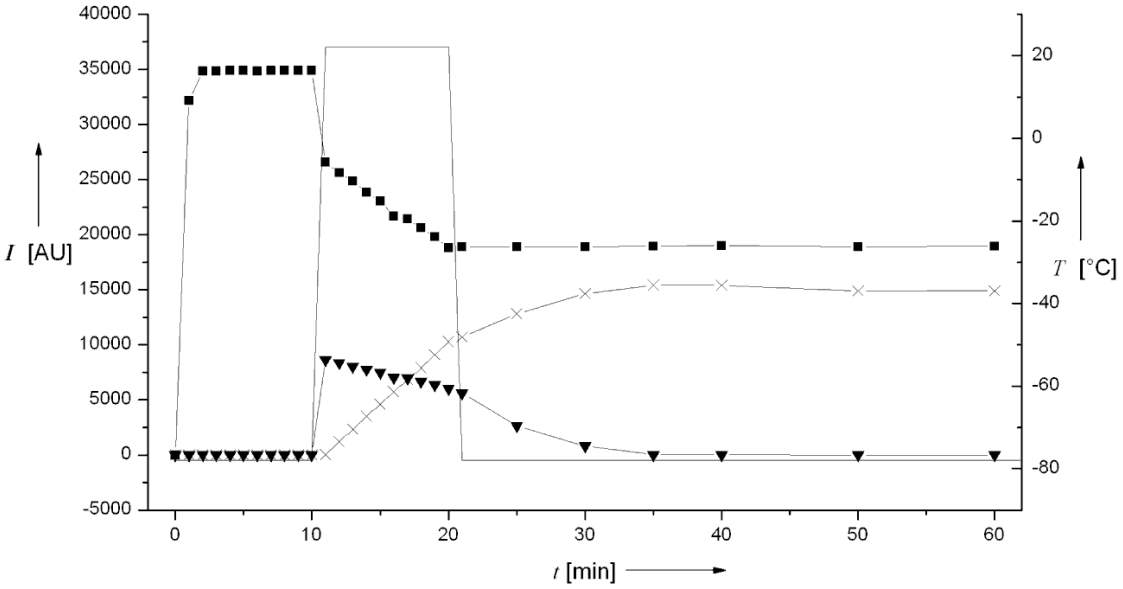

Figure 69: ^{13}C NMR signal intensities of zwitterion 52a (■), oQM 56 (▼) and xanthen 54 (×). At a temperatur (—) of -78°C zwitterion 52a is indefinitely stable. Rising the temperature to 22°C gives sufficient thermal energy to overcome the rotational barrier and turn the zwitterion into the oQM 56. This is quickly transformed into xanthen 54, the final product of this monomolecular reaction. Cooling to -78°C again stops the conversion of the zwitterion to the oQM and preserves the remaining zwitterion, whereas the still present oQM is slowly converted into the xanthene.

When oxidized at low temperature (Figure 69) the labeled compound showed one resonance at 205 ppm, corresponding to the carbocation in the zwitterionic intermediate **52a**. Thus, with this special derivative, the occurrence of a zwitterionic intermediate in the oxidation of *ortho*-alkylphenols to the corresponding oQM was directly, i.e. by direct spectroscopic observation, proven for the first time.

At increased temperatures a second resonance, that of the oQM form **56**, appeared at 128 ppm. The resonance is typical of an exocyclic methylene group. From this form, the main reaction path leads to the xanthene derivative **54** (43 ppm) which is the final stable product. It should be mentioned that spiro-dimerization, the usual reaction pathway of the oQM in the absence of coreactants, does not occur in the case of **56** due to the extreme steric crowding at C-5a. The xanthene product is not formed from the zwitterionic derivative **52a**, but only from the oQM form **56**. The interrelation between the three compounds was nicely shown with the help of the ^{13}C resonances by the following sequence: low-temperature oxidation afforded the zwitterionic **52a** only. When this was heated to r.t. for a few seconds, an equilibrium between **52a** and oQM **56** was established (two ^{13}C resonances visible) and at the same time generation of the xanthene **54** set in (the third signal appearing). During this period the ratio of the intensitites of the zwitterion´s and the oQM´s signal was constantly 3.08:1. By Arrhenius´ equation (equation 1) it was thus possible to determine the rotational barrier as 2.7 kJ/mol.

Renewed cooling to -78°C stopped the conversion of the zwitterion **52a** into the oQM **56**, but conversion of the oQM **56** into the xanthene **54** continued: the resonance at 205 ppm was unchanged,

while the resonance at 128 ppm disappeared at the expense of that at 43 ppm (Figure 69, Figure 70). Upon heating to room temperature for several hours, only the resonance of the xanthene **54** remained, with all zwitterion **52a** being converted into this compound *via* the oQM **56**.

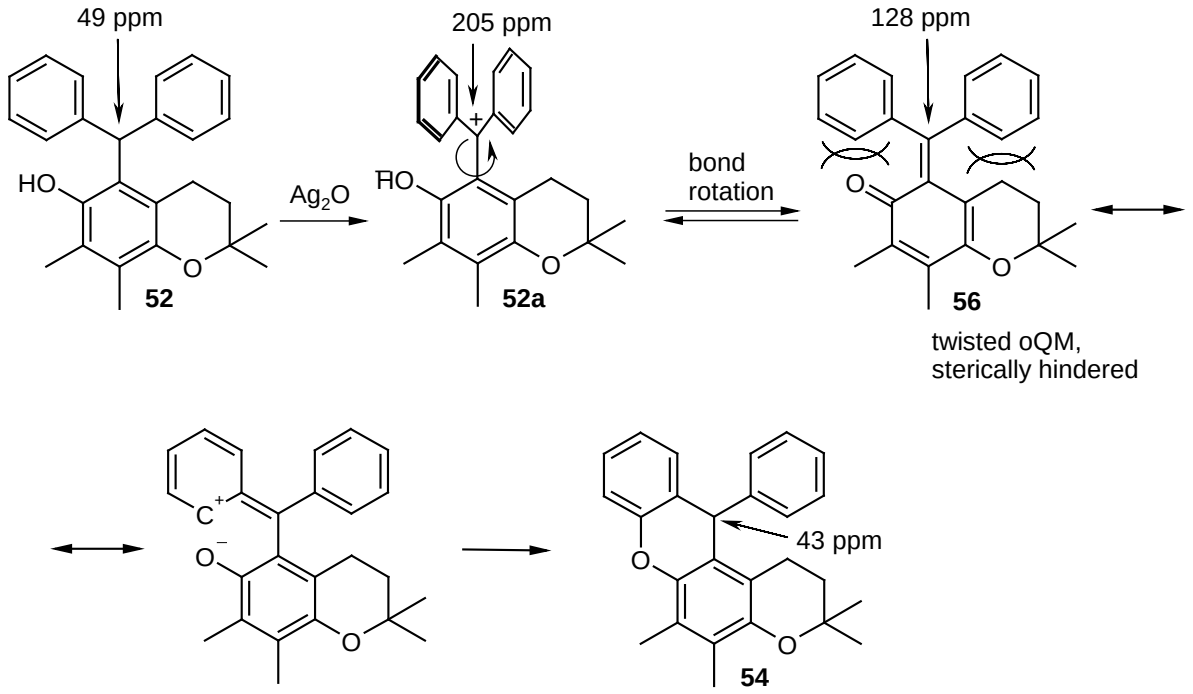

Figure 70. Summary of the ^{13}C-NMR shifts of the carbon at C-5a. They reflect the electronic environment of the atom and change dramatically during the oxidation of the model compound.

The diphenyl derivative **52** – due to its peculiar property to form equally stable zwitterion and oQM species – was a nice probe to search for conditions stabilizing the zwitterionic form. Solvent effects, for instance, were readily detected. The rates of conversion from the zwitterions into the oQM were roughly 13:8:1 when going from C_6D_6 to $CDCl_3$ to DMSO-d_6, evidently reflecting the stabilizing effect of polar solvents on the zwitterionic stage. Concluding from the stabilizing effect of amine *N*-oxide[90] and the bis(sulfonium ylide)[97] a stabilizing effect of solvents containing salts and of ionic liquids was expected. However, this stabilizing effect was only moderate, with the zwitterion-to-oQM conversion being about 22-34 times faster in C_6D_6 than in common BMIM-type ionic liquids with different anions. It was speculated that the two opposite charges in the stabilizing agent must be arranged in quite close proximity and must be quite localized to exert a large stabilizing effect. This is the case in amine *N*-oxides and in the sulfonium ylide, but not in the case of the bulky ions and additionally delocalized charges, as in the case of ions with solvent shells and ionic liquids, respectively.

Conclusions

For the first time the zwitterionic intermediate in the formation of oQMs from the parent *ortho*-alkylphenols could be observed directly by spectroscopic means without the addition of stabilizing

molecules. Steric hindrance alone was sufficient to result in an 18 times slower oQM-formation for **51**. Additional electronic effects in **52** stabilized the zwitterionic intermediate indefinitely at -78°C. At room temperature the conversion to oQM was slow enough to determine its activation energy. Oxidation rates were found to be solvent dependent, with polar solvent having a stabilizing effect on the zwitterion. By means of ^{13}C-labeling all stages of the oxidation reaction – starting material, zwitterion, oQM, oxidation product – could be observed simultaneously and kinetics became accessible. The oxidation product, a xanthene derivative, was fully characterised and its properties confirmed by total synthesis.

The occurrence of a zwitterionic intermediate upon oQM formation is one major result going far beyond tocopherol chemistry and reaching into the realm of fundamental concepts in chemistry, such as aromaticity and antiaromaticity. The finding requires revision of the decade-old, conventional teaching about oQM formation and oQM chemistry. The fact that a simple rotation around a single bond can act as a quasi switch between aromaticity and antiaromaticity might in future allow to construct molecular switches, to assemble uniformly moving molecular arrays or to drive molecular machines by the absorption energy of aromatic / antiaromatic structures.

Chemo- and Regioselectivity in the oQM Formation from Tocopherol[42]

oQM *versus* "5a-Chromanolmethyl" Radicals

In the early days of vitamin E research and up to the late 1980s the radical reactions of the tocopherols were given wide attention, and all other chemical conversions of these compounds were seen as perhaps academically interesting, but negligible side reactions which do not significantly contribute to the main reactivity picture. In the late 1980s this notion slowly started to change, and in 2007 it was shown that a major part of the reactions commonly assigned to hypothetical tautomers of the tocopheroxyl radical **5** in fact had been wrongly attributed to this primary intermediate, since they are actually reactions of another primary intermediate, the oQM **6**.[40] This changed the perception of basic tocopherol chemistry quite drastically, but also promoted the "appreciation" of the oQM **3** as a central species in tocopherol chemistry.

The occurrence of a 5a-*C*-centered tocopherol-derived radical **57**, often called "chromanolmethide radical" or "chromanolmethyl radical", had been postulated in literature articles dating back to the early days of vitamin E research,[106-113] which have been cited or supposedly reconfirmed later (Figure 5).[114-117] In some accounts, radical structure **57** has been described in the literature as being a resonance form (canonic structure) of the tocopheroxyl radical, which of course is inaccurate. If indeed existing, radical **57** represents a tautomer of tocopheroxyl radical **5**, being formed by a chemical reaction, namely a 1,4-shift of one 5a-proton to the 6-oxygen, but not just by a „shift of electrons" as in the case of resonance structures (Figure 71). In all accounts mentioning α-tocopherol-derived *C*-centered radicals, the spin density was described to be centered at 5a-C, but not at alternative carbons, such as 7a-C or 8b-C. The occurrence of 5a-*C*-radicals was concluded from experimental observations which seemed to support 5a-*C*-radicals.

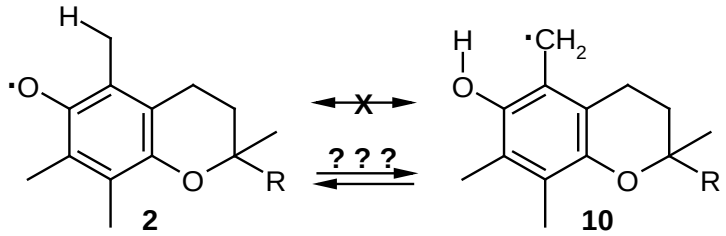

Figure 71. The hypothetical chromanolmethide radical 57 - a tautomer of α-tocopheroxyl radical 5.

Basically, three reactions were evoked to support the occurrence of 5a-*C*-centered radicals **57** in tocopherol chemistry. The first one is the formation of 5a-substituted derivatives in the reaction of α-

tocopherol **1** with radicals and radical initiators. The most prominent example is here the reaction of **1** with dibenzoyl peroxide leading to 5a-α-tocopheryl benzoate (**58**) in fair yields, so that a "typical" radical recombination mechanism was postulated (Figure 72). Similarly, low yields of 5a-alkoxy-α-tocopherols were obtained by oxidation of α-tocopherol with *tert*-butyl hydroperoxide or other peroxides in inert solvents containing various alcohols,[118,119] although the involvement of 5a-*C*-centered radicals in the formation mechanism was not evoked as explanation in these cases.

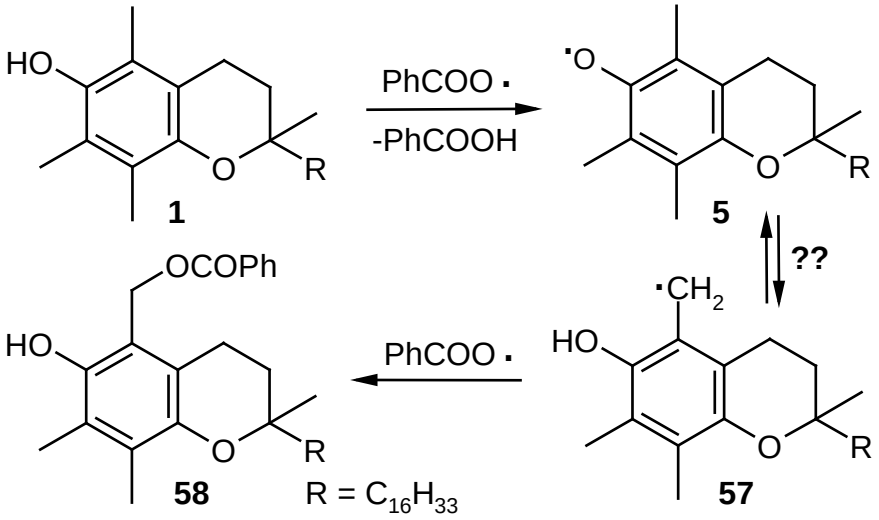

Figure 72. Hypothetical radical mechanism for the formation of 5a-α-tocopheryl benzoate (58) by reaction of α-tocopherol (1) with dibenzoyl peroxide.

The second observation cited as evidence for a radical mechanism involving radical 5 is the frequent occurrence of ethano-dimer **59**, proposed to proceed by recombination of two 5a-*C*-centered radicals **57** (Figure 73).[117,120,121]

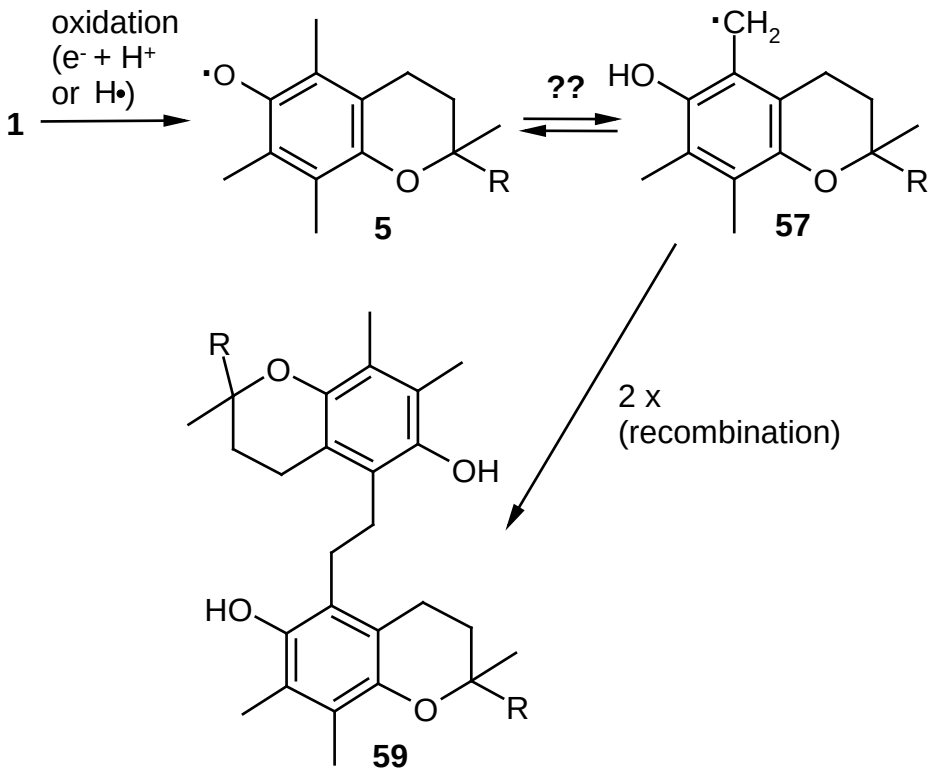

Figure 73. Formation of α-tocopherol ethano-dimer (59) as the result of a hypothetical radical recombination of two radicals 57.

The third fact that seemed to argue in favor of the occurrence of radicals **57** was the observation that reactions of α-tocopherol under typical radical conditions, i.e. at the presence of radical initiators in inert solvents or under irradiation, provided also large amounts of two-electron oxidation products such as oQM **6** and its spiro-dimerization product **8** (Figure 74).[112,120,121] This was taken as support of a disproportionation reaction involving α-tocopheroxyl radical **5** and its hypothetical tautomeric chromanolmethide radical **57**, affording one molecule of oQM **6** (oxidation) and regenerating one molecule of **1** (reduction). The term "disproportionation" was used here to describe a one-electron redox process with concomitant transfer of a proton, i.e. basically an H-atom transfer from hypothetical **57** to radical **5**.

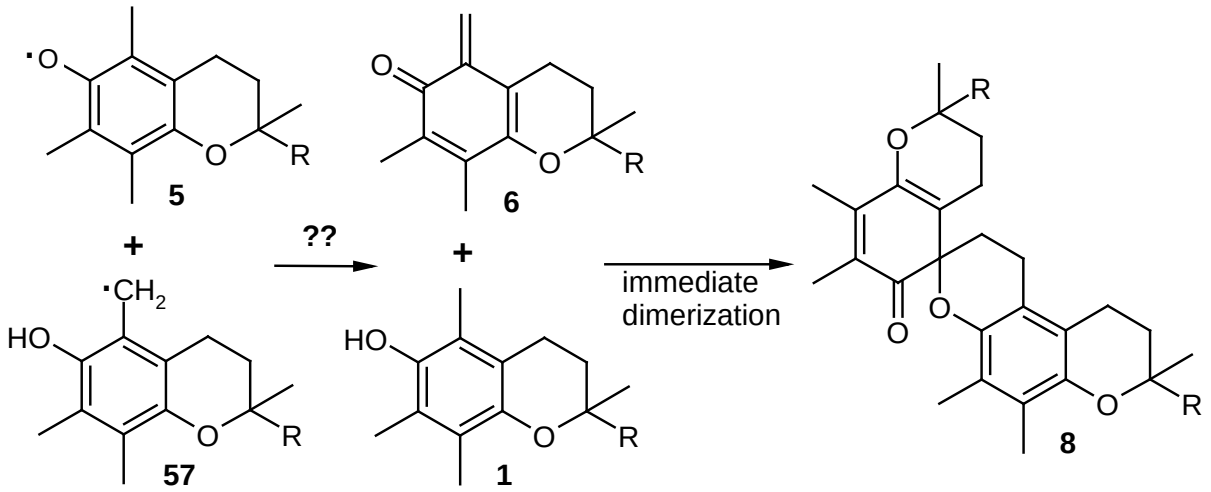

Figure 74. Hypothetical disproportionation of two α-tocopherol-derived radicals 5 and 57 in the absence of other coreactants to account for the formation of typical two-electron oxidation products (oQM 6, α-tocopherol spiro-dimer 8).

By a combination of synthetic approaches, isotopic labeling, using tocopherols with ^{13}C-labeling at C-5a and C-7a, ESR spectroscopy, and high level DFT computations it was shown that there is no radical formation at either C-5a or C-7a, and that chromanolmethide radical **57** does not occur in tocopherol.[40] ESR failed to detect those species, and computations predicted only negligibly different formation energies for the hypothetical C-5a radicals and C-7a radicals, respectively. Thus, if radicals at 5a-C and 7a-C were involved in tocopherol chemistry, then products of both species would have to be expected. The fact that in reality products of 5a-C are highly preferred over those of 7a-C – or are even formed exclusively – were already seen as an indirect proof of the underlying chemistry not being radical by nature.

The formation of 5a-α-tocopheryl benzoate (**58**) upon reaction of α-tocopherol (**1**) with dibenzoyl peroxide, which has usually been taken as "solid proof" of the involvement of 5a-*C*-centered radicals in tocopherol chemistry (see Figure 72), was shown to proceed according to a non-radical, heterolytic mechanism involving oQM **3** (Figure 75).

The initiator-derived radical products generate α-tocopheroxyl radicals (**5**) from α-tocopherol (**1**). The radicals **5** are further oxidized to *ortho*-quinone methide **6** in a formal H-atom abstraction, thereby converting benzoyloxy radicals to benzoic acid and phenyl radicals to benzene. The generated oQM **6** adds benzoic acid in a [1,4]-addition process, whereas it cannot add benzene in such a fashion. This pathway accounts for the observed occurrence of benzoate **58** and simultaneous absence of a 5a-phenyl derivative and readily explains the observed products without having to involve the hypothetical *C*-centered radical **57**.

To conclusively disprove the involvement of the chromanolmethide radical, the reaction of α-tocopherol with dibenzoyl peroxide was conducted in the presence of a large excess of ethyl vinyl

ether used as a solvent component. If 5a-α-tocopheryl benzoate (**58**) was formed homolytically according to Figure 72, the presence of ethyl vinyl ether should have no large influence on the product distribution. However, if **58** was formed heterolytically according to Figure 75, the intermediate oQM **6** would be readily trapped by ethyl vinyl ether in a hetero-*Diels-Alder* process with inverse electron demand,[90,122] thus drastically reducing the amount of **58** formed. Exactly the latter outcome was observed experimentally. In fact, using a tenfold excess of ethyl vinyl ether relative to α-tocopherol and azobis(isobutyronitrile) (AIBN), no 5a-α-tocopheryl benzoate (**58**) at all was formed but only the corresponding trapping product **60**.

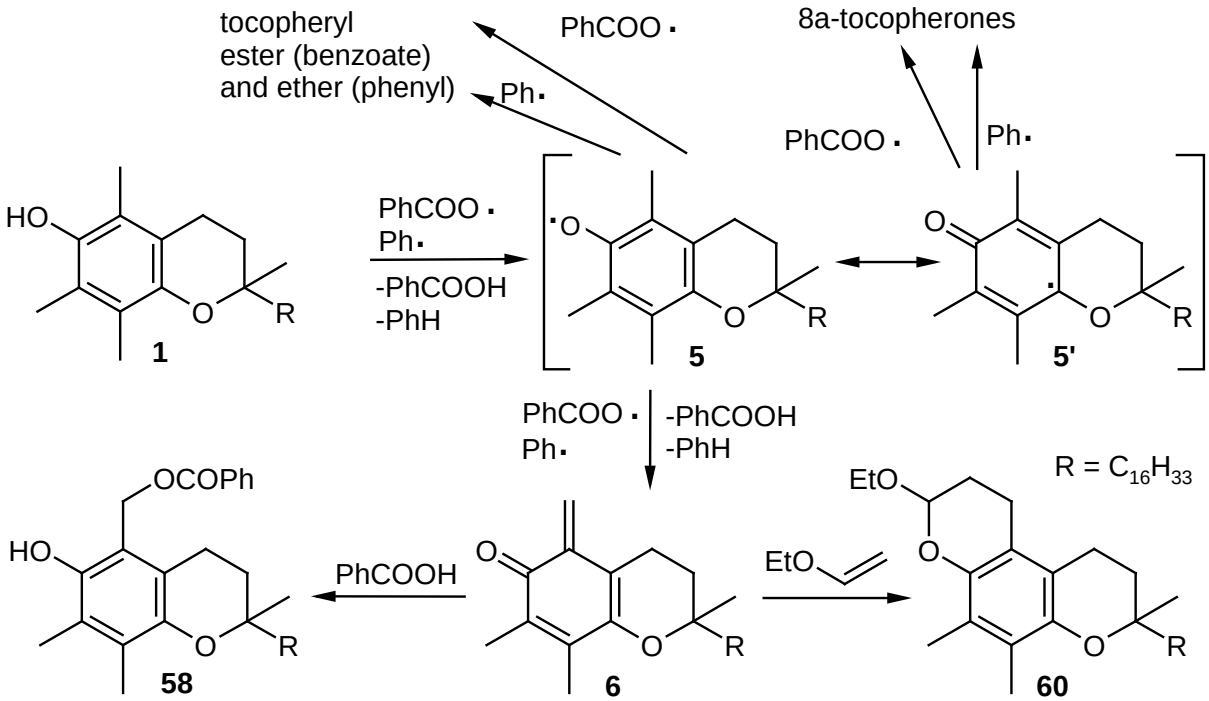

Figure 75. Confirmed heterolytic formation pathway for 5a-α-tocopheryl benzoate (58) without involvement of 5a-*C*-centered radicals and its proof by trapping of *ortho*-quinone methide 6 with ethyl vinyl ether to pyranochroman 60. Shown are the major products of the reaction of α-tocopherol (1) with dibenzoyl peroxide.

Also for the reaction that was described as "dimerization" of the chromanolmethide radicals **57** to the ethano-dimer of α-tocopherol 12, the involvement of the C-centered radicals has been disproven and these intermediates lost their role as key intermediates in favor of the oQM **6**. It was experimentally shown that ethano-dimer **59** in hydroperoxide reaction mixtures of α-tocopherol was formed according to a more complex pathway involving the reduction of the spiro-dimer **8** by α-tocopheroxyl radicals **5**, which can also be replaced by other phenoxyl radicals (Figure 76).[40] Neither the hydroperoxides themselves, nor radical initiators, such as AIBN, nor tocopherol alone were able to perform this

reaction, but combinations of tocopherol with radical initiators generating a high flux of tocopheroxyl radicals **5** afforded high yields of the ethano-dimer **59** from the spiro-dimer **8**.

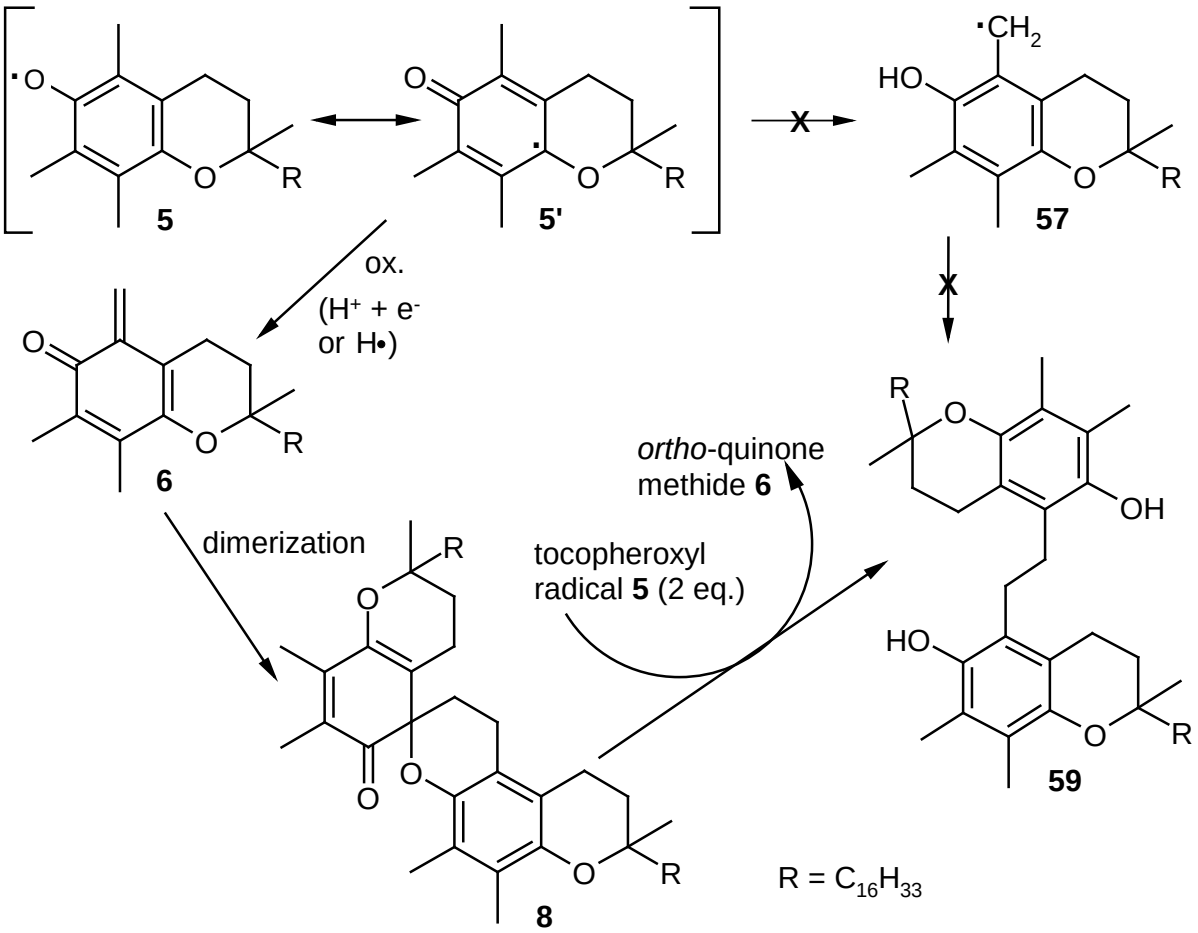

Figure 76. Confirmed generation of ethano-dimer 59 by reduction of spiro-dimer 8 in different reaction systems. 5a-*C*-centered radicals 57 are not involved in this process.

The last reaction commonly evoked to support the involvement of radical species **57** in tocopherol chemistry is the "disproportionation" of two molecules into the phenol α-tocopherol and the *ortho*-quinone methide **6** (Figure 74), the latter immediately dimerizing into spiro-dimer **8**. This dimerization is actually a hetero-*Diels-Alder* process with inverse electron demand. It is largely favored which is also reflected by the fact that spiro-dimer **8** is an almost ubiquitous product and byproduct in vitamin E chemistry.[43,123] The disproportionation mechanism was proposed to account for the fact that in reactions of tocopheroxyl radical **5** generated without chemical coreactants, i.e. by irradiation, the spiro-dimer **8** was the only major product found.

An alternative pathway (Figure 77) was proved, which did not involve the dubious 5a-*C*-centered radical **57**, but instead only the well-documented and theoretically sound structure of tocopheroxyl radical **5** and its major canonic form **5'**. According to general tocopherol chemistry (*cf* page 27), **5** and **5'** will recombine in the absence of other coreactants to afford a labile 8a-α-tocopheryl-tocopherone

(**61**), which undergoes [1,4]-elimination to afford α-tocopherol (**1**) and *ortho*-quinone methide **6**, by analogy to other 8a-tocopherones.[124-126] oQM **6**, once formed, will immediately dimerize into spiro-dimer **8** in inert media. This pathway explains the observed product readily on the basis of general tocopherol chemistry without the need to evoke the 5a-*C*-centered radical **57**. The important coupling intermediate **61** was isolated under special chromatographic conditions – elution from finely powdered potassium carbonate with *n*-hexane – and was shown to decompose into α-tocopherol and its spiro-dimer extremely readily, this decomposition being exactly the outcome of the alleged "radical disproportionation".

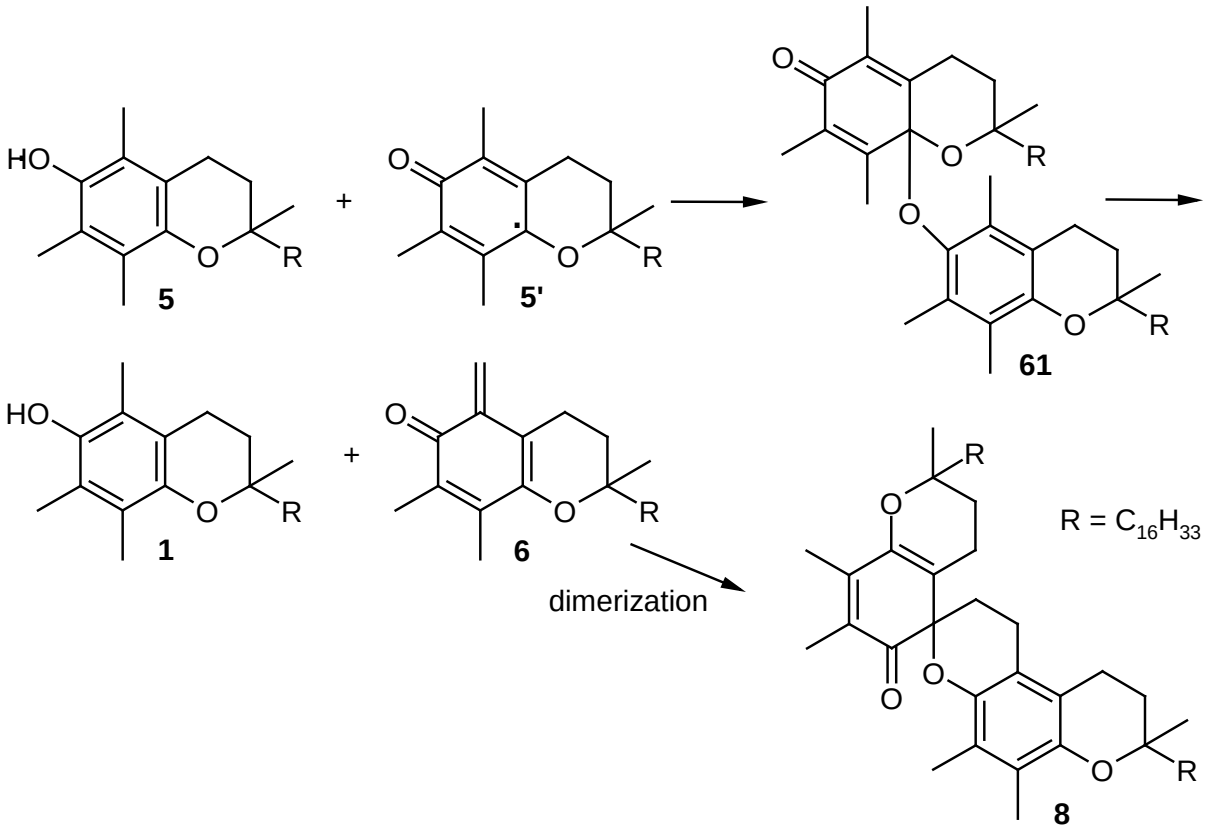

Figure 77. Confirmed pathway for the observed "disproportionation" of tocopheroxyl radical 5 into α-tocopherol (1) and oQM 6, the latter immediately dimerizing into α-tocopherol spiro-dimer (8). 5a-*C*-centered radicals 57 are not involved in this process.

The above described experiments, calculations and theroretical considerations showed that there is no theoretical or experimental evidence whatsoever for the 5a-*C*-centered radical **57**. All relevant reactions can be traced back to occurrence and reactions of oQM **6** as the central intermediate. The three reactions commonly cited to support the occurrence of the chromanol methide radical **57** in vitamin E chemistry (Figure 72 - Figure 74), are actually typical processes of the oQM intermediate (Figure 75 - Figure 77).

The questions whether 5a-*C*-centered radicals exist in oxidation chemistry of α-tocopherol and whether mechanisms proposed in early days of vitamin E research are correct might appear academic

at a first glance, but as soon as one recalls the immense medical, physiological, and economic importance of α-tocopherol and its derivatives, the significance of an exact knowledge about their basic chemistry becomes obvious. By analogy to the Mills-Nixon theory in tocopherol chemistry having been replaced by the concept of strain-induced bond localization (SIBL) recently (see next subchapter), the condoned involvement of 5a-*C*-centered radicals in oxidation reactions of α-tocopherol must be revised. The confirmed alternative heterolytic pathways involving the oQM **6** will certainly soon find their general acceptance in tocopherol chemistry.

Regioselectivity in the Oxidation of α-Tocopherol – up-oQM versus down-oQM

According to literature accounts, oxidation chemistry of α-tocopherol (**1**) and PMC (**4**) regioselectively involves C-5a, where the *ortho*-quinone methide **6** is formed, the so-called "up"-oQM (Figure 78). The isomeric compound with the exo-methylene group at C-7a ("down"-oQM) was reportedly not observed.[127,128] Usually, the so called "Mills-Nixon effect" reported for the first time in 1930,[129] is given as explanation for the regioselectivity observed,[130,131] whereas the formation of other regioisomers than the "up"-oQM was reported only very rarely.[43] The original work by Mills and Nixon, after which the effect is named, is based on three theories, today known as erroneous:

1) aromatic systems consist of two bond-shift isomers that are in equilibrium,

2) the van't-Hoff model of carbon, which implies that all the angles around the carbon are tetrahedral. Together with the first assumption, annulation of differently sized rings will shift the equilibrium between the equilibrating mesomers of benzene to that isomer which possesses the least strained angle, i.e., as close as possible to 109.5°,

3) The mechanism for electrophilic aromatic substitution is addition–elimination. Using these working hypotheses Mills and Nixon explained the regioselectivity of electrophilic substitution in 5-hydroxyindan versus 6-hydroxytetralin.

Applying the Mills-Nixon explanation to vitamin E, it is usually argued that the annulation of a pyran or furan structure to the trimethyl-substituted phenol ring causes bond localization in the aromatic part of the corresponding α-tocopherol-type benzochromanol or benzofuranol. The term "α-tocopherol-type" refers to compounds derived from trimethylhydroquinone, i.e. having three methyl substituents at the aromatic ring. Upon oxidation, only that one of the two possible oQMs is formed, which requires as little rearrangement of the π-frame (double bonds) as possible (Figure 78). In α-tocopherol-type benzo*pyranols* (chromanols), the three double bonds in the aromatic ring are positioned so that one is placed at the annulation site: the *ortho*-quinone methide will thus be formed involving C-5a (the "up"-oQM). In α-tocopherol-type benzo*furanols*, the three aromatic double bonds are positioned in a way that the annulation bond is a single bond: the favored *ortho*-quinone methide

will be at C-7a, (the “down”-oQM). Thus, a widely accepted postulate was derived, which was frequently repeated throughout the literature: tocopherol-type chromanols are regioselectively oxidized at C-5a to form “up”-oQMs, whereas tocopherol-type benzofuranols are always oxidized at C-7a to form “down”-oQMs. The strict regioselectivity is due to the different ring size of the alicycle and due to the electronic effect of the alicyclic ring exerted on the aromatic. Clearly, this explanation, which rested on theories today known as erroneous, was considered insufficient.

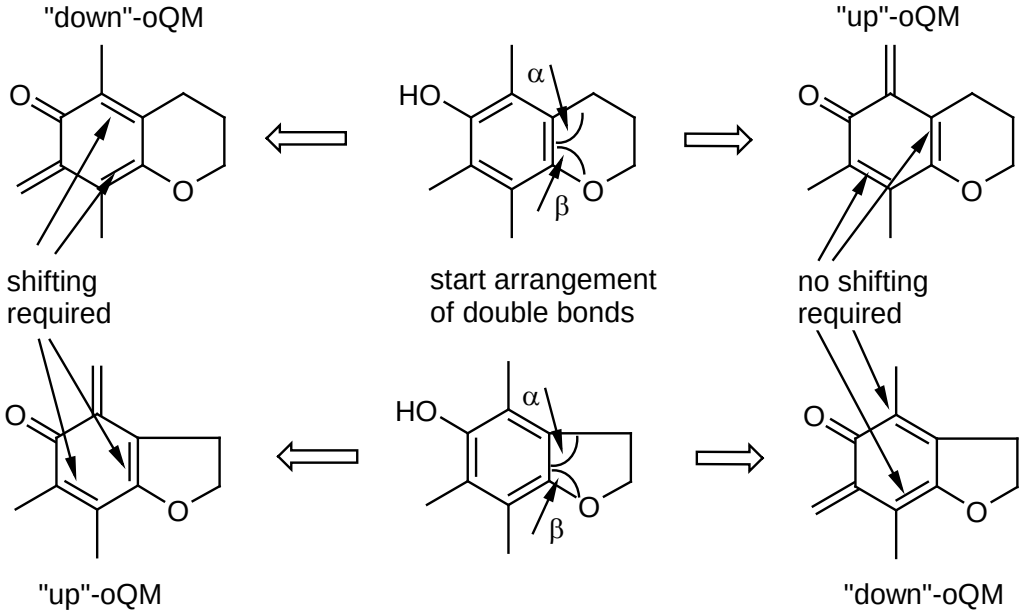

Figure 78. Traditional application of the “Mills-Nixon effect” theory to α-tocopherol-type benzopyranols and benzofuranols, having an anullation angle sum of (α + β).

The issue of regioselectivity in oxidations of α-tocopherol-type antioxidants – being an open question for more than 70 years – was recently clarified by a combined experimental and theoretical study.[44] The approach was based on measuring the ratio between the “down”-oQM and “up”-oQM products obtained upon oxidation of ten α-tocopherol-type antioxidants (**1**, **62a-i**), which carried differently sized alicycles (Figure 79). Thus, in these compounds the electronic effects were kept constant and only the angular strain of the systems was changed, as seen by the (α+β)-values, which cover an angle range between 219° (for **62a**) to 246° (for **62i**), see Figure 78, Figure 80 and Table 2. In addition, tetrasubstituted hydroquinones (**63a-b**) carrying similar substituents as α-tocopherol – but no annulated ring – were used, which thus exhibited the same electronic substituent effects, but no angular strain influence.

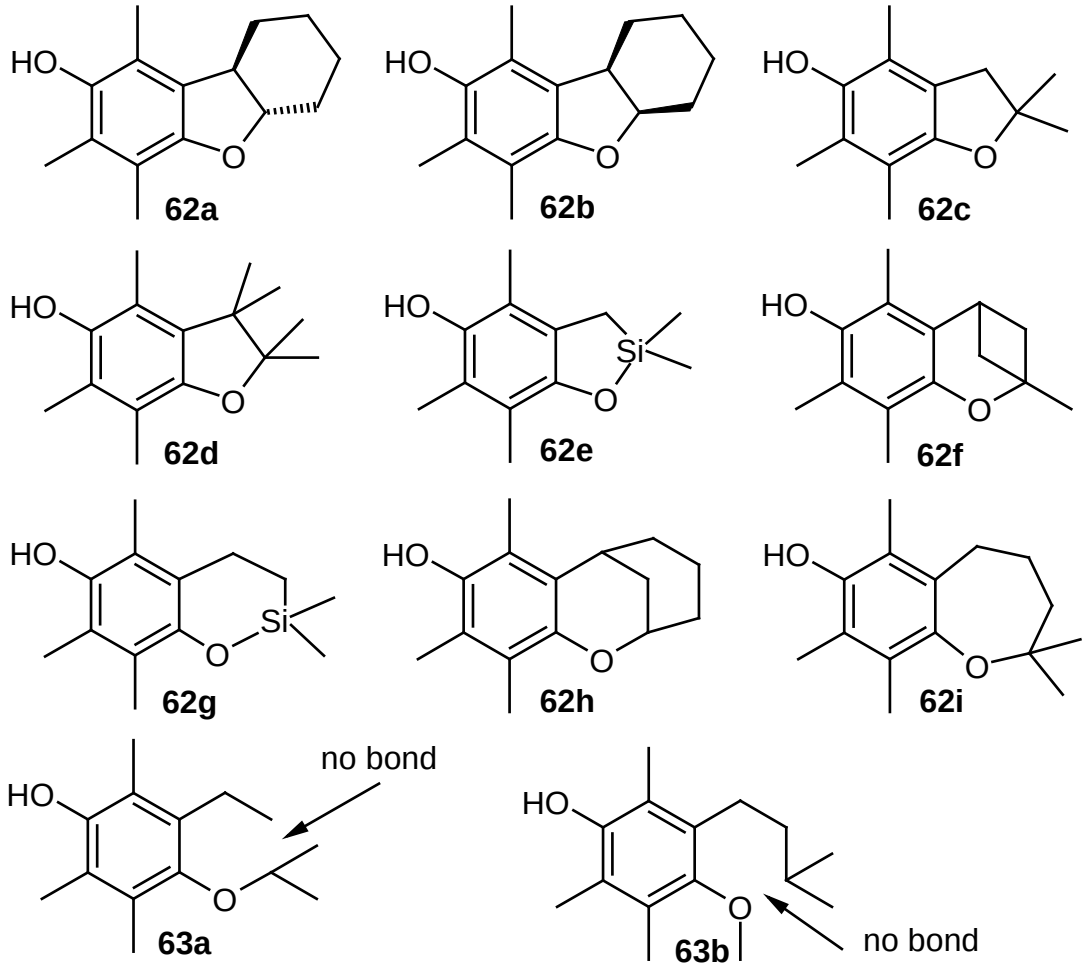

Figure 79. α-Tocopherol-type benzofurans and benzopyrans having different strain in the alicyclic ring (62a-i) and non-anullated α-toocpherol-type hydroquinones (63a-b).

The model compounds were oxidized to the corresponding oQMs, which were trapped by the fast reaction with ethyl vinyl ether (Figure 80). Product analysis provided the ratio between the two oQMs intermediates, and by measuring the ratio between the trapped "up"-oQMs and "down"-oQMs at different temperatures the activation energy difference for the formation of the two intermediates was obtained. The outcome proved unambiguously that the regioselectivity, i.e. the ratio between "up"-oQM and "down"-oQM, was not a function of the ring size: it changed gradually, but not abruptly when going from a six-membered to a five-membered ring systems, in contrast to what has been assumed so far and what was derived from the Mills-Nixon postulate (Table 2). The "up"-oQMs were increasingly favored when going from small (α+β)-values to large ones, with down-oQMs showing the opposite trend. The data clearly disproved the notion that vitamin E-related benzofuranols form only one oQM (the "down"-form), while the chromanols give only the opposite one ("up"-oQMs).

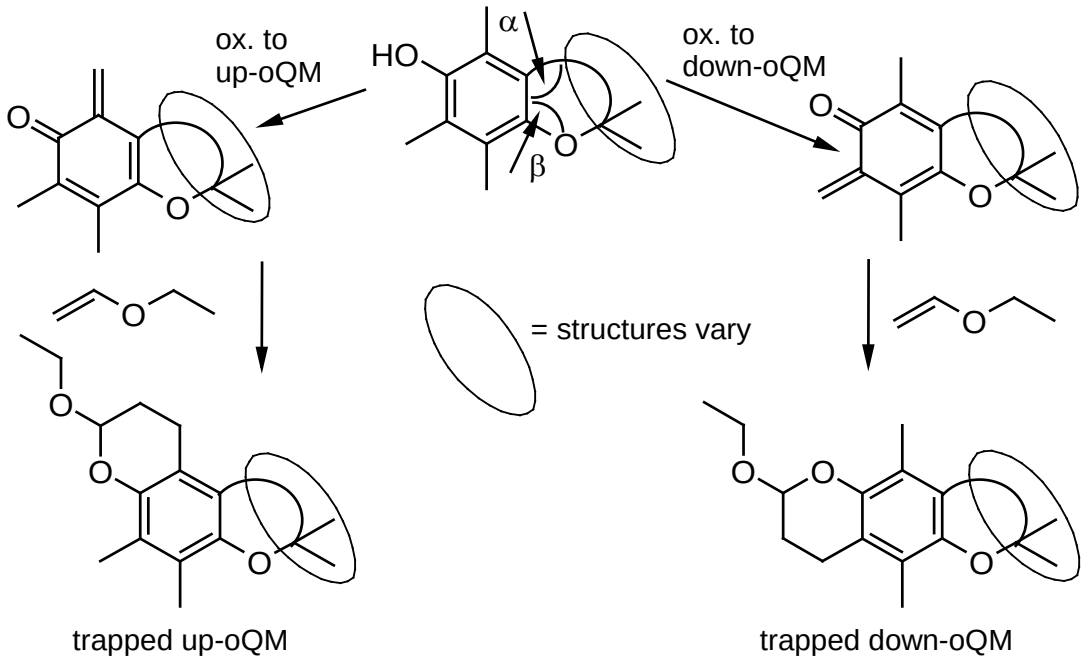

Figure 80. Oxidation of PMC-derivatives with different ring strain to mixtures of two possible *ortho*-quinone methides: the oxidation behavior and the ratio of the formed oQMs agreed fully with the theory of strain-induced bond localization (SIBL).

Cpd.	(α+β)	up-oQM [%, 373 K]	down-oQM [%, 373 K]	$\Delta\Delta H^{\ddagger}$ [kcal mol^{-1}]
62a	219	0.9	99.1	3.49±0.12
62b	221	2.3	97.7	2.86±0.08
62c	221	14.9	85.1	1.22±0.04
62d	223	43.3	56.7	0.18±0.01
62e	231	54.3	45.7	-0.109±0.002
62f	233	66.9	30.1	-0.458±0.009
62g	240	94.2	5.8	-1.96±0.06
1	242	97.9	2.1	-2.768±0.005
62h	244	99.3	0.7	-3.24±0.12
62i	246	99.8	0.2	-4.77±0.13

Table 2. Ratio between the trapped "up"-oQMs and "down"-oQMs, and kinetically determined activation enthalpy difference.

There was a clear linear correlation between (α+β)-values and the differences in activation enthalpies. The absolute value of the activation enthalpy difference went through a minimum, meaning that at "medium angle sum" there was no distinct preference of one or the other oQM type, whereas at

"extreme angle sums" – either very large or very small ones – one of the oQM types is largely preferred over the other one.

The regioselectivity in oQM formation was not a consequence of substitution, as hitherto assumed. The tetrasubstituted hydroquinones **63a** and **63b** represent the "open ring version" of the truncated α-tocopherol model PMC (**4**), having the same substituents and thus the same inductive electronic substituent effects as this chromanol, but no annulated ring (Figure 79). Upon oxidation, both compounds afforded the "up"-oQM and "down"-oQMs in a nearly perfect 50/50 ratio. This proved that the regioselectivity in oQM formation from PMC-type oxidants is not a consequence of simple substitution. Regioselectivity in oxidative oQM formation is only observed, if trimethylhydroquinone (TMHQ) is annulated, i.e. attached to another ring structure. It is not an intrinsic property of chain-substituted trimethylhydroquinone or caused by electronic substituent effects, it is moreover caused by strain imposed through annulation.

The oxidation selectivity of α-tocopherol (**1**) – having an (α+β) angle sum of 242° – is about 98.8 / 1.2 between "up"-oQM (**6**) and the corresponding "down"-oQM at room temperature; that of the corresponding benzofuranol (**62c**) is quite opposite at 11.8 / 88.2.

A comparison of the experimental data to the theoretical model of strain-induced bond localization (SIBL) was made. To sort out the factors governing the regioselectivity, comprehensive calculations were carried out using models that underwent angle deformations to mimic the angular strain imposed by annulation of the ring, according to the SIBL principle,[132-134] which was recently reviewed.[45,96,135,136] The agreement between the experimental results, such as the kinetics and the values for the activation energy differences derived from the "up"/"down" ratio of the two possible *ortho*-quinone methides, and the theoretical data according to the SIBL model was excellent, showing that the observed regioselectivity in oxidations of PMC-type antioxidants is simply a function of angular strain. This peculiar oxidation selectivity of α-tocopherol was thus fully explained by the SIBL theory, ending the decade-long Mills-Nixon controversy.

Reactions of the "Common" Tocopherol-Derived *ortho*-Quinone Methide[42]

Self-Reaction of the oQM: Spiro-Dimers and Spiro-Trimers

The oxidation of α-tocopherol (**1**) to dimers[123,137] and trimers[108,138] has been reported already in the early days of vitamin E chemistry, including standard procedures for near-quantitative preparation of these compounds. The formation generally proceeds *via ortho*-quinone methide **6** as the key intermediate. The dimerization of **6** into spiro-dimer **8** is one of the most frequently occurring reactions in tocopherol chemistry, being almost ubiquitous as side reaction as soon as the oQM **6** occurs as reaction intermediate. Early accounts proposed numerous incorrect structures,[139] which found entry into review articles and thus survived in the literature until today.[114] Also several different proposals as to the formation mechanisms of these compounds existed. Only recently, a consistent model of their formation pathways and interconversions as well as a complete NMR assignment of the different diastereomers has been achieved.[43]

The spiro-dimer of α-tocopherol (**8**) is formed as mixture of two diastereomers (Figure 81) by dimerization of the oQM **6** in a hetero-*Diels-Alder* reaction with inverse electron demand. Both isomers are linked by a fluxion process (Figure 82), which was proven by NMR spectroscopy.[140] The detailed mechanism of the interconversion, which is catalyzed by acids, was proposed to be either stepwise or concerted.[140-142]

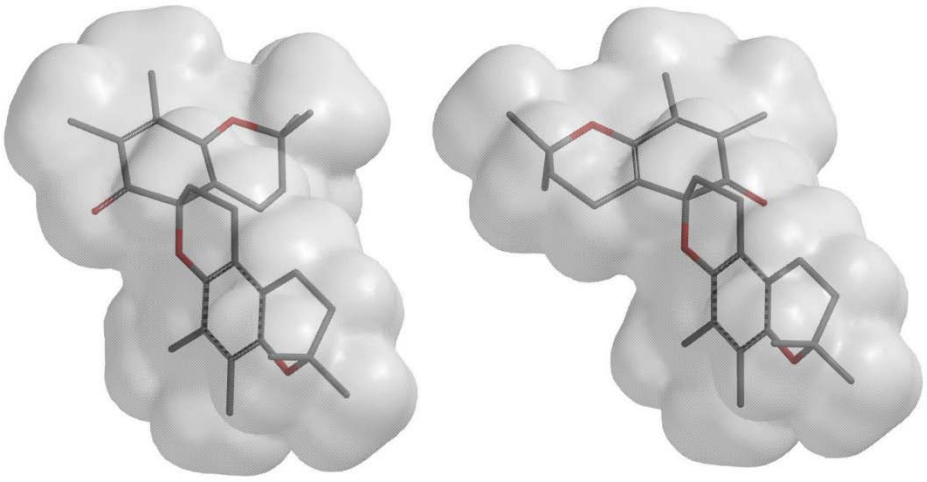

Figure 81: Calculated conformation of S- and R-spirodimer. The gray surface displays an electron density of 0.002/au³ and resembles the actual shape of the molecule.

Formation of the ethano-dimer of α-tocopherol (**59**) by reduction of spiro-dimer (**8**) proceeds readily almost independently of the reductant used. This reduction step can also be performed by

tocopheroxyl radicals as occurring upon treatment of tocopherol with high concentrations of radical initiators (see Figure 76). The ready reduction can be explained by the energy gain upon re-aromatization of the cyclohexadienone system. Since the reverse process, oxidation from **59** to **8** by various oxidants, proceeds also quantitatively, spiro-dimer **8** and ethano-dimer **59** can be regarded as a reversible redox system (Figure 82).

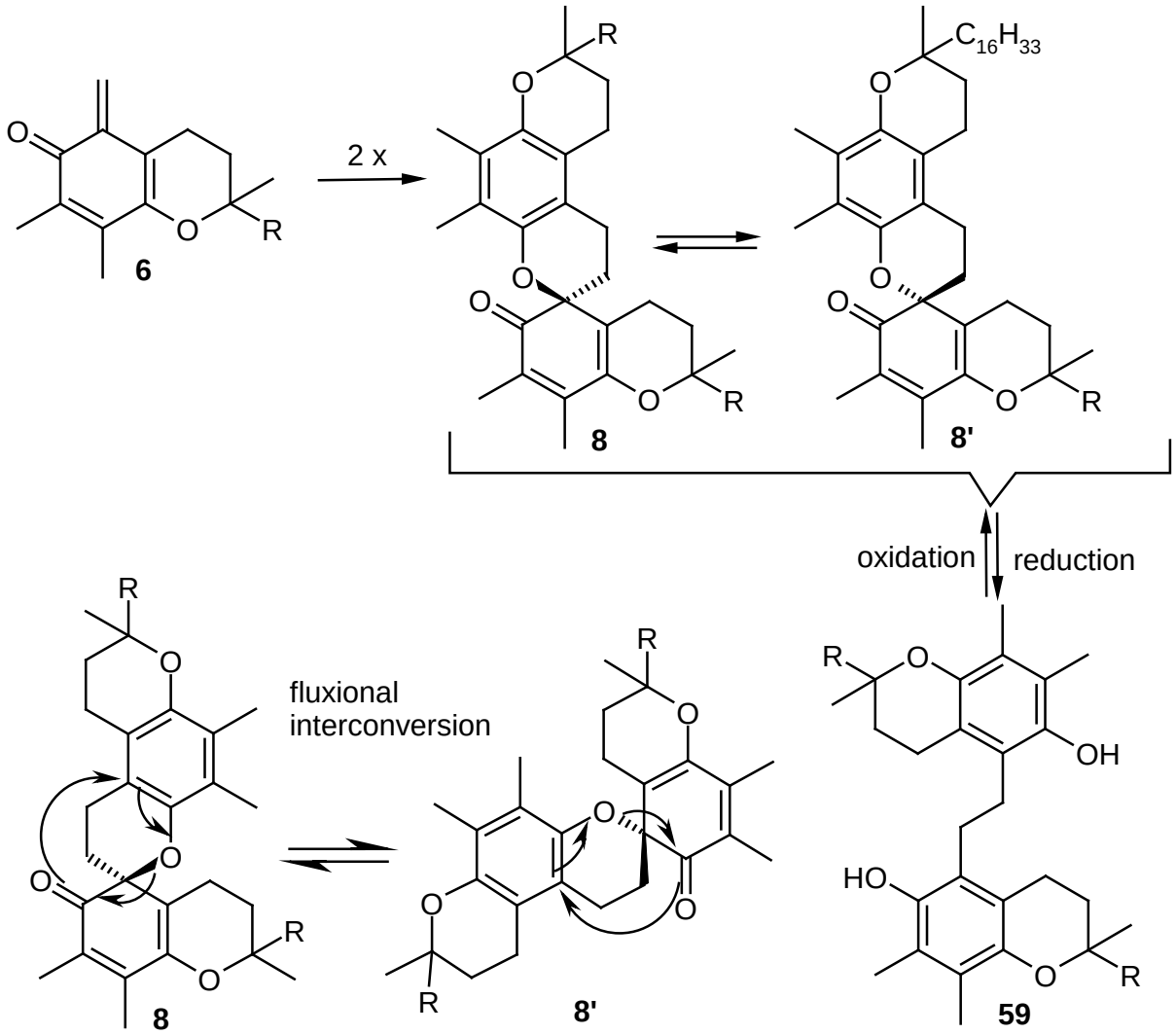

Figure 82. Spiro-dimer of α-tocopherol (8): formation, redox reactions and fluxional nature.

The methano-dimer of α-tocopherol (**64**)[137] was formed by reaction of oQM **6** as an alkylating agent towards excess γ-tocopherol. It is also the reduction product of the furano-spiro-dimer **65**, which by analogy to spiro-dimer **8** occurred as two interconvertible diastereomers,[43] see Figure 83. However, the interconversion rate was found to be slower than in the case of spiro-dimer **8**. While the reduction of furanospiro-dimer **65** to methano-dimer **64** proceeded largely quantitatively and independently of the reductant, the products of the reverse reaction, oxidation of **64** to **65**, depended on oxidant and reaction conditions, so that those two compounds did not constitute a reversible redox pair, in contrast to **8** and **59**.

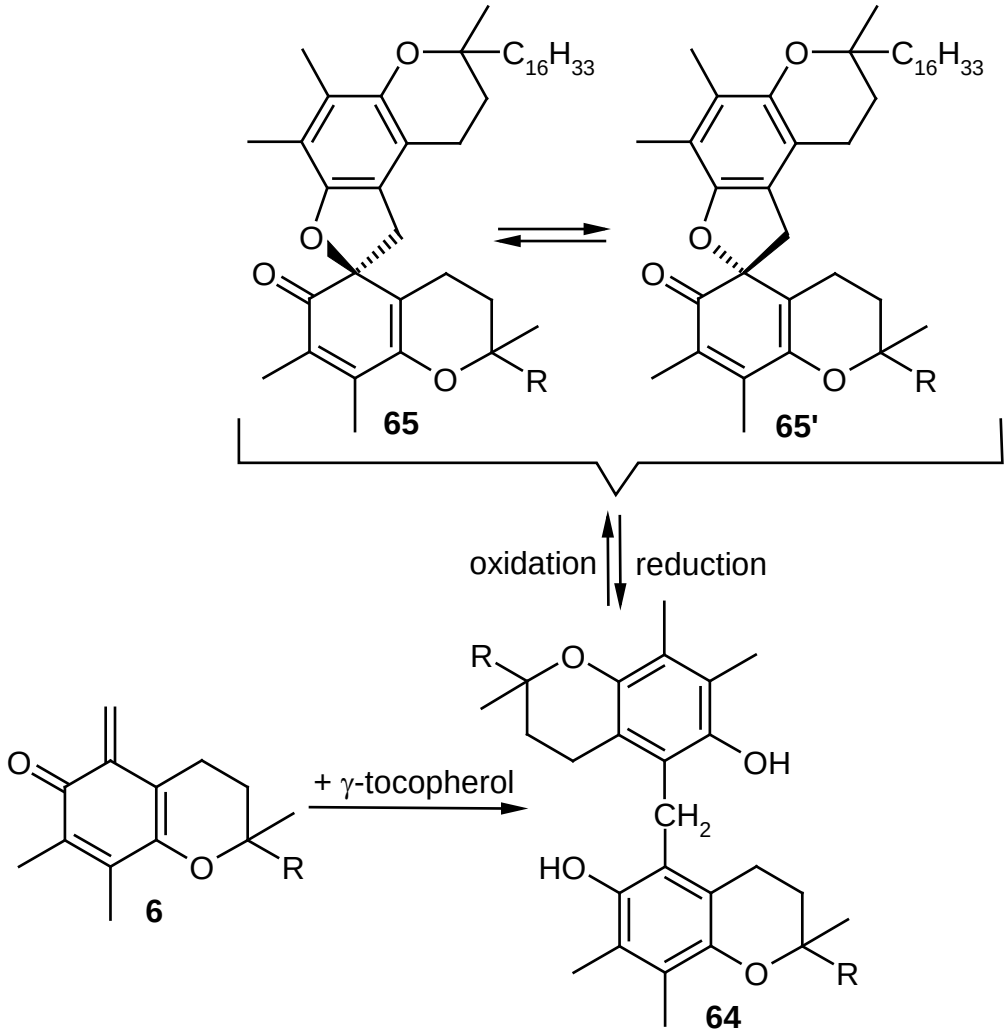

Figure 83. Methano-dimer of α-tocopherol (64): formation and redox reactions, including oxidation two the two fluxationally interconvertible diastereomers of furanospiro-dimer 65.

Treatment of methano-dimer **64** with elemental bromine revealed a remarkable reactivity: at low temperatures it proceeded quantitatively to the furano-spiro-dimer **65**, by analogy with the ethano-dimer **59** giving spiro-dimer **8** upon oxidation. With increasing temperatures the reaction mechanism changed, however, now affording a mixture of 5-bromo-γ-tocopherol **22** and spiro-dimer **8** (Figure 84). Thus, the methano-dimer **64** fragmented into an "α-tocopherol part", in the form of oQM **6** that dimerized into **8**, and a "γ-tocopherol part", which was present as the 5-bromo derivative **22** after the reaction. Thus, the overall reaction can be regarded as oxidative dealkylation.

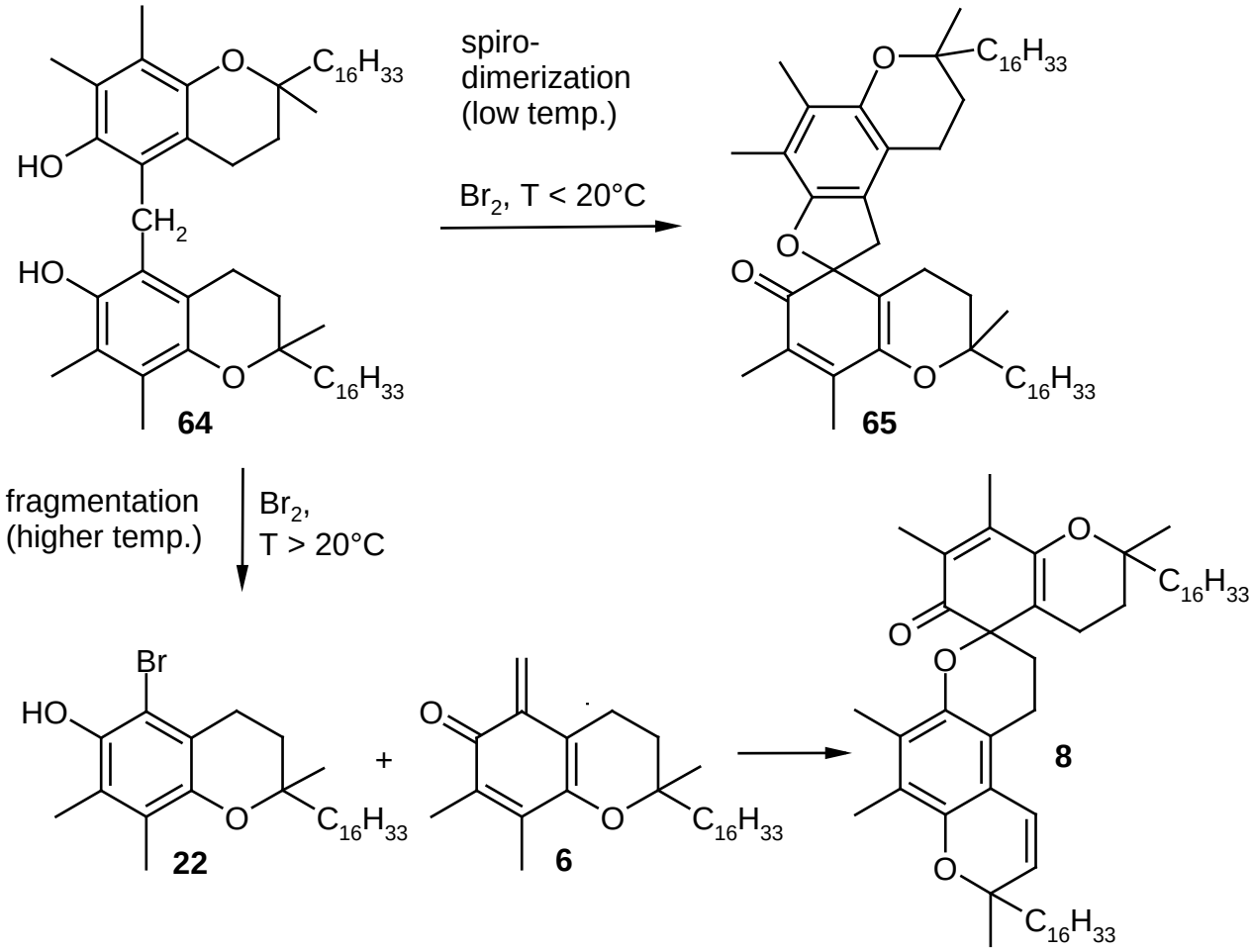

Figure 84. Redox behavior of the methano-dimer of α-tocopherol (bis(5-tocopheryl)methane, 64): temperature dependence of the oxidation with bromine.

A further hetero-*Diels-Alder* reaction with inverse electron demand between oQM **6** as the dienophile and either of the two diastereomers of spiro-dimer **8** as the diene provided the spiro-trimers **9a** and **9b** (Figure 85). The absolute configuration was derived from NMR experiments. It was moreover shown that only two of the four possible stereoisomeric trimers were formed in the hetero-*Diels-Alder* reaction: the attack of the oQM **6** occurred only from the side *syn* to the spiro-ring oxygen.[43]

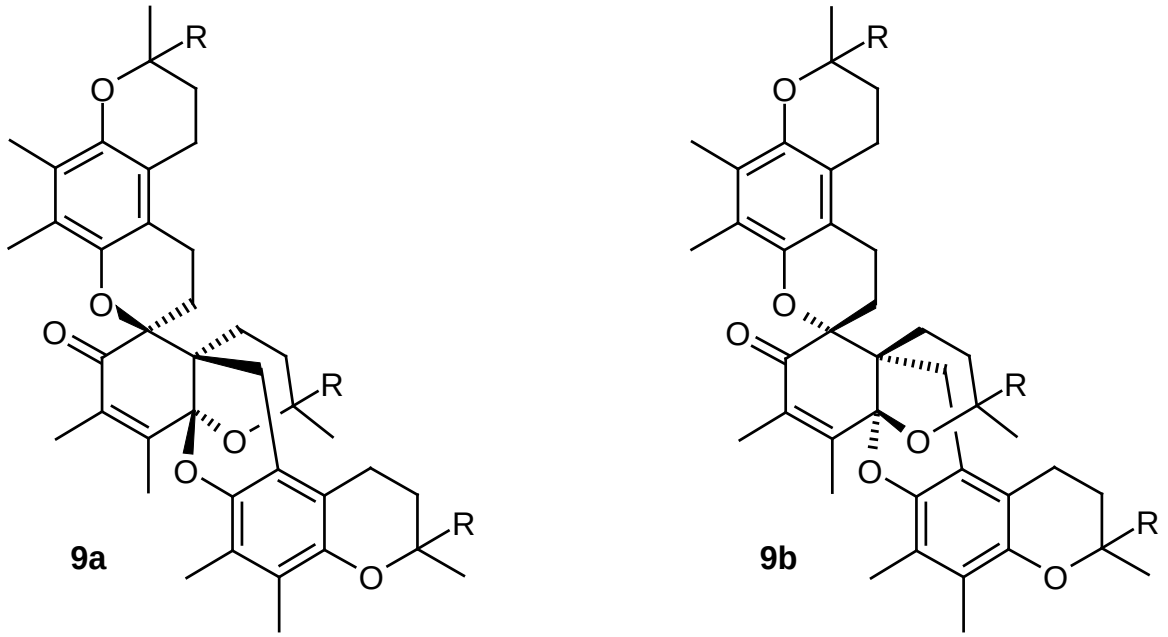

Figure 85. Spiro-trimers of α-tocopherol (9a, 9b) formed by reaction of oQM 6 with the two diastereomers of spiro-dimer 8.

Spiro-Oligomerization / Spiro-Polymerization of Tocopherol Derivatives

If a compound possesses more than one *ortho*-alkylphenol unit capable of being oxidized to an oQM, the spiro-dimerization process occurs more than once at the molecule, and becomes a spiro-oligomerization or even spiro-polymerization process eventually. Tetracycle **66**, which was obtained by condensation of trimethylhydroquinone with 1,1,3,3-tetramethoxypropane,[143] proved to be a very appropriate means to study such multiple spiro-dimerization processes. The compound consists of two chroman units of the α-tocopherol-type which are connected with each other at the alicyclic pyran ring having C-2, C-3 and C-4 in common, which gave the compound its name “Siamese twin”-tocopherol. Compound **66** is a vitamin E model which "locks" the alicyclic chroman ring into a specific geometry, but without achieving this by means of sterically demanding, large substituents. Any conformational change in one of the two chromanol moieties in **66**, which would influence oQM or radical stability[144] is accompanied by the reverse change in the second "twin" moiety, causing the opposite effect there. The chromanoxyl radical derived from **66** gave ESR spectra that resembled those of α-tocopherol **1**, but exhibit additional hyperfine structure due to the other “half” of the molecule.[143] The compound showed antioxidant properties which were superior to that of the truncated tocopherol model compound in several test systems.[145]

Since it contained *two* chromanol moieties, twin-tocopherol **66** gave all reactions characteristic of tocopherol twice, most notably *ortho*-quinone methide formation. Each one of the two "twins parts" in **66** was able to undergo a reaction similar to the spiro-dimerization of tocopherol. Thus, this simple spiro-dimerization eventually became a spiro-oligomerization / spiro-polymerization in the case of **66**:

after both sides of the twin molecule had reacted in a spiro-dimerization, each of the two newly attached twin molecules again possessed an end capable of undergoing spiro-dimerization, and so on, finally affording linear molecules consisting of twin molecules connected by spiro links that were formed in sequential hetero-*Diels-Alder* reactions. The lengths of the spiro-polymers as well as the molecular weight distribution varied according to reaction time and reaction temperature. Different oxidants, solvents, reaction times, and reaction temperatures afforded polymers with 4 to 215 units depending on the conditions.[143]

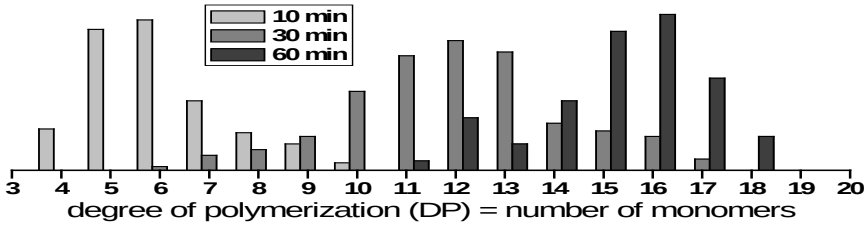

Figure 86. Oxidation of twin-tocopherol 66 by $AgNO_3$ in toluene at 25°C: molecular weight distribution of the resulting oligomers in dependence of the reaction time.[146]

After reaction of the first "twin side" of **66** by spiro-dimerization, for instance as dienophile, the second half can theoretically react either as dienophile or as diene (Figure 87). Thus, a pyrano/spiro pair (reaction of the "left twin" as diene and the "right twin" as dienophile), a pyrano/pyrano pair or a spiro/spiro couple (reaction of "both twins" as dienes or dienophiles, respectively) is formed. However, only products were observed that contained exclusively asymmetric pairs (pyrano/spiro or spiro/pyrano pairs) as the building blocks – but no symmetric (pyrano/pyrano or spiro/spiro) couples.[143]

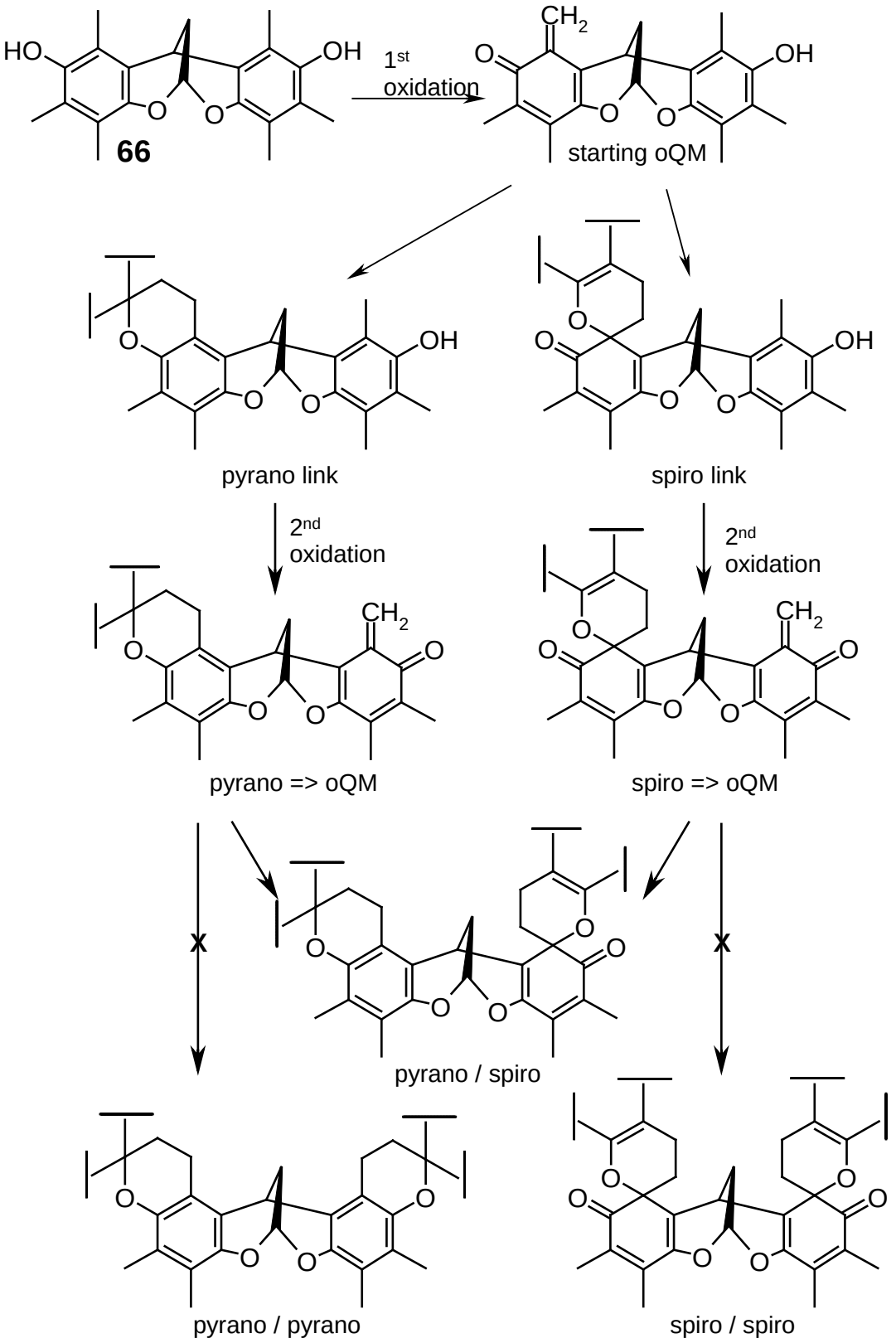

Figure 87. Regioselectivity of spiro-pyrano link formation upon dimerization of the oQMs derived from twin-tocopherol 66.

The spiro-pyrano regioselectivity was rationalized in terms of frontier orbital theory. Reaction of the first oQM as a diene (pyrano structure) resulted in an increase of the HOMO energy of the

neighboring oQM. Therefore, this oQMs will react as dienophile due to increased π-donor ability, and will thus form a spiro structure. By analogy, reaction of the first oQM as a dienophile (spiro structure) decreased the LUMO energy of the neighboring oQM leading to increased π-acceptor capability and subsequent reaction as a diene (pyrano structure). In both cases spiro/pyrano couples resulted, but no spiro/spiro or pyrano/pyrano neighbors, since there was a significantly decreased HOMO-LUMO energy difference for the asymmetric pairs as compared to the symmetric couples (Figure 88).

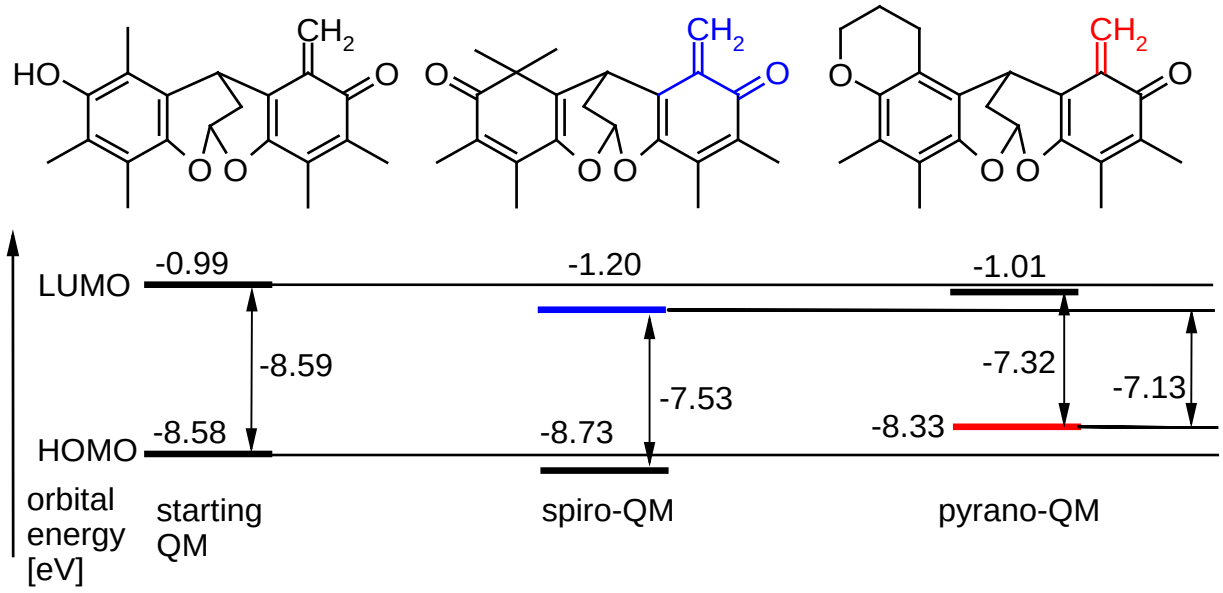

Figure 88. Influence of the reaction of the first oQM (to a pyrano or spiro structure) on the reactivity of the second oQM from 66 according to computations: only spiro/pyrano, but no pyrano/pyrano or spiro/spiro pairs are formed in the oligomeric products.[143]

When the oxidative spiro-oligomerization starting from twin-tocopherol **66** was carried out at low temperatures, the cyclic tetramer **67** was obtained instead of linear products.[143] Also **67** contained only pyrano/spiro (=spiro/pyrano) pairs as the building blocks, but no pyrano/pyrano or spiro/spiro couples. Each spiro-link in linear or cyclic spiro-oligomers and spiro-polymers was reduced in analogy to the spiro-dimer of tocopherol (**8**). Consequently, reduction of **67** provided the macrocycle **68** (Figure 89), which showed some similarities to calixarenes. In the presence of excess oxidant and reductant, respectively, **67** and **68** exchanged eight electron equivalents per molecule, by analogy to the reversible redox pair formed by the tocopherol-derived spiro-dimer (**8**) and ethano-dimer (**59**) exchanging only two electron equivalents.

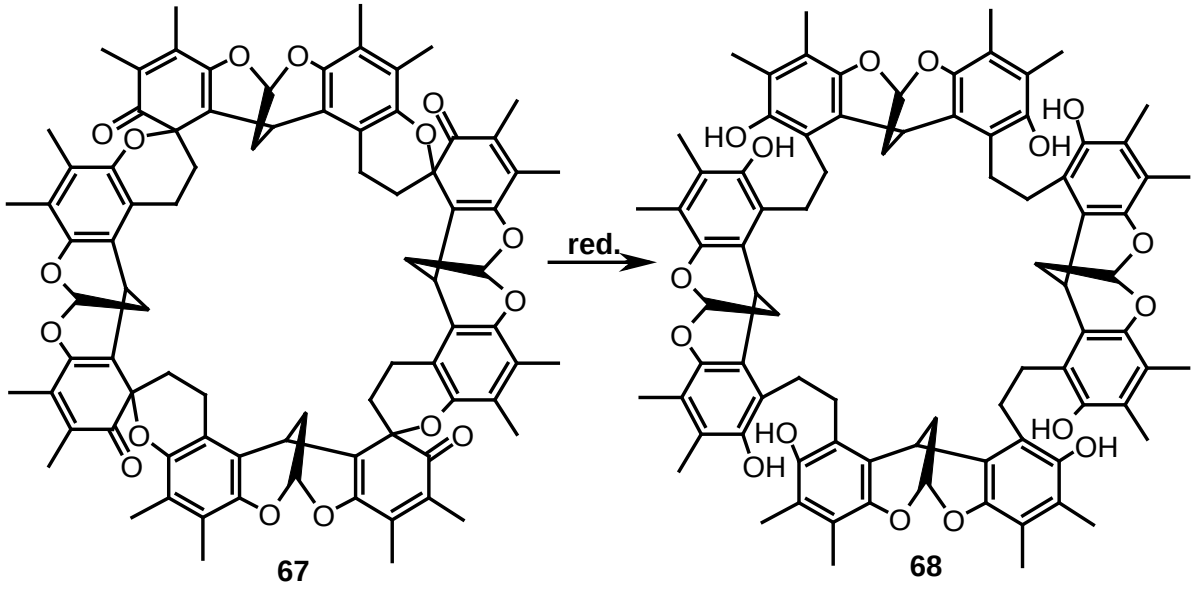

Figure 89. Cyclic spiro-tetramer 67 and its reduction product, macrocycle 68.

Spiro-dimerization of the tocopherol-derived oQM seemed to be a quite favored process, which proceeds also in the case of moderately bulky substituents at C-5a. A particularly interesting case was the oxidative spiro-dimerization of α,ω-bis(tocopheryl)alkanes (**69**), which basically present two α-tocopherol units linked at C-5a by an alkyl bridge.[147] The reaction of other α,ω-bis(hydroxyphenyl)-alkanes, such as **70** – **73**, proceeded similarly.

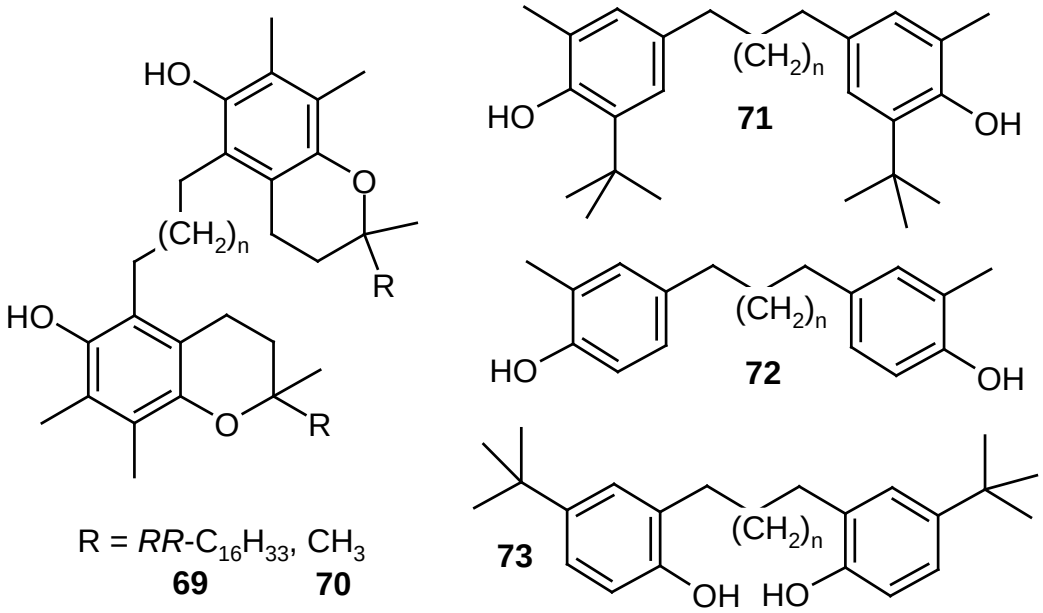

Figure 90. α,ω-Bis(tocopheryl)alkanes (69) and other α,ω-bis(hydroxyphenyl)-alkanes (70 - 73) as starting materials for the spiro-oligomerization / spiro-polymerization reaction.

Subject to typical conditions for spiro-polymerization, e.g. treatment with Ag_2O in inert solvents, each tocopherol unit of the bis(tocopheryl)alkanes **69** underwent oxidation to the respective oQM. The

subsequent dimerization process involves two different molecules as intramolecular dimerization is impossible due to steric reasons. Each "side" of the starting bis(tocopheryl)alkane forms a spiro-dimer unit. The two newly attached molecules carry another tocopherol at the opposite end, which will again be oxidized and react with two other molecules, and so on. This way, the spiro-dimerization process becomes a spiro-polymerization process, affording linear oligomers / polymers (**74**) consisting of spiro-dimers linked by alkyl chain bridges of differing lengths (Figure 91). Basically, these oligomers consist of spiro-dimers of α-tocopherol (**8**) linked at the ethano-bridges by alkyl chains. The degree of polymerization was adjustable by the choice of solvent, reaction temperature, reaction time and oxidant (*cf.* Figure 86). As an example, 1,6-bis(5-tocopheryl)hexane (**69**, n=4) afforded different spiro-polymers according to the reaction conditions (oxidant, time, temperature), the maximum of the molecular weight distributions ranging between 16 and 534 spiro-dimer units, corresponding to molecular weights between about 14500 and 483000, the distributions themselves being rather narrow.[147]

Reduction of the spiro-polymers proceeded by analogy to the reduction of the spiro-dimer (**8**) giving the ethano-dimer of α-tocopherol (**59**). Each spiro-dimer unit in the spiro-polymer was thus converted into 1,2-bis(5-tocopheryl)-ethane elements, the ethane unit being a part of the alkyl chain bridges in **69**. The resulting products **75** are basically a long alkane chain carrying vicinal 5-tocopheryl or other *ortho*-alkylphenol substituents in regular distances, which are set by the chain length of the alkyl bridges. The products thus represent polytocopherols (Figure 91).

The spiro-polymerization is a novel reaction type which uses the spiro-dimerization of oQMs to build up linear oligomers and polymers. The basic properties of the spiro-dimer of α-tocopherol, i.e. its fluxional structure and its ready reduction to the ethano-dimer, remain also active when such structural units are bound in the polymer. The products of the reaction, both in its poly(spiro-dimeric) form (**74**) and in the form of the reduced polytocopherols (**75**), are interesting materials for application as high-capacity antioxidants, polyradical precursors or organic metals, to name but a few.

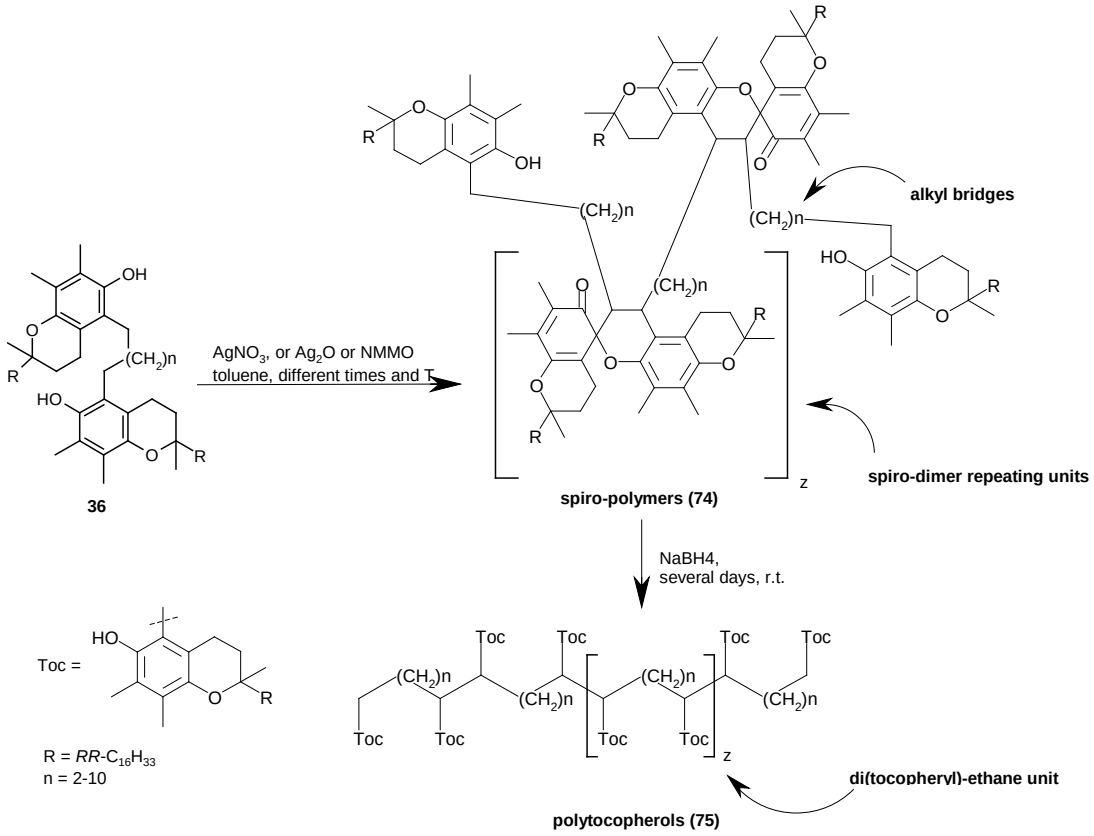

Figure 91. Spiro-polymerization of α,ω-bis(tocopheryl)alkanes 69 to linear spiro-polymers 74 carrying spiro-dimer units liked by alkyl chains. Reduction of 74 converts the spiro-dimer units into ethano-dimer units, resulting in polytocopherols 75.

A special case of the spiro-oligomerization reaction is the oxidation of 1,3-bis(5-tocopheryl)propane (**76**) which did not cause spiro-polymerization, but formation of spiro-tetramers (**77-b**), distinguished by the arrangement of pyrano/spiro links. The regioselectivity of spiro-pyrano link formation as well as the influence of already formed spiro-links on the ones to be formed was rationalized in terms of frontier orbital theory, similar to the case of the "Siamese twin" tocopherol (Figure 88). According to theory, spiro/pyrano neighbor couples would result, but no spiro/spiro or pyrano/pyrano neighbors, predicting a clear preference of **77a** over **77b**. The validity of this hypothesis was confirmed experimentally since the two compounds were formed upon Ag_2O oxidation at room temperature in a ratio of 15:1. Both spiro-tetramers were reduced to the same product, *cis*-1,2-*cis*-4,5-tetrakis(5-tocopheryl)cyclohexane (**78**). Also here, the reduced tocopherol and the spiro-tetramers establish reversible redox pair, with the ratio between the two spiro-tetramers **77a** and **77b** remaining constant during repeated redox cycles.

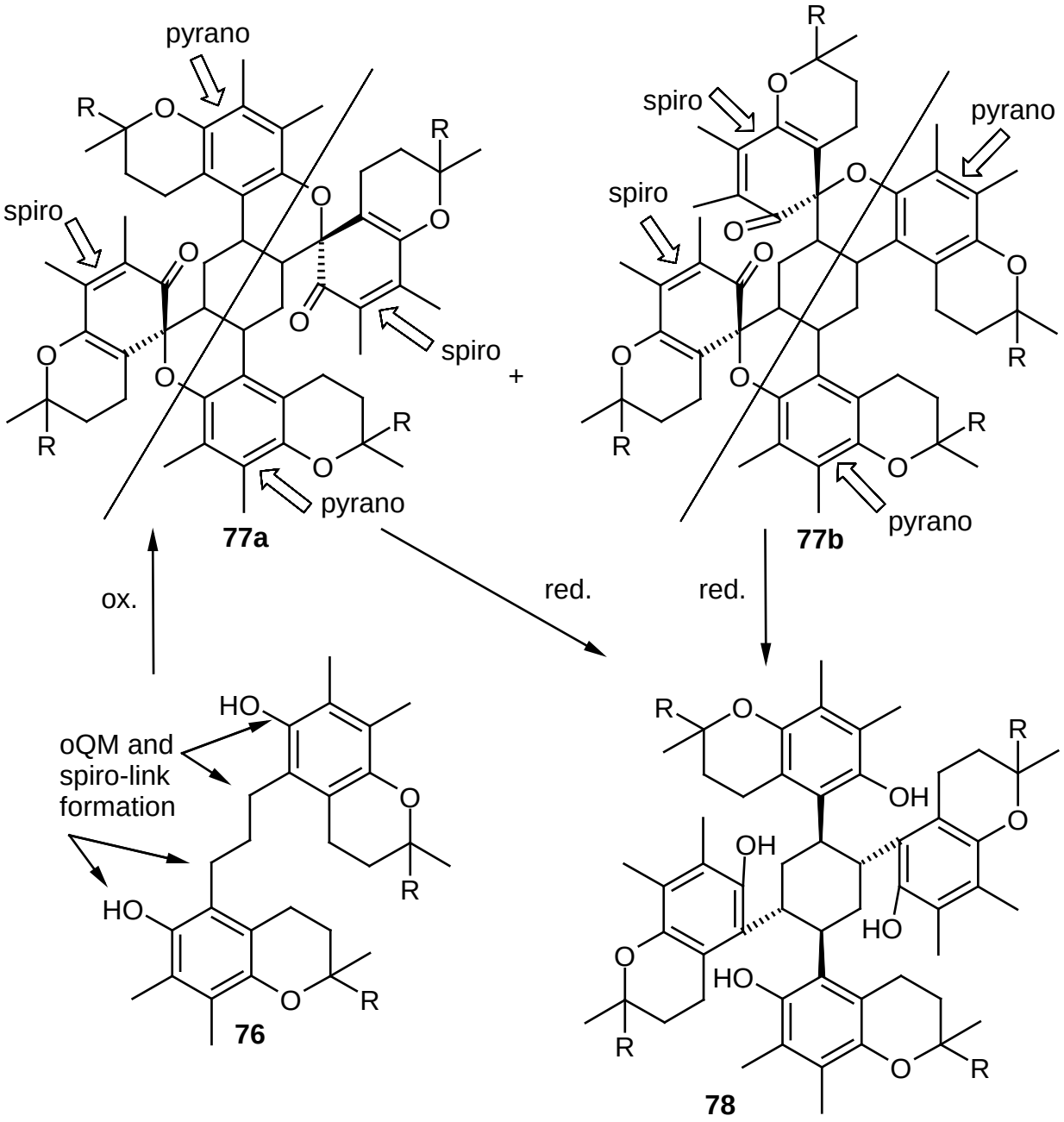

Figure 92. Configurationally different spiro-tetramers 77a and 77b formed by spiro-tetramerization of 1,3-bis(5-tocopheryl)propane (76) in a 15:1 ratio in agreement with theory. Reduction of each of the tetramers provides *cis*-1,2-*cis*- 4,5-tetrakis(5-tocopheryl)cyclohexane (78). The dashed lines separate the two former units of 76, indicating where bond formation during the spiro-oligomerization process occurred.

Bromination of α-Tocopherol and further Reactions of 5a-Bromo-α-tocopherol and other 5a-Substituted Tocopherols

Treatment of α-tocopherol (**1**) with elemental bromine provided quantitative yields of 5a-bromo-α-tocopherol (**16**). The reaction was assumed to proceed according to a radical mechanism, but later a non-radical oxidation–addition mechanism was proven (Figure 93). Bromine oxidized α-tocopherol (**1**)

to the intermediate *ortho*-quinone methide (**6**) which in turn added the HBr produced in the oxidation step.[68] If the HBr was removed by flushing with nitrogen, the spiro-dimer (**8**) became the main product, if it was purged by HCl gas, mainly 5a-chloro-α-tocopherol was produced.

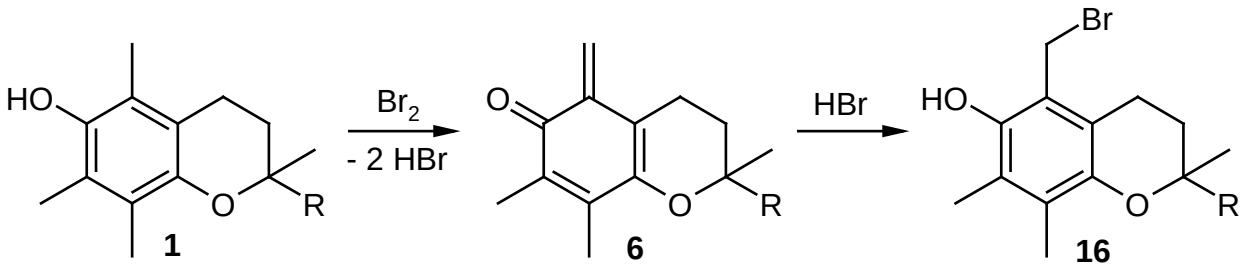

Figure 93. Synthesis of 5a-bromo-α-tocopherol (16) from α-tocopherol (1) according to an oxidation-addition mechanism involving the oQM intermediate 6.

5a-Bromo-α-tocopherol (**16**) has become a most frequently used starting material in the synthesis of 5a-substituted tocopherols. This is due to its ready availability and facile preparation in quantitative yield which makes time-consuming and tedious purification procedures unnecessary. Because of its inherent benzyl bromide structure, 5a-bromo-α-tocopherol shows high reactivity and is amenable to facile nucleophilic substitution,[148] although preparative difficulties arose because of ready elimination of hydrogen bromide in basic media or at slightly elevated temperatures – approx. above 50°C – causing re-formation of the oQM **6**, and thus the α-tocopherol spiro-dimer (**8**) as the most frequently observed by-product. Ready elimination occurred with all types of *O*-, *N*- and *S*-substituents at C-5a, inducible by treatment with alkali or at elevated temperatures.

The stability of 5a-substituted tocopherols in acidic media and their lability in basic media was used as the basis for the development of prodrugs, which showed pH-dependent drug release: while the prodrugs are stable in the acidic medium of the stomach, they are readily cleaved in the basic media of the intestinal tract, where the drug – a 5a-substituent bound to the tocopherol moiety through an oxygen or amino functionality – is released.[149] The tocopherol moiety acts as a lipophilic drug carrier. Upon release of the drug and cleavage of the carrier either spiro-dimer **8**, *para*-tocopherylquinone **79** or, by reduction, α-tocopherol (**1**) are formed, thus physiologically fully compatible compounds. One illustrative example in this respect is tocopheryl ascorbate **80**. This compound is stable under neutral and acidic conditions, but eliminates ascorbate at a pH above 8 with concomitant formation of oQM **6**. Both intermediates join in a redox reaction, and finally regenerated α-tocopherol and dehydroascorbate are produced in high yield (Figure 94). Addition of sodium ascorbate rendered the tocopherol yields quantitative. Kinetic experiments showed the main reaction to proceed in the pH range of 8 to 11 under simulated physiological conditions, and the tocopherol to be generated in a finely dispersed and thus readily absorbable manner.

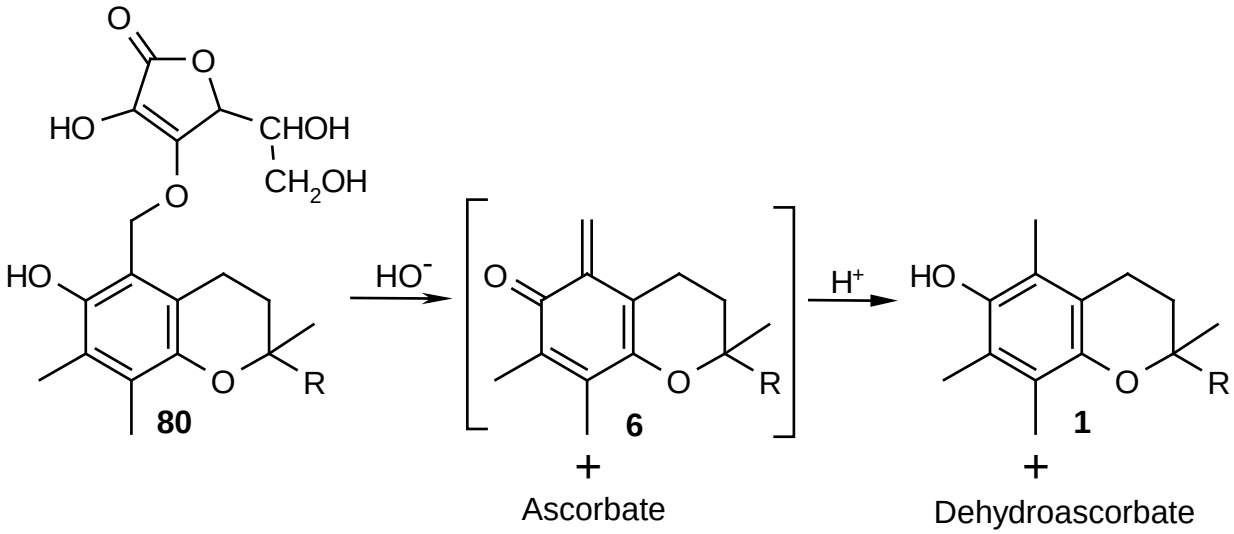

Figure 94. Regeneration of α-tocopherol by base-catalyzed fragmentation of 5a-tocopheryl ascorbate (80) followed by a redox process.

The reaction of 5a-bromo-α-tocopherol (**16**) with amines was further elaborated into a procedure to use this compound as a protecting group "Toc" for amines and amino acids (Figure 95).[68] The protection effect was due to a steric blocking of the amino function by the bulky tocopheryl moiety rather than to conversion into a non-nucleophilic amide derivative, and the Toc-protected amino acids were employed in the synthesis of dipeptides according to the dicyclohexylcarbodiimide (DCC) coupling method.[150] The overall yield of the reaction sequence was reported to be largely dependent on the coupling reaction, since both installation and removal of the protecting group were near-quantitative steps. Especially the cleavage by treatment with silver oxide or mild bases could be performed under quite mild conditions. The Toc group is cleaved off as the oQM **6** which immediately dimerizes into spiro-dimer **9**, which is the only product derived from the protecting group that due to its high lipophility can conveniently be separated. The Toc-protected amines and amino acids represent 5a-substituted tocopherols, and can be cleaved under similar conditions.

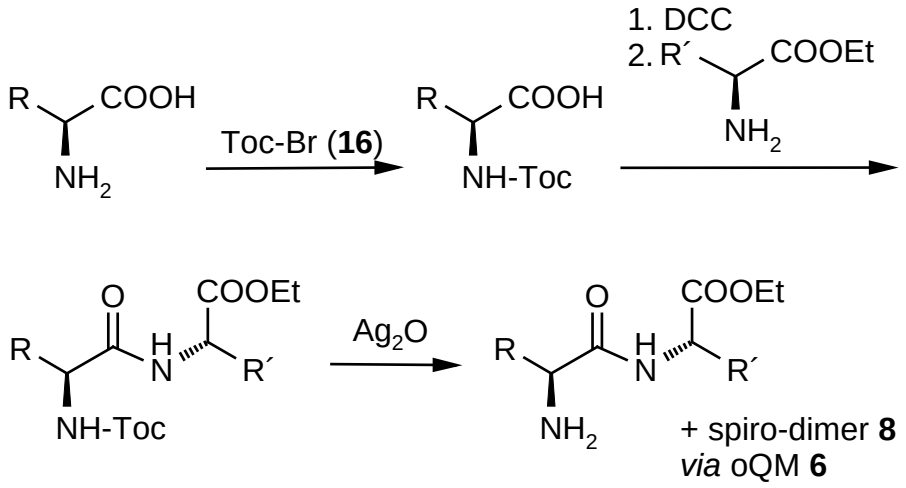

Figure 95. 5a-Bromo-α-tocopherol 16 as auxiliary in the synthesis of dipeptides: the "Toc" protecting group.

Cyclization of *para*-Tocopherylquinone into oQM

As mentioned earlier (*cf.* page 30), the chromanoxylium cation **7** can be converted into oQM **6** by elimination of a proton from the 5a-methyl group. When starting from α-tocopherol (**1**), the oxidative generation of the oQM **6** can also be performed directly (under apolar, aprotic conditions) so that there is no need to take a "detour" *via* the chromanoxylium **7** from the synthesis point of view. However, this reaction is highly valuable when the chromanoxylium is not produced from α-tocopherol by oxidation (loss of two electrons and a proton), but from *para*-tocopherylquinone (**79**) by acid-induced cyclization. For this cyclization, two mechanisms are possible, the first one involving protonation of the tertiary hydroxyl group which is released as water, followed by cyclization and deprotonation at C-5a in a concerted process (Figure 96**,** path A). The alternative path starts with the attack of the hydroxyl group at the quinone carbonyl facilitated by protonation of the carbonyl oxygen. The intermediate 8a-hydroxytocopherone, undergoes [1,4]-elimination to afford the oQM **6** (Figure 96, path B). Whether this elimination is a simultaneous process or a stepwise one involving the chromanoxylium cation **7** as an intermediate cannot be answered at present. Although the first mechanism has not been disproven to occur, the second one is supported by the fact that 8a-substituted tocopherones can be isolated under special conditions and were indeed shown to produce the oQM by [1,4]-elimination quite readily.[40] In addition, occurrence of a tertiary carbenium ion according to the former mechanism would involve side reaction such as elimination and competitive recyclization to furan derivatives, however, none of these products were found.

The cyclization of *para*-tocopherylquinone **79** and conversion into the oQM **6** converts a *para*-quinoid system into an *ortho*-quinoid one. The preparative applicability of this reaction is high as the intermediate oQM immediately reacts further with acyl halides and trimethylsilyl halides into the corresponding 5a-halo-tocopheryl esters (**81**)[151] and 5a-halo-*O*-trimethylsilyltocopherols (**82**),[152] respectively. The reagents are used in excess and are also responsible for generating traces of hydrogen halide to produce the acidic conditions necessary for triggering the cyclization. For example, by treating *para*-tocopherylquinone **7** with trimethylsilyl bromide, the corresponding *O*-trimethylsilyl-5a-bromo-α-tocopherol (**82**, E = Me_3Si, X = Br) was obtained.[152] Analogously, treatment with acetyl chloride provided 5a-chloro-α-tocopheryl acetate (**81**, E = Ac, X = Cl).[153]

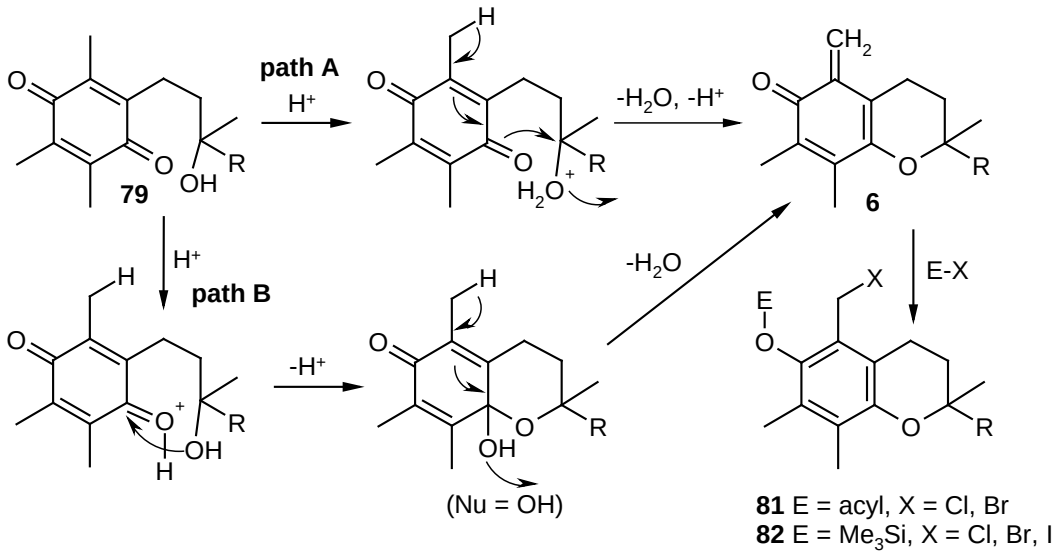

Figure 96. Two mechanistic alternatives for the cyclization of *para*-tocopherylquinone 79 into oQM 6 and subsequent reaction with acyl or trimethylsilyl halides.

Reaction Behavior of 3-(5-Tocopheryl)propionic acid and Synthesis *via* oQM

3-(5-Tocopheryl)propionic acid (**83**) is one of the rare examples to involve the oQM **6** in its preparation in a direct synthesis rather than as a non-intentionally used intermediate or byproduct. $ZnCl_2$-catalyzed, inverse hetero-*Diels-Alder* reaction between *ortho*-quinone methide **6** and an excess of *O*-methyl-*C,O*-bis-(trimethylsilyl)ketene acetal provided the acid in fair yields (Figure 97).[154] The oQM **6** was prepared *in situ* by thermal degradation of 5a-bromo-α-tocopherol (**16**). The primary cyclization product, an *ortho*-ester derivative, was not isolated, but immediately hydrolyzed to methyl 3-(5-tocopheryl)-2-trimethylsilyl-propionate, subsequently desilylated, and finally hydrolyzed into **83**.

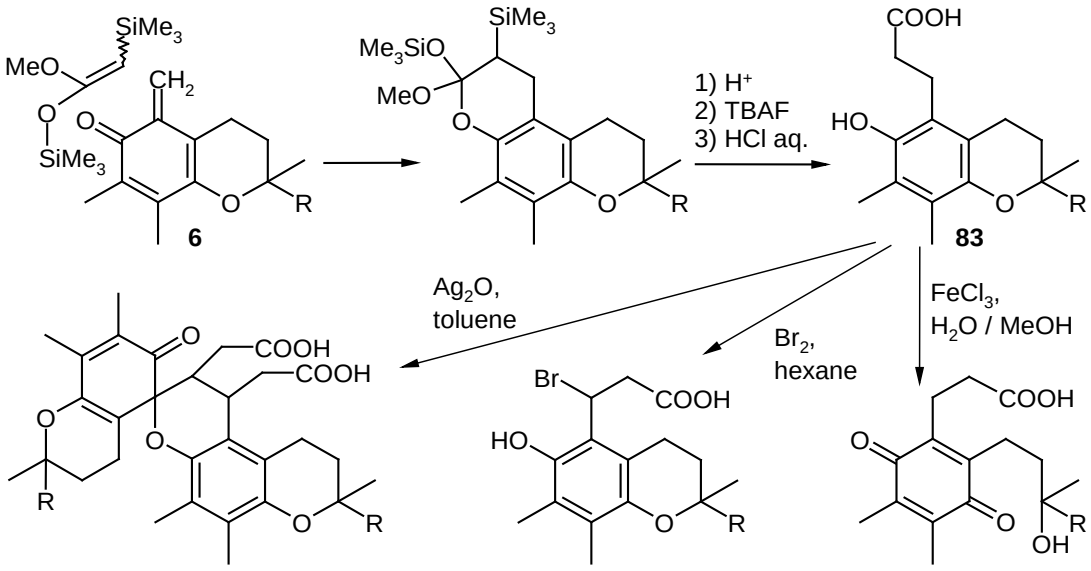

Figure 97. Synthesis of 3-(5-tocopheryl)-propionic acid (83) by trapping the intermediate oQM 6 with a ketene acetal. Reaction products of 83 that are formed as a result of a reaction behavior in complete analogy to that of α-tocopherol (1).

While tocopherylacetic acid (**84**), the lower C_1-homologue of 3-(5-tocopheryl)-propionic acid (**83**) showed a changed redox behavior (see page 124), compound **83** displayed the usual redox behavior of tocopherol derivatives, i.e. formation of both *ortho*-quinoid and *para*-quinoid oxidation intermediates and products depending on the respective reaction conditions. Evidently, the electronic substituent effects that changed the reactivity and oxidation behavior tocopherylacetic acid (**84**) and its derivatives were neutralized by homologation, so that the system returned to its "normal" behavior. All three oxidation reactions typical of α-tocopherol (**1**) – bromination with elemental bromine to the 5a-bromo derivative, oxidation with Ag_2O to an intermediate *ortho*-quinone methide which dimerized into the spiro-dimer, and oxidation in aqueous media to a *para*-quinone – proceeded with 3-(5-tocopheryl)-propionic acid (**83**) in complete similarity to α-tocopherol itself, demonstrating the analogous chemical behavior of the two compounds (Figure 97).[154]

Formation of Tocopherol-Derived oQMs Involving other Positions than C-5a[42]

5-(γ-Tocopheryl)acetic Acid

5-γ-Tocopherylacetic acid (**84**) was produced by hydrolysis of the corresponding nitrile precursor in aqueous dioxane with gaseous HCl, the precursor being obtained by reaction of 5a-bromo-α-tocopherol (**16**) with potassium cyanide in DMSO.[155] The nitrile was also the starting material for the preparation of different esters, amides and the corresponding lactone.[155]

An interesting feature of 5-tocopherylacetic acid (**84**) and its derivatives was their appreciable thermal stability up to 200°C. In contrast to 5a-substituted tocopherols carrying an electronegative substituent at C-5a, the homopolar C-C bond in the C_2-unit at the 5-position of the tocopherol skeleton was shown to be very stable. Thermal decomposition of **84** at temperatures above 250°C caused a complete breakdown of the chroman structure, the C_3-unit consisting of C-2, C-2a and C-3 being eliminated as propyne, the side chain as 4,8,12-trimethyltridec-1-ene (Figure 98). Fragmentation occurred with formation of an intermediate *ortho*-quinone methide involving C-4 and O-1, which was stabilized immediately in subsequent reactions, either by [1,2]-addition of the carboxylic OH group followed by rearomatization into lactone **85**, or by dimerization to a spiro-compound **86**, the latter reaction being a parallel of the common self-dimerization of oQM **6** into spiro-dimer **8**. From the historic perspective, this was the first report of an oQM formed from α-tocopherol other than the "usual" oQM **6**.[155]

Interestingly, tocopherylacetic acid underwent no reaction with bromine or Ag_2O – conditions that produce oQM **6** from α-tocopherol readily. Apparently the substituent effect prohibited formation of the typical 5a-oQM structure, whereas the ability to form *para*-quinoid structures was not impaired: compound **84** was neatly oxidized into its corresponding *para*-quinone, present as lactono-semiketal **87** in aqueous media, both compounds forming a reversible redox pair (Figure 98). Evidently, the electronic effects exerted by the carboxylic acid function in α-position to C-5a changed the oxidation chemistry of the tocopherol system in a way that oQM formation at C-5a was largely, if not completely, disfavored and *para*-quinoid oxidation products were largely preferred. This notion is supported by the fact that homologation in the 5-substituent, i.e. presence of a propionic acid rather than a acetic acid moiety, returns the reactivity of the system to "normal", i.e. to that of α-tocopherol. This was shown above (see page 122) for 3-(5-tocopheryl)propionic acid (**83**).

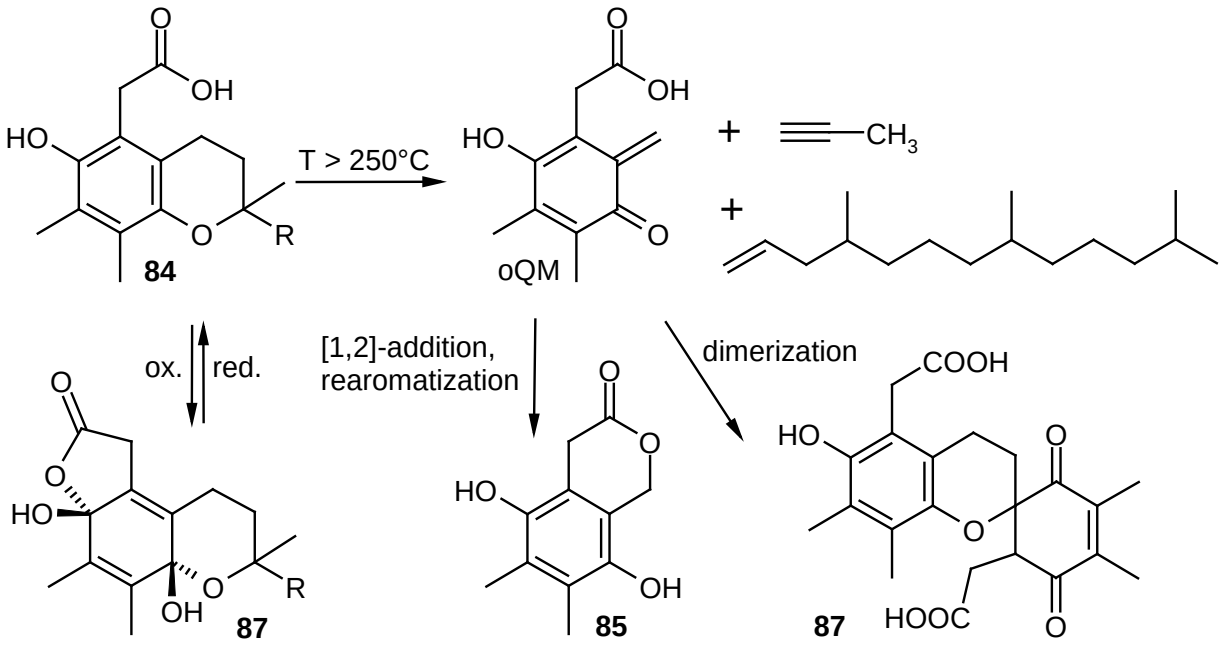

Figure 98. Redox behavior and thermal degradation of 5-tocopherylacetic acid (84), involving an oQM formed by involvement of C-4 and O-1.

4-Oxo-α-tocopherol

4-Oxo-α-tocopherol (**88**) proved to be a very interesting compound with regard to forming various intermediate tautomeric and quinoid structures. It undergoes an intriguing rearrangement of its skeleton under involvement of different oQM structures. The 4-oxo-compound was prepared from 3,4-dehydro-α-tocopheryl acetate *via* its bromohydrin, which was treated with ZnO to afford 4-oxo-α-tocopherol (**88**). The ZnO was a very effective reagent as it caused dehydrobromination, simultaneous deacetylation, and tautomerization of the resulting enol intermediate.[156]

4-Oxo-α-tocopherol (**88**) rearranged under simulated physiological, oxidative conditions into hydroquinone **89**, which was immediately oxidized into naphthalenetrione **90**, the final oxidation product, in yields of about 10%.[156] The rearrangement product possessed a carbon skeleton completely different from that of the starting tocopherol **88**. The rearrangement mechanism was shown to involve opening of the alicyclic ring, followed by formation of different tautomers, bond rotation, and electrocyclic ring closure as the key step (Figure 99). The incorporation of C-5a of 4-oxo-α-tocopherol (**88**) into the alicyclic ring in **90** was demonstrated by means of isotopic labeling: 4-oxo-α-tocopherol trideuterated at C-5a produced compound **90** bisdeuterated at C-4, the “former” C-5a position.

Apparently, introduction of the C-4 oxo-group changed the reactivity of the tocopherol system quite drastically. Enolization of the 4-carbonyl is coupled to formation of quinone dimethide structure involving C-5a and C-4. This reaction can be seen as a [1,5]-sigmatropic proton shift; it does not involve external oxidants. A similar quinone dimethide, after cleavage of the alicyclic ring and bond

rotation, undergoes an intramolecular electrocyclic reaction with the ene structure in the former pyran unit. This reaction is somehow comparable to the trapping of oQM **6** with ethyl vinyl ether, although this is of course an intermolecular process. The oxidation of the resulting annelated hydroquinone into the corresponding naphthoquinone **90** is the last step of the reaction, and probably also the driving force of the whole sequence which caused a far-reaching rearrangement of the carbon skeleton of **88**.

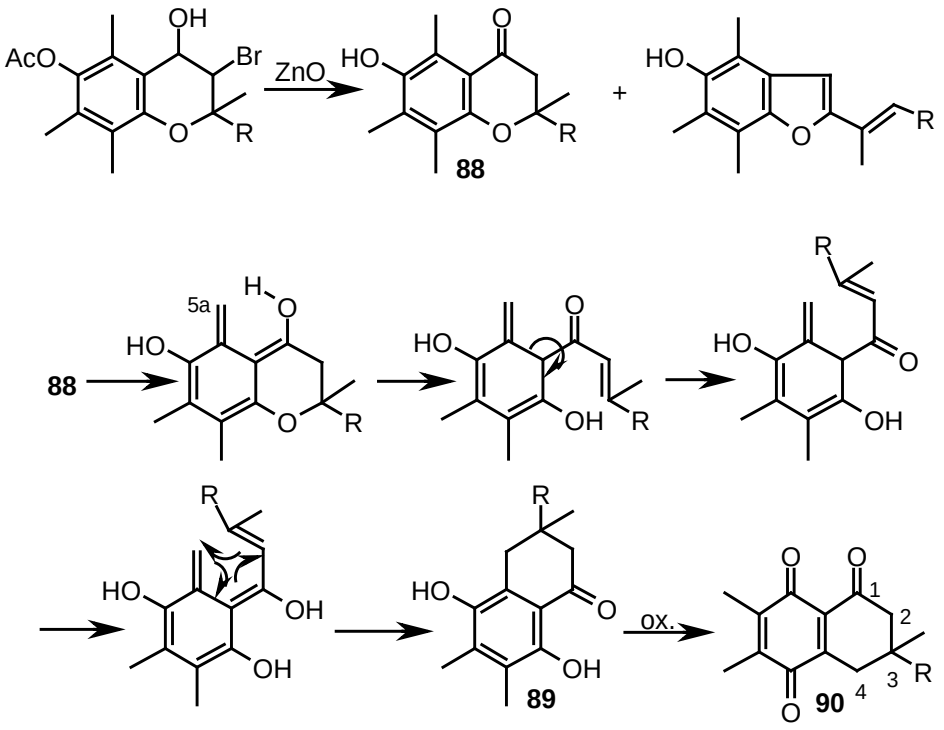

Figure 99. Synthesis of 4-oxo-α-tocopherol (88) and its oxidative rearrangement into naphthalenetrione (90).

3-Oxa-chromanols

3-Oxa-chromanols of the general formula **91** – termed 5,7,8-trimethyl-4*H*-benzo[1,3]dioxin-6-ols according to IUPAC rules – exhibit a structure quite close to tocopherols: Only the C-3 methylene group is exchanged for an oxygen. However, their reactivity is quite different from that of α-tocopherol (**1**). Their remarkable feature is the dependence of the oxidation chemistry of the available concentration of water as the coreactant, and the involvement of a rich quinone methide chemistry. Therefore, although they strictly speaking do not represent conventional tocopherol derivatives, they were regarded as oxa-derivatives of the vitamin, and their chemistry shall be included in the discussion on tocopherol-derived oQMs within this chapter.

3-Oxa-chromanols were obtained as diastereomeric mixtures by condensation of trimethylhydroquinone with the double equivalent of aldehydes in a straightforward one-pot reaction (Figure 100).[157] 3-Oxa-chromanols have recently been tested for their antioxidative properties, as they represent an interesting novel class of phenolic antioxidants.[145] ESR measurements of the radicals

derived from 3-oxa-chromanol derivatives revealed similar stabilities as compared to the α-tocopheroxyl radical (**5**), producing well-resolved multi-line spectra, the hyperfine coupling constants for the methyl substituents at the aromatic ring being quite similar to those of **5**. Distinct effects of the configuration on the long-range couplings into the heterocyclic ring were observed.[90,157]

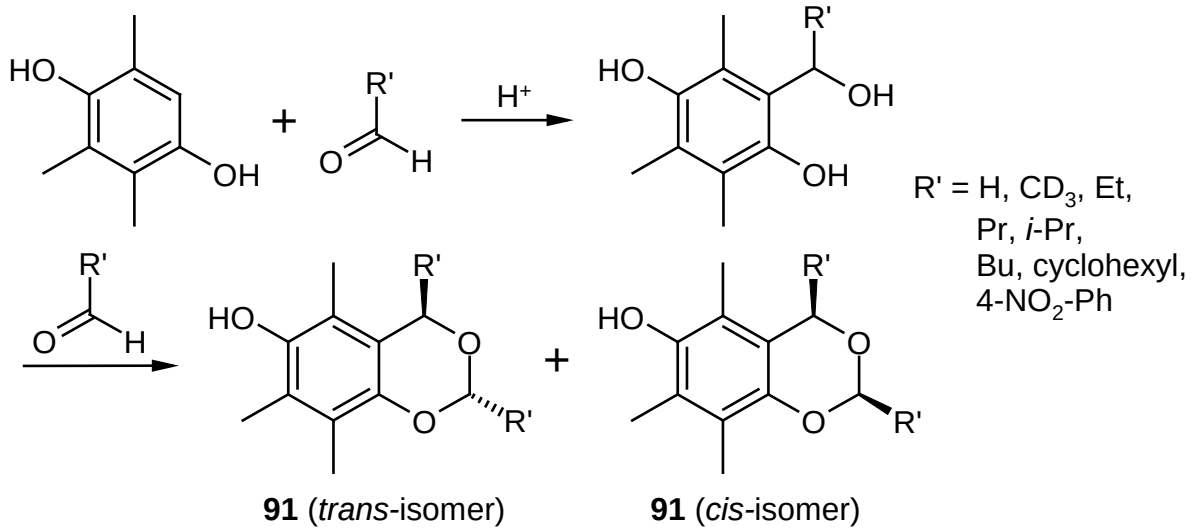

Figure 100. Synthesis of 3-oxa-chromanols (91) as mixture of *cis/trans*-isomers.

The oxidation behavior of 3-oxa-chromanols was mainly studied by means of the 2,4-dimethyl substituted compound 2,4,5,7,8-trimethyl-4*H*-benzo[1,3]dioxin-6-ol (**92**) applied as mixture of isomers;[90] it showed an extreme dependence on the amount of coreacting water present. In aqueous media, **92** was oxidized by one oxidation equivalent to 2,5-dihydroxy-3,4,6-trimethyl-acetophenone (**61**) *via* 2-(1-hydroxyethyl)-3,5,6-trimethylbenzo-1,4-quinone (**93**) that could be isolated at low temperatures (Figure 101). This "detour" explained why the seemingly quite inert benzyl ether position was oxidized while the labile hydroquinone structure remained intact. Two oxidation equivalents gave directly the corresponding *para*-quinone **95**. Upon oxidation, C-2 of the 3-oxa-chroman system carrying the methyl substituent was always lost in the form of acetaldehyde.

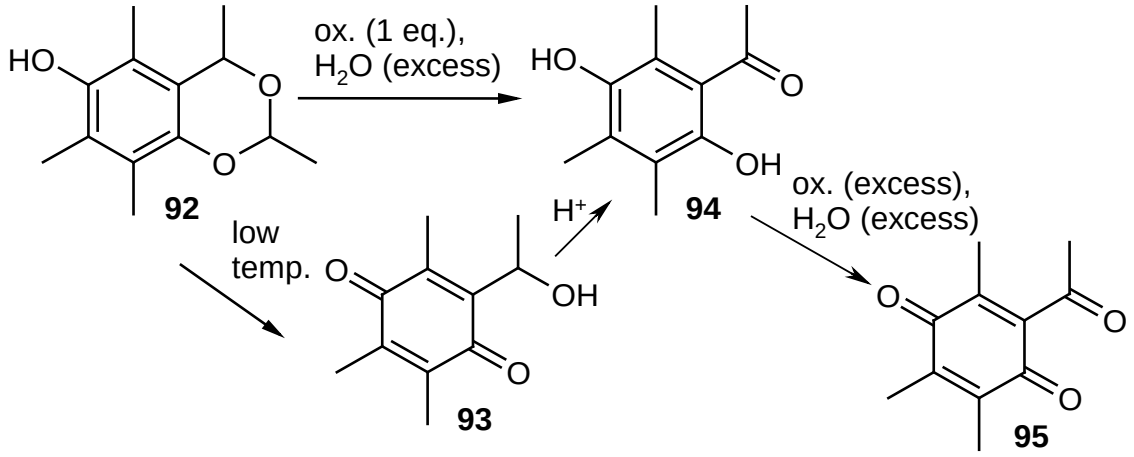

Figure 101. Oxidation of 3-oxa-chromanol 59 in aqueous media (excess water present), leading to acetophenone 61 with an equimolar amount of oxidant, and further to *para*-quinone 62 in the presence of excess oxidant.

Oxidation of 3-oxa-chromanol **92** in the presence of just one equivalent of water produced acetophenone **94** as well, but according to a different mechanism not involving *para*-quinone **93**. The process was elucidated by employing isotopically labeled starting material, selectively trideuterated at the 2- and 4-methyl groups (Figure 102). The reaction involved an *ortho*-quinone dimethide intermediate **96**.[90] Interestingly, such an intermediate was observed in the case of the chemistry of 4-oxo-α-tocopherol (**88**) which also possessed a strongly electronegative oxygen substituent at C-4, similar to the 3-oxa-chromanols. Intermediate **96** underwent a [1,5]-sigmatropic proton shift in a concerted way to give styrene derivative **97**, from which finally acetaldehyde was released by reaction with water to afford acetophenone **94**. The overall outcome of the reaction was thus the same as in the presence of excess water, but the formation mechanisms were completely different from each other. By means of deuterated starting material, the selective [1,5]-sigmatropic proton shift from the C-4a methyl group to the exocyclic methylene group was demonstrated, and the occurrence of both intermediates, *ortho*-quinone dimethide intermediate **96** and styrene derivative **97**, was additionally confirmed by trapping in hetero-*Diels-Alder* reactions.[90]

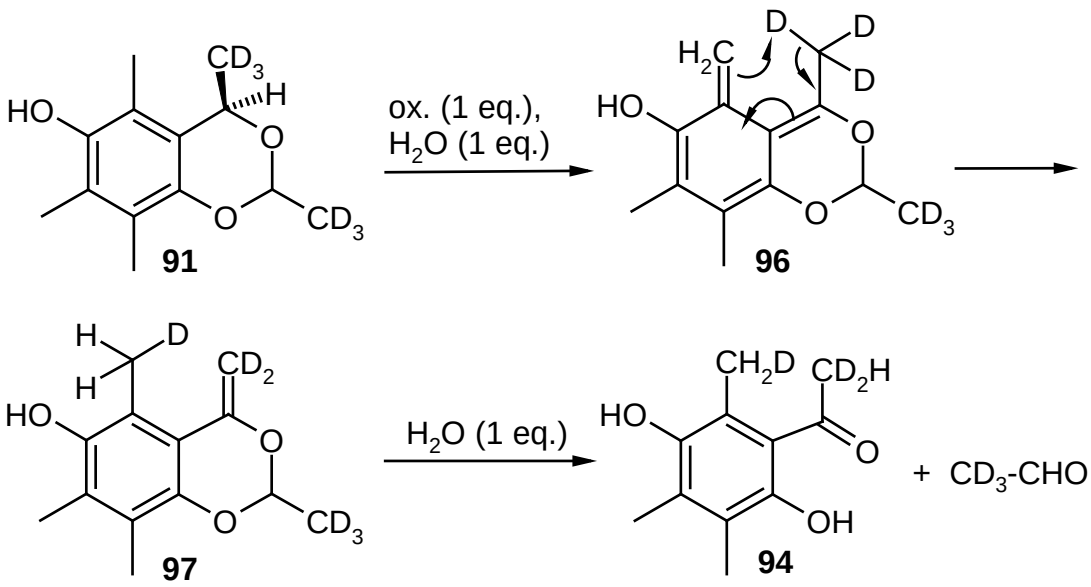

Figure 102. Oxidation of 3-oxa-chromanol 91 in the presence of 1 equivalent of water: mechanistic study by means of selectively deuterated starting material. The initially formed *ortho*-quinone dimethide 96 rearranges into styrene derivative 97, which then reacts with water to provide acetophenone 94.

In the absence of water, oxidation of **92** proceeded also *via* the *ortho*-quinone dimethide **96** and the styrene derivative **97**. However, as no water was present to react with the latter intermediate to release acetaldehyde, the C-2 – C-3 bond was broken and a bond rotation occurred in the zwitterionic intermediate followed by C-C bond formation that established a chromanone system **98**. The zwitterionic intermediate in this reaction is remarkable as it somehow represents the "opposite" of the zwitterionic intermediate encountered in the formation of oQMs from the parent phenols. In the former intermediate formed from the 3-oxa-chromanols, the negative charge is placed at the benzylic position, the positive one at the ring oxygen, both charges being stabilized by resonance. In the latter intermediate formed upon oQM production from the phenols, the charge placement is opposite: a benzyl cation and a phenolate anion, which evidently rendered this intermediate much more stable than the former one. Chromanone **98** was immediately further oxidized to chromenone **99**, the probably driving force of the reaction. The overall process from 3-oxa-chromanol **92** to chromenone **99** required two equivalents of a two-electron oxidant. In the absence of water, evidently the chromanone-to-chromenone oxidation was favored over the oxidation of the starting material **92**. Chromanone **98** was consumed before the oxa-chromanol **92** was affected, so that in the presence of less than two equivalents of oxidant, chromenone **99** was present besides non-reacted starting material.

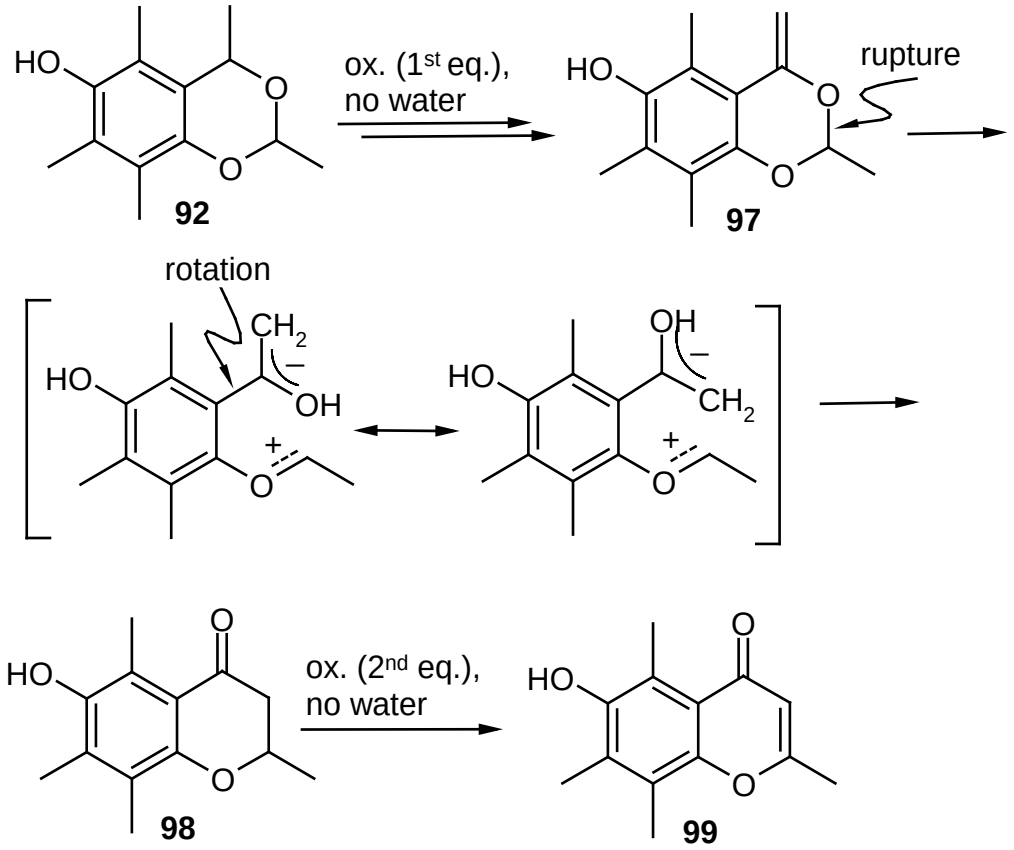

Figure 103. Oxidation of 3-oxa-chromanol 92 in the absence of water, providing chromenone 99 as the final product: mechanism and reaction intermediates.

If the formation of an exocyclic methylene group at C-4, and thus the formation of a styrene intermediate such as **97**, is impossible due to structural prerequisites, oxidation of the corresponding 3-oxa-chromanols will involve the oQM formed involving C-5a, which will react to the corresponding spiro-dimer (Figure 104), by analogy to the reactivity of the α-tocopherol-derived oQM **6**. For example, this chemical behavior was observed for 2,4-diphenyl-3-oxachromanol **100**, which upon oxidation in non-aqueous media with excess oxidant (Ag_2O), provided the sterically crowded tetraphenyl spiro-dimer **102** *via* the intermediate C-5a-oQM **101**.[90] Due to the phenyl substituent at C-4, a hypothetical *ortho*-quinone dimethide intermediate (analogous to **96**) cannot rearrange to a styrene intermediate involving C-4b. This "blocking" of C-4b returned the system to a reactivity similar to α-tocopherol: an oQM involving O-6 and C-5a as in α-tocopherol (**1**), but not the *ortho*-quinone dimethide involving C-5a and C-4 as in the 3-oxa-chromanols **91** and **92** was formed. Oxidation of 2,4-diphenyl-3-oxachromanol **67** in aqueous media produced *para*-quinone **103**, also by analogy to α-tocopherol chemistry (cf page 27).

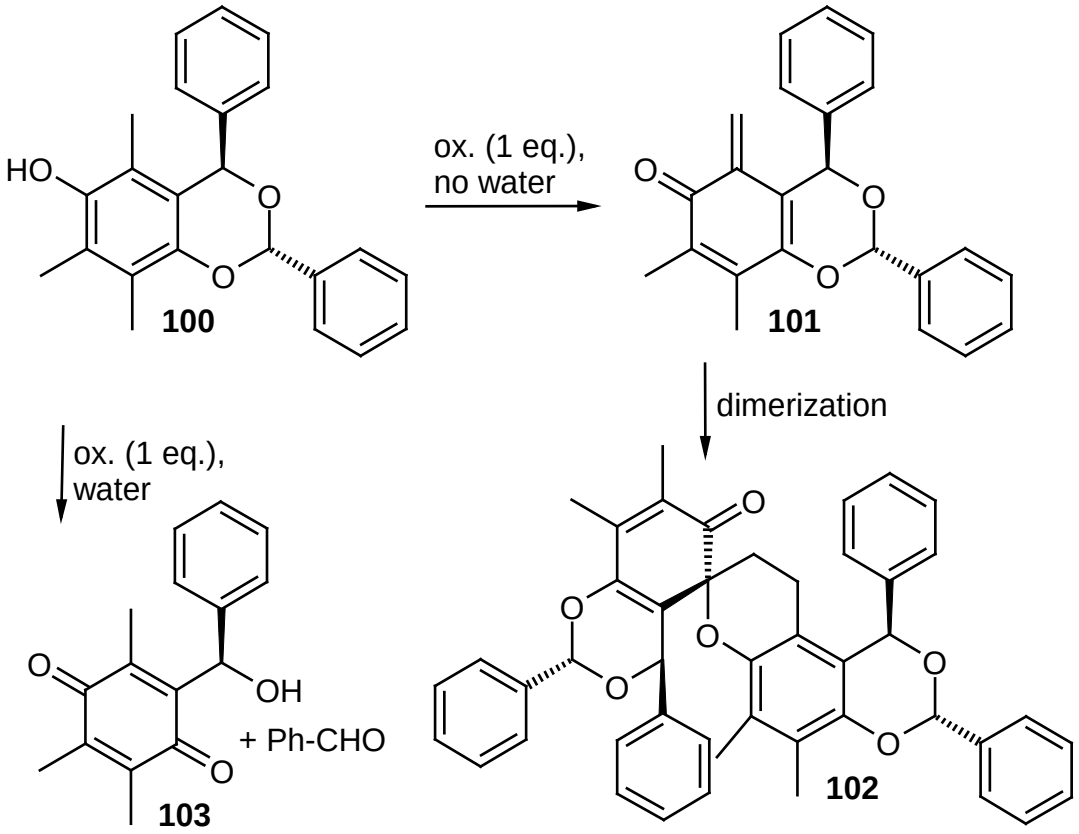

Figure 104. Oxidation of 3-oxa-chromanol 100, having no protons at position C-4b able to undergo rearrangements by analogy to 3-oxa-chromanol 92 with its oxidation intermediates 96 and 97. Due to this blocking at C-4/C-4b, the oxidation behavior of 100 resembles that of α-tocopherol (1).

The oxidation behavior of 3-oxa-chromanols showed both differences and similarities to that of α-tocopherol (**1**). Paralleling the chemistry of α-tocopherol, one-electron oxidation caused formation of the corresponding chromanoxyl radicals, which were relatively stable. Also in the absence of a C-4b substituent with protons, the oxidation behavior entirely resembled that of α-tocopherol. In the presence of a C-4b substituent with protons, the oxidation behavior changed fundamentally. The primary *ortho*-quinone dimethide formed involving C-5a and C-4 (**96**) underwent different subsequent reactions depending on the water content present. The proton transfer from C-4b to C-5a in a [1,5]-sigmatropic rearrangement giving a styrene derivative **97** with the olefinic double bond between C-4 and C-4b was the preferred reaction. The further chemistry of this styrene intermediate is then highly dependent on the amount of coreacting water available (see Figure 102 and Figure 103).

Selected Substituent-Stabilized Tocopherols and Conjugatively Stabilized *ortho*-Quinone Methides

Similar to 3-oxa-chromanols, also several other derivatives of α-tocopherol exhibit a substantially changed oxidation behavior as compared to α-tocopherol itself. Especially 5-substituted derivatives with no 5a-hydrogen belong into this class, as they are unable to form an oQM involving C-5a, which

is most typical of α-tocopherol (**1**). In 5a,5a,5a-trimethyl-α-tocopherol (5-*tert*-butyl-γ-tocopherol, **104**) and other 5a,5a,5a-trialkyl tocopherols the oxidation resistance in apolar media was greatly increased, in aqueous media the corresponding *para*-quinone was formed very readily.[158] Interestingly, blocking of C-5a with regard to oQM formation did not lead to an increased involvement of C-7a in oQM formation, but rather caused increased stability towards oxidation. This is somehow similar to the case of γ-tocopherol, where the missing 5a-methyl group (and thus the inability to form the α-tocopherol-type oQM **6**) also causes increased stability towards two-electron oxidation in apolar media, but not involvement of the 7a-oQM.

The reaction behavior of 5-phenyl-γ-tocopherol (**105**) was similar to that of the 5a,5a,5a-trialkyl tocopherols: the 5a-oQM cannot be formed, and the oxidative stability was increased. However, if a *para*-OH group was introduced into the 5-phenyl substituent as in 5-(*p*-hydroxyphenyl)-γ-tocopherol (**106**), oxidation in apolar media proceeded quite readily – comparably fast to α-tocopherol – and produced the quinoid structure **107** which can be regarded as an *ortho*-quinone methide with regard to the basic tocopherol moiety, as *para*-quinone methide with regard to the phenyl substituent, and also as phenylogous 5,6-tocopherylquinone, the latter compound being quite well known in tocopherol chemistry also as α-tocored (**108**).[153] Quinoid compound **107** is a stable compound when stored at -20°C in inert atmosphere and does not undergo cycloaddition reactions as oQM **6** does, e.g. spiro-dimerization or reaction with ethyl vinyl ether. It is neatly reduced to the starting tocopherol **106** without side reactions. Under ambient conditions in the presence of air it undergoes autoxidation to a complex product mixture.

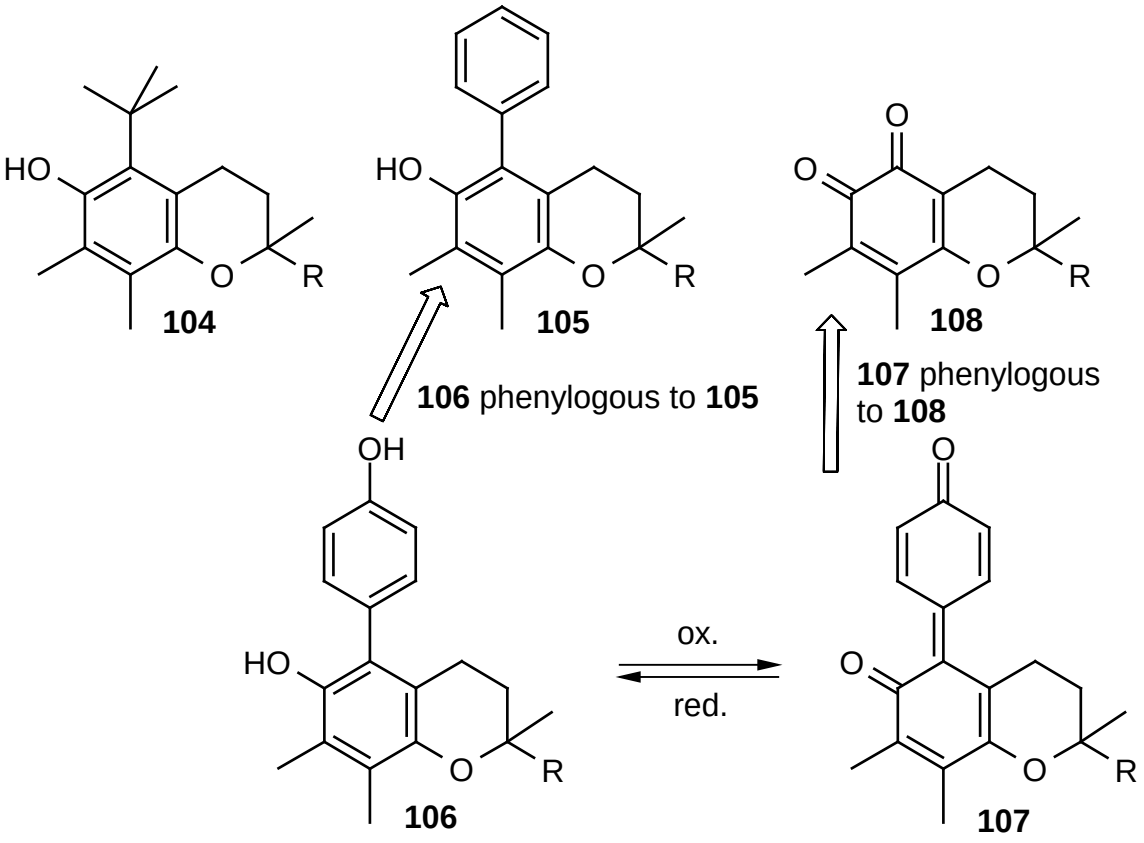

Figure 105. Inability of 5a-substituted derivatives to form structures analogous to oQM 6 causes increased oxidative stability as in compounds 104 and 105. 5-(*p*-Hydroxyphenyl)-γ-tocopherol (106) is oxidized to the conjugatively stabilized oQM 107, the phenylogous α-tocored (108).

Also 5-(4-methylphenyl)-γ-tocopherol (**109**), which can be imagined as "phenylogous α-tocopherol", was as readily oxidized as α-tocopherol (**1**) in aprotic media, providing the quinone structure **110**, which represents a phenylogous oQM **6**, by analogy.[146] The conjugative extension of oQM **6** caused an appreciable stabilization, so that intermediate **110** was stable in inert solvents at r.t. without undergoing dimerization or conjugation reactions. In the presence of HBr, a [1,8]-addition process occurred that afforded 5-(4-bromomethylphenyl)-γ-tocopherol (**111**), other nucleophiles such as water reacting in a similar way by [1,8]-addition. Also bromination of **109** with elemental bromine afforded 5-(4-bromomethylphenyl)-γ-tocopherol (**111**) quantitatively. The reaction proceeded according to an oxidation-addition mechanism *via* the phenylogous quinone methide **110** which added the HBr generated in the oxidation step (Figure 106).[68] The reaction was thus the "phenylogous version" of the bromination of α-tocopherol (**1**) (see Figure 93), with quinone **77** being the phenylogous oQM **6** and bromide **111** acting as phenylogous product 5a-bromo-α-tocopherol (**16**), see Figure 106. Also the ready elimination of HBr from **111** upon alkali treatment or thermal stress finds its parallels in the chemistry of 5a-bromo-α-tocopherol (**16**).

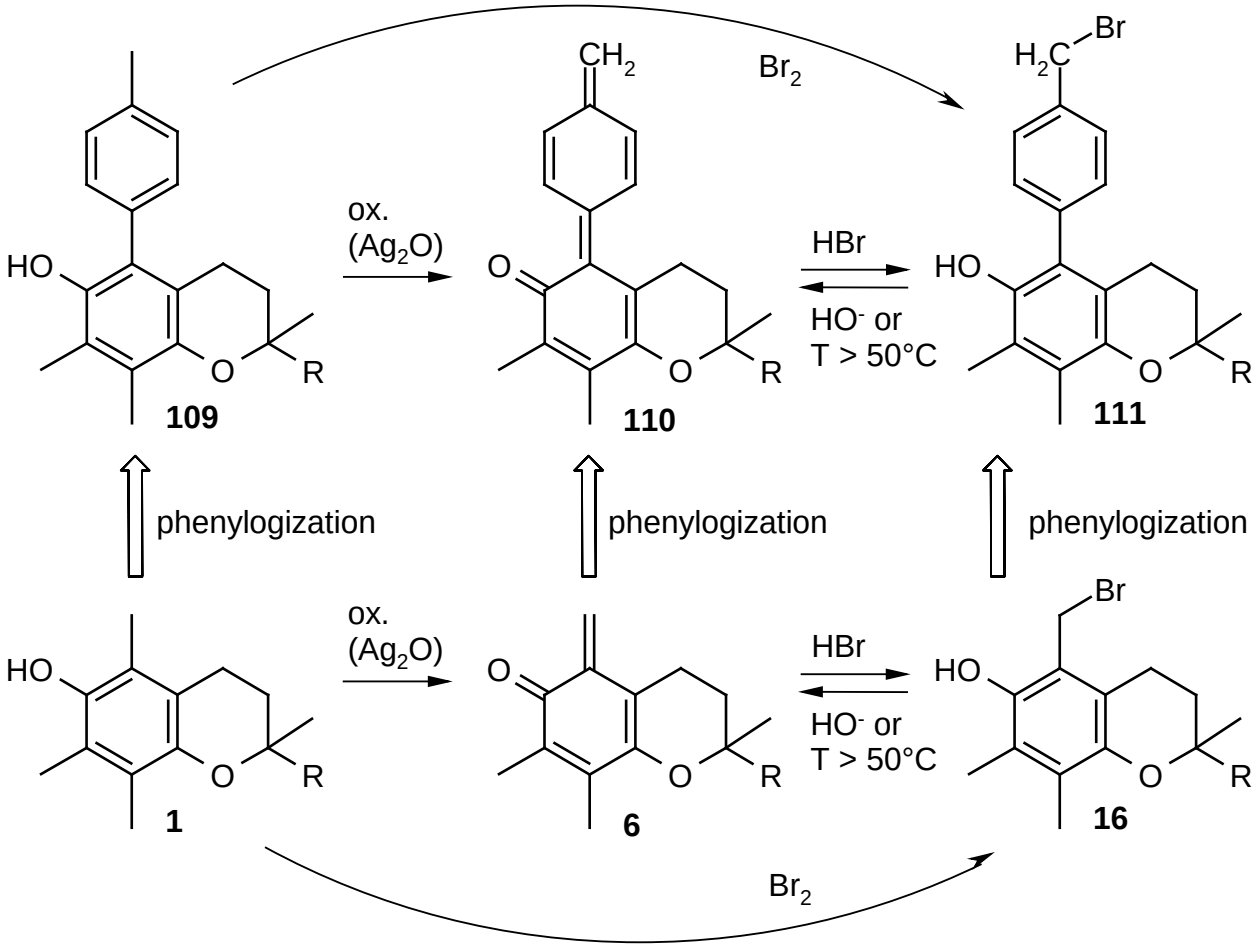

Figure 106. Oxidation chemistry of 5-(4-methylphenyl)-γ-tocopherol (109), establishing a reaction system "phenylogous" to α-tocopherol (1), with quinone methide 110 and benzyl bromide 111 being the conjugatively stabilized, phenylogous counterparts of oQM 6 and 5a-bromo-α-tocopherol (16).

The stability of the phenylogous oQM **110** allowed the conclusion that the conjugative stabilization of oQM **6** by introduction of the phenyl system was nearly as large as the rearomatization energy between oQM **6** and α-tocopherol (**1**). This was confirmed by introducing an additional double bond to the conjugatively stabilized system: oxidation of the styryltocopherol **112** produced the oQM **113**, which represents the "styrylogous" (vinylphenylogous) oQM **6**.[146] This quinoid structure was completely stable at room temperature in the absence of oxygen, also in the presence of water. It did neither undergo any dimerization nor cycloaddition reactions. Heating in the presence of water to 60°C produced the corresponding hydroxymethyl derivative **114**, which at temperatures above 80°C eliminated water again to regenerate the vinylphenylogous oQM **113** (Figure 107). In this compound the conjugative stabilization is very similar to the rearomatization energy of oQM **6** to α-tocopherol (**1**), which provided a nice means to approach this rearomatization energy experimentally.

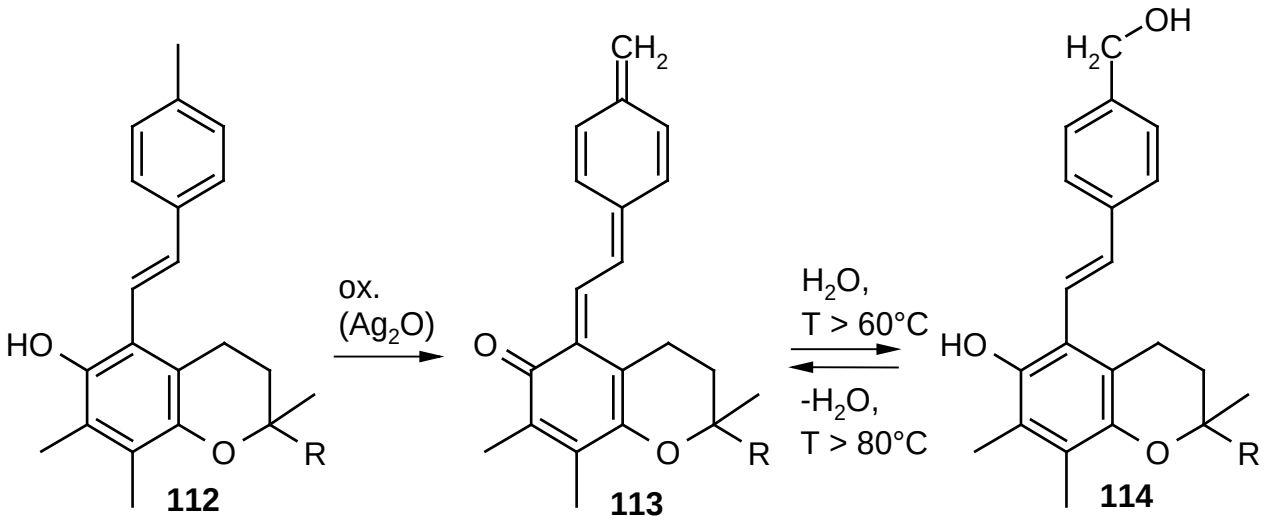

Figure 107. Oxidation of styryl-γ-tocopherol 112 to the stable oQM 113, a "styrylogous" oQM 6.

In a similar fashion, 1,4-bis(5-γ-tocopheryl)benzene (**115**) was oxidized by Ag_2O in toluene into the quinoid compound **116**, a cross-conjugated dimer of oQM **6**, and was reduced back to the parent phenol **115**. Both compounds formed a reversible redox system. Also quinone methide **116** was stable under ambient conditions and did not undergo the reactions typical of oQM **6**. Interestingly, oQM **116** was exclusively formed in the "*cis*"-form (both keto groups on the same side of the C-5 – C-5 axis), but not as the corresponding "*trans*"-structure.[146] The reason for this was an interaction of the phenolic hydroxyl groups with each other and with the oxidant that placed the hydroxyls on the same side of the phenol, exerting a certain pre-organizational effect. When oxidized by DDQ in dichloromethane at room temperature, 1,4-bis(5-γ-tocopheryl)benzene (**115**) formed a mixture of oQM **116** and the corresponding *trans*-isomer **117** in an approximate 1:19 ratio. Stability and reduction of **117** to **115** were similar to the behavior of the *cis*-isomer **116.**

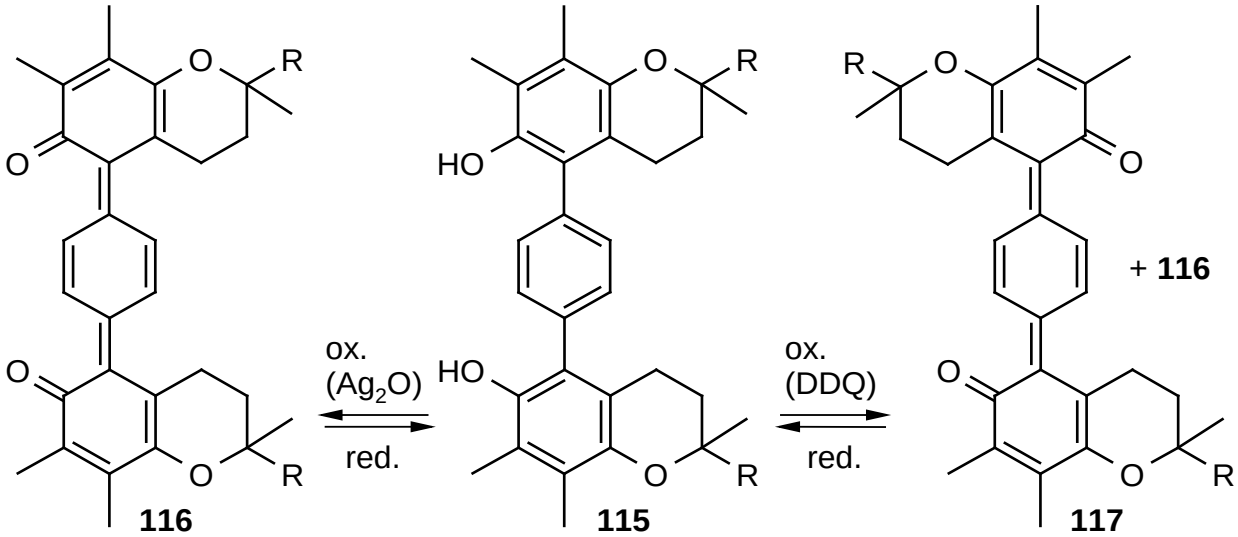

Figure 108. Oxidation of 1,4-bis(5-γ-tocopheryl)benzene (115) to the two stable oQM isomers 116 (*cis*) and 117 (*trans*) in dependence on the oxidant used.

Experimental

General

Commercial chemicals were of the highest grade available and were used without further purification. Tocopherols and tocopheramines were provided by DSM Nutritional Products. Reagent-grade solvents were used for all extractions and workup procedures. Distilled water was used for all aqueous extractions and for all aqueous solutions. All reactions involving non-aqueous conditions were conducted in oven-dried (140°C, overnight) or flame-dried glassware under argon or nitrogen. TLC was performed with Merck silica gel 60 F254 pre-coated plates. Flash chromatography was performed with Baker silica gel (40 μm particle size). All products were purified to homogeneity as checked by TLC/GC-MS analysis. The use of brine refers to saturated NaCl (aq). All given yields refer to isolated, pure products.

Melting points, determined on a Kofler-type micro hot stage with a Reichert–Biovar microscope, are uncorrected. Elemental analyses were performed at the Microanalytical Laboratory of the Institute of Physical Chemistry at the University of Vienna.

^{1}H NMR spectra were recorded at 300.13 MHz (400.13 MHz, respectively) for ^{1}H and at 75.47 MHz (100.41 MHz, respectively) for ^{13}C NMR with $CDCl_3$ as the solvent if not otherwise stated. Chemical shifts, relative to TMS as internal standard, are given as δ values, coupling constants in Hz. ^{13}C peaks were assigned with the aid of APT, HMQC, and HMBC spectra.

GC-MS was performed on a GC 6890N/MSD 5973B instrument with a fused silica HP-5ms (30 m, 0.25 mm, 25 μm) column and helium as carrier gas. Total flow was 27.5 mL min^{-1} at 46.9 kPa carrier gas pressure and the resulting column flow was 0.9 mL min^{-1}. The temperature programs were as follows: 100°C (5 min), 10°C min^{-1} to 280°C (20 min). Aliquots (0.2 μL) of the dissolved samples were injected at 230°C inlet temperature in split mode (25:1). Ionization was performed in EI mode at 70 eV.

Computations, as implemented with the Spartan Pro 04 program package, were carried out on geometries pre-optimized by the semiempirical PM3 method. For full geometry optimization the widely employed B3LYP hybrid method, which includes a mixture of HF and DFT exchange terms and the gradient-corrected correlation functional of Lee, Yang, and Parr,[159,160] parametrized by Becke,[160-162] was used, along with the double-zeta split valence basis sets 6–31+G(d,p)[163,164] which includes diffuse functions, or the higher 6-311G(2df,2p) analogue. Vibrational frequencies were calculated at the corresponding level of theory to characterize local minima (equilibrium structures) or first-order saddle points (transition states) on the potential energy surface and to determine zeropoint vibrational energies. All equilibrium geometries were characterized by real frequencies only, all transition states by one imaginary frequency. For the calculation of rotational barriers the MMFF method was employed.

X-ray Crystallographic Study: X-ray data collection was performed with a Bruker AXS Smart APEX CCD diffractometer and graphite- monochromatized Mo-*K*α radiation, λ = 0.71073 Å; corrections for absorption with the program SADABS, structure solution with direct methods, structure refinement on *F*2 (Bruker AXS, 2001: programs SMART, version 5.626; SAINT, version 6.36A; SADABS version 2.05; XPREP, version 6.12; SHELXTL, version 6.10. Bruker AXS Inc., Madison, WI, USA).

7-Bromo-β-tocopherol (**19**)

7-Bromo-6-hydroxy-2,2,5,8-tetramethylchroman (**19a**)

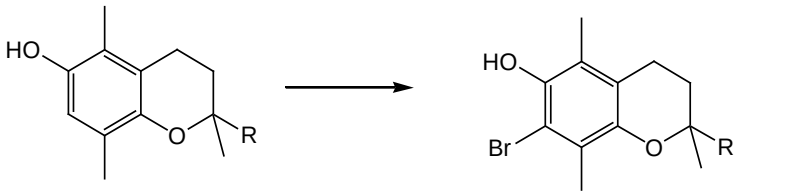

R = Me, $C_{16}H_{33}$

7-Bromo-β-tocopherol (19): A solution of Br_2 in *n*-hexane [1 M, equiv. to 0.0028 mL (0.056 mmol) of Br_2] was added dropwise at 0°C to a stirred solution of β-tocopherol (23.3 mg, 0.056 mmol) in *n*-hexane (10 mL). The solution was stirred for 1 h and allowed to warm to room temp., and the solvent was evaporated *in vacuo*. The residue was purified by flash chromatography on silica gel with an *n*-hexane/diethyl ether gradient (50:1 to 20:1 v/v) to afford **19** as a colorless oil (22.7 mg, 82%).

R_f = 0.62 (*n*-hexane/diethyl ether 9:1 v/v). ^{1}H NMR: δ = 1.72–1.85 (m, 2 H, 3-H), 2.17 (s, 3 H, 8b-H), 2.25 (s, 3 H, 5a-H), 2.59 (t, *J* = 6.9 Hz, 2 H, 4-H), 5.22 (br. s, 1 H, –OH) ppm. ^{13}C NMR: δ = 12.1 (C-5a), 15.8 (C-8b), 20.7 (C-4), 23.8 (C-2a), 31.3 (C-3), 75.3 (C-2), 111.7 (C-7), 120.04; 120.08 (C- 4a; C-5), 122.9 (C-8), 142.9 (C-8a), 145.7 (C-6), isoprenoid side chain: 19.7 (C-4a'), 19.8 (C-8a'), 21.0 (C-2'), 22.7 (C-13'), 22.7 (C- 12a'), 24.4 (C-6'), 24.8 (C-10'), 28.0 (C-12'), 32.6 (C-8'), 32.8 (C- 4'), 37.3 (C-7'), 37.39; 37.40; 37.44 (C-5'; C-9'; C-3'), 39.4 (C-11'), 39.6 (C-1') ppm. $C_{28}H_{47}BrO_2$ (495.58): calcd. C 67.86, H 9.56; found C 67.70, H 9.50.

7-Bromo-6-hydroxy-2,2,5,8-tetramethylchroman (19a): A solution of Br_2 in *n*-hexane [equiv. to 0.012 mL (0.24 mmol) of Br_2] was added dropwise at 0°C to a stirred solution of 6-hydroxy-2,2,5,8-tetramethylchroman (50 mg, 0.24 mmol) in *n*-hexane (10 mL). The solution was stirred for 1 h and allowed to warm to room temp., and the solvent was evaporated *in vacuo*. The residue was purified by flash chromatography on silica gel with *n*-hexane/diethyl ether (9:1 v/v) to afford **19a** as a waxy solid (56.1 mg, 82%).

R_f = 0.53 (*n*-hexane/ ethyl acetate 8:2 v/v). ^{1}H NMR: δ = 1.29 (s, 6 H, 2a-H), 1.79 (t, *J* = 6.9 Hz, 2 H, 3-H), 2.17 (s, 3 H, 8b-H), 2.25 (s, 3 H, 5a- H), 2.60 (t, *J* = 6.9 Hz, 2 H, 4-H), 5.23 (s, 1 H, –OH) ppm. ^{13}C NMR: δ = 12.0 (C-5a), 15.9 (C-8b), 21.0 (C-4), 26.6 (C-2a), 32.8 (C-3), 73.2 (C-2), 111.8 (C-7), 119.8; 120.0 (C-4a; C-5), 123.0 (C- 8), 143.0 (C-8a), 145.8 (C-6) ppm. $C_{13}H_{17}BrO_2$ (285.18): calcd. C 54.75, H 6.01; found C 54.60, H 5.99.

5-Bromomethyl-β-tocopherol (**20**)

5-Bromomethyl-6-hydroxy-2,2,8-trimethylchroman (**20a**)

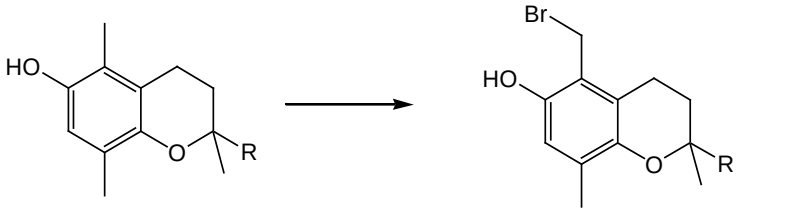

R = Me, $C_{16}H_{33}$

5-Bromomethyl-β-tocopherol (20): A solution of β-tocopherol quinone[165] (0.1 mmol, 43.3 mg) and Me_3SiBr (1.0 mmol, 0.125 g) in dry *n*-hexane (10 mL) was stirred under nitrogen at 40°C for 2 h. Solvent and excess silylating agent were removed under reduced pressure, and the residue was co-evaporated with toluene (10 mL). The residue was dissolved in diethyl ether (20 mL), and water (10 mL) and tetrabutylammonium fluoride (100 mg) were added. After vigorous stirring for 10 min at room temp., water (10 mL) was added and the phases were separated. The organic phase was dried with $MgSO_4$, and the solvent was removed *in vacuo*. The residue was purified by flash chromatography on silica gel with *n*-hexane/ diethyl ether (20:1 v/v) to afford **20** as a greenish oil (37.2 mg, 75%).

R_f = 0.52 (*n*-hexane/diethyl ether 9:1 v/v). ^{1}H NMR: δ = 1.70–1.78 (m, 2 H, 3-H), 2.14 (s, 3 H, 8b-H), 2.60 (t, *J* = 6.8 Hz, 2 H, 4-H), 4.58 (s, 2 H, 5a-H), 5.10 (s, 1 H, –OH) ppm. ^{13}C NMR: δ = 15.6 (C-8b), 19.8 (C-4), 23.8 (C-2a), 27.2 (C-5a), 31.2 (C-3), 75.2 (C-2), 116.0 (C-5), 119.4 (C-4a), 121.4 (C-7), 124.9 (C-8), 143.9 (C-8a), 146.6 (C-6), isoprenoid side chain: 19.7 (C- 4a'), 19.8 (C-8a'), 20.9 (C-2'), 22.6 (C-13'), 22.7 (C-12a'), 24.4 (C- 6'), 24.8 (C-10'), 27.8 (C-12'), 32.6 (C-8'), 32.8 (C-4'), 37.35 (C- 7'), 37.36 (C-5'), 37.40; 37.44 (C-9'; C-3'), 39.2 (C-11'), 39.5 (C- 1') ppm. $C_{28}H_{47}BrO_2$ (495.58): calcd. C 67.86, H 9.56; found C 67.80, H 9.71.

5-Bromomethyl-6-hydroxy-2,2,8-trimethylchroman (20a): A solution of 3-(3-hydroxy-3-methylbutyl)-2,5-dimethyl-1,4-benzoquinone[165] (truncated β-tocopherol quinone, 0.2 mmol, 44.4 mg) and Me_3SiBr (1.0 mmol, 0.125 g) in chloroform (10 mL) was stirred under nitrogen at 40°C for 2 h. Solvent and excess silylating agent were removed under reduced pressure, and the residue was co-evaporated with toluene (10 mL). The residue was dissolved in diethyl ether (20 mL), and water (10 mL) and tetrabutylammonium fluoride (100 mg) were added. After vigorous stirring for 10 min at room temp., water (10 mL) was added and the phases were separated. The organic phase was dried with $MgSO_4$, and the solvent was removed *in vacuo*. The residue was purified by flash chromatography on silica gel with *n*-hexane/diethyl ether (8:2 v/v) to afford **20a** as a greenish, waxy solid (35.9 mg, 63%).

R_f = 0.40 (*n*-hexane/ ethyl acetate 8:2 v/v). ^{1}H NMR: δ = 1.28 (s, 6 H, 2a-H), 1.79 (t, *J* = 6.8 Hz, 2 H, 3-H), 2.14 (s, 3 H, 8b-H), 2.61 (t, 3*J* = 6.8 Hz, 2 H, 4-H), 4.16 (s, 1 H, –OH), 4.52 (s, 2 H, 5a-H), 6.47 (s, 1 H, 7- H) ppm. ^{13}C NMR: δ = 15.8 (C-8b), 19.9 (C-4), 26.5 (C-2a.), 32.4 (C-3), 73.2 (C-2), 116.0 (C-5), 119.7 (C-4a), 121.4 (C-7), 124.6 (C- 8), 144.0 (C-8a), 146.4 (C-6) ppm. $C_{13}H_{17}BrO_2$ (285.18): calcd. C 54.75, H 6.01; found C 54.86, H 6.00.

7-Bromo-5-bromomethyl-β-tocopherol (**21**)

7-Bromo-5-bromomethyl-6-hydroxy-2,2,8-trimethylchroman (**21a**)

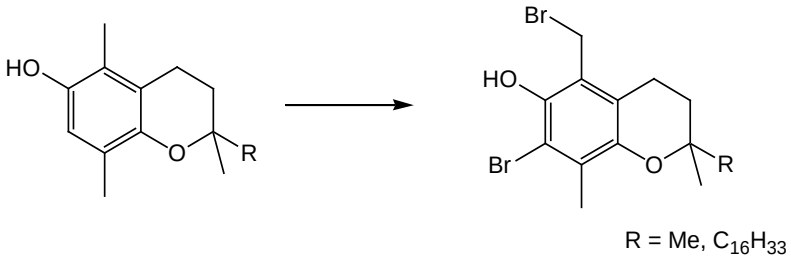

R = Me, $C_{16}H_{33}$

7-Bromo-5-bromomethyl-β-tocopherol (21): A solution of Br_2 in *n*-hexane (equiv. to 0.0087 mL, 0.174 mmol of Br_2) was added in one portion at 40°C to a stirred solution of β-tocopherol (24.1 mg, 0.058 mmol) in *n*-hexane (10 mL). The solution was stirred for 1 h and allowed to cool to room temp. The solution was purged with nitrogen to remove excess bromine until the color had changed to light yellow, and the solvent was evaporated *in vacuo*. The residue was purified by flash chromatography on silica gel with *n*-hexane/ diethyl ether (20:1 v/v) to afford **21** as a green-yellow oil (30.6 mg, 92%).

R_f = 0.54 (*n*-hexane/diethyl ether 9:1 v/v). ^{1}H NMR: δ = 1.72–1.79 (m, 2 H, 3-H), 2.15 (s, 3 H, 8b-H), 2.58 (t, J = 6.8 Hz, 2 H, 4-H), 4.60 (s, 2 H, 5a-H), 5.42 (s, 1 H, –OH) ppm. ^{13}C NMR: δ = 15.8 (C-8b), 19.9 (C-4), 23.8 (C-2a), 26.5 (C-5a), 31.3 (C-3), 75.2 (C-2), 112.0 (C-5), 119.4; 120.0 (C-4a; C-7), 127.9 (C-8), 143.6 (C-8a), 146.6 (C-6), isoprenoid side chain: 19.7 (C-4a'), 19.8 (C- 8a'), 21.0 (C-2'), 22.7 (C-13'), 22.7 (C-12a'), 24.4 (C-6'), 24.8 (C- 10'), 27.9 (C-12'), 32.6 (C-8'), 32.8 (C-4'), 37.32 (C-7'), 37.36 (C- 5'), 37.42; 37.45 (C-9'; C-3'), 39.3 (C-11'), 39.6 (C-1') ppm. $C_{28}H_{46}Br_2O_2$ (574.48): calcd. C 58.54, H 8.07; found C 58.48, H 8.11.

7-Bromo-5-bromomethyl-6-hydroxy-2,2,8-trimethylchroman (21a): A solution of Br_2 (0.037 mL, 0.72 mmol) in *n*-hexane (5 mL) was added in one portion at 40°C to a stirred solution of 6-hydroxy-2,2,5,8-tetramethylchroman (50 mg, 0.24 mmol) in *n*-hexane (10 mL). The solution was stirred for 1 h, allowed to cool to room temp., and purged with nitrogen to remove excess bromine until the color had changed to light yellow. The solvent was evaporated *in vacuo*. The residue was purified by flash chromatography on silica gel with *n*-hexane/diethyl ether (9:1 v/v) to afford **21a** as a greenish, waxy solid (77.8 mg, 89%).

R_f = 0.42 (*n*-hexane/ethyl acetate 8:2 v/v). ^{1}H NMR: δ = 1.28 (s, 6 H, 2a-H) 1.75 (m, J = 6.9 Hz, 2 H, 3-H), 2.10 (s, 3 H, 8b-H), 2.74 (t, J = 6.9 Hz, 2 H, 4-H), 4.59 (s, 2 H, 5a-H), 5.43 (s, 1 H, –OH) ppm. ^{13}C NMR: δ = 16.3 (C- 8b), 19.4 (C-4), 26.4 (C-2a), 27.1 (C-5a), 32.3 (C-3), 73.6 (C-2), 112.1 (C-5), 119.4; 119.9 (C-4a; C-7), 127.5 (C-8), 143.6 (C-8a), 146.3 (C-6) ppm. $C_{13}H_{16}Br_2O_2$ (364.08): calcd. C 42.89, H 4.43; found C 42.94, H 4.21.

5-Bromo-γ-tocopherol (**22**)

5-Bromo-6-hydroxy-2,2,7,8-tetramethylchroman (**22a**)

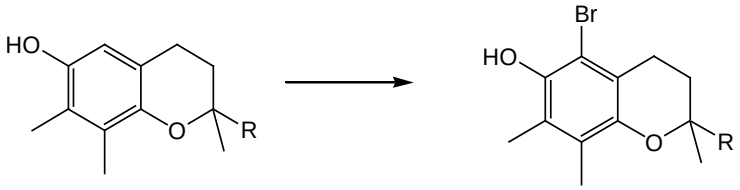

R = Me, $C_{16}H_{33}$

5-Bromo-γ-tocopherol (22): A solution of Br_2 in *n*-hexane (equiv. to 0.0036 mL, 0.072 mmol of Br_2) was added dropwise at 0°C to a stirred solution of γ-tocopherol (30 mg, 0.072 mmol) in *n*-hexane (10 mL). The solution was stirred for 1 h and allowed to warm to room temp., and the solvent was evaporated *in vacuo*. The residue was chromatographed on silica gel with an *n*-hexane/diethyl gradient (50:1 to 20:1 v/v) to give **22** as a colorless oil (25.7 mg, 72%).

R_f = 0.60 (*n*-hexane/diethyl ether 9:1 v/v). ^{1}H NMR: δ = 1.72–1.88 (m, 2 H, 3-H), 2.11 (s, 3 H, 7a/8b-H), 2.23 (s, 3 H, 7a/8b-H), 2.68 (t, J = 6.8 Hz, 2 H, 4-H), 5.21 (br. s, 1 H, –OH) ppm. ^{13}C NMR: δ = 11.8 (C-7a), 12.9 (C-8b), 21.0 (C-4), 23.7 (C-2a), 31.4 (C-3), 75.4 (C-2), 109.2 (C-5), 117.3 (C-4a), 122.3 (C-7), 125.4 (C-8), 143.4 (C-6), 145.9 (C-8a), isoprenoid side chain: 19.6 (C-4a'), 19.6 (C- 8a'), 19.7 (C-2'), 22.6 (C-13'), 22.7 (C-12a'), 24.5 (C-6'), 24.6 (C- 10'), 28.0 (C-12'), 32.6 (C-8'), 32.8 (C-4'), 37.50; 37.55; 37.56 (C- 5'; C-7'; (C-9'), 37.5 (C-3'), 39.55 (C-11'), 39.6 (C-1') ppm. $C_{28}H_{47}BrO_2$ (495.58): calcd. C 67.86, H 9.56; found C 67.70, H 9.50.

5-Bromo-6-hydroxy-2,2,7,8-tetramethylchroman (22a): A solution of Br_2 (0.012 mL, 0.24 mmol) in *n*-hexane (10 mL) was added dropwise at 0°C to a stirred solution of 6-hydroxy-2,2,5,8-tetramethylchroman (50 mg, 0.24 mmol) in *n*-hexane (10 mL). The solution was stirred for 1 h and allowed to warm to room temp., and the solvent was evaporated *in vacuo*. The residue was purified by flash chromatography on silica gel with *n*-hexane/diethyl ether (9:1 v/v) to afford **22a** as a waxy solid (47.9 mg, 70%).

R_f = 0.55 (*n*-hexane/ ethyl acetate 8:2 v/v). ^{1}H NMR: δ = 1.29 (s, 6 H, 2a-H), 1.78 (t, J = 7.2 Hz, 2 H, 3-H), 2.08 (s, 3 H, 7a-H), 2.21 (s, 3 H, 8b-H), 2.68 (t, J = 7.2 Hz, 2 H, 4-H), 5.19 (s, 1 H, OH) ppm. ^{13}C NMR: δ = 11.8 (C-7a), 12.9 (C-8b), 24.3 (C-4), 26.5 (C-2a and C-2b), 33.0 (C- 3), 73.3 (C-2), 109.3 (C-5), 117.1 (C-4a), 122.4 (C-7), 125.4 (C-8), 143.4 (C-6), 146.0 (C-8a) ppm. $C_{13}H_{17}BrO_2$ (285.18): calcd. C 54.75, H 6.01; found C 54.72, H 6.28.

5-Bromo-δ-tocopherol (**25**)

7-Bromo-δ-tocopherol (**27**)

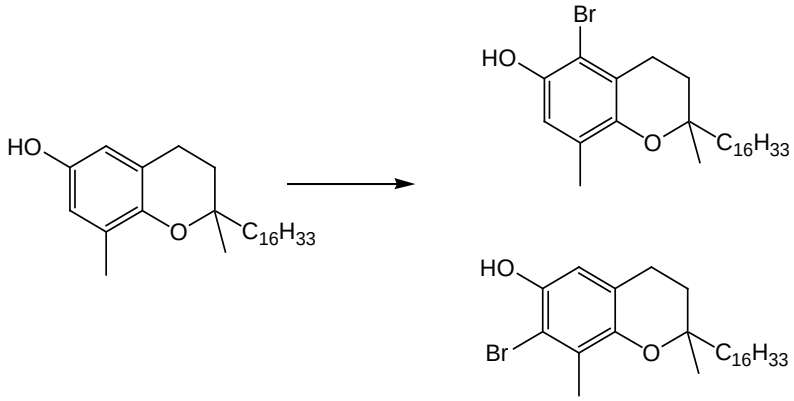

5-Bromo-δ-tocopherol (25) and 7-Bromo-δ-tocopherol (27): A solution of Br_2 in *o*-dichlorobenzene (equiv. to 0.003 mL, 0.06 mmol of Br_2) was added dropwise at 80°C to a stirred solution of δ-tocopherol (48.3 mg, 0.12 mmol) in *o*-dichlorobenzene (10 mL). The solution was stirred for 30 min and allowed to cool to room temp., and the solvent was evaporated *in vacuo*. The residue was purified by flash chromatography on silica gel (*n*-hexane/diethyl ether 50:1 v/v) to give **25** as a colorless oil (19.1 mg, 33%), **27** as a colorless oil (6.9 mg, 12%), and unreacted δ-tocopherol (22.7 mg, 47%) in the order of elution.

5-Bromo-δ-tocopherol (25): TLC: R_f = 0.34 (*n*-hexane/diethyl ether 9:1 v/v). ^{1}H NMR: δ = 1.73–1.86 (m, 2 H, 3-H), 2.11 (s, 3 H, 8b- H), 2.68 (t, J = 6.8 Hz, 2 H, 4-H), 5.05 (s, 1 H, OH), 6.73 (s, 1 H, Ar-H) ppm. ^{13}C NMR: δ = 15.9 (C-8b), 21.2 (C-4), 22.6 (C-2a), 31.3 (C-3), 75.4 (C-2), 109.0 (C-5), 115.1 (CH, C-4a), 120.1 (C-7), 127.0 (C-8), 144.8 (C-8a), 146.3 (C-6), isoprenoid side chain: 19.6 (C-4a'), 19.7 (C-8a'), 20.9 (C-2'), 22.7 (C-13'), 23.7 (C-12a'), 24.1 (C-6'), 24.4 (C-10'), 28.0 (C-12'), 32.7 (C-8'), 32.8 (C-4'), 37.28; 37.39; 37.43; 37.44 (C-3'; C-5'; C-7'; C-9'), 39.3 (C-11'), 39.4 (C- 1') ppm. $C_{27}H_{45}BrO_2$ (481.56): calcd. C 67.34, H 9.42; found C 67.24, H 9.39.

7-Bromo-δ-tocopherol (27): TLC: R_f = 0.27 (*n*-hexane/ethyl acetate 9:1 v/v), 0.31 (*n*-hexane/diethyl ether 9:1 v/v). ^{1}H NMR: δ = 1.69– 1.84 (m, 2 H, 3-H), 2.26 (s, 3 H, 8b-H), 2.68 (m, 2 H, 4-H), 5.11 (s, 1 H, –OH), 6.63 (s, 1 H, Ar-H) ppm. ^{13}C NMR: δ = 15.9 (C- 8b), 22.3 (C-4), 22.6 (C-2a), 31.2 (C-3), 75.4 (C-2), 111.5 (C-7), 112.4 (C-5), 121.1 (C-4a), 126.0 (C-8), 144.8 (C-8a), 146.0 (C-6), isoprenoid side chain: 19.6 (C-4a'), 19.8 (C-8a'), 20.9 (C-2'), 22.7 (C-13'), 23.7 (C-12a'), 24.0 (C-6'), 24.4 (C-10'), 28.0 (C-12'), 32.6 (C-8'), 32.8 (C-4'), 37.2 (C-7'), 37.28; 37.39; 37.40; 37.44 (C-3'; C- 5'; C-7'; C-9'), 39.4 (C-11'), 39.9 (C-1') ppm. $C_{27}H_{45}BrO_2$ (481.56): calcd. C 67.34, H 9.42; found C 67.2, H 9.35.

5-Bromo-6-hydroxy-2,2,8-trimethylchroman (**25a**)

7-Bromo-6- hydroxy-2,2,8-trimethylchroman (**27a**)

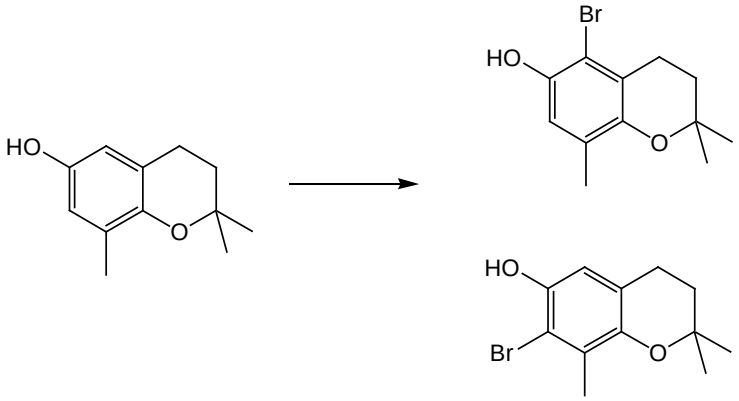

5-Bromo-6-hydroxy-2,2,8-trimethylchroman (25a) and 7-Bromo-6-hydroxy-2,2,8-trimethylchroman (27a): A solution of Br_2 in *o*-dichlorobenzene (equiv. to 0.007 mL, 0.14 mmol of Br_2) was added dropwise at 40°C to a stirred solution of 6-hydroxy-2,2,8-trimethylchroman[54] (50 mg, 0.26 mmol) in *o*-dichlorobenzene (10 mL). The solution was stirred for 30 min and allowed to cool to room temp., and the solvent was evaporated *in vacuo*. The residue was purified by flash chromatography on silica gel (*n*-hexane/diethyl ether 9:1 v/v) to give **25a** as a yellow wax (21.9 mg, 31%), **27a** as a yellow wax (11.2 mg, 16%), and unreacted starting material (21 mg, 42%) in the order of elution.

5-Bromo-6-hydroxy-2,2,8-trimethylchroman (25a): TLC: R_f = 0.34 (*n*-hexane/diethyl ether 8:2 v/v). ^{1}H NMR: δ = 1.29 (s, 6 H, 2a-H), 1.81 (t, J = 6.8 Hz, 2 H, 3-H), 2.11 (s, 3 H, 8b-H), 2.70 (t, J = 6.8 Hz, 2 H, 4-H), 5.00 (s, 1 H, –OH), 6.73 (s, 1 H, Ar-H) ppm. ^{13}C NMR: δ = 16.0 (C-8b), 24.4 (C-4), 26.5 (C-2a), 32.7 (C-3), 73.4 (C-2), 109.0 (C-5), 115.1 (CH, C-4a), 119.9 (C-7), 126.9 (C-8), 144.8 (C-8a), 146.4 (C-6) ppm. $C_{12}H_{15}BrO_2$ (271.15): calcd. C 53.16, H 5.58; found C 53.34, H 5.37.

7-Bromo-6-hydroxy-2,2,8-trimethylchroman (27a): TLC: R_f = 0.28 (*n*-hexane/diethyl ether 8:2 v/v). ^{1}H NMR: δ = 1.29 (s, 6 H, 2a-H), 1.80 (t, J = 6.8 Hz, 2 H, 3-H), 2.19 (s, 3 H, 8b-H), 2.68 (t, J = 6.8 Hz, 2 H, 4-H), 5.35 (s, 1 H, –OH), 6.75 (s, 1 H, Ar-H) ppm. ^{13}C NMR: δ = 15.8 (C-8b), 24.8 (C-4), 26.3 (C-2a), 32.7 (C-3), 73.2 (C-2), 111.5 (C-7), 112.4 (CH, C-5), 121.1 (C-4a), 127.0 (C-8), 144.8 (C-8a), 145.7 (C-6) ppm. $C_{12}H_{15}BrO_2$ (271.15): calcd. C 53.16, H 5.58; found C 53.24, H 5.26.

5,7-Dibromo-δ-tocopherol (**26**)

5,7-Dibromo-6-hydroxy-2,2,8-trimethylchroman (**26a**)

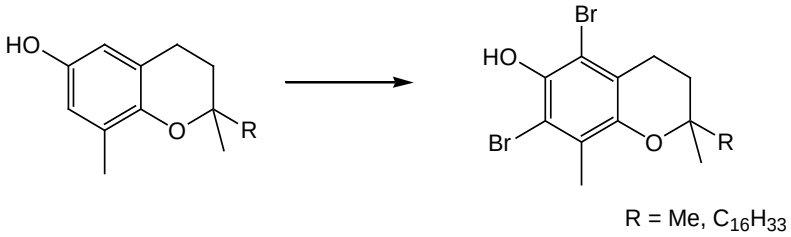

R = Me, $C_{16}H_{33}$

5,7-Dibromo-δ-tocopherol (26): A solution of Br_2 (0.015 mL, 0.30 mmol) in *n*-hexane (5 mL) was added in one portion at 40°C to a stirred solution of δ-tocopherol (48.3 mg, 0.12 mmol) in *n*-hexane (10 mL). The solution was stirred for 30 min and allowed to cool to room temp., and excess bromine was removed by purging with nitrogen. The solvent was evaporated *in vacuo* and the residue was purified by flash chromatography on silica gel (*n*-hexane/diethyl ether 50:1 v/v) to give **26** as a colorless oil (53.8 mg, 80%).

TLC:R_f = 0.46 (*n*-hexane/diethyl ether 9:1 v/v). ^{1}H NMR: δ = 1.74–1.87 (m, 2 H, 3-H), 2.25 (s, 3 H, 8b-H), 2.68 (t, J = 6.8 Hz, 2 H, 4-H), 5.55 (br. s, 1 H, –OH) ppm. ^{13}C NMR: δ = 15.0 (C-8b), 20.2 (C-4), 21.7 (C-2a), 31.6 (C-3), 75.1 (C-2), 107.5 (C-7), 109.8 (C-5), 119.4 (C-4a), 125.2 (C-8), 141.3 (C-8a), 145.8 (C-6), isoprenoid side chain: 18.6 (C-4a'), 19.7 (C-8a'), 19.9 (C-2'), 22.6 (C- 13'), 22.6 (C-12a'), 23.0 (C-6'), 23.4 (C-10'), 27.0 (C-12'), 31.6 (C- 8'), 31.7 (C-4'), 36.2 (C-7'), 36.33; 36.35 (C-5'; C-9'), 36.4 (C-3'), 38.3 (C-11'), 38.4 (C-1') ppm. $C_{27}H_{44}Br_2O_2$ (560.45): calcd. C 57.86, H 7.91; found C 57.72, H 7.89.

5,7-Dibromo-6-hydroxy-2,2,8-trimethylchroman (26a): A solution of Br_2 (0.033 mL, 0.65 mmol) in *n*-hexane (8 mL) was added in one portion at 40°C to a stirred solution of 6-hydroxy-2,2,8-trimethylchroman[54] (50 mg, 0.26 mmol) in *n*-hexane (10 mL). The solution was stirred for 30 min and allowed to cool to room temp., and excess bromine was removed by flushing with nitrogen. The solvent was evaporated *in vacuo* and the residue was purified by flash chromatography on silica gel (*n*-hexane/diethyl ether, 50:1 v/v) to give **26a** as a brownish wax (83.7 mg, 92%).

TLC: R_f = 0.33 (*n*-hexane/ ethyl acetate, 9:1 v/v). ^{1}H NMR: δ = 1.30 (s, 6 H, 2a-H), 1.80 (t, J = 6.8 Hz, 2 H, 3-H), 2.25 (s, 3 H, 8b-H), 2.69 (t, J = 6.8 Hz, 2 H, 4-H), 5.55 (s, 1 H, –OH) ppm. ^{13}C NMR: δ = 16.0 (C-8b), 24.5 (C-4), 26.4 (C-2a), 32.6 (C-3), 74.1 (C-2), 108.5 (C-7), 110.8 (C-5), 120.0 (C-4a), 126.2 (C-8), 142.4 (C-8a), 146.4 (C- 6) ppm. $C_{12}H_{14}Br_2O_2$ (350.05): calcd. C 41.17, H 4.03; found C 41.36, H 3.94.

Methanesulfonic acid 2,2,5,7,8-pentamethylchroman-6-yl ester

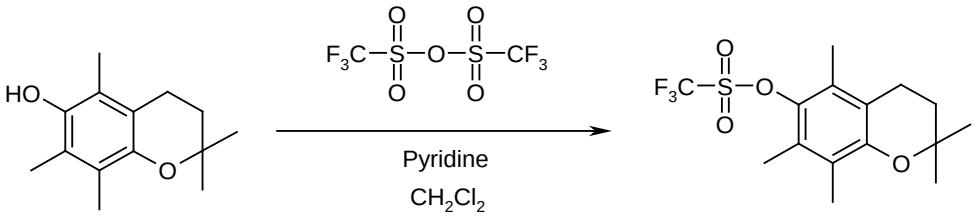

$C_{14}H_{20}O_2$
220.31 g/mole

$C_{15}H_{19}O_4S_1F_3$
352.37 g/mole

Substance	Quant.	M.W.	mmol	Eq.
6-Hydroxy-2,2,5,7,8-pentamethylchroman	4.0 g	220.31	18.15	1
Triflic anhydride (d= 1.7)	6.71 g (3.94 mL)	282.13	23.78	1.31

Procedure: A oven dried single necked 250-mL round-bottom flask equipped with a nitrogen inlet, rubber septum and magnetic stir bar was charged with 6-hydroxy-2,2,5,7,8-pentamethylchroman, anhydrous dichloromethane (66 mL) and anhydrous pyridine. The solution was cooled in an ice bath (0 - 4ºC) and triflic anhydride was added dropwise *via* a syringe. The cold bath was removed and the reaction mixture was allowed to warm to ambient temperature and stir for 15 min. The progress of the reaction was monitored by TLC. Upon completion, the mixture was diluted with cold 5% aq. $NaHCO_3$ (66 mL) and the organic and aqueous layers were separated in a separatory funnel. The aqueous layer was extracted two times with dichloromethane (2 × 50 mL). The combined organic extracts were washed with brine and dried over Na_2SO_4 and then concentrated on a rotary evaporator. Flash chromatography (SiO_2, *n*-hexane → *n*-hexane with drops of ethyl acetate) of the crude product furnished the pure product (methanesulfonic acid 2,2,5,7,8-pentamethylchroman-6-yl ester 6.22 g = 97% yield) as a colorless oil.

TLC: R_f = 0.60 (SiO_2; *n*-hexane:ethyl acetate 9:1 (v/v)). Color reaction of the spot with *p*-anisaldehyde reagent: violet, also visible under UV. ^{1}H NMR ($CDCl_3$): δ = 1.31 (s, 6H, H-2a), 1.80 (t, 2H, ^3J = 6.8 Hz, H-3), 2.10, 2.19, 2.22 (s, 9H, H-5a,7a,8b), 2.61 (t, 2H, ^3J = 6.8 Hz, H-4).

Benzhydrylidene-(2,2,5,7,8-pentamethylchroman-6-yl)-amine [86]

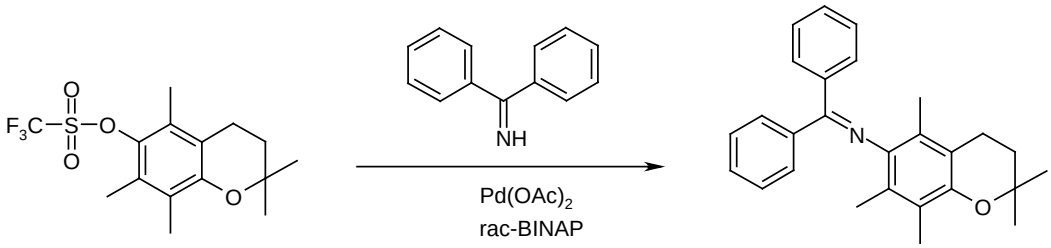

$C_{15}H_{19}O_4S_1F_3$
352.37 g/mole

$C_{27}H_{29}O_1N_1$
383.54 g/mole

Substance	Quant.	M.W.	mmol	Eq.
Methanesulfonic acid 2,2,5,7,8-pentamethylchroman-6-yl ester	0.5196 g	352.37	1.47	1
Benzophenone imine (*d*= 1.084)	0.3189 g (0.295 mL)	181.23	1.76	1.2
Sodium *tert*-butoxide	0.1835 g	96.11	1.91	1.3
(Palladium(II) acetate	0.0163 g	224.49	0.073	0.05
((±)-2,2'-Bis(diphenylphosphino)-1,1'-binaphthalene)	0.0596 g	622.69	0.0958	0.065

Procedure: A oven dried two necked 25-mL round-bottom flask equipped with a condenser, nitrogen inlet, rubber septum and magnetic stir bar was charged with palladium(II) acetate and (±)-2,2'-bis(diphenylphosphino)-1,1'-binaphthalene in anhydrous toluene (4.5mL). The mixture was stirred for 30 min. at 23ºC. Then, first a solution of 2,2,5,7,8-pentamethylchroman triflate (and benzophenone imine in anhydrous toluene (4.5 mL) and after 5 minutes, sodium *tert*-butoxide were added to the catalyst mixture at 23ºC. The resulting mixture was heated at 80ºC for 90 minutes. The progress of the reaction was monitored by TLC. Upon completion, the reaction mixture was allowed to cool to room temperature, diluted with diethyl ether (60 mL)) and filtered through a plug of 3 cm silica gel topped with 1 cm of celite. The crude product was concentrated and partially purified by short flash chromatography (SiO_2, *n*-hexane → *n*-hexane with drops of ethyl acetate) and crude product was then recrystallized from methanol to furnish the pure product (benzhydrylidene-(2,2,5,7,8-pentamethylchroman-6-yl)-amine) 0.52 g = 93% yield) as a yellow-orange solid.

TLC: R_f = 0.42 (SiO_2; *n*-hexane:ethyl acetate 9:1 (v/v)). Color reaction of the spot with *p*-anisaldehyde reagent: yellow, also visible under UV. ^{1}H NMR - 300 MHz ($CDCl_3$): δ = 1.22 (s, 3H, H-2a), 1.27 (s, 3H, H-2a), 1.74 (m, 2H, H-3), 1.87 (s, 3H, H-5a/7a/8a), 1.94 (s, 3H, H-5a/7a/8a), 2.01 (s, 3H, H-5a/7a/8a), 2.49 (m, 2H, H-4), 7.18 (m, 3H, Ar-H), 7.42 (m, 4H, Ar-H), 7.79 (m, 3H, Ar-H).

2,2,5,7,8-Pentamethylchroman-6-ylamine (**30**)[86]

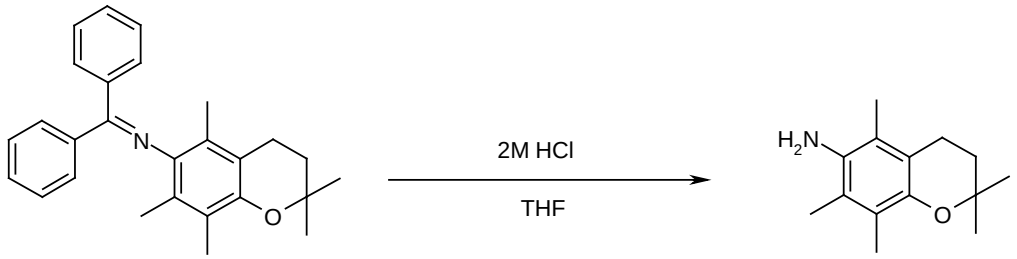

$C_{27}H_{29}O_1N_1$
383.54 g/mole

$C_{14}H_{21}O_1N_1$
219.32 g/mole

Substance	Quant.	M.W.	mmols
Benzhydrylidene-(2,2,5,7,8-pentamethylchroman-6-yl)-amine	0.511 g	383.54	1.33

Procedure: A single necked 25-mL round-bottom flask equipped with a magnetic stir bar was charged with 6-imine-2,2,5,7,8-pentamethylchroman and THF (7.5 mL). 2 M HCl solution (5 mL) was added at 23 ºC. The resulting orange solution was stirred at 23 ºC for overnight. The progress of the reaction was monitored by TLC. Upon completion, 1 M NaOH aq. solution (15 mL) was added and the aqueous phase extracted with diethyl ether (3 × 15 mL). The combined organic phase was washed with brine and dried over $MgSO_4$. After the removal of the solvent under vacuum, flash chromatography (short path of SiO_2, *n*-hexane with drops of ethyl acetate → 9:1) furnished the pure product (2,2,5,7,8-Pentamethylchroman-6-ylamine) 0.21 g = 72% yield) as a light brownish white solid.

TLC: R_f = 0.16 (SiO_2; *n*-hexane:ethyl acetate 8:2 (v/v)). Color reaction of the spot with ninhydrin reagent: green. ^{1}H NMR ($CDCl_3$): δ = 1.23 (s, 6H, H-2a), 1.73 (t, 2H, ^3J = 6.8 Hz, H-3), 2.02 (s, 6H, H-5a,8b), 2.05 (s, 3H, H-7a), 2.54 (t, 2H, ^3J = 6.8 Hz, H-4). ^{13}C NMR ($CDCl_3$): δ = 11.88 (C-5a), 15.85 (C-8b), 21.33 (C-4), 26.65 (C-2a), 33.21 (C-3), 72.20 (C-2), 116.68 (C-7), 118.90 (C-8), 119.53 (C-5), 124.04 (C-4a), 135.47 (C-6), 145.64 (C-8a). Elemental Anal. Calcd. for $C_{14}H_{21}O_1N_1$ (219.32): C: 76.67, H: 9.65, N, 6.39; found: C: 76.62, H, 9.72, N: 6.35.

Methanesulfonic acid 2,2,5,8-tetramethylchroman-6-yl ester [85]

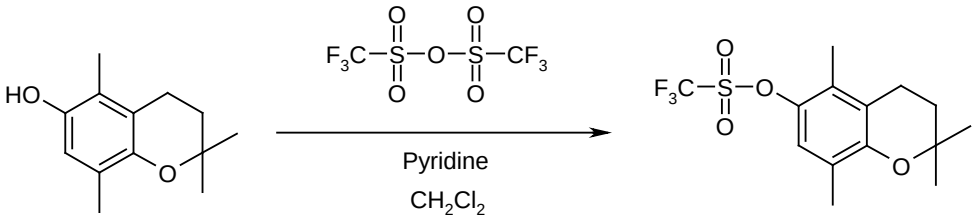

$C_{13}H_{18}O_2$
206.28 g/mole

$C_{14}H_{17}O_4S_1F_3$
338.34 g/mole

Substance	Quant.	M.W.	mmol	Eq.
6-Hydroxy-2,2,5,8-tetramethylchroman	0.6 g	206.28	2.9	1
Triflic anhydride (d= 1.7)	1.075 g (0.63 mL)	282.13	3.8	1.31

Procedure: A oven dried single necked 25-mL round-bottom flask equipped with a nitrogen inlet, rubber septum and magnetic stir bar was charged with 6-hydroxy-2,2,5,8-tetramethylchroman, anhydrous dichloromethane (11 mL) and anhydrous pyridine (0.5 mL). The solution was cooled in an ice bath (0 - 4°C) and triflic anhydride was added dropwise *via* a syringe. The cold bath was removed and the reaction mixture was allowed to warm to ambient temperature and stir for 15 min. The progress of the reaction was monitored by TLC. Upon completion, the reaction was diluted with cold 5% aq. $NaHCO_3$ (12 mL) and the organic and aqueous layers were separated in a separatory funnel. The aqueous layer was extracted two times with dichloromethane (2 × 12 mL). The combined organic extracts were washed with brine and dried over Na_2SO_4 and then concentrated on a rotary evaporator. Flash chromatography (SiO_2, *n*-hexane → *n*-hexane with drops of ethyl acetate) of the crude product furnished the pure product (methanesulfonic acid 2,2,5,8-tetramethylchroman-6-yl ester 0.94 g = 96% yield) as a white solid.

TLC: R_f = 0.53 (SiO_2; *n*-hexane:ethyl acetate 9:1 (v/v)). Color reaction of the spot with *p*-anisaldehyde reagent: violet, also visible under UV. ^{1}H NMR ($CDCl_3$): δ = 1.31 (s, 6H, H-2a), 1.81 (t, 2H, ^3J = 6.8 Hz, H-3), 2.13, 2.18 (s, 6H, H-5a,8b), 2.61 (t, 2H, ^3J = 6.8 Hz, H-4), 6.85 (s, 1H, H-7).

Benzhydrylidene-(2,2,5,8-tetramethylchroman-6-yl)-amine [86]

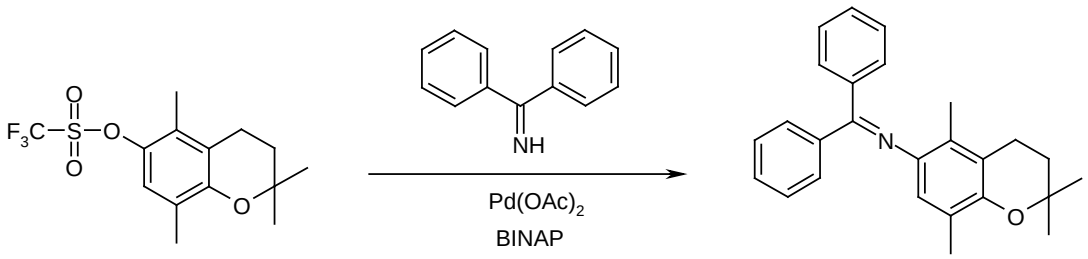

$C_{14}H_{17}O_4S_1F_3$
338.34 g/mole

$C_{26}H_{27}O_1N_1$
369.51 g/mole

Substance	Quant.	M.W.	mmol	Eq.
Methanesulfonic acid 2,2,5,8-tetramethylchroman-6-yl ester	0.9385 g	338.34	2.77	1
Benzophenone imine (*d*= 1.084)	0.6016 g (0.55 mL)	181.23	3.32	1.2
Sodium *tert*-butoxide	0.3459 g	96.11	3.60	1.3
Palladium(II) acetate	0.0310 g	224.49	0.1385	0.05
(±)-2,2'-Bis(diphenylphosphino)-1,1'-binaphthalene	0.1120 g	622.69	0.180	0.065

Procedure: A oven dried two necked 50-mL round-bottom flask equipped with a condenser, nitrogen inlet, rubber septum and magnetic stir bar was charged with palladium(II) acetate and (±)-2,2'-bis(diphenylphosphino)-1,1'-binaphthalene in anhydrous toluene (8.5mL). The mixture was stirred for 30 min. at 23ºC. Then, first a solution of 2,2,5,8-tetramethylchroman triflate and benzophenone imine in anhydrous toluene (8.5 mL) and after 5 minutes, sodium *tert*-butoxide were added to the catalyst mixture at 23ºC. The resulting mixture was heated at 80ºC for 3.5 h. The progress of the reaction was monitored by TLC. Upon completion, the reaction mixture was allowed to cool to room temperature, diluted with diethyl ether (120 mL) and filtered through a plug of 3 cm silica gel topped with 1 cm of celite. The crude product was concentrated, flash chromatography (SiO_2, *n*-hexane → *n*-hexane with drops of ethyl acetate) of the crude product furnished the pure product (Benzhydrylidene-(2,2,5,8-tetramethylchroman-6-yl)-amine) 0.97 g = 95% yield) as a yellow-orange oil.

TLC: R_f = 0.45 (SiO_2; *n*-hexane:ethyl acetate 9:1 (v/v)). Color reaction of the spot with *p*-anisaldehyde reagent: yellow, also visible under UV. ^{1}H NMR - 300 MHz ($CDCl_3$): δ = 1.26 (s, 6H, H-2a), 1.76 (t, 2H, H-3), 1.95 (s, 3H, H-8b), 2.06 (s, 3H, H-5a), 2.54 (t, 2H, H-4), 7.43-7.52 (m, 5H, H-7, H-3', H-5'), 7.59 (t, 2H, H-4'), 7.80 (d, 4H, H-2', H-6').

2,2,5,8-Tetramethylchroman-6-ylamine (**31**)[86]

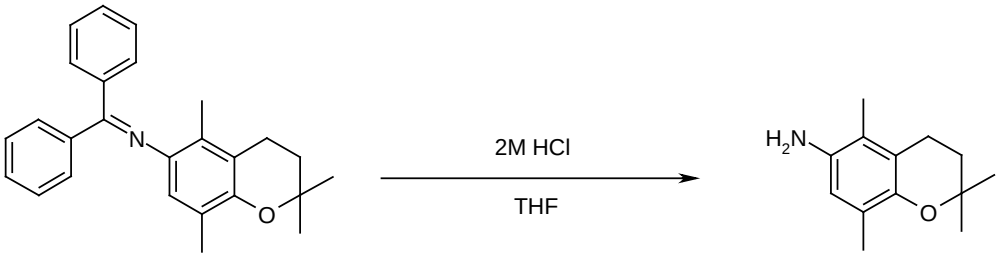

$C_{26}H_{27}O_1N_1$
369.51 g/mole

$C_{13}H_{19}O_1N_1$
205.30 g/mole

Substance	Quant.	M.W.	mmol
Benzhydrylidene-(2,2,5,8-tetramethylchroman-6-yl)-amine	0.5184 g	369.51	1.40

Procedure: A single necked 25-mL round-bottom flask equipped with a magnetic stir bar was charged with 6-imine-2,2,5,8-tetramethylchroman and THF (8 mL). 2 M HCl solution (5.3 mL) was added at 23ºC. The resulting orange solution stirred at 23 ºC for 30 min. The progress of the reaction was monitored by TLC. Upon completion, 1 M NaOH aq. solution (16 mL) was added and the aqueous phase extracted with diethyl ether (3 × 16 mL). The combined organic phase was washed with brine and dried over $MgSO_4$. After the removal of the solvent under vacuum, flash chromatography (SiO_2, *n*-hexane with drops of ethyl acetate→ 7:3) furnished the pure product (2,2,5,8-tetramethylchroman-6-ylamine) 0.20 g = 69% yield) as a light brownish white solid.

Mp (ºC): 72-74. TLC: R_f = 0.2 (SiO_2; *n*-hexane:ethyl acetate 7:3 (v/v)). Color reaction of the spot with *p*-anisaldehyde reagent: yellow, also visible under UV. ^{1}H NMR ($CDCl_3$): δ = 1.28 (s, 6H, H-2a), 1.77 (t, 2H, ^3J = 6.8 Hz, H-3), 2.03 (s, 3H, H-5a/8b), 2.09 (s, 3H, H-5a/8b), 2.63 (t, 2H, ^3J = 6.8 Hz, H-4) 3.52 (br, 2H, -NH_2), 6.46 (s, 1H, H-7). ^{13}C NMR ($CDCl_3$): δ = 12.27 (C-5a), 15.85 (C-8b), 21.28 (C-4), 26.64 (C-2a), 33.05 (C-3), 72.20 (C-2), 116.68 (C-7), 118.90 (C-8), 119.53 (C-5), 124.04 (C-4a), 135.47 (C-6), 145.64 (C-8a). Elemental Anal. Calcd. for $C_{13}H_{19}O_1N_1$ (205.30): C: 76.06, H: 9.33, N: 6.82; found: C: 75.99, H: 9.38, N: 6.80.

Methanesulfonic acid 2,2,7,8-tetramethylchroman-6-yl ester [85]

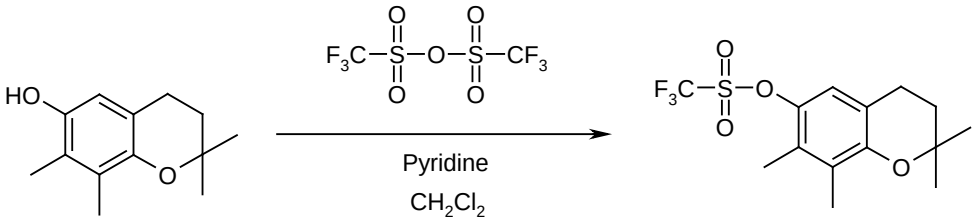

$C_{13}H_{18}O_2$
206.28 g/mole

$C_{14}H_{17}O_4S_1F_3$
338.34 g/mole

Substance	Quant.	M.W.	mmol	Eq.
6-Hydroxy-2,2,7,8-tetramethylchroman	1.0 g	206.28	4.847	1
Triflic anhydride (d= 1.7)	1.79 g (1.05 mL)	282.13	6.350	1.31

Procedure: A oven dried single necked 250-mL round-bottom flask equipped with a nitrogen inlet, rubber septum and magnetic stir bar was charged with 6-hydroxy-2,2,7,8-tetramethylchroman, anhydrous dichloromethane (19 mL) and anhydrous pyridine. The solution was cooled in an ice bath (0 - 4°C) and triflic anhydride was added dropwise *via* a syringe. The cold bath was removed and the reaction mixture was allowed to warm to ambient temperature and stir for 30 min. The progress of the reaction was monitored by TLC. Upon completion, the reaction was diluted with cold 5% aq. $NaHCO_3$ (20 mL) and the organic and aqueous layers were separated in a separatory funnel. The aqueous layer was extracted two times with dichloromethane (2 × 20 mL). The combined organic extracts were washed with brine and dried over Na_2SO_4 and then concentrated on a rotary evaporator. Flash chromatography (SiO_2, *n*-hexane → *n*-hexane with drops of ethyl acetate) of the crude product furnished the pure product (methanesulfonic acid 2,2,7,8-tetramethylchroman-6-yl ester 1.56 g = 95% yield) as a colorless oil.

TLC: R_f = 0.57 (SiO_2; *n*-hexane:ethyl acetate 9:1 (v/v)). Color reaction of the spot with *p*-anisaldehyde reagent: violet, also visible under UV. ^{1}H NMR ($CDCl_3$): δ = 1.32 (s, 6H, H-2a), 1.77 (t, 2H, ^3J = 6.8 Hz, H-3), 2.11, 2.20 (s, 6H, H-7a, 8b), 2.74 (t, 2H, ^3J = 6.8 Hz, H-4), 6.80 (s, 1H, H-5).

Benzhydrylidene-(2,2,7,8-tetramethylchroman-6-yl)-amine [86]

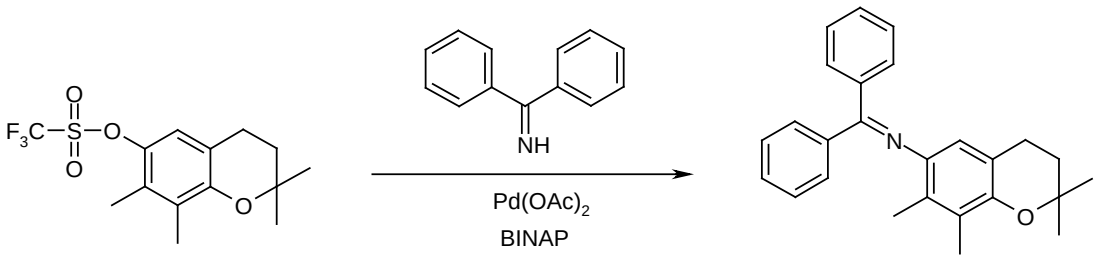

$C_{14}H_{17}O_4S_1F_3$
338.34 g/mole

$C_{26}H_{27}O_1N_1$
369.51 g/mole

Substance	Quant.	MW.	mmols	Eq.
Methanesulfonic acid 2,2,7,8-tetramethylchroman-6-yl ester	1.5482 g	338.34	4.57	1
Benzophenone imine (*d*= 1.084)	0.9949 g (0.91 mL)	181.23	5.49	1.2
Sodium *tert*-butoxide	0.5708 g	96.11	5.94	1.3
Palladium(II) acetate	0.0513 g	224.49	0.22	0.05
(±)-2,2'-Bis(diphenylphosphino)-1,1'-binaphthalene	0.1852 g	622.69	0.29	0.065

Procedure: A oven dried two necked 25-mL round-bottom flask equipped with a condenser, nitrogen inlet, rubber septum and magnetic stir bar was charged with palladium(II) acetate and (±)-2,2'-bis(diphenylphosphino)-1,1'-binaphthalene in anhydrous toluene (14 mL). The mixture was stirred for 30 min. at 23ºC. Then, first a solution of 2,2,7,8-tetramethylchroman triflate and benzophenone imine in anhydrous toluene (14 mL) and after 5 minutes, sodium *tert*-butoxide were added to the catalyst mixture at 23ºC. The resulting mixture was heated at 80ºC for 60 minutes. The progress of the reaction was monitored by TLC. Upon completion, the reaction mixture was allowed to cool to room temperature, diluted with diethyl ether (185 mL) and filtered through a plug of celite. The crude product was concentrated, and flash chromatography (SiO_2, *n*-hexane → *n*-hexane with drops of ethyl acetate) of the crude product furnished the pure product (benzhydrylidene-(2,2,7,8-tetramethyl-chroman-6-yl)-amine) 1.60 g = 95% yield) as a yellow-orange oil.

TLC: R_f = 0.46 (SiO_2; *n*-hexane:ethyl acetate 9:1 (v/v)). Color reaction of the spot with *p*-anisaldehyde reagent: yellow, also visible under UV. ^{1}H NMR - 300 MHz ($CDCl_3$): δ = 1.25 (s, 6H, H-2a), 1.66 (t, 2H, H-3), 2.06 (s, 3H, H-8b), 2.10 (s, 3H, H-7a), 2.48 (t, 2H, H-4), 7.26 (s, 1H, H-5), 7.40-7.60 (m, 6H, H-3', H-4', H-5'), 7.81 (d, 4H, H-2', H-6').

2,2,7,8-Tetramethylchroman-6-ylamine (**32**)[86]

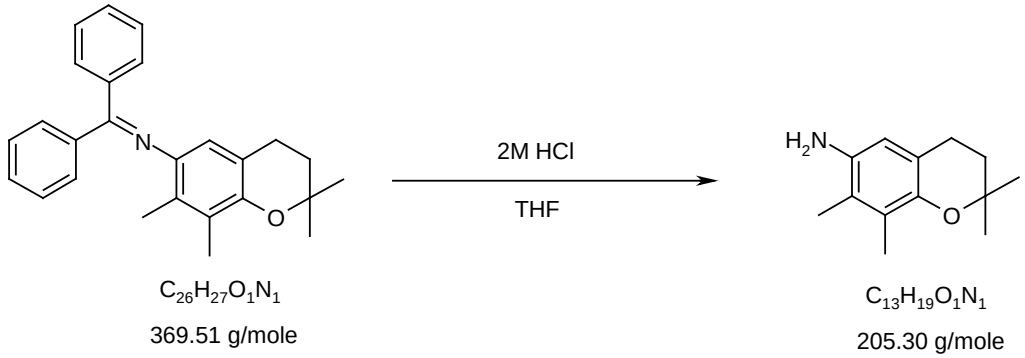

$C_{26}H_{27}O_1N_1$
369.51 g/mole

$C_{13}H_{19}O_1N_1$
205.30 g/mole

Substance	Quant.	M.W.	mmol
Benzhydrylidene-(2,2,7,8-tetramethylchroman-6-yl)-amine	1.6046 g	369.51	4.34

Procedure: A single necked 25-mL round-bottom flask equipped with a magnetic stir bar was charged with 6-imine-2,2,7,8-tetramethylchroman and THF (25 mL). 2 M HCl solution (16.2 mL) was added at 23ºC. The resulting orange solution stirred at 23 ºC for 30 min. The progress of the reaction was monitored by TLC. Upon completion, 1 M NaOH aq. solution (49 mL) was added and the aqueous phase extracted with diethyl ether (3 × 50 mL). The combined organic phase was washed with brine and dried over $MgSO_4$. After the removal of the solvent under vacuum flash chromatography (SiO_2, *n*-hexane with drops of ethyl acetate→ 7:3) furnished the pure product (2,2,7,8-Tetramethylchroman-6-ylamine) 0.6 g = 67% yield) as a white solid.

TLC: R_f = 0.15 (SiO_2; *n*-hexane:ethyl acetate 7:3 (v/v)). Color reaction of the spot with ninhydrin reagent: green. Color reaction of the spot with $KMnO_4$ reagent: yellow. ^{1}H NMR ($CDCl_3$): δ = 1.23 (s, 6H, H-2a), 1.73 (t, 2H, ^3J = 6.8 Hz, H-3), 2.02 (s, 6H, H-5a,8b), 2.05 (s, 3H, H-7a), 2.54 (t, 2H, ^3J = 6.8 Hz, H-4), 6.29 (s, 1H, C5-H). ^{13}C NMR ($CDCl_3$): δ = 16.00 (C-8b), 22.77 (C-4), 26.94 (C-2a), 32.98 (C-3), 73.33 (C-2), 113.97 (C-5), 116.50 (C-7), 120.92 (C-8), 127.01 (C-4a), 137.19 (C-6), 145.63 (C-8a). Elemental Anal. Calcd. for $C_{13}H_{19}O_1N_1$ (205.30): C: 76.06, H: 9.33, N: 6.82; found: C: 76.12, H: 9.42, N: 6.76.

Methanesulfonic acid 2,2,8-trimethylchroman-6-yl ester [85]

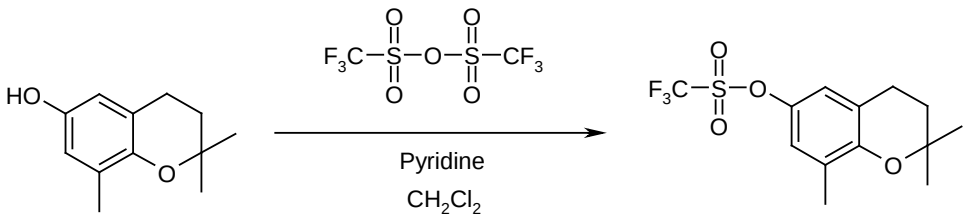

$C_{12}H_{16}O_2$
192.25 g/mole

$C_{13}H_{15}O_4S_1F_3$
324.31 g/mole

Substance	Quant.	M.W.	mmol	Eq.
6-Hydroxy-2,2,8-trimethylchroman	0.3 g	192.25	1.56	1
Triflic anhydride (d= 1.7)	0.576 g (0.33 mL)	282.13	2.04	1.31

Procedure: A oven dried single necked 25-mL round-bottom flask equipped with a nitrogen inlet, rubber septum and magnetic stir bar was charged with 6-hydroxy-2,2,8-trimethylchroman, anhydrous dichloromethane (6 mL) and anhydrous pyridine (0.3 mL). The solution was cooled in an ice bath (0 - 4ºC) and triflic anhydride was added dropwise *via* a syringe. The cold bath was removed and the reaction mixture was allowed to warm to ambient temperature and stir for 20 min. The progress of the reaction was monitored by TLC. Upon completion, the reaction was diluted with cold 5% aq. $NaHCO_3$ (6 mL) and the organic and aqueous layers were separated in a separatory funnel. The aqueous layer was extracted two times with dichloromethane (2 × 5 mL). The combined organic extracts were washed with brine and dried over Na_2SO_4 and then concentrated on a rotary evaporator. Flash chromatography (SiO_2, *n*-hexane → *n*-hexane with drops of ethyl acetate) of the crude product furnished the pure product (methanesulfonic acid 2,2,8-trimethylchroman-6-yl ester 0.46 g = 92% yield) as a colorless oil.

TLC: R_f = 0.56 (SiO_2; *n*-hexane:ethyl acetate 9:1 (v/v)). Color reaction of the spot with *p*-anisaldehyde reagent: violet, also visible under UV. ^{1}H NMR ($CDCl_3$): δ = 1.25 (s, 6H, H-2a), 1.72 (t, 2H, ^3J = 6.8 Hz, H-3), 2.09 (s, 3H, H-8b), 2.70 (t, 2H, ^3J = 6.8 Hz, H-4), 6.74, 6.77 (s, 2H, H-5, H-7).

Benzhydrylidene-(2,2,8-trimethyl-chroman-6-yl)-amine [86]

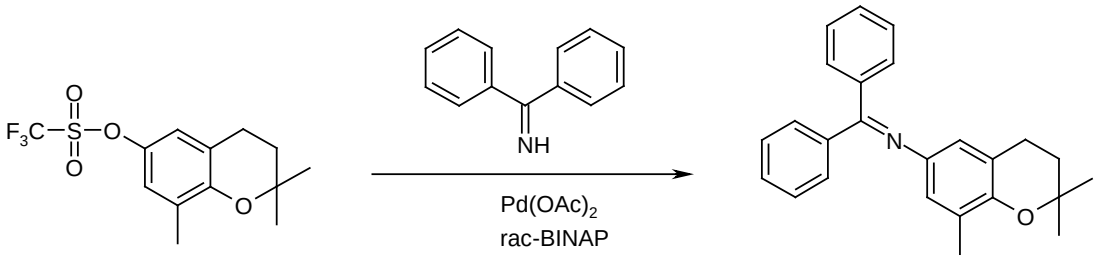

$C_{13}H_{15}O_4S_1F_3$
324.31 g/mole

$C_{25}H_{25}O_1N_1$
355.48 g/mole

Substance	Quant.	M.W.	mmol	Eq.
Methanesulfonic acid 2,2,8-trimethylchroman-6-yl ester	0.4377 g	324.31	1.34	1
Benzophenone imine (*d*= 1.084)	0.2899 g (0.26 mL)	181.23	1.60	1.2
Sodium *tert*-butoxide	0.1672 g	96.11	1.74	1.3
Palladium(II) acetate	0.0150 g	224.49	0.067	0.05
(±)-2,2'-Bis(diphenylphosphino)-1,1'-binaphthalene	0.0541 g	622.69	0.087	0.065

Procedure: A oven dried two necked 25-mL round-bottom flask equipped with a condenser, nitrogen inlet, rubber septum and magnetic stir bar was charged with palladium(II) acetate and (±)-2,2'-bis(diphenylphosphino)-1,1'-binaphthalene in anhydrous toluene (4 mL). The mixture was stirred for 30 min. at 23ºC. Then, first a solution of 2,2,8-trimethylchroman triflate and benzophenone imine in anhydrous toluene (4 mL) and after 5 minutes, sodium *tert*-butoxide were added to the catalyst mixture at 23ºC. The resulting mixture was heated at 80ºC for overnight. The progress of the reaction was monitored by TLC. Upon completion, the reaction mixture was allowed to cool to room temperature, diluted with diethyl ether (60 mL) and filtered through a plug of celite. The crude product was concentrated and flash chromatography (SiO_2, *n*-hexane → *n*-hexane with drops of ethyl acetate) of the crude product furnished the pure product (benzhydrylidene-(2,2,8-trimethylchroman-6-yl)-amine) 0.43 g = 91% yield) as a yellow-orange oil.

TLC: R_f = 0.43 (SiO_2; *n*-hexane:ethyl acetate 9:1 (v/v)). Color reaction of the spot with *p*-anisaldehyde reagent: yellow, also visible under UV. ^{1}H NMR - 300 MHz ($CDCl_3$): δ = 1.27 (s, 6H, H-2a), 1.71 (t, 2H, H-3), 1.99 (s, 3H, H-8b), 2.58 (t, 2H, H-4), 7.48 (m, 5H, H-5, H-2', H-6'), 7.57 (m, 5H, H-7, H-3', H-5'), 7.79 (d, 2H, H-4').

2,2,8-Trimethylchroman-6-ylamine (**33**)[85,166]

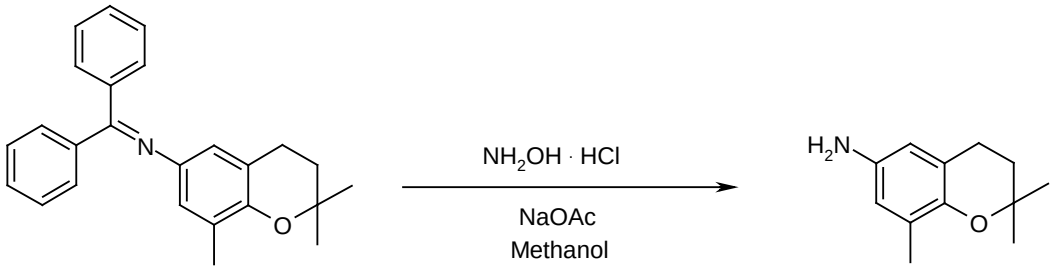

$C_{25}H_{25}O_1N_1$
355.48 g/mole

$C_{12}H_{17}O_1N_1$
191.28 g/mole

Substance	Quant.	M.W.	m.moles	Eq.
Benzhydrylidene-(2,2,8-trimethylchroman-6-yl)-amine	0.4064 g	355.48	1.14	1
Hydroxylamine hydrochloride	0.1429 g	69.49	2.05	1.8
Sodium acetate	0.2250 g	82.03	2.74	2.4

Procedure: A single necked 25-mL round-bottom flask equipped with a magnetic stir bar was charged with 6-imine-2,2,8-trimethylchroman, methanol (11.5 mL), hydroxylamine hydrochloride and sodium acetate. The mixture was stirred for 15 to 30 min. at 23ºC. The solution was then partitioned between 0.1 M NaOH aq. solution (13 mL) and dichloromethane (13 mL) and the organic and aqueous layers were separated in a separatory funnel. The aqueous layer was extracted two times with dichloromethane (2 × 5 mL). The combined organic extracts were washed with brine and dried over $MgSO_4$ and then concentrated on a rotary evaporator. Flash chromatography (short path of SiO_2, *n*-hexane with drops of ethyl acetate → 8:2) of the crude product furnished the pure product (2,2,8-trimethylchroman-6-ylamine 0.14 g = 65% yield) as a light brownish solid.

TLC: R_f = 0.08 (SiO_2; *n*-hexane:ethyl acetate 8:2 (v/v)). Color reaction of the spot with *p*-anisaldehyde reagent: yellow, also visible under UV. ^{1}H NMR ($CDCl_3$): δ = 1.28 (s, 6H, H-2a), 1.74 (t, 2H, ^3J = 6.8 Hz, H-3), 2.09 (s, 3H, H-8b), 2.67 (t, 2H, ^3J = 6.8 Hz, H-4) 3.62 (br, 2H, -NH_2), 6.32 (s, 1H, H-7), 6.41 (s, 1H, H-5). ^{13}C NMR ($CDCl_3$): δ = 16.00 (C-8b), 22.77 (C-4), 26.94 (C-2a), 32.98 (C-3), 73.33 (C-2), 113.97 (C-5), 116.50 (C-7), 120.92 (C-8), 127.01 (C-4a), 137.19 (C-6), 145.63 (C-8a). Elemental Anal. Calcd. for $C_{12}H_{17}O_1N_1$ (191.28): C: 75.35, H: 8.96, N: 7.32, found: C: 75.24, H: 9.20, N: 7.28.

Methyl-(2,2,5,7,8-pentamethylchroman-6-yl)-amine (**38**)

Dimethyl-(2,2,5,7,8-pentamethylchroman-6-yl)-amine (**39**)

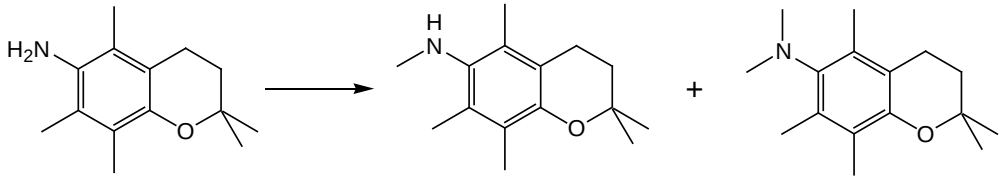

2,2,5,7,8-Pentamethylchroman-6-ylamine	223 mg	219,32 g/mol	1,02 µmol	1 eq
Iodomethane	216 mg	141,94 g/mol	1,53 µmol	1,5 eq
Sodium hydroxide	300 mg			

Chromanylamine was dissolved in 2.5 ml DMSO under an argon atmosphere. Sodium hydroxide and iodomethane were added, and the reaction was stirred at room temperature. Distilled water was added after 5 h and the mixture was extracted three times with DCM. The organic extract was washed four times with distilled water and once with brine, dried with $MgSO_4$, filtrated and evaporated in vacuo. Column chromatography (5 g silica gel, hexane:EE 5:1) yielded 94 mg dimethyl-(2,2,5,7,8-pentamethylchroman-6-yl)-amine (37% yield) as a yellow oil and 85 mg methyl-(2,2,5,7,8-pentamethylchroman-6-yl)-amine (36% yield) as a colourless oil.

Methyl-(2,2,5,7,8-pentamethylchroman-6-yl)-amine (38): TLC: R_f =0.19 (hexane:EE 5:1 (v/v)). Color reaction of the spot with *p*-anisaldehyde reagent: brown, also visible under UV. ^{1}H NMR ($CDCl_3$): δ = 1.30 (s, 6H, H-2a), 1.78 (t, $^3J_{HH}$= 6.8 Hz, H-3), 2.08 (s, 3H, H-7a), 2.13 (s, 3H, H-8b), 2.17 (s, 3H, H-5a), 2.59 (t, 2H, $^3J_{HH}$= 6.8 Hz, H-4), 2.80 (s, 6H, N-CH_3). ^{13}C NMR ($CDCl_3$): δ = 12.0 (C-8b), 14.2 (C-5a), 15.1 (C-7a), 21.2 (C4), 27.0 (C2a), 33.0 (NH-CH_3), 43.0 (N-CH_3), 72.6 (C2), 100.0 (C-4a), 117.0 (C-8), 133.3 (C-7), 135.0 (C-5), 141.4 (C-6), 188.0 (C-8b). EI-MS (70 eV): 233 (100%), 177 (95%), 178 (41%), 149 (36%), 134 (19%), 234 (16%), 148 (13%). Elemental Anal. Calcd. for $C_{16}H_{25}ON$ (247.38): C: 77.68, H: 10.19, N: 5.66, found: C: 77.68, H: 10.32, N: 5.60.

Dimethyl-(2,2,5,7,8-pentamethylchroman-6-yl)-amine (39): TLC: R_f = 0.72 (hexane:EE 5:1 (v/v)). Color reaction of the spot with *p*-anisaldehyde reagent: brown, also visible under UV. ^{1}H NMR ($CDCl_3$): δ = 1.30 (s, 6H, H-2a), 1.80 (t, $^3J_{HH}$= 6.8 Hz, H-3), 2.12 (s, 3H, H-8b), 2.19 (s, 3H, H-7a), 2.24 (s, 3H, H-5a), 2.63 (t, $^3J_{HH}$= 6.8 Hz, H-4), 2.65 (s, 3H, N-CH_3), 2.81 (br, 1H, NH). . ^{13}C NMR ($CDCl_3$): δ = 12.4 (C-8b), 13.6 (C-5a), 14.5 (C-7a), 21.7 (C-4), 27.2 (C-2a), 33.4 (C-3), 37.0 (N-CH_3), 72.9 (C-2), 117.5 (C-4a), 122.9 (C-8), 127.4 (C-5), 129.3 (C-7), 139.1 (C-6), 148.4 (C-8a). EI-MS (70 eV): 247 (100 %), 192 (43%), 148 (30%), 191 (27%), 176 (19%), 248 (17%), 190 (14%), 232 (13%), 177 (10%).Elemental Anal. Calcd. for $C_{15}H_{23}ON$ (233.36): C: 77.21, H: 9.93, N: 6.00, found: C: 77.14, H: 10.00, N: 5.92.

2,2,5,7,8-Pentamethylchroman (**36**)[167]

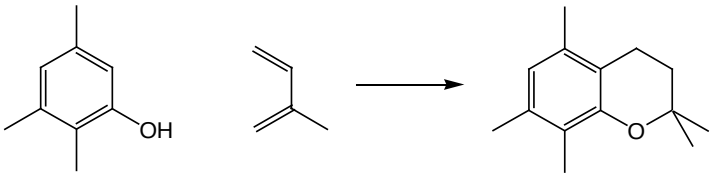

A 500 ml round-bottom flask equipped with a magnetic stirrer, a reflux condenser and a septum was flame dried, purged with Ar and charged with 2,3,5-trimethylphenol (45.40 g, 333 mmol) and 40 mL of anhydrous glacial acetic acid, which failed to dissolve the phenol completely. Anhydrous zinc chloride (5.00 g, 36.7 mmol) was added directly from the ampule. After the addition of isoprene (33.40 ml, 22.70 g, 333 mmol), the mixture was stirred overnight. After 17 h the solution was heated to reflux for another 8 h (changing its color from brown to black), allowed to cool down again and was stirred at r.t. for another three days. After that, water was added and the solution was extracted three times with *n*-hexane. The combined organic layers were washed three times with a saturated solution of sodium bicarbonate, twice with distilled water and once with brine. The organic solution was dried over $MgSO_4$, filtered and evaporated *in vacuo*. The resulting brown oil was purified by kugelrohr distillation to provide **1** as a white solid (9.34 g, 13.7 %).

^{1}H NMR: δ = 6.68 (s, 1H, 6-CH), 2.73 (t, 2H, ^3J= 6.7 Hz, 4-CH_2), 2.34; (s, 3H, 8b-CH_3), 2.30 (s, 3H, 7a-CH_3), 2.22 (s, 3H, 5a-CH_3), 1.92 (t, 2H, ^3J= 6.6 Hz, 3-CH_2), 1.44 (s, 6H, 2a-CH_3). ^{13}C NMR: δ = 152.2 (C-8a), 135.1 (C-7), 133.9 (C-5), 122.8 (HC-6), 122.4 (C-8), 117.1 (C-4a), 73.5 (C-2), 33.3 (C-3), 27.4 (C-2a), 21.3 (C-4), 20.3 (C-7a), 19.3 (C-5a), 11.9 (C-8b). EI-MS (70 eV): 149 (100%), 204 (66%), 148 (24%), 105 (20%), 150 (14%), 189 (10%), 205 (10%). R_f (*n*-hexane / ethyl acetate, v/v = 5:1): 0.75. Microanalysis calcd. for $C_{14}H_{20}O$ (204.31): C: 82.30, H: 9.87; found C: 82.27, H: 9.94.

6-Nitro-2,2,5,7,8-pentamethylchromane-^{15}N (**37**)

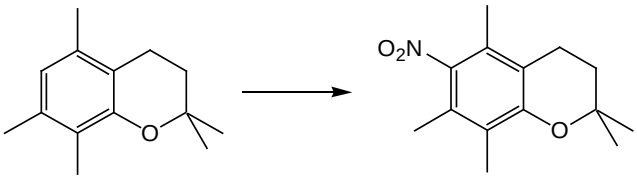

(Caution! Explosive acetyl nitrate is a possible intermediate / byproduct of this reaction. Failing to remove this compound before work-up and solvent evaporation can result in an explosion.) 2,2,5,7,8-Pentamethylchroman (600 mg, 2.94 mmol) was dissolved in glacial acetic acid (3 ml) in a 10 ml round bottom flask, and the solution was kept at 14°C with a cold water bath. ^{15}N-Nitric acid (10 N, 1 ml) was added slowly, and the acid ampule was rinsed with 0.3 ml of glacial acetic acid, which was added to the solution. The greenish-brown solution was stirred for five hours and then added carefully to a beaker containing 75 ml of a saturated aqueous sodium bicarbonate solution and 5 ml of ethyl acetate. The aqueous solution was extracted four times with ethyl acetate (25 ml each), and the combined organic layers were washed with saturated sodium bicarbonate solution and brine, dried over $MgSO_4$, filtered and evaporated to give a brown oil (725 mg) which was used without purification in the next step. 10% of the crude intermediate were kept for analytical studies, the pure compound **2** being isolated by flash chromatography (*n*-hexane / ethyl acetate, v/v = 10:1).

^{1}H NMR: δ = 2.62 (2H, t, ^3J = 6.80 Hz, 4-CH_2), 2.14 (s, 3H, 8b-CH_3), 2.11 (s, 6H, 5a-CH_3, 7a-CH_3), 1.82 (t, 2H, ^3J = 6.80 Hz, 3-CH_2), 1.32 (s, 6H, 2a-CH_3).^{13}C NMR: δ = 153.0 (C-8a), 146.6 (d, C-6, $J_{C,N}$ = 14.2 Hz), 126.5 (C-7), 125.4 (C-5), 124.1 (C-8), 117.8 (C-4a), 74.4 (C-2), 32.5 (C-3), 27.1 (C-2a), 21.2 (C-4), 14.9 (C-7a), 14.1 (C-5a), 12.1 (C-8b). EI-MS (70 eV): 195 (100 %), 250 (64 %), 233 (30 %), 177 (23 %), 178 (22 %), 91 (14 %), 196 (11 %),251 (10 %), 77 (10 %). R_f (*n*-hexane / ethyl acetate, v/v = 5:1): 0.63. Microanalysis calcd. for $C_{14}H_{19}NO_2$ (249.31): C: 67.14, H: 7.65, N: 5.62; found C: 67.12, H: 7.76, N: 5.39.

2,2,5,7,8-Pentamethyl-6-chromanylamine-^{15}N hydrochloride (**35**)

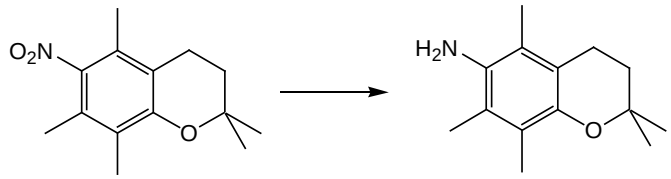

The crude 6-Nitro-2,2,5,7,8-pentamethylchromane-^{15}N as obtained above was dissolved in THF (6 ml, dried over sodium and distilled) in a 10 ml round bottom flask, and the solution was cooled with an ice/water bath. Lithium aluminium hydride (200 mg, 5.29 mmol) was added in small quantities. The reaction mixture was allowed to warm to r.t. and was stirred overnight. The resulting suspension was slowly poured into a beaker with ice cold water. The mixture was extracted four times with ethyl acetate, and the combined organic layers were washed with brine, dried over $MgSO_4$, filtered and the solvent evaporated *in vacuo*. The resulting brownish oil was dissolved in diethyl ether, and product **3** was precipitated as the hydrochloride by adding HCl in diethyl ether (1 M) to afford 201 mg of a brown powder (26.7 %). For NMR analysis the hydrochloride was converted to the free amine with sodium hydroxide solution.

^{1}H NMR: δ = 2.66 (2H, t, ^3J = 6.80 Hz, 4-CH_2), 2.14 (s, 3H, 8b-CH_3), 2.12 (s, 3H, 7a-CH_3), 2.06 (s, 3H, 5a-CH_3), 1.79 (t, 2H, ^3J = 6.80 Hz, 3-CH_2), 1.29 (s, 6H, 2a-CH_3). ^{13}C NMR: δ = 145.5 (C-8a), 134.7 (d, $J_{C,N}$ = 9.4 Hz, C-6), 122.6 (C-8), 121.1 (C-7), 118.4 (C-4a), 117.3 (C-5), 72.6 (C-2), 33.2 (C-3), 27.0 (C-2a), 21.7 (C-4), 13.9 (C-7a), 12.9 (C-5a), 12.2 (C-8b). ^{15}N NMR: δ = -331.4. EI-MS (70 eV): 164 (100 %), 220 (58 %), 165 (37 %), 136 (19 %), 121 (15 %), 135 (11 %), 221 (10 %). R_f (*n*-hexane / ethyl acetate, v/v = 5:1): 0.30. Microanalysis calcd. for $C_{14}H_{21}NO$ (219.33): C: 76.32, H: 9.61, N: 6.39; found C: 76.31, H: 9.68, N: 6.33.

2,3-Dimethyl-5-(1-propyl-pentyl)-[1,4]benzoquinone

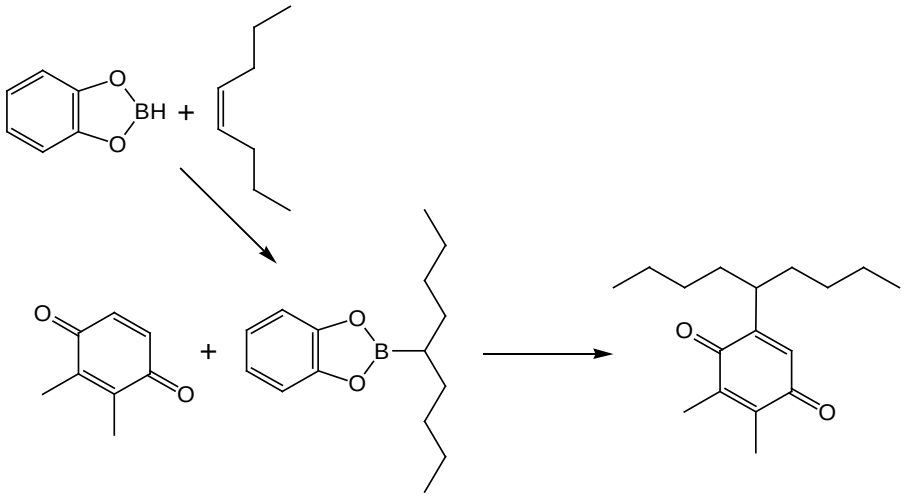

(*Z*)-4-Octene	659 mg	112.22 g/mol	5.88 mmol	2 eq
N,*N*-Dimethylacetamide	51 mg	87.12 g/mol	588 µmol	0.2 eq
1,3,2-Benzodioxaborole	880 mg	119.91 g/mol	7.34 mmol	2.5 eq
Water	317 mg	18.00 g/mol	17.6 mmol	6 eq
DMPU	753 mg	128.17 g/mol	5.88 mmol	2 eq
2,3-Dimethyl-[1,4]benzoquinone	400 mg	136.17 g/mol	2.94 mmol	1 eq

Octene and DMAc were dissolved in 6 ml dry DCM under an atmosphere of argon. The solution was cooled to 0°C and the borane was added slowly. The solution was heated to reflux for 5 h, the water was slowly added and two mixture stirred for another 20 min. DMPU was added and the benzoquinone – dissolved in 5 ml DCM - as well. 3 ml air were bubbled into the solutions with a syringe to increase radical formation. After two hours the reaction was quenched with saturated NH_4Cl-solution and extracted two times with diethyl ether. The organic extract was washed with brine, dried with $MgSO_4$, filtrated and evaporated *in vacuo*. Column chromatography (silica gel, hexane:EE 50:1) yielded 245 mg 2,3-dimethyl-5-(1-propyl-pentyl)-[1,4]benzoquinone (34% yield) as a yellow oil.

^{1}H NMR: δ = 0.78-0.99 (m, 6H, alkyl CH_3), 1.07-1.61 (m, 12H, alkyl CH_2), 2.00-2.03 (m, 6H, H-2a, H-3a), 2.86 (m, 1H, H-5a), 6.44 (s, 1H, 6-H). ^{13}C NMR: δ = 12.0 (C2a/C3a), 12.5 (C3a/C2a), 13.9 (Cε), 14.1 (Cγ'), 20.4 (Cβ'), 22.7 (Cδ), 29.5 (Cγ), 34.2 (Cβ), 36.8 (Cα'), 37.1 (Cα), 131.5 (C6), 140.1 (C2/C3), 141.2 (C3/C2), 152.7 (C5), 187.9 (C1, C4). EI-MS (70 eV): 151 (100%), 150 (93%), 122 (82%), 248 (55%), 137 (37%), 91 (31%), 205 (28%), 177 (28%), 178 (27%), 152 (27%), 135 (26%), 138 (25%), 163 (25%), 41 (25%), 179 (24%), 191 (23%), 192 (22%), 77 (20%), 164 (20 %), 53 (19%), 79 (%), 165 (19%), 219(18%), 107 (18%), 55 (18%), 123 (17%), 136 (16%), 43 (16%), 159 (15%), 121 (15%), 149 (15%), 105 (15%), 206 (14%), 193 (14%), 39 (13%), 93 (13%), 67 (13%), 161 (10%), 81 (10%), 249 (10%), 54 (10%). R_f (*n*-hexane:ethyl acetate, v/v = 5:1): 0.51.

2,2,7,8-Tetramethyl-5-(1-propyl-pentyl)-chroman-6-ol (**51**)

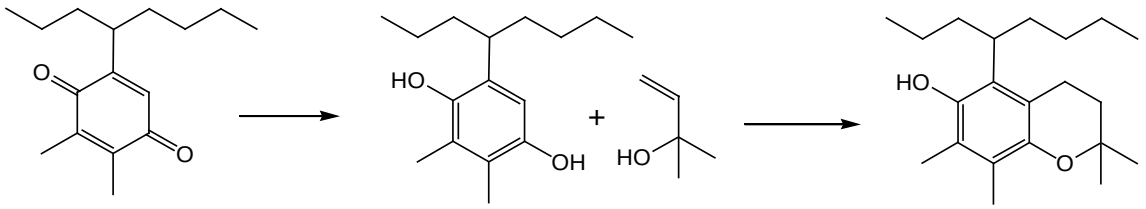

2,3-Dimethyl-5-(1-propyl-pentyl)-[1,4]benzoquinone	195 mg	248.37 g/mol	785µmol	1 eq
Sodium borohydride	45 mg	37.83 g/mol	1.18 mmol	1.5 eq
2-Methyl-3-buten-2-ol	135 mg	86.13 g/mol	1.57 mmol	2 eq
Formic acid				

Benzoquinone was dissolved under an argon-atmosphere in 2 ml THF and cooled to 0°C. Sodium borohydride was added. The reaction mixture was stirred at 0°C for five minutes and for 130 minutes at room temperature. 8 ml of formic acid were added, the flask equipped with a condenser and the mixture heated to 110°C. After 4 hours the reaction was stopped with ice water and extracted three times with diethyl ether (alltogether ~40 ml). 40 ml of *n*-hexane were added to the organic extract. It was washed with distilled water, dried with $MgSO_4$, filtrated and evaporated *in vacuo*.

The residue was dissolved in 25 ml of methanol and 1 ml of concentrated hydrochloric acid and heated to 65°C. After 70 minutes the solvent was evaporated, and diethyl ether was added. The organic solution was washed two times with distilled water and once with saturated $NaHCO_3$-solution, dried with $MgSO_4$, filtrated and exaporated *in vacuo*. Column chromatography (silica gel, hexane:EE 100:1) yielded 104 mg 2,2,7,8-Tetramethyl-5-(1-propyl-pentyl)-chroman-6-ol as a yellow oil (42% yield).

^{1}H NMR: δ = 0.80-0.89 (m, 6H, H-ε, H-γ'), 1.07-1.32 (m, 6H, H-δ, H-γ, H-β'), 1.26 (s, 6H, H-2a), 1.60-1.90 (m, 4H, H-β, H-α'), 1.76 (t, $^3J_{HH}$= 6.9 Hz, H-3), 2.10 (s, 3H, H-7a), 2.11 (s, 3H, H-8b), 2.66 (t, $^3J_{HH}$= 6.9 Hz, H-4), 2.87 (m, 1H, H-α), 4.21 (s, 1H, OH). ^{13}C NMR: δ = 12.0 (C-8b/C-7a), 12.1 (C-7a/C-8b), 14.1 (C-ε), 14.8 (C-γ') , 21.7 (C-4/ C-β'), 21.8 (C-β'/C-4), 23.1 (C-δ), 26.5 (C-2a), 26.6 (C-2a), 30.8 (C-γ), 33.5 (C-3), 34.1 (C-β/C-α'), 36.6 (C-α'/ C-β), 38.5 (C-α), 72.1 (C-2), 117.5 (C-8), 121.7 (C-7), 122.9 (C-4a), 126.3(C-5), 127.1 (C-6), 145.5 (C-8a). EI-MS (70 eV): 318 (10%), 219 (62%), 319 (22%), 165 (21%), 164 (13%), 220 (10%). R_f (*n*-hexane / ethyl acetate, v/v = 5:1): 0.53.

5-Benzhydryl-2,2,7,8-tetramethylchroman-6-ol (**52**)

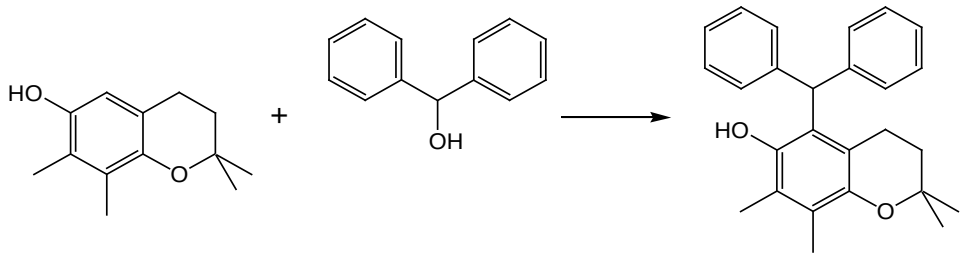

101 mg	2,2,7,8-Tetramethylchroman-6-ol	206.29 g/mol	490 µmol	1 eq
90 mg	Diphenyl carbinol	184.23 g/mol	490 µmol	1 eq
262 mg	Aluminium chloride	133.34 g/mol	1.96 mmol	4 eq

Aluminium chloride and 2,2,7,8-Tetramethylchroman-6-ol were placed in a dry 2-necked 10 ml-round bottom flask equipped with a drying tube and dissolved in 3 ml of dry THF. Diphenylcarbinol was dissolved in 1 ml of dry THF and added to the reaction mixture. The reaction was stirred at room temperature for 42 h, then distilled water was added. The aqueous mixture was extracted three times with EE. The organic layers were combined, washed three times with saturated $NaHCO_3$-solution and two times with brine. Then the organic phase was dried with Na_2SO_4, filtrated and evaporated *in vacuo*.The crude product (172 mg of yellow oil) was purified by column chromatography (hexane:ethyl acetate 50:1, 6 g silica gel, dry sample)

Yield: 151 mg colourless crystals (83%)

^{1}H NMR: δ = 1.27 (s, 6H, H-2a), 1.72 (t, 2H, $^3J_{HH}$ = 6.4 Hz, H-3), 2.08 (s, 3H, H-8b), 2.13 (s, 3H, H-7a), 2.69 (t, 2H, $^3J_{HH}$ = 6.4 Hz, H-4), 4.36 (s, 1H, OH), 5.77 (s, 1H, H-5a), 7.17-7.34 (m, 10 H, Ar-H). ^{13}C NMR: δ = 12.1 (C-7a), 12.2 (C-8b), 21.3 (C-4), 26.6 (C-2a), 33.2 (C-3), 49.1 (C-5a), 72.3 (C-2), 116.7 (C-8), 124.2 (C-5), 124.3 (C-4a), 125.2 (C-7), 126.9 (C-4'), 128.9 (C-2', C-6'), 129.0 (C-3', C-5'), 141.6 (C-1') 145.7 (C-8a), 145.9 (C-6). EI-MS (70 eV): 372 (100%), 239 (39%), 238 (31%), 373 (28%), 225 (19%), 315 (15%), 301 (14%), 165 (12%), 224 (12%), 316 (10%). R_f (*n*-hexane / ethyl acetate, v/v = 5:1): 0.56

5-Benzhydryl-2,2,7,8-tetramethylchroman-6-ol-^{13}C (**53**)

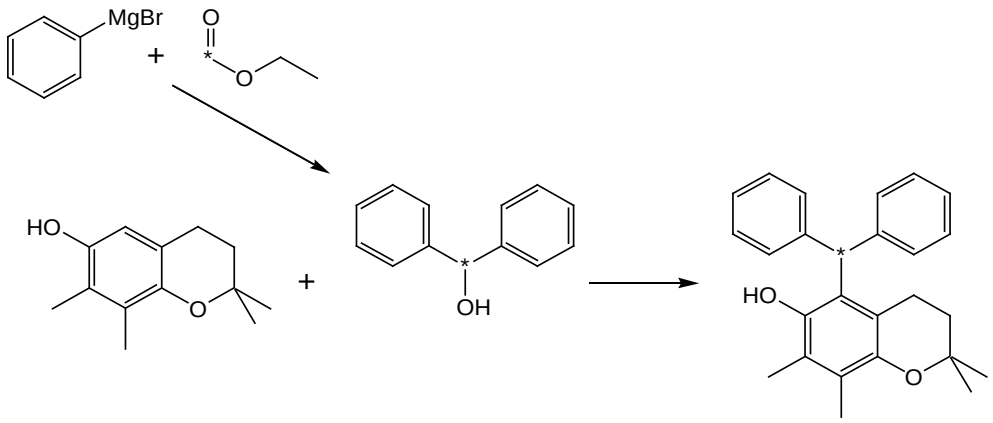

Ethyl formate-^{13}C	75 mg	75.07 g/mol	999 µmol	1 eq
Phenylmagnesium bromide	666 µl	3 mol/L	1.99 mmol	2 eq
2,2,7,8-Tetramethylchroman-6-ol	207 mg	206.29 g/mol	1.00 mmol	1 eq
Aluminium chloride	268 mg	133.34 g/mol	2,01 mmol	2 eq

Ethyl formate was dissolved in 2 ml of dry THF under argon and cooled to 0°C. The Grignard reagent was diluted with 3 ml of dry THF and added dropwise. The solution was stirred at 0°C for two hours, after that it was quenched with distilled water. The mixture was extracted three times with EE. The organic extract was washed with water, dried with Na_2SO_4, filtrated and evaporated *in vacuo*.

2.5 ml of dry THF were added to chromanol and aluminium chloride under argon. The raw benzhydrol was dissolved in 1 ml of dry THF and added dropwise to this second reaction mixture. After 15 h at room temperature another 5 ml of dry THF and some aluminium chloride were added to the suspension. The reaction was quenched after 70 h at room temperature by the addition of distilled water. The mixture was extracted three times with EE. The organic extract was washed with saturated $NaHCO_3$-solution and water, dried with Na_2SO_4, filtrated and evaporated *in vacuo*. Column chromatography (16 g silica gel, hexane:EE 50:1) yielded 252 mg of 5-Benzhydryl-2,2,7,8-tetramethylchroman-6-ol-^{13}C as colourless crystals (68% yield)

^{1}H NMR: δ = 1.27 (s, 6H, H-2a), 1.72 (t, 2H, $^3J_{HH}$ = 6.8 Hz, H-3), 2.08 (s, 3H, H-8b), 2.13 (s, 3H, H-7a), 2.69 (t, 2H, $^3J_{HH}$ = 6.8 Hz, H-4), 4.36 (s, 1H, OH), 5.77 (d, 1H, $^1J_{CH}$= 125 Hz), 7.17-7.36 (m, 10H, Ar-H) ^{13}C NMR: δ = 12.1 (C-7a), 12.2 (C-8b), 21.3 (C-4), 26.6 (C-2a), 33.2 (C-3), 49.1 (C-5a), 72.3 (C-2), 116.7 (C-8), 124.2 (C-5), 124.3 (C-4a), 125.2 (C-7), 126.9 (C-4'), 128.9 (C-2', C-6'), 129.0 (C-3', C-5'), 141.6 (C-1'), 145.7 (C-8a), 145.9 C-6). EI-MS (70 eV): 373 (100%), 240 (44%), 239 (36%), 374 (27%), 225 (21%), 226 (18%), 316 (17%), 302 (15%), 166 (14%), 317 (10%), 179 (10%). R_f (*n*-hexane / ethyl acetate, v/v = 5:1): 0.58.

3,3,5,6-Tetramethyl-12-phenyl-1,2,3,12-tetrahydropyrano[3,2-a]xanthene (**54**)

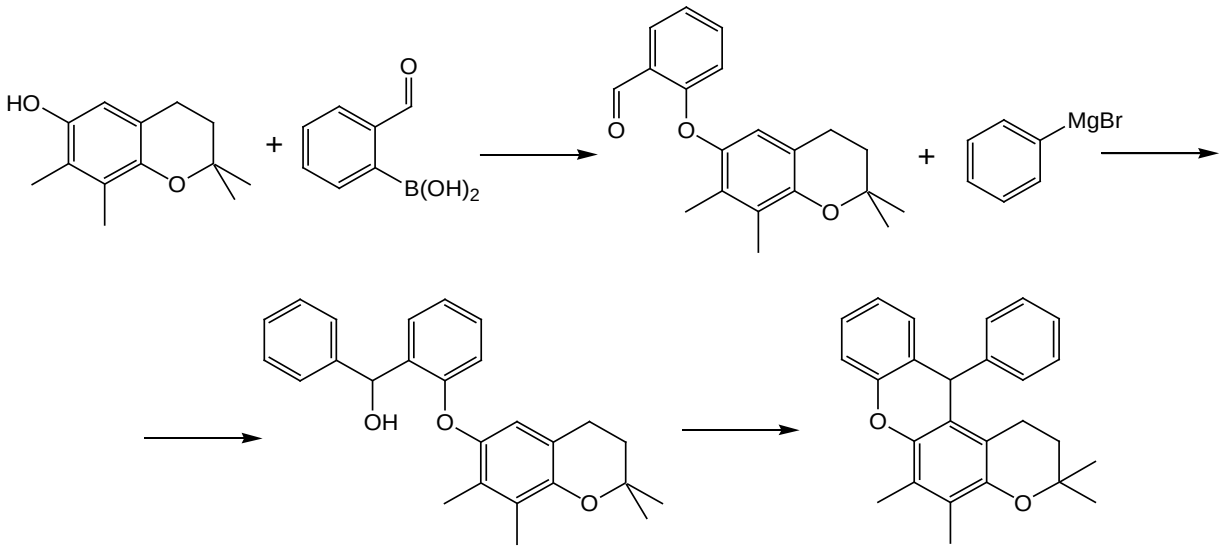

2,2,7,8-Tetramethylchroman-6-ol	241 mg	206.29 g/mol	1.17 mmol	1 eq
2-Formylphenylboronic acid	350 mg	149.94 g/mol	2.33 mmol	2eq
Copper(II) acetate	318 mg	181.63 g/mol	1.75 mmol	1 eq
Triethylamine	354 mg	101.19 g/mol	3.50 mmol	3 eq
4 Å molecular sieve				
Phenylmagnesium bromide	930 µl	2.5 mol/l	2.33 mmol	2 eq
Sulfuric Acid				

Chromanol, boronic acid, copper acetate amine and molecular sieve were dissolved in 10 ml of DCM under argon and stirred at room temperature. After 17 hours distilled water was added and the mixture was extracted three times with DCM. The organic extract was washed with saturated $NaHCO_3$-solution, dried with Na_2SO_4, filtrated and evaporated *in vacuo*.

The residue was dissolved in 10 ml dry THF and the Grignard reagent was added dropwise. After 30 minutes the reaction was quenched with saturated NH_4Cl-solution. The mixture was extracted three times with EE. The organic extract was washed with brine, dried with $MgSO_4$, filtrated and evaporated *in vacuo*. Column chromatography yielded 103 mg (23 %) of phenyl-[2-(2,2,7,8-tetramethylchroman-6-yloxy)-phenyl]-methanol as a colourless solid.

10 mg of this intermediate were dissolved in 2 ml of dry THF under argon and cooled to 0°C. A few microliters of concentrated sulfuric acid were added. The solution was evaporated *in vacuo* and the resulting black oil dissolved in EE. The organic solution was washed with saturated $NaHCO_3$-solution, dried with $MgSO_4$, filtrated and evaporated. 9 mg of 3,3,5,6-tetramethyl-12-phenyl-1,2,3,12-tetrahydropyrano[3,2-a]xanthene were obtained as colourless oil (~95% yield).

2-(2,2,7,8-Tetramethyl-chroman-6-yloxy)-benzaldehyde:

^{1}H NMR: δ = 1.36 (s, 6H, 2a), 1.80 (t, 2H, J = 6.7 Hz, H-3), 2.09 (s, 3H, N-7a), 2.17 (s, 3H, H-8b), 2.74 (t, 2H, $^3J_{HH}$ = 6.7 Hz, H-4), 6.62 (s, 1H, H-5), 6.65 (ddd, 1H, J_1 = 8.43 Hz, J_2 = 1.00 Hz, J_3 = 0.46 Hz, H-6'), 7.06 (dddd, 1H, J_1 = 7.75 Hz, J_2 = 7.25 Hz, J_3 = 0.96 Hz, J_4 = 0.84 Hz, H-4'), 7.42 (ddd, 1H, J_1 = 8.46 Hz, J_2 = 7.25 Hz, J_3 = 1.85 Hz, H-5'), 7.91 (ddd, 1H, J_1 = 7.74 Hz, J_2 = 1.84 Hz, J_3 = 0.45 Hz,

H-3'), 10.67 (d, 1H, J_1 = 0.87 Hz, CHO).^{13}C NMR: δ = 12.2 (C-7a), 12.6 (C-8b), 22.6 (C4), 27.0 (C-2a), 32.7 (C-3), 74.0 (C2), 115.6 (C-6'), 118.4 (C-5), 118.9 (C-5), 121.5 (C-4'), 125.1 (C-8), 126.5 (C-7), 127.8 (C-2'), 128.1 (C-3'), 135.7 (C-5'), 145.2 (C-6), 149.2 (C-8a), 161.7 (C-1'), 189.8 (CHO). EI-MS (70 eV): 310 (100%), 121 (30%), 255 (27%), 135 (23%), 311 (22%), 211 (16%), 239 (13%), 91 (12%), 134 (11%), 77 (10%). R_f (*n*-hexane / ethyl acetate, v/v = 5:1): 0.48.

Phenyl-[2-(2,2,7,8-tetramethylchroman-6-yloxy)-phenyl]-methanol (55)

^{1}H NMR: δ = 1.24 (s, 6H, H-2a), 1.67 (t, 2H, J = 6.9 Hz, H-3), 1.78 (s, 3H, H-7a), 2.03 (s, 3H, H-8b), 2.57 (t, 2H, J = 6.9 Hz, H-4), 2.88 (br, 1H, OH), 6.11 (s, 1H, CHOH), 6.30 (s, 1H, H-5), 6.41 (d, 1H, J = 8.2 Hz, H-2'), 6.91 (t, 1H, J = 7.6 Hz, H-4'), 7.03 (t, 1H, J = 7.6 Hz, H-3'), 7.13-7.28 (m, 3H, H-3'', H-4'', H-5''), 7.33-7.40 (m, 3H, H-5', H-2'', H-6'').

^{13}C NMR: δ = 12.0 (C-7a), 12.3 (C-8b), 22.5 (C-4), 27.0 (C-2a), 32.7 (C-3), 72.5 (CHOH), 73.9 (C-2), 114.6 (C-2'), 118.2 (C-5), 118.7 (C-4a), 121.5 (C-4'), 126.1 (C-8), 126.6 (C-2'', C-6''), 127.2 (C-4''), 127.7 (C-5'), 127.9 (C-7), 128.2 (H-3'', H-5''), 128.5 (C-3'), 132.2 (C-6'), 143.5 (C-1''), 145.5 (C-6), 148.7 (C-8a), 156.2 (C-1').

EI-MS (70 eV): 135 (100%), 388 (73%), 190 (65%), 207 (26%), 197 (25%), 293 (22%), 370 (21%), 181 (21%), 77 (20%), 389 (19%), 105 (19%), 91 (18%), 372 (16%), 165 (16%), 121 (16%), 191 (15%), 313 (15%), 175 (14%), 69 (13%), 136 (11%), 301 (11%), 79 (11%), 152 (10%), 314 (10%), 134 (10%). R_f (*n*-hexane / ethyl acetate, v/v = 5:1): 0.33.

3,3,5,6-Tetramethyl-12-phenyl-1,2,3,12-tetrahydropyrano[3,2-a]xanthenes (54)

^{1}H NMR: δ = 1.08 (s, 3H, H-3a), 1.19 (s, 3H, H-3a), 1.52-1.70 (m, 1H, H-2), 2.09 (s, 3H, H-5a/H-6b), 2.21-2.32 (m, 1H, H-1), 2.30 (s, 3H, H-6b/H-5a), 2.60-2.70 (m, 1H, H-1), 5.09 (s, 1H, H-12), 6.87 (t, 1H, J = 7.2 Hz, H-4'), 6.98-7.14 (m, 6H, H-8, H-9, H-10, H-11, H-2', H-6'), 7.19 (2 H, d, J = 7.8 Hz, H-3', H-5'). ^{13}C NMR: δ = 11.9 (C-5a/C-6b), 12.1 (C-6b/C-5a), 19.8 (C-1), 26.6 (C-3a), 26.7 (C-3a), 32.6 (C-2), 42.8 (C-12), 72.8 (C-3), 115.5 (c-12b), 116.7 (C-8), 119.3 (C-11a), 122.7 (C-4'), 123.1 (C-5), 124.9 (C-6), 125.7 (C-12a), 126.3 (C-10), 127.3 (C-9, C-2', C-6'), 128.6 (C-3', C-5'), 128.7 (C-11), 143.6 (C-6a), 145.7 (C-1'), 147.5 (C-4a), 151.5 (C-7a). EI-MS (70 eV): 370 (100%), 293 (88%), 313 (68%), 314 (41%), 237 (29%), 371 (28%), 315 (25%), 294 (19%), 299 (17%), 209 (25%), 194 (11%), 298 (10%), 195 (10%), 249 (10%). R_f (*n*-hexane / ethyl acetate, v/v = 5:1): 0.61.

Appendix

Abbreviations

α-TTP	α-tocopherol transport protein
Ac	acetyl, -C(O)CH_3
AIBN	2,2'-azobis(2-methylpropionitrile)
APT	attached proton test, ^{13}C NMR spectroscopy
BINAP	2,2'-bis(diphenylphosphino)-1,1'-binaphthyl
BMIM	1-butyl-3-methylimidazolium
Bu	butyl, -$CH_2CH_2CH_2CH_3$
CEHC	carboxyethyl hydroxychroman
CYP	cytochrome P
δ	chemical shift (NMR)
DCM	dichloromethane
DDQ	2,3-dichloro-5,6-dicyano-1,4-benzoquinone
ΔE_A	difference in activation energy
DFT	density functional theory
$\Delta H^{\neq}$	difference in activation enthalpy
DMAc	*N*,*N*-dimethylacetamide
DMPU	1,3-dimethyl-3,4,5,6-tetrahydro-2(1*H*)-pyrimidinone
DMSO	dimethyl sulfoxide
E_A	activation energy
EE	ethyl acetate
EI	electron impact (MS)
EPR	electron paramagnetic resonance
ESR	electron spin resonance
Et	ethyl, -CH_2CH_3

GC	gas chromatography
g_n	*g*-factor of the nucleus
γ-TMT	γ-tocopherol methyltransferase
HF	Hartree-Fock
HMBC	heteronuclear multiple bond coherence (NMR)
HOMO	highest occupied molecular orbital
HPT	homogentisate phytyltransferase
HSBC	heteronuclear single quantum coherence (NMR)
I	nuclear spin quantum number
*i*Pr	*iso*-propyl, -$CH(CH_3)_2$
IR	infrared
IUPAC	International Union of Pure and Applied Chemistry
J	*J*-coupling
k	kinetic rate constant
L	multiplicity of the ESR signal
LAH	lithium aluminium hydride
LUMO	lowest unoccupied molecular orbital
μ_0	permeabilty of vacuum
Me	methyl, -CH_3
MMFF	Merck Molecular Force Field
μ_N	nuclear magneton
MS	mass spectrometry
n	number of chemically equivalent nuclei
NMMO	*N*-methylmorpholine *N*-oxide
NMR	nuclear magnetic resonance
Nu	nucleophile
oQIM	*ortho*-quinoneimine methide
oQM	*ortho*-quinone methide

ox	oxidation
Ph	phenyl, -C_6H_5
PMC	2,2,5,7,8-pentamethyl-6-chromanol, α-tocopherol model
ppm	parts per million
Pr	propyl, -$CH_2CH_2CH_3$
R	gas constant (in formulae)
R	arbitrary substituent (in schemes)
red	reduction
R_f	retention factor (TLC)
$\rho_s(0)$	spin density at the nucleus
S	spin quantum number
SAM	S-adenosyl methionine
SDS	sodium dodecyl sulphate
SIBL	strain-induced bond localization
TAP	tocopherol–associated protein
TBAF	tetrabutylammonium fluoride
*t*Bu	*tert*-butyl, -$C(CH_3)_3$
Tf	triflate, -$S(O)_2CF_3$
TFA	trifluoroacetic acid
THF	tetrahydrofuran
TLC	thin-layer chromatography
TMS	tetramethylsilane
UV	ultraviolet
XRD	X-ray diffraction
ZPE	zero-point energy

Crystal Structures

2,2,5,7,8-Pentamethyl-chroman-6-ylamine, 4-methylbenzenesulfonate

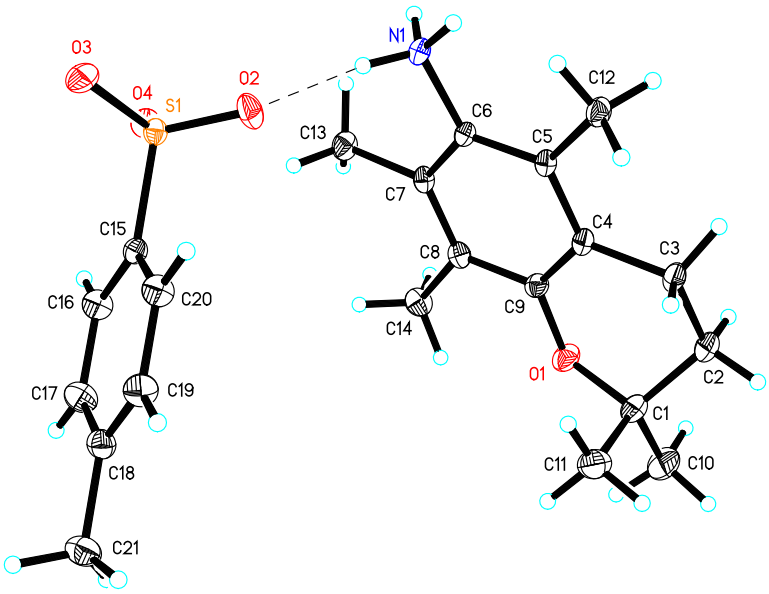

Platy crystals from methanol. The 6-aminochromane is N-protonated and all 3 N-bonded hydrogen atoms make hydrogen bonds with 3 equivalent tosylate anions. A short intramolecular H-H contact between H1Nc (ammonium) and H12c (methyl) of about 1.8 A is caused by N-H---O and C-H---O bonding to the same tosylate oxygen O3. The hydrogen bonds link cations and anions into chains along the a-axis

Fig. 1. Thermal ellipsoid plots (50% ellipsoids) of 2,2,5,7,8-pentamethyl-chroman-6-ylamine, 4-methylbenzenesulfonate

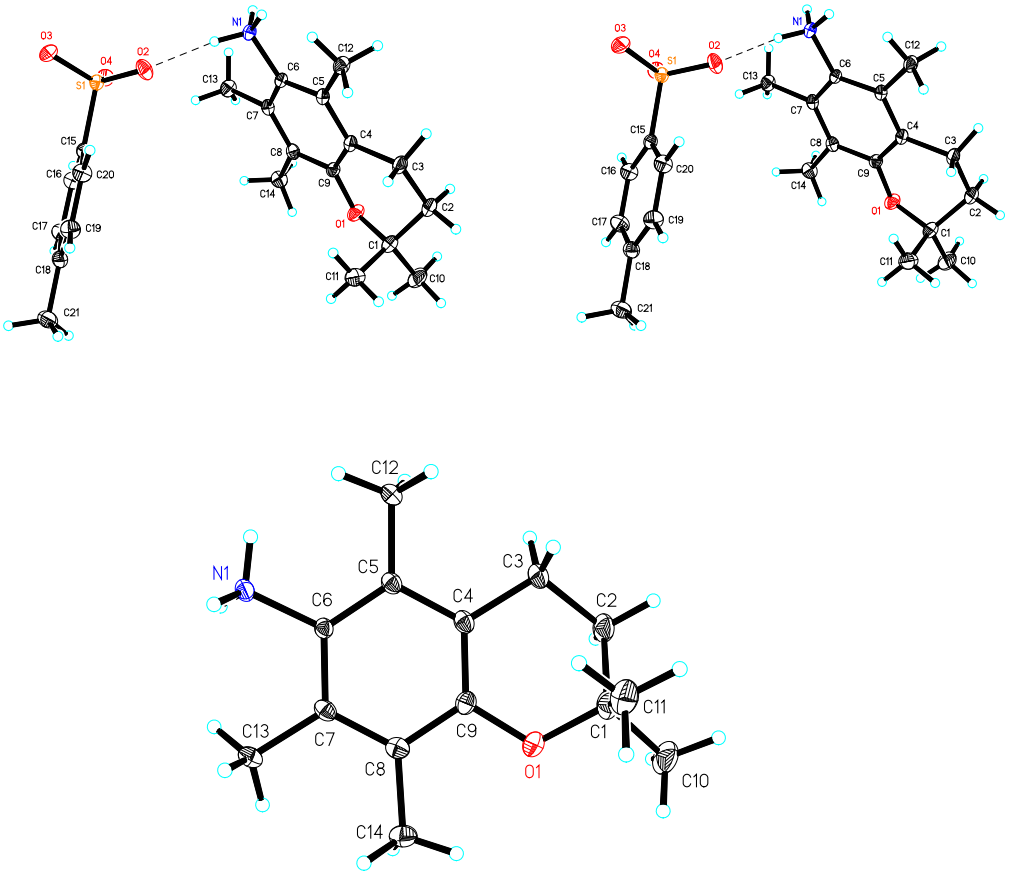

Fig. 2. Asymmetric unit of 2,2,5,7,8-pentamethyl-chroman-6-ylamine, 4-methylbenzenesulfonate.

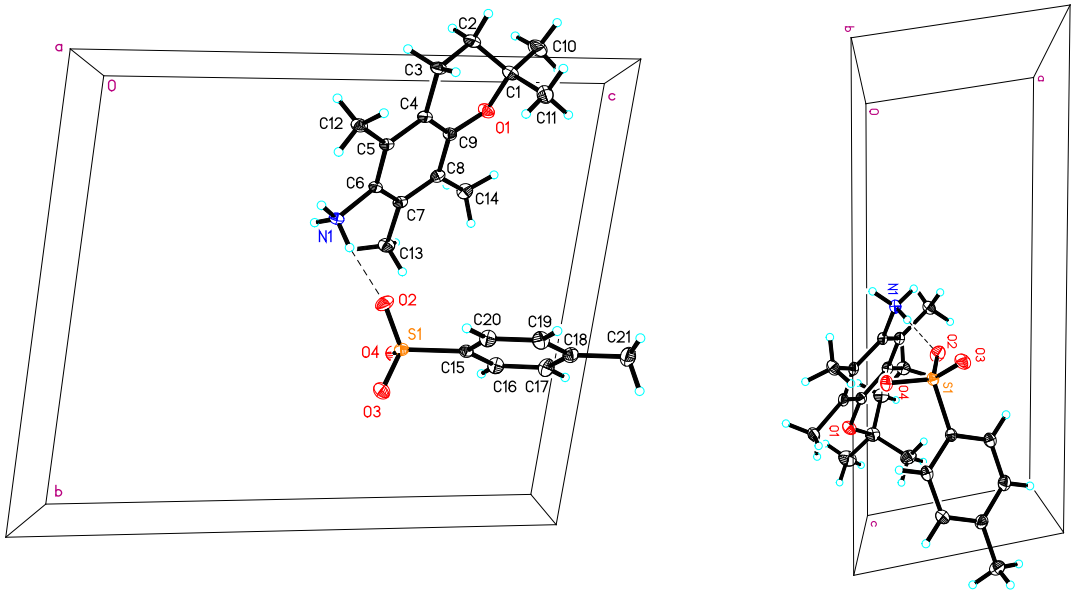

Fig. 3. Packing diagrams of 2,2,5,7,8-pentamethyl-chroman-6-ylamine, 4-methylbenzenesulfonate.

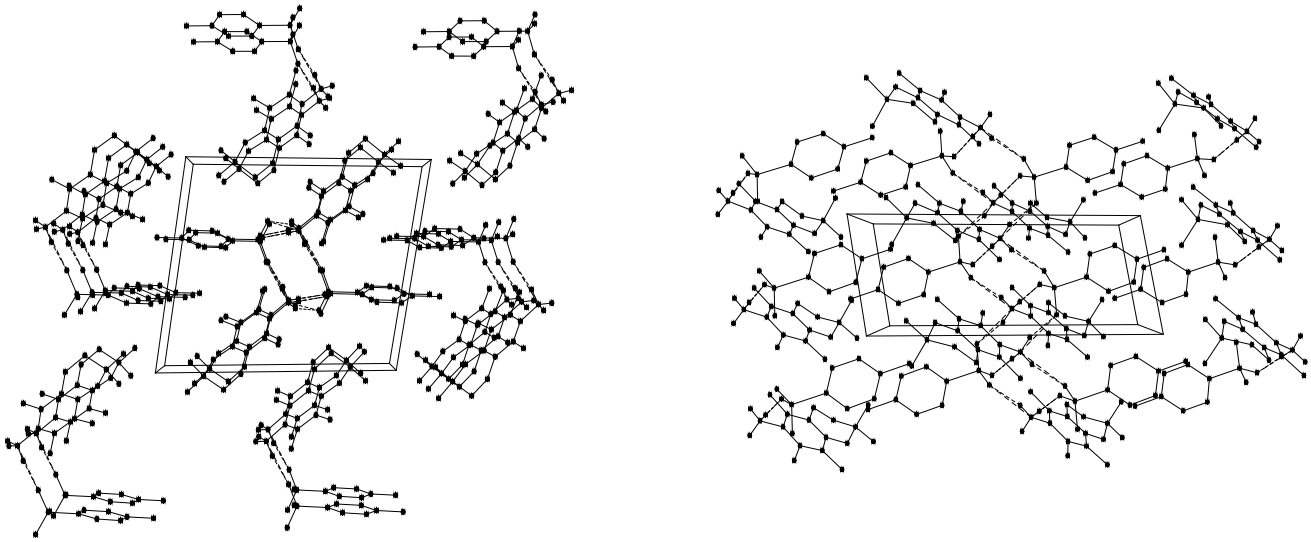

Table 1. Crystal data and structure refinement for 2,2,5,7,8-pentamethyl-chroman-6-ylamine, 4-methylbenzenesulfonate.

Identification code	1421_0m
Empirical formula	C21 H29 N O4 S
Formula weight	391.51
Temperature	100(2) K
Wavelength	0.71073 A
Crystal system, space group	Triclinic, P-1
Unit cell dimensions	a = 5.9615(7) A alpha = 97.299(2) deg. b = 12.4391(14) A beta = 98.514(2) deg. c = 14.0120(15) A gamma = 98.498(2) deg.
Volume	1004.5(2) A^3
Z, Calculated density	2, 1.294 Mg/m^3
Absorption coefficient	0.187 mm^-1
F(000)	420
Crystal size	0.50 x 0.30 x 0.10 mm
Diffractometer	Bruker KAPPA CCD (sealed X-raytube, Mo Kalfa rad., graphite monochromator CCD in 512x512 pixel mode)
Scan type / width / speed	full sphere data collection
Theta range for data collection	2.97 to 30.00 deg.
Index ranges	-8<=h<=8, -17<=k<=17, -19<=l<=19
Reflections collected / unique	14144 / 5772 [R(int) = 0.0291]
Completeness to theta = 30.00	98.2%
Absorption correction	Multi-scan (program SADABS; Sheldrick, 1996)
Max. and min. transmission	0.98 and 0.85
Structure solution	Direct methods (program SHELXS97)
Absorption correction	Semi-empirical from equivalents
Refinement method	Full-matrix least-squares on F2 (prg SHELXL97)
Data / restraints / parameters	5772 / 0 / 251
Goodness-of-fit on F2	1.047
Final R indices [I>2sigma(I)]	R1 = 0.0435, wR2 = 0.1094
R indices (all data)	R1 = 0.0640, wR2 = 0.1213
Largest diff. peak and hole	0.751 and -0.358 eA-3

$R1 = \Sigma||F_o|-|F_c||/\Sigma|F_o|$, $wR2 = [\Sigma(w(F_o^2-F_c^2)^2)/\Sigma(w(F_o^2)^2)]^{½}$

Table 2. Atomic coordinates (x 10^4) and equivalent isotropic displacement parameters ($Å^2$ x 10^3) for 2,2,5,7,8-pentamethyl-chroman-6-ylamine, 4-methylbenzenesulfonate. U_{eq} is defined as one third of the trace of the *ortho*gonalized U_{ij} tensor.

	x	y	z	U_{eq}
S(1)	3820(1)	6264(1)	6667(1)	13(1)
O(1)	-1007(2)	630(1)	7696(1)	20(1)
O(2)	4096(2)	5196(1)	6181(1)	21(1)
O(3)	5307(2)	7167(1)	6385(1)	22(1)
O(4)	1425(2)	6422(1)	6569(1)	18(1)
N(1)	1794(2)	3253(1)	4986(1)	14(1)
C(1)	320(3)	-193(1)	8017(1)	21(1)
C(2)	823(3)	-879(1)	7119(1)	22(1)
C(3)	2188(3)	-176(1)	6514(1)	19(1)
C(4)	1271(2)	886(1)	6417(1)	14(1)
C(5)	1985(2)	1554(1)	5741(1)	13(1)
C(6)	1056(2)	2507(1)	5664(1)	12(1)
C(7)	-562(2)	2827(1)	6228(1)	14(1)
C(8)	-1198(2)	2186(1)	6922(1)	15(1)
C(9)	-266(3)	1221(1)	7007(1)	15(1)
C(10)	-1273(4)	-872(2)	8548(1)	31(1)
C(11)	2501(3)	398(2)	8703(1)	27(1)
C(12)	3723(3)	1194(1)	5143(1)	17(1)
C(13)	-1577(3)	3850(1)	6098(1)	19(1)
C(14)	-2850(3)	2510(1)	7583(1)	20(1)
C(15)	4774(2)	6293(1)	7927(1)	13(1)
C(16)	3503(3)	6670(1)	8614(1)	18(1)
C(17)	4320(3)	6702(1)	9602(1)	21(1)
C(18)	6389(3)	6357(1)	9919(1)	18(1)
C(19)	7640(3)	5989(1)	9215(1)	20(1)
C(20)	6860(3)	5957(1)	8225(1)	18(1)
C(21)	7239(3)	6382(2)	10993(1)	24(1)

Table 3. Hydrogen coordinates (x 10^4) and isotropic displacement parameters (Å^2 x 10^3) for 2,2,5,7,8-pentamethyl-chroman-6-ylamine, 4-methylbenzenesulfonate.

	x	y	z	U_{eq}
H(1NA)	2468	3922	5331	21
H(1NB)	547	3332	4556	21
H(1NC)	2821	2965	4653	21
H(2A)	-647	-1259	6710	26
H(2B)	1708	-1448	7327	26
H(3A)	3826	-2	6829	22
H(3B)	2098	-596	5856	22
H(10A)	-1712	-391	9073	46
H(10B)	-479	-1426	8826	46
H(10C)	-2655	-1239	8087	46
H(11A)	3420	883	8354	40
H(11B)	3400	-145	8935	40
H(11C)	2085	836	9262	40
H(12A)	2974	572	4641	26
H(12B)	4973	972	5569	26
H(12C)	4350	1806	4830	26
H(13A)	-562	4489	6502	28
H(13B)	-3094	3775	6297	28
H(13C)	-1736	3952	5411	28
H(14A)	-2473	3303	7817	29
H(14B)	-2722	2109	8142	29
H(14C)	-4427	2329	7219	29
H(16)	2085	6904	8411	22
H(17)	3450	6965	10071	25
H(19)	9058	5754	9417	24
H(20)	7741	5709	7756	22
H(21A)	8461	5937	11073	36
H(21B)	5963	6082	11302	36
H(21C)	7844	7142	11300	36

Hydrogen atoms inserted in idealized positions and refined riding with the atoms to which they were bonded. All H atoms had $U_{iso} = U_{eq}$ x 1.2 (x 1.5 for CH_3) of their carrier atoms.

Table 4. Anisotropic displacement parameters ($Å^2$ x 10^3) for 2,2,5,7,8-pentamethyl-chroman-6-ylamine, 4-methylbenzenesulfonate. The anisotropic displacement factor exponent takes the form: $-2\pi^2 [h^2 a^{*2} U_{11} + ... + 2 h k a^* b^* U_{12}]$

	U_{11}	U_{22}	U_{33}	U_{23}	U_{13}	U_{12}
S(1)	13(1)	12(1)	15(1)	1(1)	3(1)	3(1)
O(1)	24(1)	18(1)	23(1)	9(1)	9(1)	4(1)
O(2)	22(1)	17(1)	23(1)	-5(1)	-1(1)	8(1)
O(3)	23(1)	22(1)	21(1)	7(1)	8(1)	-1(1)
O(4)	14(1)	21(1)	21(1)	4(1)	2(1)	6(1)
N(1)	14(1)	11(1)	18(1)	3(1)	3(1)	3(1)
C(1)	26(1)	16(1)	22(1)	7(1)	4(1)	3(1)
C(2)	30(1)	13(1)	24(1)	6(1)	6(1)	3(1)
C(3)	23(1)	13(1)	21(1)	4(1)	5(1)	6(1)
C(4)	14(1)	11(1)	18(1)	2(1)	2(1)	2(1)
C(5)	13(1)	11(1)	16(1)	1(1)	2(1)	2(1)
C(6)	11(1)	10(1)	15(1)	3(1)	2(1)	2(1)
C(7)	11(1)	12(1)	17(1)	0(1)	1(1)	2(1)
C(8)	11(1)	14(1)	17(1)	0(1)	2(1)	1(1)
C(9)	15(1)	13(1)	15(1)	3(1)	2(1)	0(1)
C(10)	41(1)	23(1)	31(1)	13(1)	13(1)	1(1)
C(11)	31(1)	26(1)	22(1)	6(1)	1(1)	2(1)
C(12)	19(1)	15(1)	21(1)	5(1)	7(1)	8(1)
C(13)	18(1)	18(1)	24(1)	4(1)	7(1)	9(1)
C(14)	16(1)	22(1)	21(1)	1(1)	7(1)	4(1)
C(15)	13(1)	13(1)	15(1)	3(1)	3(1)	0(1)
C(16)	14(1)	22(1)	20(1)	3(1)	4(1)	6(1)
C(17)	18(1)	26(1)	19(1)	1(1)	6(1)	5(1)
C(18)	17(1)	18(1)	18(1)	2(1)	1(1)	-1(1)
C(19)	15(1)	24(1)	22(1)	4(1)	2(1)	5(1)
C(20)	15(1)	21(1)	20(1)	2(1)	5(1)	6(1)
C(21)	24(1)	28(1)	18(1)	2(1)	0(1)	2(1)

Table 5. Bond lengths [Å] and angles [deg] for 2,2,5,7,8-pentamethyl-chroman-6-ylamine, 4-methylbenzenesulfonate.

Bond distances

S(1)-O(2)	1.4566(11)
S(1)-O(3)	1.4578(12)
S(1)-O(4)	1.4591(11)
S(1)-C(15)	1.7668(15)
O(1)-C(9)	1.3714(18)
O(1)-C(1)	1.4583(19)
N(1)-C(6)	1.4783(18)
N(1)-H(1NA)	0.9100
N(1)-H(1NB)	0.9100
N(1)-H(1NC)	0.9100
C(1)-C(10)	1.517(2)
C(1)-C(2)	1.522(2)
C(1)-C(11)	1.524(2)
C(2)-C(3)	1.526(2)
C(2)-H(2A)	0.9900
C(2)-H(2B)	0.9900
C(3)-C(4)	1.516(2)
C(3)-H(3A)	0.9900
C(3)-H(3B)	0.9900
C(4)-C(9)	1.394(2)
C(4)-C(5)	1.408(2)
C(5)-C(6)	1.3910(19)
C(5)-C(12)	1.508(2)
C(6)-C(7)	1.4033(19)
C(7)-C(8)	1.394(2)
C(7)-C(13)	1.508(2)
C(8)-C(9)	1.407(2)
C(8)-C(14)	1.511(2)
C(10)-H(10A)	0.9800
C(10)-H(10B)	0.9800
C(10)-H(10C)	0.9800
C(11)-H(11A)	0.9800
C(11)-H(11B)	0.9800
C(11)-H(11C)	0.9800
C(12)-H(12A)	0.9800
C(12)-H(12B)	0.9800
C(12)-H(12C)	0.9800
C(13)-H(13A)	0.9800
C(13)-H(13B)	0.9800
C(13)-H(13C)	0.9800
C(14)-H(14A)	0.9800
C(14)-H(14B)	0.9800
C(14)-H(14C)	0.9800
C(15)-C(16)	1.388(2)
C(15)-C(20)	1.393(2)
C(16)-C(17)	1.391(2)
C(16)-H(16)	0.9500
C(17)-C(18)	1.396(2)
C(17)-H(17)	0.9500
C(18)-C(19)	1.393(2)
C(18)-C(21)	1.509(2)
C(19)-C(20)	1.390(2)
C(19)-H(19)	0.9500
C(20)-H(20)	0.9500
C(21)-H(21A)	0.9800
C(21)-H(21B)	0.9800
C(21)-H(21C)	0.9800

Bond angles

O(2)-S(1)-O(3)	112.16(7)
O(2)-S(1)-O(4)	113.14(7)
O(3)-S(1)-O(4)	112.55(7)
O(2)-S(1)-C(15)	106.50(7)
O(3)-S(1)-C(15)	105.76(7)
O(4)-S(1)-C(15)	106.06(7)
C(9)-O(1)-C(1)	118.00(12)
C(6)-N(1)-H(1NA)	109.5
C(6)-N(1)-H(1NB)	109.5
H(1NA)-N(1)-H(1NB)	109.5
C(6)-N(1)-H(1NC)	109.5
H(1NA)-N(1)-H(1NC)	109.5
H(1NB)-N(1)-H(1NC)	109.5
O(1)-C(1)-C(10)	103.72(14)
O(1)-C(1)-C(2)	108.50(13)
C(10)-C(1)-C(2)	111.47(14)
O(1)-C(1)-C(11)	108.44(13)
C(10)-C(1)-C(11)	111.56(14)
C(2)-C(1)-C(11)	112.67(15)
C(1)-C(2)-C(3)	111.85(13)
C(1)-C(2)-H(2A)	109.2
C(3)-C(2)-H(2A)	109.2
C(1)-C(2)-H(2B)	109.2
C(3)-C(2)-H(2B)	109.2
H(2A)-C(2)-H(2B)	107.9
C(4)-C(3)-C(2)	111.39(13)
C(4)-C(3)-H(3A)	109.4
C(2)-C(3)-H(3A)	109.4
C(4)-C(3)-H(3B)	109.4
C(2)-C(3)-H(3B)	109.4
H(3A)-C(3)-H(3B)	108.0
C(9)-C(4)-C(5)	119.23(13)
C(9)-C(4)-C(3)	120.31(13)
C(5)-C(4)-C(3)	120.45(13)
C(6)-C(5)-C(4)	118.25(13)
C(6)-C(5)-C(12)	123.72(13)
C(4)-C(5)-C(12)	118.03(12)
C(5)-C(6)-C(7)	122.82(13)
C(5)-C(6)-N(1)	120.46(12)
C(7)-C(6)-N(1)	116.71(12)
C(8)-C(7)-C(6)	118.74(13)
C(8)-C(7)-C(13)	120.28(13)
C(6)-C(7)-C(13)	120.97(13)

C(7)-C(8)-C(9)	118.85(13)
C(7)-C(8)-C(14)	121.45(13)
C(9)-C(8)-C(14)	119.70(14)
O(1)-C(9)-C(4)	122.85(13)
O(1)-C(9)-C(8)	115.13(13)
C(4)-C(9)-C(8)	122.01(13)
C(1)-C(10)-H(10A)	109.5
C(1)-C(10)-H(10B)	109.5
H(10A)-C(10)-H(10B)	109.5
C(1)-C(10)-H(10C)	109.5
H(10A)-C(10)-H(10C)	109.5
H(10B)-C(10)-H(10C)	109.5
C(1)-C(11)-H(11A)	109.5
C(1)-C(11)-H(11B)	109.5
H(11A)-C(11)-H(11B)	109.5
C(1)-C(11)-H(11C)	109.5
H(11A)-C(11)-H(11C)	109.5
H(11B)-C(11)-H(11C)	109.5
C(5)-C(12)-H(12A)	109.5
C(5)-C(12)-H(12B)	109.5
H(12A)-C(12)-H(12B)	109.5
C(5)-C(12)-H(12C)	109.5
H(12A)-C(12)-H(12C)	109.5
H(12B)-C(12)-H(12C)	109.5
C(7)-C(13)-H(13A)	109.5
C(7)-C(13)-H(13B)	109.5
H(13A)-C(13)-H(13B)	109.5
C(7)-C(13)-H(13C)	109.5
H(13A)-C(13)-H(13C)	109.5
H(13B)-C(13)-H(13C)	109.5
C(8)-C(14)-H(14A)	109.5
C(8)-C(14)-H(14B)	109.5
H(14A)-C(14)-H(14B)	109.5
C(8)-C(14)-H(14C)	109.5
H(14A)-C(14)-H(14C)	109.5
H(14B)-C(14)-H(14C)	109.5
C(16)-C(15)-C(20)	120.18(14)
C(16)-C(15)-S(1)	120.89(11)
C(20)-C(15)-S(1)	118.91(11)
C(15)-C(16)-C(17)	119.55(14)
C(15)-C(16)-H(16)	120.2
C(17)-C(16)-H(16)	120.2
C(16)-C(17)-C(18)	121.35(15)
C(16)-C(17)-H(17)	119.3
C(18)-C(17)-H(17)	119.3
C(19)-C(18)-C(17)	117.99(15)
C(19)-C(18)-C(21)	121.22(15)
C(17)-C(18)-C(21)	120.79(15)
C(20)-C(19)-C(18)	121.49(15)
C(20)-C(19)-H(19)	119.3
C(18)-C(19)-H(19)	119.3
C(19)-C(20)-C(15)	119.43(14)
C(19)-C(20)-H(20)	120.3
C(15)-C(20)-H(20)	120.3
C(18)-C(21)-H(21A)	109.5
C(18)-C(21)-H(21B)	109.5
H(21A)-C(21)-H(21B)	109.5
C(18)-C(21)-H(21C)	109.5
H(21A)-C(21)-H(21C)	109.5
H(21B)-C(21)-H(21C)	109.5

Torsion angles

C9-O1-C1-C10	-165.54(13)
C9-O1-C1-C2	-46.91(18)
C9-O1-C1-C11	75.77(17)
O1-C1-C2-C3	59.64(17)
C10-C1-C2-C3	173.25(15)
C11-C1-C2-C3	-60.44(18)
C1-C2-C3-C4	-42.92(18)
C2-C3-C4-C9	13.1(2)
C2-C3-C4-C5	-167.87(14)
C9-C4-C5-C6	-2.3(2)
C3-C4-C5-C6	178.63(13)
C9-C4-C5-C12	177.49(13)
C3-C4-C5-C12	-1.6(2)
C4-C5-C6-C7	-0.3(2)
C12-C5-C6-C7	179.96(13)
C4-C5-C6-N1	178.29(12)
C12-C5-C6-N1	-1.5(2)
C5-C6-C7-C8	2.7(2)
N1-C6-C7-C8	-175.92(12)
C5-C6-C7-C13	-178.11(14)
N1-C6-C7-C13	3.3(2)
C6-C7-C8-C9	-2.5(2)
C13-C7-C8-C9	178.33(13)
C6-C7-C8-C14	177.27(13)
C13-C7-C8-C14	-1.9(2)
C1-O1-C9-C4	17.7(2)
C1-O1-C9-C8	-163.31(13)
C5-C4-C9-O1	-178.61(13)
C3-C4-C9-O1	0.5(2)
C5-C4-C9-C8	2.5(2)
C3-C4-C9-C8	-178.42(14)
C7-C8-C9-O1	-179.03(13)
C14-C8-C9-O1	1.2(2)
C7-C8-C9-C4	-0.1(2)
C14-C8-C9-C4	-179.81(14)
O2-S1-C15-C16	-134.40(13)
O3-S1-C15-C16	106.10(13)
O4-S1-C15-C16	-13.62(14)
O2-S1-C15-C20	47.19(14)
O3-S1-C15-C20	-72.30(13)
O4-S1-C15-C20	167.98(12)
C20-C15-C16-C17	-0.4(2)
S1-C15-C16-C17	-178.83(12)
C15-C16-C17-C18	-0.4(2)
C16-C17-C18-C19	0.8(2)
C16-C17-C18-C21	-179.17(15)
C17-C18-C19-C20	-0.4(2)
C21-C18-C19-C20	179.60(15)
C18-C19-C20-C15	-0.4(2)
C16-C15-C20-C19	0.9(2)
S1-C15-C20-C19	179.28(12)

Hydrogen-bonds

D-H...A	d(D-H)	d(H...A)	d(D...A)	<(DHA)
N(1)-H(1NA)...O(2)	0.91	1.90	2.8002(17)	171.5
N(1)-H(1NC)...O(3)#1	0.91	1.97	2.8187(17)	155.6
N(1)-H(1NB)...O(4)#2	0.91	1.91	2.7943(16)	163.8
C(12)-H(12C)...O(3)#1	0.98	2.27	3.1936(19)	156.8

Symmetry transformations used to generate equivalent atoms:
#1 -x+1,-y+1,-z+1 #2 -x,-y+1,-z+1

2,2,5,8-Tetramethyl-chroman-6-ylamine

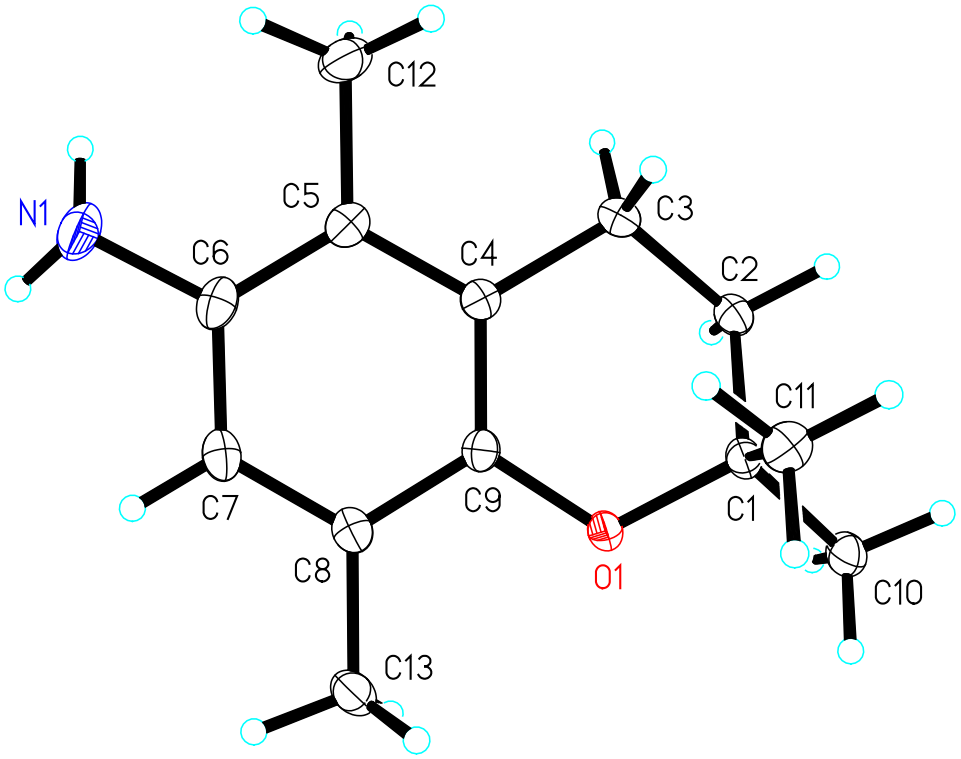

The compound crystallized in large colorless prisms of low melting point. The compound appears to be *ortho*rhombic at room temperature or close to it. At 100 K it is definitely monoclinic with two independent but closely similar molecules per asymmetric unit. The aromatic NH_2-group appears to have a pyramidal coordination. Each of the two independent nitrogen atoms has only one weak N-H---O hydrogen bond.

Fig. 1. Thermal ellipsoid plots (50% ellipsoids) of 2,2,5,8-tetramethyl-chroman-6-ylamine.

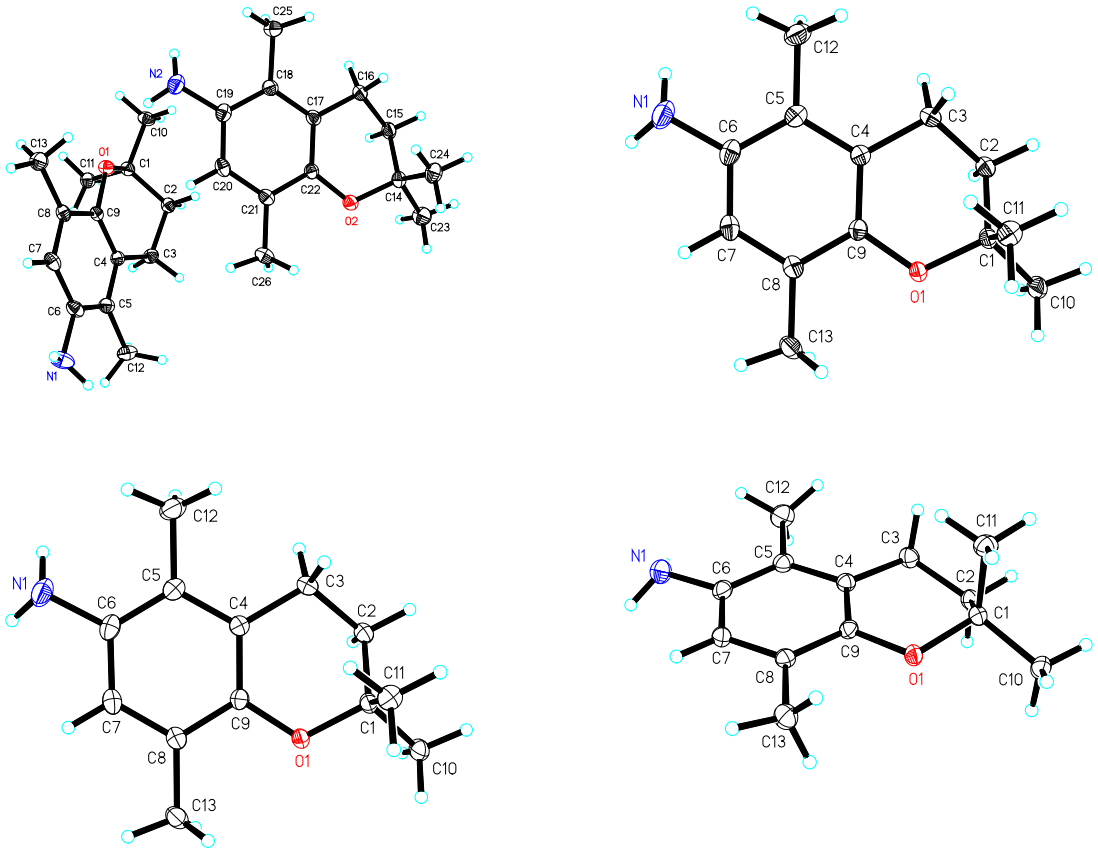

Fig. 2. Asymmetric unit of 2,2,5,8-tetramethyl-chroman-6-ylamine.

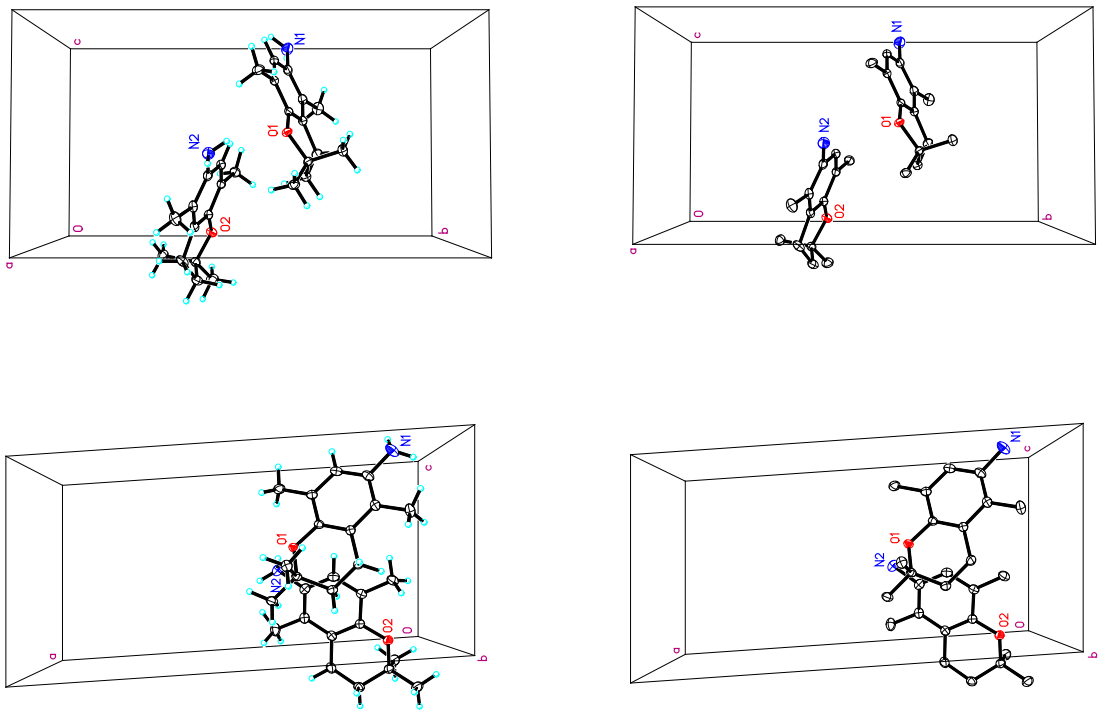

Fig. 3. Packing diagrams of 2,2,5,8-tetramethyl-chroman-6-ylamine.

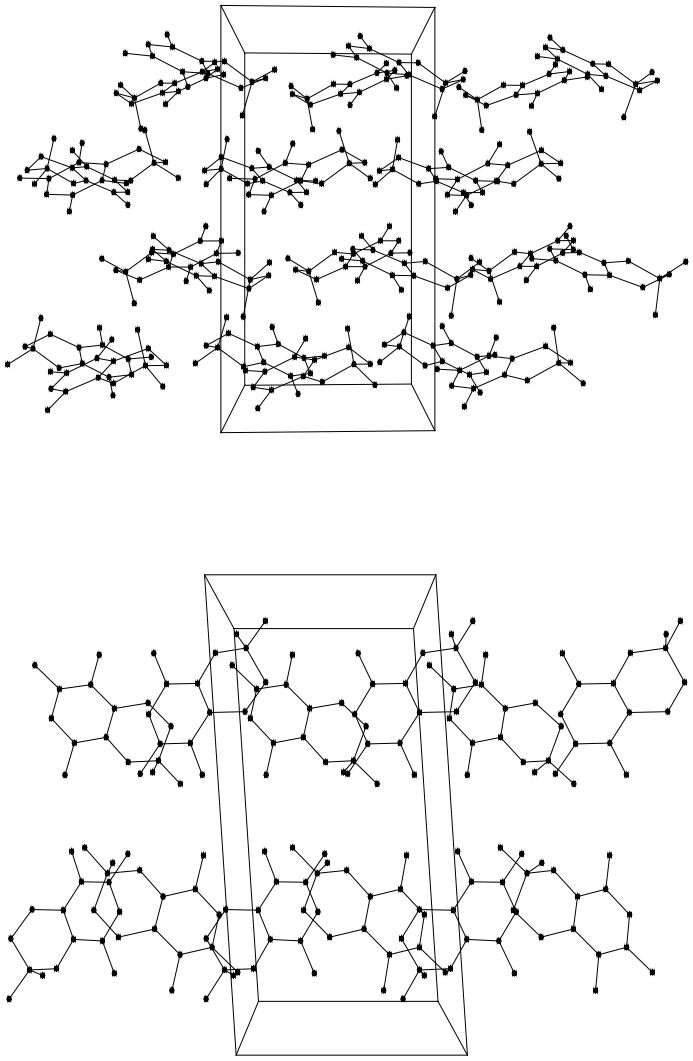

Table 1. Crystal data and structure refinement for 2,2,5,8-tetramethyl-chroman-6-ylamine..

Identification code	1423tt
Empirical formula	C13 H19 N O
Formula weight	205.29
Temperature	100(2) K
Wavelength	0.71073 A
Crystal system, space group	Monoclinic, P2(1)/c
Unit cell dimensions	a = 16.815(3) A alpha = 90 deg. b = 16.409(2) A beta = 93.866(2) deg. c = 8.2877(12) A gamma = 90 deg.
Volume	2281.6(6) A^3
Z, Calculated density	8 (Z' = 2), 1.195 Mg/m^3
Absorption coefficient	0.075 mm^-1
F(000)	896
Crystal size	0.45 x 0.40 x 0.35 mm
Diffractometer	Bruker Kappa APEX-II CCD 4-axis (sealed X-ray tube, Mo Kalfa rad., graphite monochromator detector.distance 55 mm, 512x512 pixels)
Scan type / width / speed	ome-scan frames / dome=0.3deg / 20sec per fram full sphere data collection.
Theta range for data collection	2.76 to 30.00 deg.
Index ranges	-23<=h<=23, -23<=k<=23, -11<=l<=11
Reflections collected / unique	32090 / 6519 [R(int) = 0.0294]
Completeness to theta = 30.00	97.9%
Absorption correction	Multi-scan (program SADABS; Sheldrick, 1996)
Max. and min. transmission	0.97 and 0.87
Structure solution	Direct methods (program SHELXS97)
Refinement method	Full-matrix least-squares on F2 (prg SHELXL97)
Data / restraints / parameters	6519 / 7 / 295
Goodness-of-fit on F2	1.073
Final R indices [I>2sigma(I)]	R1 = 0.0557, wR2 = 0.1503
R indices (all data)	R1 = 0.0618, wR2 = 0.1559
Largest diff. peak and hole	0.46 and -0.29 eA-3

$R1 = \Sigma||F_o|-|F_c||/\Sigma|F_o|$, $wR2 = [\Sigma(w(F_o^2-F_c^2)^2)/\Sigma(w(F_o^2)^2)]^{½}$

Table 2. Atomic coordinates (x 10^5) and equivalent isotropic displacement parameters ($Å^2$ x 10^3) for 2,2,5,8-tetramethyl-chroman-6-ylamine. U_{eq} is defined as one third of the trace of the *ortho*gonalized U_{ij} tensor.

	x	y	z	U_{eq}
O(1)	37114(6)	59213(6)	53452(11)	16(1)
N(1)	13451(9)	59889(8)	97666(17)	26(1)
C(1)	36599(8)	64496(8)	39230(15)	15(1)
C(2)	28129(8)	64338(8)	31579(15)	16(1)
C(3)	22149(8)	67355(8)	43240(16)	17(1)
C(4)	23766(7)	63623(8)	59809(15)	15(1)
C(5)	17882(8)	63825(8)	71131(16)	17(1)
C(6)	19258(8)	59890(8)	86020(17)	18(1)
C(7)	26619(8)	56166(8)	89849(16)	18(1)
C(8)	32585(8)	56103(8)	79057(15)	16(1)
C(9)	31045(8)	59813(7)	63950(15)	14(1)
C(10)	42397(9)	60750(9)	28059(16)	20(1)
C(11)	39241(8)	73033(8)	44501(17)	19(1)
C(12)	10112(8)	68204(9)	67085(19)	24(1)
C(13)	40425(9)	51971(9)	83433(17)	22(1)
O(2)	12418(6)	39643(6)	2974(12)	19(1)
N(2)	40469(8)	39542(8)	43041(16)	24(1)
C(14)	11716(8)	35325(8)	-12399(16)	17(1)
C(15)	19503(8)	36054(9)	-20667(16)	20(1)
C(16)	26471(8)	32477(9)	-10214(17)	21(1)
C(17)	26479(8)	35606(8)	6938(16)	16(1)
C(18)	33495(8)	35483(8)	17202(17)	17(1)
C(19)	33529(8)	39194(8)	32403(17)	18(1)
C(20)	26469(8)	42402(8)	37671(16)	18(1)
C(21)	19411(8)	42324(8)	27980(16)	16(1)
C(22)	19525(8)	38988(8)	12387(15)	15(1)
C(23)	4994(10)	39650(10)	-22125(18)	26(1)
C(24)	9487(9)	26502(9)	-9242(18)	23(1)
C(25)	40895(9)	31347(9)	11820(20)	25(1)
C(26)	11887(9)	45875(9)	33946(17)	21(1)

Remarks: Two independent molecules per asymmetric unit.

Table 3. Hydrogen coordinates (x 10^4) and isotropic displacement parameters (Å^2 x 10^3) for 2,2,5,8-tetramethyl-chroman-6-ylamine.

	x	y	z	U_{eq}
H(1NA)	840(8)	5982(13)	9370(30)	41(6)
H(1NB)	1411(13)	5550(11)	10390(30)	48(7)
H(2A)	2674	5870	2820	19
H(2B)	2780	6781	2179	19
H(3A)	2248	7336	4410	21
H(3B)	1669	6592	3899	21
H(7)	2756	5362	10009	21
H(10A)	4079	5513	2550	29
H(10B)	4777	6076	3342	29
H(10C)	4237	6394	1805	29
H(11A)	4473	7283	4926	29
H(11B)	3572	7509	5254	29
H(11C)	3896	7666	3509	29
H(12A)	787	7001	7709	36
H(12B)	636	6450	6125	36
H(12C)	1106	7294	6029	36
H(13A)	4096	4718	7653	33
H(13B)	4063	5027	9479	33
H(13C)	4480	5578	8184	33
H(2NA)	4053(13)	4407(10)	4900(20)	40(6)
H(2NB)	4503(9)	3948(13)	3820(30)	39(6)
H(15A)	2058	4187	-2285	24
H(15B)	1899	3315	-3116	24
H(16A)	2606	2646	-1020	26
H(16B)	3155	3398	-1484	26
H(20)	2650	4471	4819	22
H(23A)	645	4537	-2368	38
H(23B)	12	3937	-1629	38
H(23C)	407	3700	-3268	38
H(24A)	442	2633	-408	34
H(24B)	1366	2396	-210	34
H(24C)	895	2353	-1951	34
H(25A)	4420	2953	2133	37
H(25B)	4392	3520	559	37
H(25C)	3936	2663	506	37
H(26A)	1285	4753	4527	32
H(26B)	765	4177	3308	32
H(26C)	1027	5063	2737	32

Hydrogen atoms inserted in idealized positions and refined riding with the atoms to which they were bonded. All H atoms had $U_{iso} = U_{eq}$ x 1.2 (x 1.5 for CH_3) of their carrier atoms. N-bonded H-atoms refined in x,y,z,U_{iso} with hard SADI distance restraints for N-H and H-H distances.

Table 4. Anisotropic displacement parameters ($Å^2$ x 10^3) for 2,2,5,8-tetramethyl-chroman-6-ylamine. The anisotropic displacement factor exponent takes the form: $-2\pi^2 [h^2 a^{*2} U_{11} + ... + 2 h k a^* b^* U_{12}]$

	U_{11}	U_{22}	U_{33}	U_{23}	U_{13}	U_{12}
O(1)	17(1)	18(1)	13(1)	3(1)	3(1)	3(1)
N(1)	30(1)	25(1)	27(1)	4(1)	15(1)	3(1)
C(1)	17(1)	15(1)	13(1)	2(1)	2(1)	1(1)
C(2)	18(1)	17(1)	14(1)	1(1)	0(1)	1(1)
C(3)	16(1)	19(1)	17(1)	3(1)	0(1)	2(1)
C(4)	15(1)	14(1)	15(1)	0(1)	1(1)	-1(1)
C(5)	16(1)	15(1)	19(1)	-2(1)	3(1)	-1(1)
C(6)	22(1)	15(1)	19(1)	-2(1)	7(1)	-3(1)
C(7)	25(1)	14(1)	14(1)	0(1)	4(1)	-1(1)
C(8)	20(1)	13(1)	14(1)	-1(1)	1(1)	0(1)
C(9)	16(1)	13(1)	12(1)	-2(1)	2(1)	-1(1)
C(10)	23(1)	22(1)	15(1)	2(1)	5(1)	6(1)
C(11)	19(1)	17(1)	22(1)	-2(1)	2(1)	-1(1)
C(12)	17(1)	26(1)	30(1)	1(1)	5(1)	3(1)
C(13)	24(1)	26(1)	16(1)	3(1)	-1(1)	6(1)
O(2)	18(1)	22(1)	16(1)	-3(1)	0(1)	3(1)
N(2)	22(1)	24(1)	23(1)	1(1)	-5(1)	0(1)
C(14)	19(1)	18(1)	15(1)	-1(1)	0(1)	-1(1)
C(15)	21(1)	23(1)	16(1)	-5(1)	3(1)	-5(1)
C(16)	18(1)	25(1)	21(1)	-10(1)	3(1)	-2(1)
C(17)	17(1)	14(1)	18(1)	-2(1)	3(1)	-1(1)
C(18)	17(1)	13(1)	22(1)	-1(1)	2(1)	-1(1)
C(19)	20(1)	14(1)	20(1)	2(1)	-2(1)	-2(1)
C(20)	24(1)	15(1)	15(1)	-1(1)	2(1)	-2(1)
C(21)	20(1)	13(1)	16(1)	0(1)	4(1)	-1(1)
C(22)	17(1)	14(1)	15(1)	0(1)	1(1)	-1(1)
C(23)	27(1)	30(1)	20(1)	3(1)	-3(1)	6(1)
C(24)	23(1)	21(1)	23(1)	2(1)	-1(1)	-4(1)
C(25)	18(1)	24(1)	32(1)	-6(1)	2(1)	3(1)
C(26)	24(1)	21(1)	19(1)	-1(1)	7(1)	3(1)

Table 5. Bond lengths [Å] and angles [deg] for 2,2,5,8-tetramethyl-chroman-6-ylamine.

Bond distances

O(1)-C(9)	1.3885(15)
O(1)-C(1)	1.4611(15)
N(1)-C(6)	1.4185(17)
N(1)-H(1NA)	0.890(12)
N(1)-H(1NB)	0.890(12)
C(1)-C(10)	1.5190(18)
C(1)-C(2)	1.5197(18)
C(1)-C(11)	1.5247(18)
C(2)-C(3)	1.5235(18)
C(2)-H(2A)	0.99
C(2)-H(2B)	0.99
C(3)-C(4)	1.5113(18)
C(3)-H(3A)	0.99
C(3)-H(3B)	0.99
C(4)-C(9)	1.3965(17)
C(4)-C(5)	1.4092(17)
C(5)-C(6)	1.3981(19)
C(5)-C(12)	1.5088(19)
C(6)-C(7)	1.397(2)
C(7)-C(8)	1.3884(18)
C(7)-H(7)	0.95
C(8)-C(9)	1.4005(17)
C(8)-C(13)	1.5048(19)
C(10)-H(10A)	0.98
C(10)-H(10B)	0.98
C(10)-H(10C)	0.98
C(11)-H(11A)	0.98
C(11)-H(11B)	0.98
C(11)-H(11C)	0.98
C(12)-H(12A)	0.98
C(12)-H(12B)	0.98
C(12)-H(12C)	0.98
C(13)-H(13A)	0.98
C(13)-H(13B)	0.98
C(13)-H(13C)	0.98
O(2)-C(22)	1.3865(16)
O(2)-C(14)	1.4557(16)
N(2)-C(19)	1.4156(18)
N(2)-H(2NA)	0.890(12)
N(2)-H(2NB)	0.890(12)
C(14)-C(23)	1.5193(19)
C(14)-C(24)	1.5226(19)
C(14)-C(15)	1.5229(19)
C(15)-C(16)	1.527(2)
C(15)-H(15A)	0.99
C(15)-H(15B)	0.99
C(16)-C(17)	1.5113(18)
C(16)-H(16A)	0.99
C(16)-H(16B)	0.99
C(17)-C(22)	1.3966(18)
C(17)-C(18)	1.4073(18)
C(18)-C(19)	1.3989(19)
C(18)-C(25)	1.5109(19)
C(19)-C(20)	1.3953(19)
C(20)-C(21)	1.3875(19)
C(20)-H(20)	0.95
C(21)-C(22)	1.4048(18)
C(21)-C(26)	1.5063(19)
C(23)-H(23A)	0.98
C(23)-H(23B)	0.98
C(23)-H(23C)	0.98
C(24)-H(24A)	0.98
C(24)-H(24B)	0.98
C(24)-H(24C)	0.98
C(25)-H(25A)	0.98
C(25)-H(25B)	0.98
C(25)-H(25C)	0.98
C(26)-H(26A)	0.98
C(26)-H(26B)	0.98
C(26)-H(26C)	0.98

Bond angles

C(9)-O(1)-C(1)	117.22(10)
C(6)-N(1)-H(1NA)	115.7(15)
C(6)-N(1)-H(1NB)	109.4(16)
H(1NA)-N(1)-H(1NB)	106.4(15)
O(1)-C(1)-C(10)	104.24(10)
O(1)-C(1)-C(2)	109.23(10)
C(10)-C(1)-C(2)	111.15(11)
O(1)-C(1)-C(11)	108.28(10)
C(10)-C(1)-C(11)	111.09(11)
C(2)-C(1)-C(11)	112.47(11)
C(1)-C(2)-C(3)	111.71(11)
C(1)-C(2)-H(2A)	109.3
C(3)-C(2)-H(2A)	109.3
C(1)-C(2)-H(2B)	109.3
C(3)-C(2)-H(2B)	109.3
H(2A)-C(2)-H(2B)	107.9
C(4)-C(3)-C(2)	111.02(10)
C(4)-C(3)-H(3A)	109.4
C(2)-C(3)-H(3A)	109.4
C(4)-C(3)-H(3B)	109.4
C(2)-C(3)-H(3B)	109.4
H(3A)-C(3)-H(3B)	108.0
C(9)-C(4)-C(5)	119.34(12)
C(9)-C(4)-C(3)	120.38(11)
C(5)-C(4)-C(3)	120.27(11)
C(6)-C(5)-C(4)	119.67(12)
C(6)-C(5)-C(12)	120.36(12)
C(4)-C(5)-C(12)	119.97(12)
C(7)-C(6)-C(5)	119.59(12)
C(7)-C(6)-N(1)	119.03(13)
C(5)-C(6)-N(1)	121.33(13)
C(8)-C(7)-C(6)	121.63(12)

C(8)-C(7)-H(7)	119.2
C(6)-C(7)-H(7)	119.2
C(7)-C(8)-C(9)	118.32(12)
C(7)-C(8)-C(13)	120.50(12)
C(9)-C(8)-C(13)	121.17(12)
O(1)-C(9)-C(4)	123.14(11)
O(1)-C(9)-C(8)	115.46(11)
C(4)-C(9)-C(8)	121.37(12)
C(1)-C(10)-H(10A)	109.5
C(1)-C(10)-H(10B)	109.5
H(10A)-C(10)-H(10B)	109.5
C(1)-C(10)-H(10C)	109.5
H(10A)-C(10)-H(10C)	109.5
H(10B)-C(10)-H(10C)	109.5
C(1)-C(11)-H(11A)	109.5
C(1)-C(11)-H(11B)	109.5
H(11A)-C(11)-H(11B)	109.5
C(1)-C(11)-H(11C)	109.5
H(11A)-C(11)-H(11C)	109.5
H(11B)-C(11)-H(11C)	109.5
C(5)-C(12)-H(12A)	109.5
C(5)-C(12)-H(12B)	109.5
H(12A)-C(12)-H(12B)	109.5
C(5)-C(12)-H(12C)	109.5
H(12A)-C(12)-H(12C)	109.5
H(12B)-C(12)-H(12C)	109.5
C(8)-C(13)-H(13A)	109.5
C(8)-C(13)-H(13B)	109.5
H(13A)-C(13)-H(13B)	109.5
C(8)-C(13)-H(13C)	109.5
H(13A)-C(13)-H(13C)	109.5
H(13B)-C(13)-H(13C)	109.5
C(22)-O(2)-C(14)	118.08(10)
C(19)-N(2)-H(2NA)	110.9(15)
C(19)-N(2)-H(2NB)	114.5(15)
H(2NA)-N(2)-H(2NB)	106.4(15)
O(2)-C(14)-C(23)	104.51(11)
O(2)-C(14)-C(24)	108.59(11)
C(23)-C(14)-C(24)	110.63(12)
O(2)-C(14)-C(15)	109.52(11)
C(23)-C(14)-C(15)	110.86(12)
C(24)-C(14)-C(15)	112.40(12)
C(14)-C(15)-C(16)	111.39(11)
C(14)-C(15)-H(15A)	109.3
C(16)-C(15)-H(15A)	109.3
C(14)-C(15)-H(15B)	109.3
C(16)-C(15)-H(15B)	109.3
H(15A)-C(15)-H(15B)	108.0
C(17)-C(16)-C(15)	110.80(11)
C(17)-C(16)-H(16A)	109.5
C(15)-C(16)-H(16A)	109.5
C(17)-C(16)-H(16B)	109.5
C(15)-C(16)-H(16B)	109.5
H(16A)-C(16)-H(16B)	108.1
C(22)-C(17)-C(18)	119.76(12)
C(22)-C(17)-C(16)	119.44(12)
C(18)-C(17)-C(16)	120.74(12)
C(19)-C(18)-C(17)	119.37(12)
C(19)-C(18)-C(25)	120.52(12)
C(17)-C(18)-C(25)	120.11(12)
C(20)-C(19)-C(18)	119.62(12)
C(20)-C(19)-N(2)	118.23(13)
C(18)-C(19)-N(2)	122.11(13)
C(21)-C(20)-C(19)	121.86(12)
C(21)-C(20)-H(20)	119.1
C(19)-C(20)-H(20)	119.1
C(20)-C(21)-C(22)	118.16(12)
C(20)-C(21)-C(26)	120.73(12)
C(22)-C(21)-C(26)	121.10(12)
O(2)-C(22)-C(17)	123.88(12)
O(2)-C(22)-C(21)	115.01(11)
C(17)-C(22)-C(21)	121.06(12)
C(14)-C(23)-H(23A)	109.5
C(14)-C(23)-H(23B)	109.5
H(23A)-C(23)-H(23B)	109.5
C(14)-C(23)-H(23C)	109.5
H(23A)-C(23)-H(23C)	109.5
H(23B)-C(23)-H(23C)	109.5
C(14)-C(24)-H(24A)	109.5
C(14)-C(24)-H(24B)	109.5
H(24A)-C(24)-H(24B)	109.5
C(14)-C(24)-H(24C)	109.5
H(24A)-C(24)-H(24C)	109.5
H(24B)-C(24)-H(24C)	109.5
C(18)-C(25)-H(25A)	109.5
C(18)-C(25)-H(25B)	109.5
H(25A)-C(25)-H(25B)	109.5
C(18)-C(25)-H(25C)	109.5
H(25A)-C(25)-H(25C)	109.5
H(25B)-C(25)-H(25C)	109.5
C(21)-C(26)-H(26A)	109.5
C(21)-C(26)-H(26B)	109.5
H(26A)-C(26)-H(26B)	109.5
C(21)-C(26)-H(26C)	109.5
H(26A)-C(26)-H(26C)	109.5
H(26B)-C(26)-H(26C)	109.5

Torsion angles

C9-O1-C1-C10	-163.67(11)
C9-O1-C1-C2	-44.80(14)
C9-O1-C1-C11	77.98(13)
O1-C1-C2-C3	60.28(13)
C10-C1-C2-C3	174.75(11)
C11-C1-C2-C3	-59.98(14)
C1-C2-C3-C4	-45.22(14)
C2-C3-C4-C9	15.51(17)
C2-C3-C4-C5	-163.32(12)
C9-C4-C5-C6	-2.99(19)
C3-C4-C5-C6	175.85(12)
C9-C4-C5-C12	177.60(12)

C3-C4-C5-C12	-3.56(19)	C14-C15-C16-C17	-48.24(15)
C4-C5-C6-C7	3.36(19)	C15-C16-C17-C22	18.72(17)
C12-C5-C6-C7	-177.24(13)	C15-C16-C17-C18	-158.39(12)
C4-C5-C6-N1	-179.38(12)	C22-C17-C18-C19	-3.79(19)
C12-C5-C6-N1	0.0(2)	C16-C17-C18-C19	173.32(12)
C5-C6-C7-C8	-1.5(2)	C22-C17-C18-C25	175.98(12)
N1-C6-C7-C8	-178.82(12)	C16-C17-C18-C25	-6.91(19)
C6-C7-C8-C9	-0.73(19)	C17-C18-C19-C20	4.92(19)
C6-C7-C8-C13	-179.36(13)	C25-C18-C19-C20	-174.85(13)
C1-O1-C9-C4	15.55(17)	C17-C18-C19-N2	-177.63(12)
C1-O1-C9-C8	-166.23(11)	C25-C18-C19-N2	2.6(2)
C5-C4-C9-O1	178.88(11)	C18-C19-C20-C21	-2.6(2)
C3-C4-C9-O1	0.04(19)	N2-C19-C20-C21	179.82(12)
C5-C4-C9-C8	0.75(19)	C19-C20-C21-C22	-0.83(19)
C3-C4-C9-C8	-178.08(12)	C19-C20-C21-C26	-179.65(12)
C7-C8-C9-O1	-177.16(11)	C14-O2-C22-C17	11.16(18)
C13-C8-C9-O1	1.46(18)	C14-O2-C22-C21	-171.37(11)
C7-C8-C9-C4	1.10(19)	C18-C17-C22-O2	177.63(12)
C13-C8-C9-C4	179.72(12)	C16-C17-C22-O2	0.49(19)
C22-O2-C14-C23	-159.29(11)	C18-C17-C22-C21	0.31(19)
C22-O2-C14-C24	82.61(14)	C16-C17-C22-C21	-176.83(12)
C22-O2-C14-C15	-40.47(15)	C20-C21-C22-O2	-175.55(11)
O2-C14-C15-C16	59.51(14)	C26-C21-C22-O2	3.26(18)
C23-C14-C15-C16	174.32(12)	C20-C21-C22-C17	1.99(19)
C24-C14-C15-C16	-61.28(15)	C26-C21-C22-C17	-179.20(12)

Hydrogen-bonds

D-H...A	d(D-H)	d(H...A)	d(D...A)	<(DHA)
N(1)-H(1NB)...O(2)#1	0.890(12)	2.619(18)	3.3573(18)	141(2)
N(2)-H(2NA)...O(1)	0.890(12)	2.584(15)	3.3982(17)	153(2)

Symmetry transformations used to generate equivalent atoms:
#1 x,y,z+1 #2 -x,-y+1,-z+1 #3 -x+1,-y+1,-z+1

2,2,7,8-Tetramethyl-chroman-6-ylamine, 4-methylbenzenesulfonate

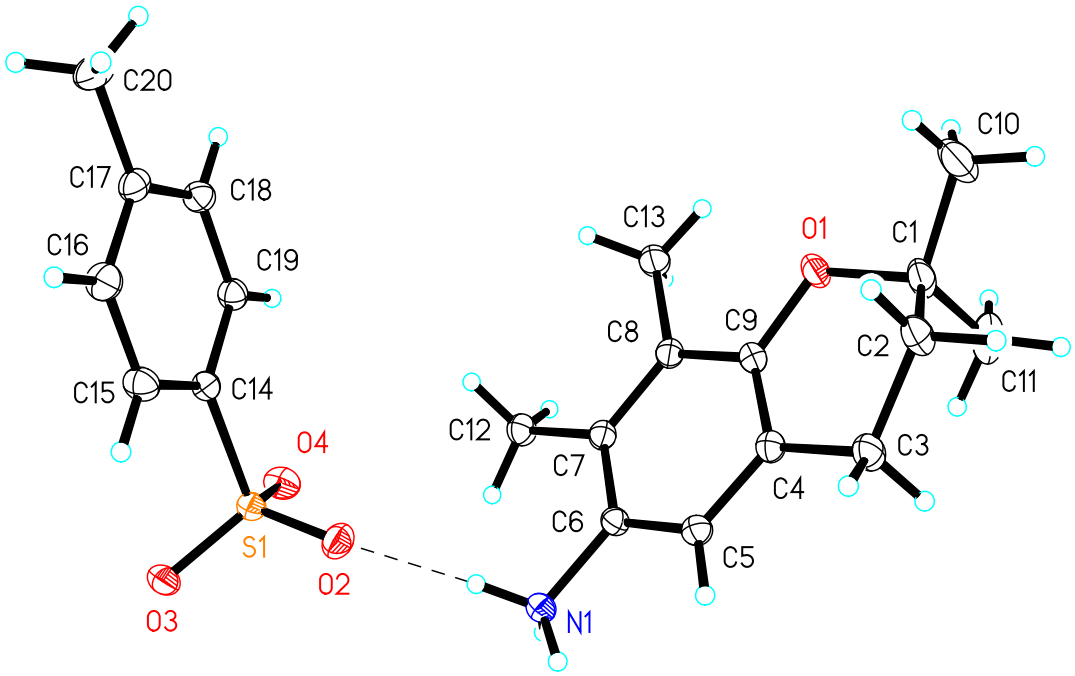

Prismatic crystals from methanol by evaporation.

Fig. 1. Thermal ellipsoid plots (50% ellipsoids) of 2,2,7,8-tetramethyl-chroman-6-ylamine, 4-methylbenzenesulfonate.

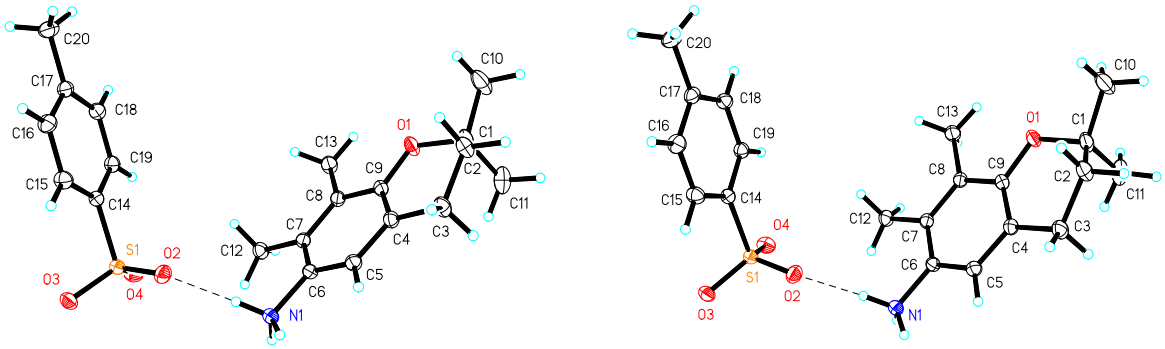

Fig. 2. Asymmetric unit of 2,2,7,8-tetramethyl-chroman-6-ylamine, 4-methylbenzenesulfonate.

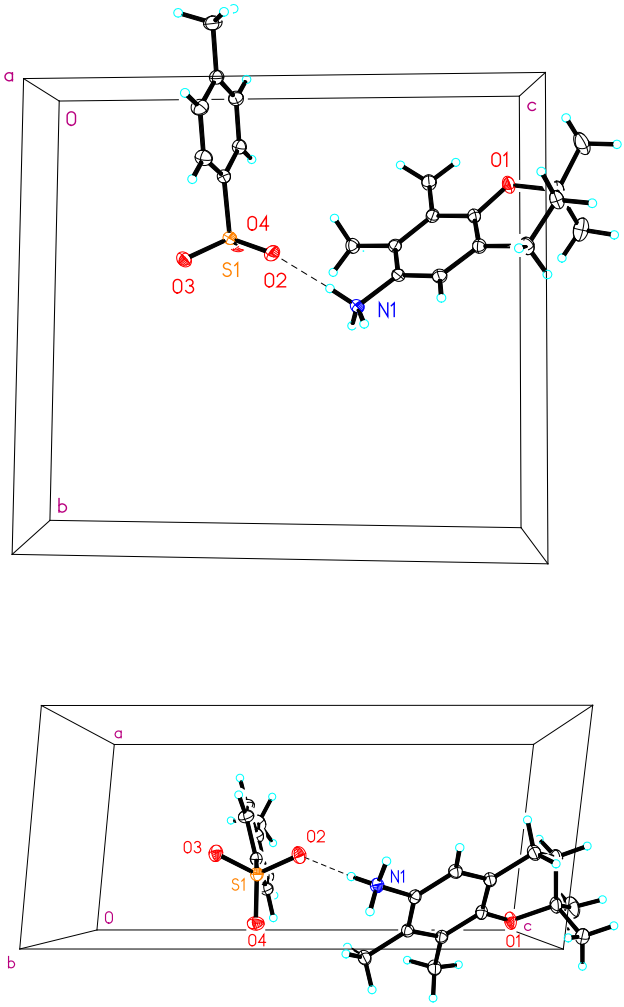

Fig. 3. Packing diagrams of 2,2,7,8-tetramethyl-chroman-6-ylamine, 4-methylbenzenesulfonate.

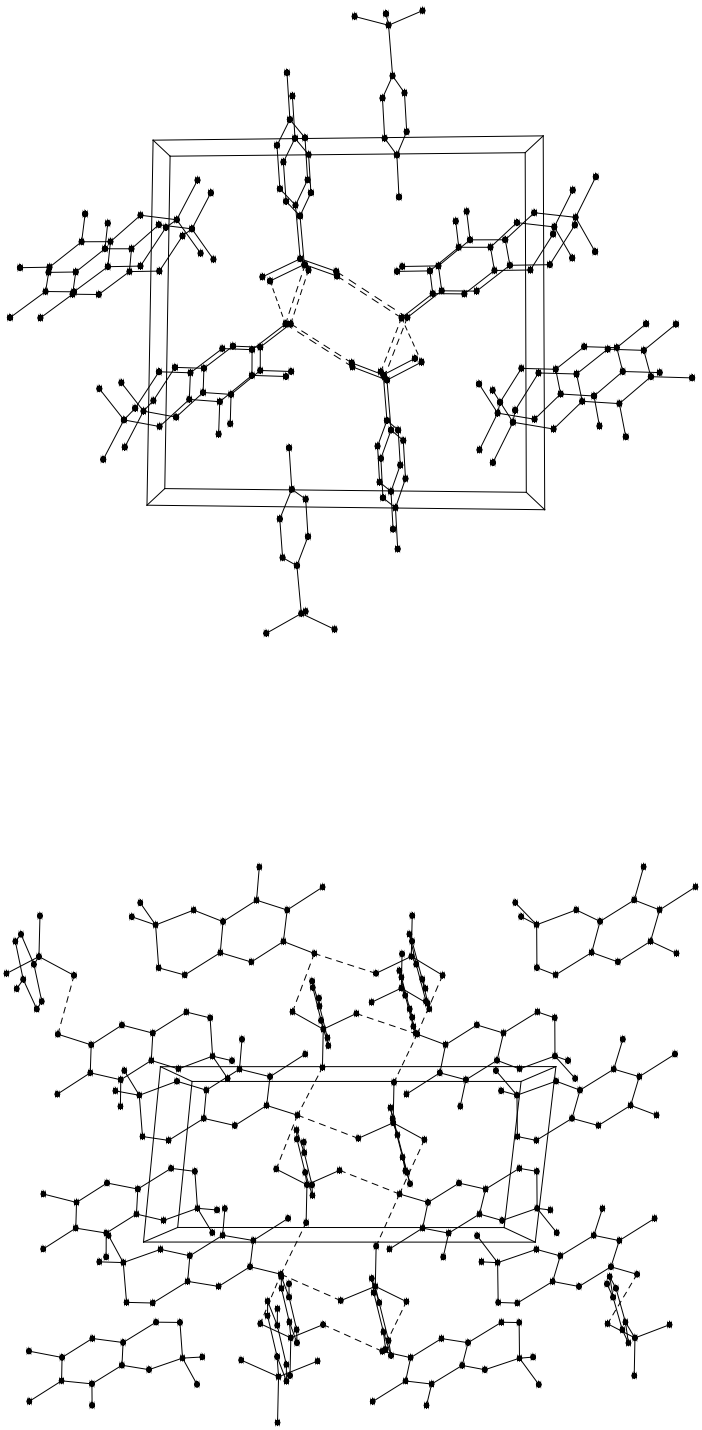

Table 1. Crystal data and structure refinement for 2,2,7,8-tetramethyl-chroman-6-ylamine, 4-methylbenzenesulfonate.

Identification code	1427
Empirical formula	C20 H27 N O4 S
Formula weight	377.49
Temperature	100(2) K
Wavelength	0.71073 A
Crystal system, space group	Triclinic, P-1
Unit cell dimensions	a = 5.9954(9) A alpha = 89.797(2) deg. b = 12.4742(18) A beta = 83.892(2) deg. c = 13.3179(19) A gamma = 84.546(2) deg.
Volume	985.9(2) A^3
Z, Calculated density	2, 1.272 Mg/m^3
Absorption coefficient	0.188 mm^-1
F(000)	404
Crystal size	0.55 x 0.40 x 0.30 mm
Diffractometer	Bruker Kappa APEX-II CCD 4-axis (sealed X-ray tube, Mo Kalfa rad., graphite monochromator CCD in 512x512 pixel mode)
Scan type / width / speed	w-scan frames / dw = 0.3ø / 10 sec. per frame full sphere data collection, 4 x 606 frames
Theta range for data collection	3.08 to 30.00 deg.
Index ranges	-8<=h<=8, -17<=k<=17, -18<=l<=18
Reflections collected / unique	10517 / 5597 [R(int) = 0.0159]
Completeness to theta = 30.00	96.9%
Absorption correction	Multi-scan (program SADABS; Sheldrick, 1996)
Max. and min. transmission	0.95 and 0.88
Structure solution	Direct methods (program SHELXS97)
Refinement method	Full-matrix least-squares on F2 (prg SHELXL97)
Data / restraints / parameters	5597 / 0 / 241
Goodness-of-fit on F2	1.045
Final R indices [I>2sigma(I)]	R1 = 0.0342, wR2 = 0.0931
R indices (all data)	R1 = 0.0375, wR2 = 0.0968
Largest diff. peak and hole	0.562 and -0.360 eA-3

$R1 = \Sigma||F_o|-|F_c||/\Sigma|F_o|$, $wR2 = [\Sigma(w(F_o^2-F_c^2)^2)/\Sigma(w(F_o^2)^2)]^{½}$

Table 2. Atomic coordinates (x 10^5) and equivalent isotropic displacement parameters (Å^2 x 10^3) for 2,2,7,8-tetramethyl-chroman-6-ylamine, 4-methylbenzenesulfonate. U_{eq} is defined as one third of the trace of the *ortho*gonalized U_{ij} tensor.

	x	y	z	U_{eq}
O(1)	6473(13)	21059(6)	97382(5)	22(1)
N(1)	25281(14)	49117(6)	65453(6)	16(1)
C(1)	14646(19)	22590(9)	107149(7)	22(1)
C(2)	39101(18)	25254(9)	105536(8)	21(1)
C(3)	41240(18)	35536(9)	99408(8)	21(1)
C(4)	27849(16)	35462(8)	90415(7)	16(1)
C(5)	31979(16)	42241(8)	82199(7)	16(1)
C(6)	19583(16)	42037(7)	74010(7)	15(1)
C(7)	2558(16)	35189(7)	73573(7)	15(1)
C(8)	-1300(16)	28097(8)	81636(7)	16(1)
C(9)	11205(16)	28392(8)	89968(7)	16(1)
C(10)	12820(20)	11755(11)	112270(9)	35(1)
C(11)	-760(20)	31457(11)	112813(9)	30(1)
C(12)	-11068(17)	35107(8)	64685(7)	19(1)
C(13)	-18022(18)	19861(8)	81283(8)	21(1)
S(1)	30591(4)	33580(2)	38890(2)	15(1)
O(2)	39987(13)	37095(6)	47868(6)	21(1)
O(3)	40829(13)	38476(6)	29734(5)	20(1)
O(4)	6036(12)	34862(6)	39825(6)	21(1)
C(14)	38292(16)	19595(7)	37683(7)	15(1)
C(15)	60441(17)	16006(8)	34165(8)	20(1)
C(16)	66761(17)	5012(8)	33444(8)	21(1)
C(17)	51412(17)	-2502(8)	36295(7)	18(1)
C(18)	29353(17)	1281(8)	39793(7)	18(1)
C(19)	22657(16)	12287(8)	40466(7)	17(1)
C(20)	58881(19)	-14359(8)	35578(8)	24(1)

Table 3. Hydrogen coordinates (x 10^4) and isotropic displacement parameters (Å^2 x 10^3) for 2,2,7,8-tetramethyl-chroman-6-ylamine, 4-methylbenzenesulfonate.

	x	y	z	U_{eq}
H(1A)	1304	5374	6447	24
H(1B)	2951	4506	5978	24
H(1C)	3683	5293	6681	24
H(2A)	4475	2617	11217	26
H(2B)	4849	1920	10195	26
H(3A)	3566	4187	10374	25
H(3B)	5730	3614	9705	25
H(5)	4338	4703	8222	20
H(10A)	2295	623	10844	53
H(10B)	-272	987	11252	53
H(10C)	1706	1218	11915	53
H(11A)	-1608	2925	11394	45
H(11B)	-88	3807	10882	45
H(11C)	473	3277	11933	45
H(12A)	-647	2854	6068	28
H(12B)	-847	4142	6047	28
H(12C)	-2711	3531	6712	28
H(13A)	-1707	1503	8707	31
H(13B)	-1460	1567	7501	31
H(13C)	-3328	2353	8154	31
H(15)	7110	2102	3228	24
H(16)	8181	254	3096	25
H(18)	1871	-372	4175	22
H(19)	753	1478	4281	20
H(20A)	6030	-1668	2850	35
H(20B)	4772	-1837	3952	35
H(20C)	7349	-1576	3825	35

Hydrogen atoms inserted in idealized positions and refined riding with the atoms to which they were bonded. All H atoms had $U_{iso} = U_{eq}$ x 1.2 (x 1.5 for CH_3) of their carrier atoms.

Table 4. Anisotropic displacement parameters ($Å^2$ x 10^3) for 2,2,7,8-tetramethyl-chroman-6-ylamine, 4-methylbenzenesulfonate. The anisotropic displacement factor exponent takes the form: $-2\pi^2 [h^2 a^{*2} U_{11} + ... + 2 h k a^* b^* U_{12}]$

	U_{11}	U_{22}	U_{33}	U_{23}	U_{13}	U_{12}
O(1)	29(1)	24(1)	13(1)	5(1)	-5(1)	-12(1)
N(1)	18(1)	15(1)	15(1)	2(1)	-2(1)	-2(1)
C(1)	25(1)	29(1)	13(1)	4(1)	-4(1)	-8(1)
C(2)	22(1)	27(1)	16(1)	5(1)	-4(1)	-4(1)
C(3)	22(1)	24(1)	17(1)	3(1)	-5(1)	-7(1)
C(4)	18(1)	17(1)	14(1)	0(1)	-3(1)	-3(1)
C(5)	17(1)	16(1)	16(1)	0(1)	-2(1)	-3(1)
C(6)	17(1)	14(1)	14(1)	1(1)	-1(1)	-1(1)
C(7)	16(1)	15(1)	14(1)	-1(1)	-2(1)	-1(1)
C(8)	17(1)	17(1)	14(1)	-1(1)	-1(1)	-3(1)
C(9)	19(1)	17(1)	13(1)	1(1)	-1(1)	-3(1)
C(10)	46(1)	41(1)	24(1)	15(1)	-10(1)	-20(1)
C(11)	23(1)	48(1)	19(1)	-6(1)	-1(1)	-6(1)
C(12)	20(1)	21(1)	17(1)	1(1)	-5(1)	-3(1)
C(13)	23(1)	23(1)	18(1)	1(1)	-3(1)	-9(1)
S(1)	17(1)	14(1)	15(1)	1(1)	-2(1)	-2(1)
O(2)	26(1)	19(1)	18(1)	-3(1)	-5(1)	-2(1)
O(3)	24(1)	19(1)	17(1)	4(1)	-2(1)	-6(1)
O(4)	17(1)	19(1)	26(1)	3(1)	-2(1)	1(1)
C(14)	16(1)	15(1)	14(1)	1(1)	-2(1)	-1(1)
C(15)	16(1)	19(1)	23(1)	2(1)	1(1)	-3(1)
C(16)	17(1)	21(1)	23(1)	0(1)	0(1)	1(1)
C(17)	22(1)	16(1)	16(1)	-1(1)	-5(1)	0(1)
C(18)	20(1)	18(1)	18(1)	0(1)	-3(1)	-5(1)
C(19)	16(1)	18(1)	17(1)	0(1)	-1(1)	-2(1)
C(20)	29(1)	17(1)	26(1)	-2(1)	-9(1)	2(1)

Table 5. Bond lengths [Å] and angles [deg] for 2,2,7,8-tetramethyl-chroman-6-ylamine, 4-methylbenzenesulfonate.

Bond distances	
O(1)-C(9)	1.3695(11)
O(1)-C(1)	1.4574(12)
N(1)-C(6)	1.4707(11)
N(1)-H(1A)	0.91
N(1)-H(1B)	0.91
N(1)-H(1C)	0.91
C(1)-C(11)	1.5196(17)
C(1)-C(10)	1.5197(16)
C(1)-C(2)	1.5269(15)
C(2)-C(3)	1.5262(14)
C(2)-H(2A)	0.99
C(2)-H(2B)	0.99
C(3)-C(4)	1.5116(13)
C(3)-H(3A)	0.99
C(3)-H(3B)	0.99
C(4)-C(5)	1.3962(12)
C(4)-C(9)	1.3991(13)
C(5)-C(6)	1.3851(13)
C(5)-H(5)	0.95
C(6)-C(7)	1.3977(13)
C(7)-C(8)	1.4030(12)
C(7)-C(12)	1.5087(13)
C(8)-C(9)	1.4062(13)
C(8)-C(13)	1.5063(13)
C(10)-H(10A)	0.98
C(10)-H(10B)	0.98
C(10)-H(10C)	0.98
C(11)-H(11A)	0.98
C(11)-H(11B)	0.98
C(11)-H(11C)	0.98
C(12)-H(12A)	0.98
C(12)-H(12B)	0.98
C(12)-H(12C)	0.98
C(13)-H(13A)	0.98
C(13)-H(13B)	0.98
C(13)-H(13C)	0.98
S(1)-O(4)	1.4577(8)
S(1)-O(2)	1.4607(8)
S(1)-O(3)	1.4640(7)
S(1)-C(14)	1.7651(10)
C(14)-C(19)	1.3904(13)
C(14)-C(15)	1.3926(13)
C(15)-C(16)	1.3885(14)
C(15)-H(15)	0.95
C(16)-C(17)	1.3988(14)
C(16)-H(16)	0.95
C(17)-C(18)	1.3930(14)
C(17)-C(20)	1.5044(14)
C(18)-C(19)	1.3938(14)
C(18)-H(18)	0.95
C(19)-H(19)	0.95
C(20)-H(20A)	0.98
C(20)-H(20B)	0.98
C(20)-H(20C)	0.98

Bond angles	
C(9)-O(1)-C(1)	117.83(8)
C(6)-N(1)-H(1A)	109.5
C(6)-N(1)-H(1B)	109.5
H(1A)-N(1)-H(1B)	109.5
C(6)-N(1)-H(1C)	109.5
H(1A)-N(1)-H(1C)	109.5
H(1B)-N(1)-H(1C)	109.5
O(1)-C(1)-C(11)	108.19(9)
O(1)-C(1)-C(10)	103.71(9)
C(11)-C(1)-C(10)	111.57(10)
O(1)-C(1)-C(2)	109.36(8)
C(11)-C(1)-C(2)	112.43(10)
C(10)-C(1)-C(2)	111.15(10)
C(3)-C(2)-C(1)	111.14(9)
C(3)-C(2)-H(2A)	109.4
C(1)-C(2)-H(2A)	109.4
C(3)-C(2)-H(2B)	109.4
C(1)-C(2)-H(2B)	109.4
H(2A)-C(2)-H(2B)	108.0
C(4)-C(3)-C(2)	110.62(8)
C(4)-C(3)-H(3A)	109.5
C(2)-C(3)-H(3A)	109.5
C(4)-C(3)-H(3B)	109.5
C(2)-C(3)-H(3B)	109.5
H(3A)-C(3)-H(3B)	108.1
C(5)-C(4)-C(9)	117.79(9)
C(5)-C(4)-C(3)	121.33(9)
C(9)-C(4)-C(3)	120.86(8)
C(6)-C(5)-C(4)	120.52(9)
C(6)-C(5)-H(5)	119.7
C(4)-C(5)-H(5)	119.7
C(5)-C(6)-C(7)	122.25(8)
C(5)-C(6)-N(1)	117.81(8)
C(7)-C(6)-N(1)	119.92(8)
C(6)-C(7)-C(8)	117.83(9)
C(6)-C(7)-C(12)	121.96(8)
C(8)-C(7)-C(12)	120.19(8)
C(7)-C(8)-C(9)	119.67(9)
C(7)-C(8)-C(13)	120.73(9)
C(9)-C(8)-C(13)	119.55(8)
O(1)-C(9)-C(4)	122.71(9)
O(1)-C(9)-C(8)	115.37(8)
C(4)-C(9)-C(8)	121.88(8)
C(1)-C(10)-H(10A)	109.5
C(1)-C(10)-H(10B)	109.5
H(10A)-C(10)-H(10B)	109.5
C(1)-C(10)-H(10C)	109.5
H(10A)-C(10)-H(10C)	109.5
H(10B)-C(10)-H(10C)	109.5
C(1)-C(11)-H(11A)	109.5

C(1)-C(11)-H(11B)	109.5	C9-O1-C1-C11	77.58(11)
H(11A)-C(11)-H(11B)	109.5	C9-O1-C1-C10	-163.83(10)
C(1)-C(11)-H(11C)	109.5	C9-O1-C1-C2	-45.18(12)
H(11A)-C(11)-H(11C)	109.5	O1-C1-C2-C3	60.05(12)
H(11B)-C(11)-H(11C)	109.5	C11-C1-C2-C3	-60.15(12)
C(7)-C(12)-H(12A)	109.5	C10-C1-C2-C3	173.96(9)
C(7)-C(12)-H(12B)	109.5	C1-C2-C3-C4	-45.49(12)
H(12A)-C(12)-H(12B)	109.5	C2-C3-C4-C5	-161.54(9)
C(7)-C(12)-H(12C)	109.5	C2-C3-C4-C9	16.99(14)
H(12A)-C(12)-H(12C)	109.5	C9-C4-C5-C6	1.23(14)
H(12B)-C(12)-H(12C)	109.5	C3-C4-C5-C6	179.80(9)
C(8)-C(13)-H(13A)	109.5	C4-C5-C6-C7	0.23(15)
C(8)-C(13)-H(13B)	109.5	C4-C5-C6-N1	-177.99(8)
H(13A)-C(13)-H(13B)	109.5	C5-C6-C7-C8	-2.16(14)
C(8)-C(13)-H(13C)	109.5	N1-C6-C7-C8	176.02(8)
H(13A)-C(13)-H(13C)	109.5	C5-C6-C7-C12	179.24(9)
H(13B)-C(13)-H(13C)	109.5	N1-C6-C7-C12	-2.58(14)
O(4)-S(1)-O(2)	113.30(5)	C6-C7-C8-C9	2.60(14)
O(4)-S(1)-O(3)	113.04(4)	C12-C7-C8-C9	-178.78(9)
O(2)-S(1)-O(3)	111.40(5)	C6-C7-C8-C13	-174.90(9)
O(4)-S(1)-C(14)	105.72(4)	C12-C7-C8-C13	3.73(14)
O(2)-S(1)-C(14)	106.44(4)	C1-O1-C9-C4	16.60(14)
O(3)-S(1)-C(14)	106.28(4)	C1-O1-C9-C8	-165.56(9)
C(19)-C(14)-C(15)	120.60(9)	C5-C4-C9-O1	176.96(9)
C(19)-C(14)-S(1)	120.51(7)	C3-C4-C9-O1	-1.62(15)
C(15)-C(14)-S(1)	118.87(7)	C5-C4-C9-C8	-0.73(15)
C(16)-C(15)-C(14)	119.18(9)	C3-C4-C9-C8	-179.32(9)
C(16)-C(15)-H(15)	120.4	C7-C8-C9-O1	-179.07(9)
C(14)-C(15)-H(15)	120.4	C13-C8-C9-O1	-1.54(13)
C(15)-C(16)-C(17)	121.32(9)	C7-C8-C9-C4	-1.21(15)
C(15)-C(16)-H(16)	119.3	C13-C8-C9-C4	176.32(9)
C(17)-C(16)-H(16)	119.3	O4-S1-C14-C19	-17.64(9)
C(18)-C(17)-C(16)	118.44(9)	O2-S1-C14-C19	103.13(8)
C(18)-C(17)-C(20)	121.52(9)	O3-S1-C14-C19	-138.02(8)
C(16)-C(17)-C(20)	120.04(9)	O4-S1-C14-C15	164.13(8)
C(17)-C(18)-C(19)	121.00(9)	O2-S1-C14-C15	-75.11(9)
C(17)-C(18)-H(18)	119.5	O3-S1-C14-C15	43.75(9)
C(19)-C(18)-H(18)	119.5	C19-C14-C15-C16	0.12(15)
C(14)-C(19)-C(18)	119.45(9)	S1-C14-C15-C16	178.35(8)
C(14)-C(19)-H(19)	120.3	C14-C15-C16-C17	-0.80(16)
C(18)-C(19)-H(19)	120.3	C15-C16-C17-C18	0.79(15)
C(17)-C(20)-H(20A)	109.5	C15-C16-C17-C20	-179.03(10)
C(17)-C(20)-H(20B)	109.5	C16-C17-C18-C19	-0.11(15)
H(20A)-C(20)-H(20B)	109.5	C20-C17-C18-C19	179.71(9)
C(17)-C(20)-H(20C)	109.5	C15-C14-C19-C18	0.54(14)
H(20A)-C(20)-H(20C)	109.5	S1-C14-C19-C18	-177.66(7)
H(20B)-C(20)-H(20C)	109.5	C17-C18-C19-C14	-0.55(15

Torsion angles

Hydrogen-bonds for 1427 [A and deg.].

D-H...A	d(D-H)	d(H...A)	d(D...A)	<(DHA)
N(1)-H(1A)...O(4)#1	0.91	1.87	2.7515(11)	163.9
N(1)-H(1B)...O(2)	0.91	1.89	2.8009(11)	176.3
N(1)-H(1C)...O(3)#2	0.91	1.89	2.7958(11)	175.6

Symmetry transformations used to generate equivalent atoms:
#1 -x,-y+1,-z+1 #2 -x+1,-y+1,-z+1

5-Benzhydryl-2,2,7,8-tetramethylchroman-6-ol

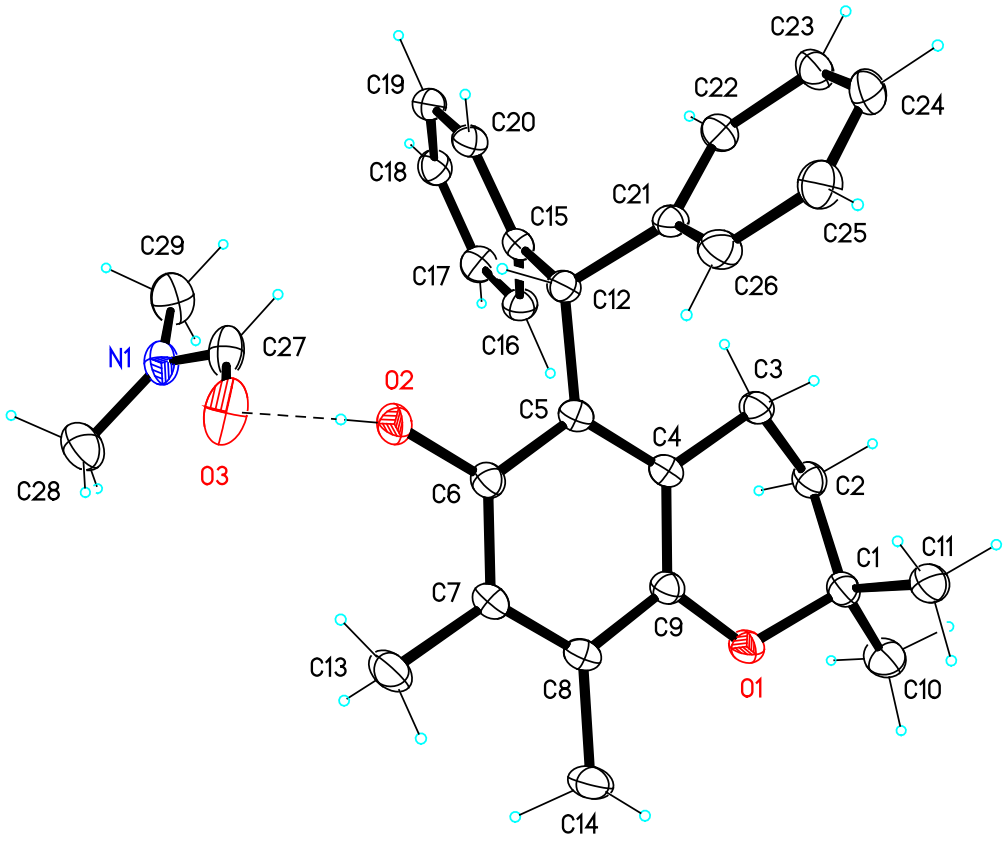

The solvate is stable in air but dissolves readily in ethanol, yielding a different crystal structure. The chromanol has the usual geometry, the OH has a hydrogen bond to DMF.

Fig. 1. Thermal ellipsoid plots (50% ellipsoids) of 5-benzhydryl-2,2,7,8-tetramethylchroman-6-ol.

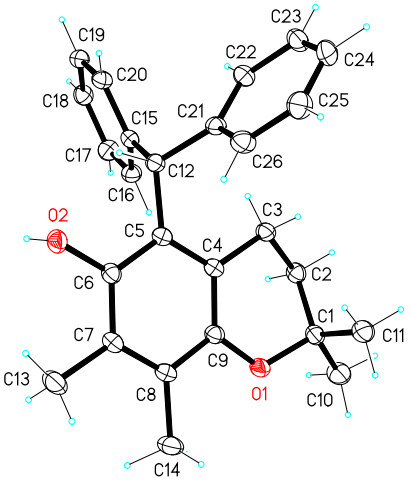

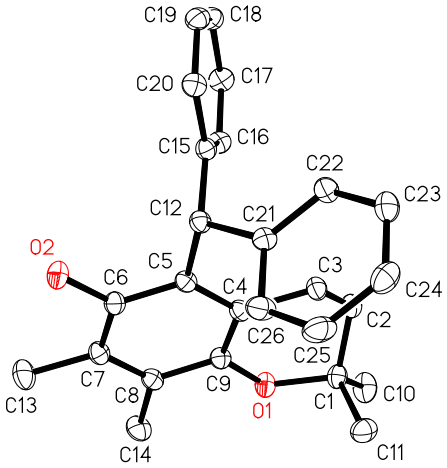

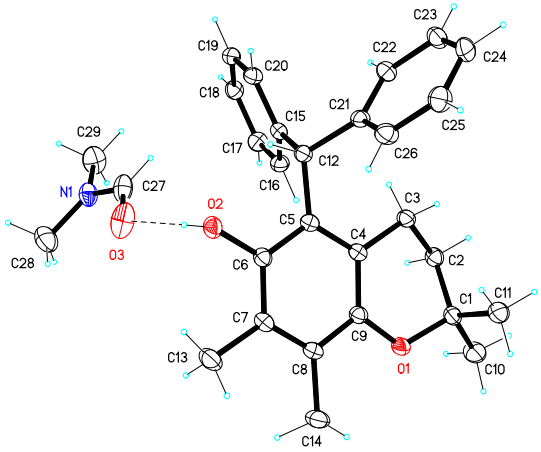

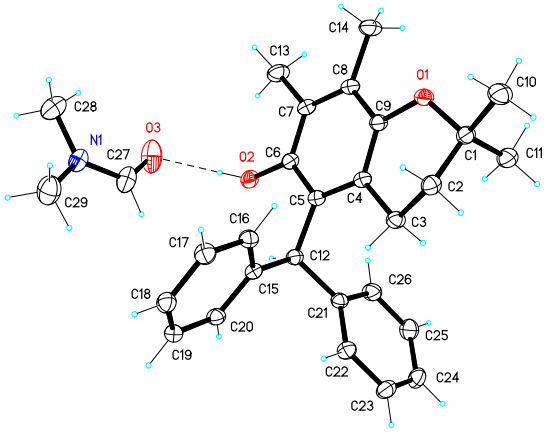

Fig. 2. Asymmetric unit of 5-benzhydryl-2,2,7,8-tetramethylchroman-6-ol.

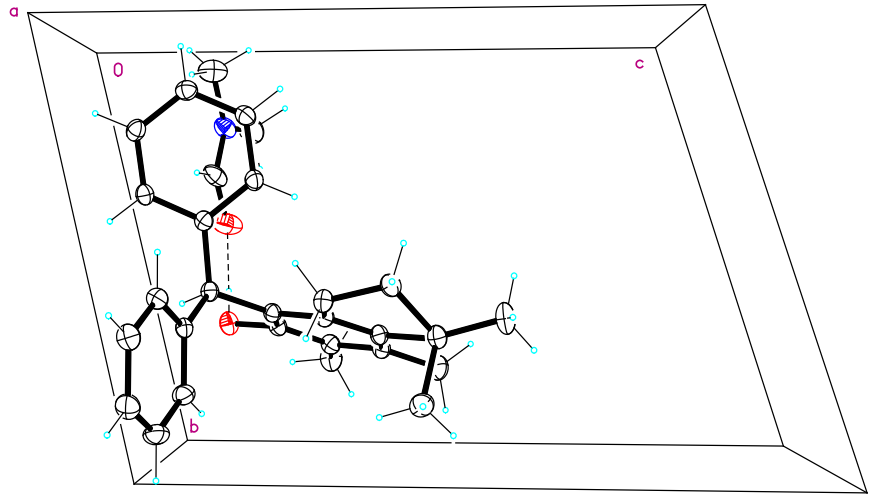

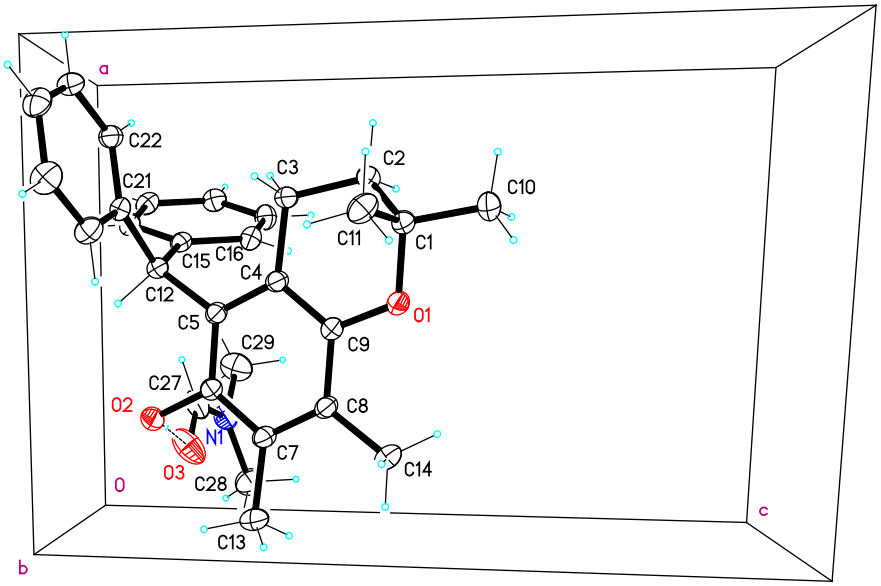

Fig. 3. Packing diagrams of 5-benzhydryl-2,2,7,8-tetramethylchroman-6-ol.

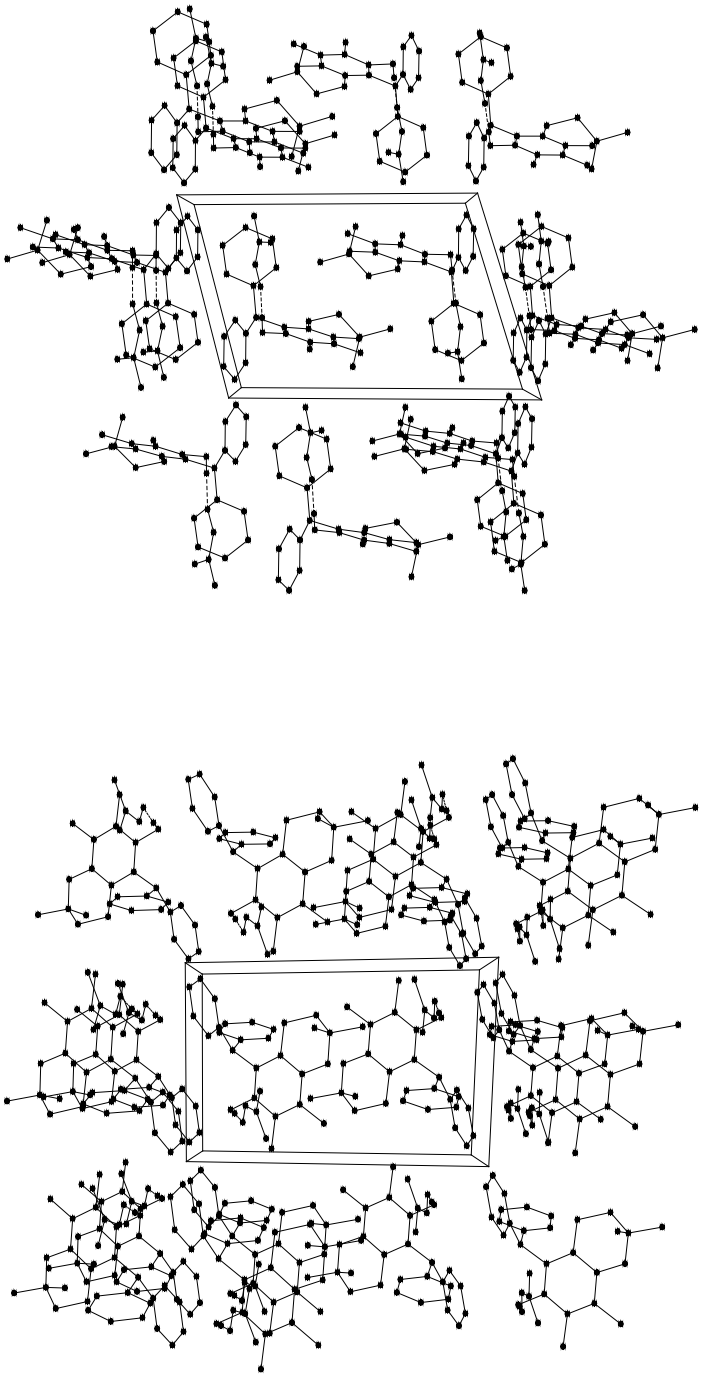

Table 1. Crystal data and structure refinement for 5-benzhydryl-2,2,7,8-tetramethylchroman-6-ol.

Identification code	1325fr
Empirical formula	C29 H35 N O3
Formula weight	445.58
Temperature	100(2) K
Wavelength	0.71073 Å
Crystal system, space group	Triclinic, P-1
Unit cell dimensions	a = 9.3872(12) A alpha = 73.183(3) deg. b = 10.1989(13) A beta = 83.963(3) deg. c = 14.0812(16) A gamma = 72.555(3) deg.
Volume	1230.9(3) A^3
Z, Calculated density	2, 1.202 Mg/m^3
Absorption coefficient	0.077 mm^-1
F(000)	480
Crystal size	0.58 x 0.35 x 0.20 mm, colorless block
Diffractometer	Bruker SMART APEX CCD platform type 3-circle (sealed X-ray tube, Mo Kα radiation, graphite monochr., CCD at 50 mm in 512x512 pixel mode)
Scan type / width / speed	ω-scan frames / Δω = 0.3° / 20 sec. per frame hemisphere data collection
Theta range for data collection	2.67 to 30.01 deg.
Index ranges	-13<=h<=12, -14<=k<=14, -16<=l<=19
Reflections collected / unique	9528 / 6909 [R(int) = 0.0123]
Completeness to theta = 30.01	96.1%
Absorption correction	Multi-scan (program SADABS; Sheldrick, 1996)
Max. and min. transmission	0.98 and 0.86
Structure solution	Direct methods (program SHELXS97)
Refinement method	Full-matrix least-squares on F2 (prg SHELXL97)
Data / restraints / parameters	6909 / 85 / 305
Goodness-of-fit on F2	1.078
Final R indices [I>2sigma(I)]	R1 = 0.0424, wR2 = 0.1195
R indices (all data)	R1 = 0.0516, wR2 = 0.1256
Largest diff. peak and hole	0.372 and -0.349 eA-3

$R1 = \Sigma||F_o|-|F_c||/\Sigma|F_o|$, $wR2 = [\Sigma(w(F_o^2-F_c^2)^2)/\Sigma(w(F_o^2)^2)]^{½}$

Table 2. Atomic coordinates (x 10^5) and equivalent isotropic displacement parameters (Å^2 x 10^3) for 5-benzhydryl-2,2,7,8-tetramethylchroman-6-ol. U_{eq} is defined as one third of the trace of the *ortho*gonalized U_{ij} tensor.

	x	y	z	U_{eq}
O(1)	49892(8)	72506(8)	47326(5)	21(1)
O(2)	25937(8)	70027(8)	13889(5)	22(1)
C(1)	65623(11)	71420(11)	47806(7)	20(1)
C(2)	74900(11)	59900(11)	43015(7)	20(1)
C(3)	71019(10)	63467(11)	32151(7)	19(1)
C(4)	54231(10)	67539(10)	31075(7)	17(1)
C(5)	47797(10)	66806(10)	22720(7)	17(1)
C(6)	32266(10)	70427(10)	22213(7)	18(1)
C(7)	22868(10)	75070(10)	29722(7)	19(1)
C(8)	29147(10)	75744(10)	38068(7)	18(1)
C(9)	44785(10)	71879(10)	38661(7)	18(1)
C(10)	68696(13)	67196(14)	58799(8)	30(1)
C(11)	67809(13)	86064(12)	42721(8)	26(1)
C(12)	57019(10)	61714(10)	14200(7)	17(1)
C(13)	6148(12)	79211(13)	28567(9)	28(1)
C(14)	19625(12)	80693(13)	46394(8)	26(1)
C(15)	62712(10)	45504(10)	16376(7)	17(1)
C(16)	63637(11)	36201(11)	25939(7)	20(1)
C(17)	68628(12)	21453(11)	27395(8)	22(1)
C(18)	72709(11)	15714(11)	19360(8)	21(1)
C(19)	71739(11)	24854(11)	9807(8)	21(1)
C(20)	66715(11)	39522(11)	8376(7)	19(1)
C(21)	68836(10)	69571(10)	9763(7)	17(1)
C(22)	83685(11)	62743(11)	7990(7)	20(1)
C(23)	93556(11)	70598(12)	3350(8)	24(1)
C(24)	88776(13)	85345(12)	407(8)	26(1)
C(25)	73981(13)	92322(12)	2167(9)	28(1)
C(26)	64155(12)	84463(11)	6845(8)	23(1)
O(3)	18459(11)	45808(9)	17244(8)	40(1)
N(1)	23598(10)	21742(10)	21305(7)	25(1)
C(27)	27153(14)	33962(12)	17753(8)	28(1)
C(28)	8635(14)	21575(15)	24994(10)	36(1)
C(29)	34706(15)	8108(13)	22220(11)	37(1)

Table 3. Hydrogen coordinates (x 10^4) and isotropic displacement parameters (Å^2 x 10^3) for 5-benzhydryl-2,2,7,8-tetramethylchroman-6-ol.

	x	y	z	U_{eq}
H(2)	2382	6227	1502	33
H(2A)	7309	5064	4665	24
H(2B)	8563	5892	4350	24
H(3A)	7487	7149	2822	23
H(3B)	7582	5510	2956	23
H(10A)	6695	5788	6196	44
H(10B)	6202	7437	6183	44
H(10C)	7910	6661	5971	44
H(11A)	6166	9302	4613	39
H(11B)	6482	8900	3578	39
H(11C)	7835	8560	4298	39
H(12)	4971	6465	877	20
H(13A)	392	8031	2169	42
H(13B)	155	8826	3025	42
H(13C)	213	7175	3302	42
H(14A)	955	7986	4614	39
H(14B)	1908	9068	4567	39
H(14C)	2407	7476	5277	39
H(16)	6083	3998	3151	24
H(17)	6924	1528	3394	26
H(18)	7613	566	2037	26
H(19)	7452	2104	426	25
H(20)	6598	4564	181	23
H(22)	8714	5261	997	24
H(23)	10366	6577	220	28
H(24)	9553	9066	-279	32
H(25)	7058	10246	17	33
H(26)	5409	8932	807	28
H(27)	3713	3348	1545	34
H(28A)	904	1592	3195	54
H(28B)	429	1732	2103	54
H(28C)	245	3137	2450	54
H(29A)	3123	241	1893	55
H(29B)	3630	303	2926	55
H(29C)	4411	966	1909	55

Hydrogen atoms inserted in idealized positions and refined riding with the atoms to which they were bonded. All H atoms had $U_{iso} = U_{eq}$ x 1.2 (x 1.5 for CH_3) of their carrier atoms.

Table 4. Anisotropic displacement parameters ($Å^2$ x 10^3) for 5-benzhydryl-2,2,7,8-tetramethylchroman-6-ol.
The anisotropic displacement factor exponent takes the form: $-2\pi^2 [h^2 a^{*2} U_{11} + ... + 2 h k a^* b^* U_{12}]$

	U_{11}	U_{22}	U_{33}	U_{23}	U_{13}	U_{12}
O(1)	18(1)	31(1)	17(1)	-9(1)	2(1)	-9(1)
O(2)	19(1)	29(1)	19(1)	-6(1)	-2(1)	-9(1)
C(1)	18(1)	25(1)	17(1)	-5(1)	0(1)	-9(1)
C(2)	18(1)	23(1)	19(1)	-4(1)	-2(1)	-6(1)
C(3)	15(1)	24(1)	18(1)	-7(1)	0(1)	-5(1)
C(4)	15(1)	18(1)	18(1)	-5(1)	2(1)	-5(1)
C(5)	16(1)	17(1)	16(1)	-4(1)	2(1)	-5(1)
C(6)	17(1)	19(1)	17(1)	-4(1)	0(1)	-6(1)
C(7)	16(1)	21(1)	20(1)	-4(1)	2(1)	-6(1)
C(8)	16(1)	20(1)	18(1)	-5(1)	3(1)	-5(1)
C(9)	17(1)	20(1)	16(1)	-5(1)	1(1)	-6(1)
C(10)	27(1)	45(1)	18(1)	-8(1)	-1(1)	-13(1)
C(11)	28(1)	25(1)	29(1)	-10(1)	7(1)	-12(1)
C(12)	15(1)	19(1)	16(1)	-5(1)	1(1)	-5(1)
C(13)	16(1)	39(1)	28(1)	-10(1)	2(1)	-7(1)
C(14)	21(1)	32(1)	23(1)	-10(1)	6(1)	-6(1)
C(15)	15(1)	19(1)	18(1)	-5(1)	2(1)	-6(1)
C(16)	22(1)	21(1)	17(1)	-5(1)	2(1)	-8(1)
C(17)	26(1)	20(1)	19(1)	-2(1)	-1(1)	-7(1)
C(18)	22(1)	19(1)	24(1)	-5(1)	1(1)	-7(1)
C(19)	21(1)	23(1)	21(1)	-9(1)	4(1)	-9(1)
C(20)	19(1)	21(1)	17(1)	-4(1)	3(1)	-7(1)
C(21)	18(1)	18(1)	14(1)	-5(1)	2(1)	-6(1)
C(22)	18(1)	20(1)	21(1)	-4(1)	0(1)	-5(1)
C(23)	18(1)	29(1)	25(1)	-7(1)	2(1)	-9(1)
C(24)	29(1)	28(1)	27(1)	-7(1)	3(1)	-17(1)
C(25)	34(1)	19(1)	33(1)	-8(1)	4(1)	-11(1)
C(26)	24(1)	19(1)	27(1)	-7(1)	4(1)	-5(1)
O(3)	49(1)	25(1)	46(1)	-1(1)	-23(1)	-11(1)
N(1)	26(1)	25(1)	25(1)	-2(1)	-4(1)	-12(1)
C(27)	34(1)	27(1)	25(1)	2(1)	-11(1)	-15(1)
C(28)	30(1)	42(1)	37(1)	-6(1)	3(1)	-17(1)
C(29)	35(1)	27(1)	47(1)	-7(1)	-6(1)	-8(1)

Table 5. Bond lengths [Å] and angles [deg] for 5-benzhydryl-2,2,7,8-tetramethylchroman-6-ol.

Bond distances

O(1)-C(9)	1.3818(11)
O(1)-C(1)	1.4546(12)
O(2)-C(6)	1.3846(12)
O(2)-H(2)	0.84
C(1)-C(10)	1.5161(14)
C(1)-C(2)	1.5217(15)
C(1)-C(11)	1.5230(14)
C(2)-C(3)	1.5235(13)
C(2)-H(2A)	0.99
C(2)-H(2B)	0.99
C(3)-C(4)	1.5167(13)
C(3)-H(3A)	0.99
C(3)-H(3B)	0.99
C(4)-C(9)	1.4008(13)
C(4)-C(5)	1.4077(13)
C(5)-C(6)	1.3968(13)
C(5)-C(12)	1.5267(13)
C(6)-C(7)	1.4013(14)
C(7)-C(8)	1.3965(14)
C(7)-C(13)	1.5116(14)
C(8)-C(9)	1.4061(13)
C(8)-C(14)	1.5098(14)
C(10)-H(10A)	0.98
C(10)-H(10B)	0.98
C(10)-H(10C)	0.98
C(11)-H(11A)	0.98
C(11)-H(11B)	0.98
C(11)-H(11C)	0.98
C(12)-C(15)	1.5246(13)
C(12)-C(21)	1.5363(13)
C(12)-H(12)	1.00
C(13)-H(13A)	0.98
C(13)-H(13B)	0.98
C(13)-H(13C)	0.98
C(14)-H(14A)	0.98
C(14)-H(14B)	0.98
C(14)-H(14C)	0.98
C(15)-C(20)	1.3977(14)
C(15)-C(16)	1.3989(13)
C(16)-C(17)	1.3939(14)
C(16)-H(16)	0.95
C(17)-C(18)	1.3881(15)
C(17)-H(17)	0.95
C(18)-C(19)	1.3915(14)
C(18)-H(18)	0.95
C(19)-C(20)	1.3869(14)
C(19)-H(19)	0.95
C(20)-H(20)	0.95
C(21)-C(22)	1.3912(13)
C(21)-C(26)	1.3949(14)
C(22)-C(23)	1.3937(14)
C(22)-H(22)	0.95
C(23)-C(24)	1.3817(16)
C(23)-H(23)	0.95
C(24)-C(25)	1.3906(16)
C(24)-H(24)	0.95
C(25)-C(26)	1.3918(15)
C(25)-H(25)	0.95
C(26)-H(26)	0.95
O(3)-C(27)	1.2254(15)
N(1)-C(27)	1.3298(13)
N(1)-C(29)	1.4466(16)
N(1)-C(28)	1.4488(15)
C(27)-H(27)	0.95
C(28)-H(28A)	0.98
C(28)-H(28B)	0.98
C(28)-H(28C)	0.98
C(29)-H(29A)	0.98
C(29)-H(29B)	0.98
C(29)-H(29C)	0.98

Bond angles

C(9)-O(1)-C(1)	118.23(7)
C(6)-O(2)-H(2)	109.5
O(1)-C(1)-C(10)	104.78(8)
O(1)-C(1)-C(2)	109.03(8)
C(10)-C(1)-C(2)	110.87(9)
O(1)-C(1)-C(11)	108.04(8)
C(10)-C(1)-C(11)	110.80(9)
C(2)-C(1)-C(11)	112.95(8)
C(1)-C(2)-C(3)	111.38(8)
C(1)-C(2)-H(2A)	109.4
C(3)-C(2)-H(2A)	109.4
C(1)-C(2)-H(2B)	109.4
C(3)-C(2)-H(2B)	109.4
H(2A)-C(2)-H(2B)	108.0
C(4)-C(3)-C(2)	110.24(8)
C(4)-C(3)-H(3A)	109.6
C(2)-C(3)-H(3A)	109.6
C(4)-C(3)-H(3B)	109.6
C(2)-C(3)-H(3B)	109.6
H(3A)-C(3)-H(3B)	108.1
C(9)-C(4)-C(5)	118.68(8)
C(9)-C(4)-C(3)	119.49(8)
C(5)-C(4)-C(3)	121.82(8)
C(6)-C(5)-C(4)	119.34(9)
C(6)-C(5)-C(12)	117.52(8)
C(4)-C(5)-C(12)	123.10(8)
O(2)-C(6)-C(5)	119.31(8)
O(2)-C(6)-C(7)	118.93(8)
C(5)-C(6)-C(7)	121.70(9)
C(8)-C(7)-C(6)	119.36(9)
C(8)-C(7)-C(13)	121.68(9)
C(6)-C(7)-C(13)	118.96(9)
C(7)-C(8)-C(9)	118.97(9)
C(7)-C(8)-C(14)	121.88(9)

C(9)-C(8)-C(14)	119.15(9)
O(1)-C(9)-C(4)	123.54(8)
O(1)-C(9)-C(8)	114.53(8)
C(4)-C(9)-C(8)	121.92(9)
C(1)-C(10)-H(10A)	109.5
C(1)-C(10)-H(10B)	109.5
H(10A)-C(10)-H(10B)	109.5
C(1)-C(10)-H(10C)	109.5
H(10A)-C(10)-H(10C)	109.5
H(10B)-C(10)-H(10C)	109.5
C(1)-C(11)-H(11A)	109.5
C(1)-C(11)-H(11B)	109.5
H(11A)-C(11)-H(11B)	109.5
C(1)-C(11)-H(11C)	109.5
H(11A)-C(11)-H(11C)	109.5
H(11B)-C(11)-H(11C)	109.5
C(15)-C(12)-C(5)	113.54(8)
C(15)-C(12)-C(21)	114.58(8)
C(5)-C(12)-C(21)	113.84(8)
C(15)-C(12)-H(12)	104.5
C(5)-C(12)-H(12)	104.5
C(21)-C(12)-H(12)	104.5
C(7)-C(13)-H(13A)	109.5
C(7)-C(13)-H(13B)	109.5
H(13A)-C(13)-H(13B)	109.5
C(7)-C(13)-H(13C)	109.5
H(13A)-C(13)-H(13C)	109.5
H(13B)-C(13)-H(13C)	109.5
C(8)-C(14)-H(14A)	109.5
C(8)-C(14)-H(14B)	109.5
H(14A)-C(14)-H(14B)	109.5
C(8)-C(14)-H(14C)	109.5
H(14A)-C(14)-H(14C)	109.5
H(14B)-C(14)-H(14C)	109.5
C(20)-C(15)-C(16)	117.86(9)
C(20)-C(15)-C(12)	118.41(8)
C(16)-C(15)-C(12)	123.69(9)
C(17)-C(16)-C(15)	120.76(9)
C(17)-C(16)-H(16)	119.6
C(15)-C(16)-H(16)	119.6
C(18)-C(17)-C(16)	120.53(9)
C(18)-C(17)-H(17)	119.7
C(16)-C(17)-H(17)	119.7
C(17)-C(18)-C(19)	119.25(9)
C(17)-C(18)-H(18)	120.4
C(19)-C(18)-H(18)	120.4
C(20)-C(19)-C(18)	120.10(9)
C(20)-C(19)-H(19)	119.9
C(18)-C(19)-H(19)	119.9
C(19)-C(20)-C(15)	121.48(9)
C(19)-C(20)-H(20)	119.3
C(15)-C(20)-H(20)	119.3
C(22)-C(21)-C(26)	118.19(9)
C(22)-C(21)-C(12)	123.98(8)
C(26)-C(21)-C(12)	117.73(8)
C(21)-C(22)-C(23)	120.77(9)
C(21)-C(22)-H(22)	119.6
C(23)-C(22)-H(22)	119.6
C(24)-C(23)-C(22)	120.60(10)
C(24)-C(23)-H(23)	119.7
C(22)-C(23)-H(23)	119.7
C(23)-C(24)-C(25)	119.29(10)
C(23)-C(24)-H(24)	120.4
C(25)-C(24)-H(24)	120.4
C(24)-C(25)-C(26)	120.04(10)
C(24)-C(25)-H(25)	120.0
C(26)-C(25)-H(25)	120.0
C(25)-C(26)-C(21)	121.11(10)
C(25)-C(26)-H(26)	119.4
C(21)-C(26)-H(26)	119.4
C(27)-N(1)-C(29)	121.38(10)
C(27)-N(1)-C(28)	121.07(11)
C(29)-N(1)-C(28)	117.43(10)
O(3)-C(27)-N(1)	124.58(12)
O(3)-C(27)-H(27)	117.7
N(1)-C(27)-H(27)	117.7
N(1)-C(28)-H(28A)	109.5
N(1)-C(28)-H(28B)	109.5
H(28A)-C(28)-H(28B)	109.5
N(1)-C(28)-H(28C)	109.5
H(28A)-C(28)-H(28C)	109.5
H(28B)-C(28)-H(28C)	109.5
N(1)-C(29)-H(29A)	109.5
N(1)-C(29)-H(29B)	109.5
H(29A)-C(29)-H(29B)	109.5
N(1)-C(29)-H(29C)	109.5
H(29A)-C(29)-H(29C)	109.5
H(29B)-C(29)-H(29C)	109.5

Torsion angles

C9-O1-C1-C10	-160.48(9)
C9-O1-C1-C2	-41.75(11)
C9-O1-C1-C11	81.35(10)
O1-C1-C2-C3	60.66(10)
C10-C1-C2-C3	175.50(8)
C11-C1-C2-C3	-59.46(11)
C1-C2-C3-C4	-49.20(11)
C2-C3-C4-C9	19.76(12)
C2-C3-C4-C5	-158.89(9)
C9-C4-C5-C6	0.11(14)
C3-C4-C5-C6	178.78(8)
C9-C4-C5-C12	-177.76(8)
C3-C4-C5-C12	0.91(14)
C4-C5-C6-O2	178.49(8)
C12-C5-C6-O2	-3.52(13)
C4-C5-C6-C7	1.35(14)
C12-C5-C6-C7	179.34(8)
O2-C6-C7-C8	-178.90(8)
C5-C6-C7-C8	-1.75(15)
O2-C6-C7-C13	1.16(14)

C5-C6-C7-C13	178.31(9)	C20-C15-C16-C17	1.00(14)
C6-C7-C8-C9	0.68(14)	C12-C15-C16-C17	178.50(9)
C13-C7-C8-C9	-179.39(9)	C15-C16-C17-C18	-0.33(15)
C6-C7-C8-C14	179.83(9)	C16-C17-C18-C19	-0.12(15)
C13-C7-C8-C14	-0.24(15)	C17-C18-C19-C20	-0.13(15)
C1-O1-C9-C4	12.80(13)	C18-C19-C20-C15	0.84(15)
C1-O1-C9-C8	-168.25(8)	C16-C15-C20-C19	-1.26(14)
C5-C4-C9-O1	177.69(8)	C12-C15-C20-C19	-178.90(8)
C3-C4-C9-O1	-1.00(14)	C15-C12-C21-C22	-1.36(13)
C5-C4-C9-C8	-1.17(14)	C5-C12-C21-C22	131.66(10)
C3-C4-C9-C8	-179.87(9)	C15-C12-C21-C26	174.98(9)
C7-C8-C9-O1	-178.19(8)	C5-C12-C21-C26	-52.00(11)
C14-C8-C9-O1	2.64(13)	C26-C21-C22-C23	-0.52(15)
C7-C8-C9-C4	0.77(14)	C12-C21-C22-C23	175.81(9)
C14-C8-C9-C4	-178.40(9)	C21-C22-C23-C24	-0.06(16)
C6-C5-C12-C15	-97.33(10)	C22-C23-C24-C25	0.33(17)
C4-C5-C12-C15	80.58(11)	C23-C24-C25-C26	-0.01(17)
C6-C5-C12-C21	129.16(9)	C24-C25-C26-C21	-0.58(17)
C4-C5-C12-C21	-52.93(12)	C22-C21-C26-C25	0.84(16)
C5-C12-C15-C20	158.62(8)	C12-C21-C26-C25	-175.72(10)
C21-C12-C15-C20	-68.22(11)	C29-N1-C27-O3	-176.23(11)
C5-C12-C15-C16	-18.87(12)	C28-N1-C27-O3	-0.22(18)
C21-C12-C15-C16	114.29(10)		

Hydrogen-bond

D-H...A	d(D-H)	d(H...A)	d(D...A)	<(DHA)
O(2)-H(2)...O(3)	0.84	1.83	2.6669(12)	177.6

Citations

(1) Funk, C. *The Journal of State Medicine* **1912**, *XX*, 341-368.
(2) Funk, C. *British Medical Journal* **1913**, *19*, 812-814.
(3) McCollum, E. V.; Pitz, W. *The Journal of Biological Chemistry* **1917**, *31*, 229-253.
(4) McCollum, E. V.; Kennedy, C. *The Journal of Biological Chemistry* **1916**, *24*, 491-502.
(5) Drummond, J. C. *Biochemical Journal* **1919**, *13*, 77-80.
(6) Evans, H. M.; Burr, G. O. *Proceedings of the National Academy of Sciences of the United States of America* **1925**, *11*, 334-341.
(7) Evans, H. M.; Emerson, O. H.; Emerson, G. A. *The Journal of Biological Chemistry* **1936**, *113*, 319-332.
(8) Olcott, H. S.; Emerson, O. H. *Journal of the American Chemical Society* **1937**, *59*, 1008-1009.
(9) Fernholz, E. *Journal of the American Chemical Society* **1937**, *59*, 1154-5.
(10) Fernholz, E. *Journal of the American Chemical Society* **1938**, *60*, 700-5.
(11) Karrer, P.; Fritzsche, H.; Ringier, B. H.; Salomon, H. *Helvetica Chimica Acta* **1938**, *21*, 520-5.
(12) Karrer, P.; Fritzsche, H.; Ringier, B. H.; Salomon, H. *Helvetica Chimica Acta* **1938**, *21*, 820-5.
(13) Bergel, F.; Copping, A. M.; Jacob, A.; Todd, A. R.; Work, T. S. *Journal of the Chemical Society* **1938**, 1382-4.
(14) Mayer, H.; Schudel, P.; Ruegg, R.; Isler, O. *Helvetica Chimica Acta* **1963**, *46*, 963-82.
(15) Mayer, H.; Schudel, P.; Ruegg, R.; Isler, O. *Helvetica Chimica Acta* **1963**, *46*, 650-71.
(16) Isler, O.; Brubacher, G. *Vitamine I - fettlösliche Vitamine*; Thieme: Stuttgart, New York, 1982.
(17) Biesalski, H. K.; Grimm, P. *Taschenatlas der Ernährung*; 2 ed.; Thieme: Stuttgart, New York, 2002.
(18) Brigelius-Flohé, R.; Traber, M. G. *The FASEB Journal* **1999**, *13*, 1145-1155.
(19) Brigelius-Flohé, R.; Kelly, F. J.; Salonen, J. T.; Neuzil, J.; Zingg, J.-M.; Azzi, A. *American Journal of Clinical Nutrition* **2002**, *76*, 703-716.
(20) Brigelius-Flohé, R. *Nutrition Research Reviews* **2006**, *19*, 174-186.
(21) Azzi, A. *Free Radical Biology and Medicine* **2007**, *43*, 16-21.
(22) Traber, M. G.; Atkinson, J. *Free Radical Biology and Medicine* **2007**, *43*, 4-15.
(23) Brigelius-Flohé, R.; Davies, K. J. A. *Free Radical Biology and Medicine* **2007**, *43*, 2-3.
(24) Atkinson, J.; Epand, R. F.; Epand, R. M. *Free Radical Biology and Medicine* **2008**, *44*, 739-764.
(25) Brigelius-Flohé, R. *Free Radical Biology and Medicine* **2009**, *46*, 543-554.
(26) Traber, M. G.; Ramakrishnan, R.; Kayden, H. J. *Proceedings of the National Academy of Sciences of the United States of America* **1994**, *91*, 10005-10008.
(27) DellaPenna, D. *Journal of Plant Physiology* **2005**, *162*, 729-737.
(28) Bonrath, W.; Netscher, T. *Applied Catalysis A: General* **2005**, *280*, 55-73.
(29) Karrer, P.; Isler, O.; US2411967, 1946.
(30) Karrer, P.; Isler, O.; US2411968, 1946.
(31) Karrer, P.; Isler, O.; US2411969, 1946.
(32) Karrer, P.; Isler, O.; US2411970, 1946.
(33) Netscher, T.; Scalone, M.; Schmid, R. *Asymmetric Catalysis on Industrial Scale* **2004**, 71-89.
(34) Netscher, T.; Bonrath, W. *Die aktuelle Wochenschau der GDCh* **2008**.
(35) Netscher, T.; Bonrath, W. *Die aktuelle Wochenschau der GDCh* **2008**.
(36) Bonrath, W.; Karge, R.; Netscher, T. *Journal of Molecular Catalysis B: Enzymatic* **2002**, *19-20*, 67-72.
(37) Rosenau, T. In *Encyclopedia of Vitamin E*; Preedy, V. R., Watson, R. R., Eds.; CABI: Wallingford, Cambridge, 2007, p 69-95.
(38) Rosenau, T. In *Encyclopedia of Vitamin E*; Preedy, V. R., Watson, R. R., Eds.; CABI: Wallingford, Cambridge, 2007, p 21-43.
(39) *European Journal of Biochemistry* **1982**, *123*, 473-475.
(40) Rosenau, T.; Kloser, E.; Gille, L.; Mazzini, F.; Netscher, T. *Journal of Organic Chemistry* **2007**, *72*, 3268-3281.
(41) Williams, L. L.; Webster, R. D. *Journal of the American Chemical Society* **2004**, *126*, 12441-12450.

(42) Rosenau, T.; Böhmdorfer, S. In *Quinone Methides*; Steven, E. R., Ed.; Wiley-VCH: Weinheim, 2009; Vol. 1, p 163-215.
(43) Schröder, H.; Netscher, T. *Magnetic Resonance in Chemistry* **2001**, *39*, 701-708.
(44) Rosenau, T.; Ebner, G.; Stanger, A.; Perl, S.; Nuri, L. *Chemistry--A European Journal* **2005**, *11*, 280-287.
(45) Stanger, A.; Vollhardt, K. P. C. *Journal of Organic Chemistry* **1988**, *53*, 4889-90.
(46) Stanger, A. *Journal of the American Chemical Society* **1991**, *113*, 8277-80.
(47) Patel, A.; Böhmdorfer, S.; Hofinger, A.; Netscher, T.; Rosenau, T. *European Journal of Organic Chemistry* **2009**, 4873-4881.
(48) D'Ischia, M. *Tetrahedron Letters* **1995**, *36*, 8881-8884.
(49) D'Ischia, M.; Novellino, L. *Bioorganic and Medicinal Chemistry* **1996**, *4*, 1747-1753.
(50) Morton, L. W.; Ward, N. C.; Croft, K. D.; Puddey, I. B. *Biochemical Journal* **2002**, *364*, 625-628.
(51) McGeer, P. L.; McGeer, E. G. In *Annals of the New York Academy of Sciences* 2004; Vol. 1035, p 104-116.
(52) Coulter, I. D.; Hardy, M. L.; Morton, S. C.; Hilton, L. G.; Tu, W.; Valentine, D.; Shekelle, P. G. *Journal of General Internal Medicine* **2006**, *21*, 735-744.
(53) Patel, A.; Liebner, F.; Mereiter, K.; Netscher, T.; Rosenau, T. *Tetrahedron* **2007**, *63*, 4067-4073.
(54) Patel, A.; Liebner, F.; Netscher, T.; Mereiter, K.; Rosenau, T. *Journal of Organic Chemistry* **2007**, *72*, 6504-6512.
(55) Hoglen, N. C.; Waller, S. C.; Sipes, I. G.; Liebler, D. C. *Chemical Research in Toxicology* **1997**, *10*, 401-407.
(56) Marcinkiewicz, S. *Acta Poloniae Pharmaceutica* **1967**, *24*, 375-378.
(57) Yenes, S.; Messeguer, A. *Tetrahedron* **1999**, *55*, 14111-14122.
(58) Cooney, R. V.; Franke, A. A.; Harwood, P. J.; Hatch-Pigott, V.; Custer, L. J.; Mordan, L. J. *Proceedings of the National Academy of Sciences of the United States of America* **1993**, *90*, 1771-1775.
(59) Cooney, R. V.; Harwood, P. J.; Franke, A. A.; Narala, K.; Sundstrom, A. K.; Berggren, P. O.; Mordan, L. J. *Free Radical Biology and Medicine* **1995**, *19*, 259-269.
(60) Christen, S.; Woodall, A. A.; Shigenaga, M. K.; Southwell-Keely, P. T.; Duncan, M. W.; Ames, B. N. *Proceedings of the National Academy of Sciences of the United States of America* **1997**, *94*, 3217-3222.
(61) Singh, R. J.; Goss, S. P. A.; Joseph, J.; Kalyanaraman, B. *Proceedings of the National Academy of Sciences of the United States of America* **1998**, *95*, 12912-12917.
(62) Rosenau, T.; Adelwöhrer, C.; Kloser, E.; Mereiter, K.; Netscher, T. *Tetrahedron* **2006**, *62*, 1772-1776.
(63) Nguyen, Q.; Southwell-Keely, P. T. *Lipids* **2007**, *42*, 171-178.
(64) Ho, H.; Soldevilla, J.; Hook, J. M.; Southwell-Keely, P. T. *Sedox Sep.* **2000**, *5*, 60-62.
(65) Urano, S.; Hattori, Y.; Yamanoi, S.; Matsuo, M. *Chemical and Pharmaceutical Bulletin* **1980**, *28*, 1992-1998.
(66) Brownstein, S.; Burton, G. W.; Hughes, L.; Ingold, K. U. *Journal of Organic Chemistry* **1989**, *54*, 560-569.
(67) Rosenau, T.; Habicher, W. D. *Tetrahedron* **1995**, *51*, 7919-7926.
(68) Rosenau, T.; Chen, C. L.; Habicher, W. D. *Journal of Organic Chemistry* **1995**, *60*, 8120-8121.
(69) Baker, J. K.; Myers, C. W. *Pharmaceutical Research* **1991**, *8*, 763-770.
(70) Stern, M. H.; Robeson, C. D.; Weisler, L.; Baxter, J. G. *Journal of the American Chemical Society* **1947**, *69*, 869-874.
(71) Smith, L. I.; Renfrow, W. B., Jr.; Opie, J. W. *Journal of the American Chemical Society* **1942**, *64*, 1082-4.
(72) Schwieter, U.; Tamm, R.; Weiser, H.; Wiss, O. *Helvetica Chimica Acta* **1966**, *49*, 2297-303.
(73) Gloor, U.; Wuersch, J.; Schwieter, U.; Wiss, O. *Helvetica Chimica Acta* **1966**, *49*, 2303-12.
(74) Bieri, J. G.; Prival, E. L. *Biochemistry* **1967**, *6*, 2153-8.
(75) Bieri, J. G.; Mason, K. E. *Journal of Nutrition* **1968**, *96*, 192-4.

(76) Soendergaard, E.; Dam, H. *Zeitschrift fuer Ernaehrungswissenschaft* **1970**, *10*, 71-8.
(77) Schwieter, U.; Tamm, R.; Schlegel, W.; CH463533, 1968.
(78) Schwieter, U.; Tamm, R.; Schlegel, W.; CH463534, 1968.
(79) Itoh, S.; Nagaoka, S.-i.; Mukai, K.; Ikesu, S.; Kaneko, Y. *Lipids* **1994**, *29*, 799-802.
(80) Neuzil, J.; Tomasetti, M.; Zhao, Y.; Dong, L.-F.; Birringer, M.; Wang, X.-F.; Low, P.; Wu, K.; Salvatore Brian, A.; Ralph Steven, J. *Molecular pharmacology* **2007**, *71*, 1185-99.
(81) Eytina, H. J.; Lynn, A.; Mahdavian, E.; Chapman, J. M.; Salvatore, B. A. In *Abstracts of Papers, 224th ACS National Meeting, Boston, MA, United States, August 18-22, 2002* 2002, p ORGN-102.
(82) Tomic-Vatic, A.; EyTina, J.; Chapman, J.; Mahdavian, E.; Neuzil, J.; Salvatore, B. A. *International Journal of Cancer* **2005**, *117*, 188-193.
(83) Ralph, S. J.; Neuzil, J.; 2008.
(84) Ralph, S. J.; Neuzil, J.; 2009.
(85) Mahdavian, E.; Sangsura, S.; Landry, G.; Eytina, J.; Salvatore, B. A. *Tetrahedron Letters* **2009**, *50*, 19-21.
(86) Mazzini, F.; Netscher, T.; Salvadori, P. *European Journal of Organic Chemistry* **2009**, 2063-2068.
(87) Yang, B. H.; Buchwald, S. L. *Journal of Organometallic Chemistry* **1999**, *576*, 125-146.
(88) McMurry, J. E.; Mohanraj, S. *Tetrahedron Letters* **1983**, *24*, 2723-6.
(89) Kubota, S.; Iwaizumi, M.; Ikegami, Y.; Shimokoshi, K. *The Journal of Chemical Physics* **1979**, *71*, 4771-4776.
(90) Rosenau, T.; Potthast, A.; Elder, T.; Lange, T.; Sixta, H.; Kosma, P. *Journal of Organic Chemistry* **2002**, *67*, 3607-3614.
(91) Lee, S. B.; Willis, A. C.; Webster, R. D. *Journal of the American Chemical Society* **2006**, *128*, 9332-9333.
(92) Gaussian 03W, 6.1; Frisch, M. J.; Trucks, G. W.; Schlegel, H. B.; Scuseria, G. E.; Robb, M. A.; Cheeseman, J. R.; Montgomery, J. A. J.; Vreven, T.; Kudin, K. N.; Burant, J. C.; Millam, J. M.; Iyengar, S. S.; Tomasi, J.; Barone, V.; Mennucci, B.; Cossi, M.; Scalmani, G.; Rega, N.; Petersson, G. A.; Nakatsuji, H.; Hada, M.; Ehara, M.; Toyota, K.; Fukuda, R.; Hasegawa, J.; Ishida, M.; Nakajima, T.; Honda, Y.; Kitao, O.; Nakai, H.; Klene, M.; Li, X.; Knox, J. E.; Hratchian, H. P.; Cross, J. B.; Adamo, C.; Jaramillo, J.; Gomperts, R.; Stratmann, R. E.; Yazyev, O.; Austin, A. J.; Cammi, R.; Pomelli, C.; Ochterski, J. W.; Ayala, P. Y.; Morokuma, K.; Voth, G. A.; Salvador, P.; Dannenberg, J. J.; Zakrzewski, V. G.; Dapprich, S.; Daniels, A. D.; Strain, M. C.; Farkas, O.; Malick, D. K.; Rabuck, A. D.; Raghavachari, K.; Foresman, J. B.; Ortiz, J. V.; Cui, Q.; Baboul, A. G.; Clifford, S.; Cioslowski, J.; Stefanov, B. B.; Liu, G.; Liashenko, A.; Piskorz, P.; Komaromi, I.; Martin, R. L.; Fox, D. J.; Keith, T.; Al-Laham, M. A.; Peng, C. Y.; Nanayakkara, A.; Challacombe, M.; Gill, P. M. W.; Johnson, B.; Chen, W.; Wong, M. W.; Gonzalez, C.; Pople, J. A.; Gaussian Inc., Pittsburgh, 2003.
(93) Barone, V. In *Recent Advances in Density Functional Method*; 1 ed.; Chong, D. P., Ed.; World Scientific: Singapore, 1996; Vol. 1.
(94) Qiao, G. G.; Lenghaus, K.; Solomon, D. H.; Reisinger, A.; Bytheway, I.; Wentrup, C. *The Journal of Organic Chemistry* **1998**, *63*, 9806-9811.
(95) Rosenau, T.; Stanger, A. *Tetrahedron Letters* **2005**, *46*, 7845-7848.
(96) Kalinowski, H. O.; Berger, S.; Braun, S. *^{13}C-NMR Spektroskopie*; Georg Thieme Verlag: Stuttgart, 1984.
(97) Patel, A.; Netscher, T.; Rosenau, T. *Tetrahedron Letters* **2008**, *49*, 2442-2445.
(98) Rosenau, T.; Mereiter, K.; Jager, C.; Schmid, P.; Kosma, P. *Tetrahedron* **2004**, *60*, 5719-5723.
(99) Witkowski, S.; Markowska, A. *Polish Journal of Chemistry* **1996**, *70*, 656-657.
(100) Adelwöhrer, C.; Rosenau, T.; Kosma, P. *Tetrahedron* **2003**, *59*, 8177-8182.
(101) Kumli, E.; Montermini, F.; Renaud, P. *Organic Letters* **2006**, *8*, 5861-5864.
(102) Brown, H. C.; Negishi, E. *Journal of the American Chemical Society* **1971**, *93*, 3777-3779.
(103) Garrett, C. E.; Fu, G. C. *The Journal of Organic Chemistry* **1996**, *61*, 3224-3225.
(104) Cadot, C.; Dalko, P. I.; Cossy, J.; Ollivier, C.; Chuard, R.; Renaud, P. *The Journal of Organic Chemistry* **2002**, *67*, 7193-7202.
(105) Chan, D. M. T.; Monaco, K. L.; Wang, R.-P.; Winters, M. P. *Tetrahedron Letters* **1998**, *39*, 2933-2936.

(106) Knapp, F. W.; Tappel, A. L. *Journal of the American Oil Chemists' Society* **1961**, *38*, 151-6.
(107) Inglett, G. E.; Mattill, H. A. *Journal of the American Chemical Society* **1955**, *77*, 6552-4.
(108) Skinner, W. A.; Alaupovic, P. *Journal of Organic Chemistry* **1963**, *28*, 2854-8.
(109) Skinner, W. A. *Biochemical and Biophysical Research Communications* **1964**, *15*, 469-72.
(110) Goodhue, C. T.; Risley, H. A. *Biochemical and Biophysical Research Communications* **1964**, *17*, 549-53.
(111) Skinner, W. A.; Parkhurst, R. M.; Scholler, J.; Alaupovic, P.; Crider, Q. E.; Schwarz, K. *Journal of Medicinal Chemistry* **1967**, *10*, 657-61.
(112) Nilsson, J. L. G.; Daves, G. D., Jr.; Folkers, K. *Acta Chemica Scandinavica* **1968**, *22*, 207-18.
(113) Fujimaki, M.; Kanamaru, K.; Kurata, T.; Igarashi, O. *Agricultural and Biological Chemistry* **1970**, *34*, 1781-6.
(114) Kamal-Eldin, A.; Appelqvist, L. A. *Lipids* **1996**, *31*, 671-701.
(115) Fukuzawa, K.; Gebicki, J. M. *Archives of biochemistry and biophysics* **1983**, *226*, 242-51.
(116) Tsuchiya, J.; Niki, E.; Kamiya, Y. *Bulletin of the Chemical Society of Japan* **1983**, *56*, 229-232.
(117) Matsuo, M.; Matsumoto, S.; Iitaka, Y.; Niki, E. *Journal of the American Chemical Society* **1989**, *111*, 7179-85.
(118) Suarna, C.; Southwell-Keely, P. T. *Lipids* **1989**, *24*, 56-60.
(119) Suarna, C.; Southwell-Keely, P. T. *Lipids* **1988**, *23*, 137-9.
(120) Rousseau-Richard, C.; Richard, C.; Martin, R. *FEBS Letters* **1988**, *233*, 307-10.
(121) Nilsson, J. L.; Daves, G. D., Jr.; Folkers, K. *Acta Chemica Scandinavica* **1968**, *22*, 200-6.
(122) Rosenau, T.; Potthast, A.; Elder, T.; Kosma, P. *Organic Letters* **2002**, *4*, 4285-4288.
(123) Schudel, P.; Mayer, H.; Metzger, J.; Ruegg, R.; Isler, O. *Helvetica Chimica Acta* **1963**, *46*, 636-49.
(124) Dürckheimer, W.; Cohen, L. A. *Biochemical and Biophysical Research Communications* **1962**, *9*, 262-5.
(125) Omura, K. *Journal of Organic Chemistry* **1989**, *54*, 1987-90.
(126) Kohar, I.; Southwell-Keely, P. T. *Redox Report* **2002**, *7*, 251-255.
(127) Machlin, L. J. *Vitamin E, a Comprehensive Treatise*; Marcel Dekker Inc.: New York, 1980.
(128) Parkhurst, R. M.; Skinner, W. A. *Chromans and Tocopherols*; Wiley: New York, 1981; Vol. 36.
(129) Mills, W. H.; Nixon, I. G. *Journal of the Chemical Society* **1930**, 2510-24.
(130) Badger, G. M. *Quart. Revs. (London)* **1951**, *5*, 147-70.
(131) Behan, J. M.; Dean, F. M.; Johnstone, R. A. W. *Tetrahedron* **1976**, *32*, 167-71.
(132) Stanger, A.; Boese, R.; Askenazi, N.; Stellberg, P. *Journal of Organometallic Chemistry* **1997**, *542*, 19-24.
(133) Stanger, A.; Boese, R.; Askenazi, N.; Stellberg, P. *Journal of Organometallic Chemistry* **1997**, *548*, 113.
(134) Stanger, A.; Boese, R.; Ashkenazi, N.; Stellberg, P. *Journal of Organometallic Chemistry* **1998**, *556*, 249-250.
(135) Frank, N. L. *Advances in Theoretically Interesting Molecules*; AI Press Inc.: Greenwich, 1995; Vol. 3.
(136) Maksic, Z. B.; M, M.; Mo, O.; Yanez, M. *Pauling´s Legacy: Modern Modelling of the Chemical Bond in Theor. Comp. Chem.*; Elsevier: Amsterdam, 1999; Vol. 6.
(137) Nelan, D. R.; Robeson, C. D. *Journal of the American Chemical Society* **1962**, *84*, 2963-5.
(138) Skinner, W. A.; Parkhurst, R. M. *Journal of Organic Chemistry* **1964**, *29*, 3601-3.
(139) Skinner, W. A.; Parkurst, R. M. *Journal of Organic Chemistry* **1966**, *31*, 1248-51.
(140) Fales, H. M.; Lloyd, H. A.; Ferretti, J. A.; Silverton, J. V.; Davis, D. G.; Kon, H. J. *Journal ot the Chemical Society: Perkin Transactions 2* **1990**, 1005-1010.
(141) Dixie, C. J.; Sutherland, I. O. *Journal of the Chemical Society, Chemical Communications* **1972**, 646-7.
(142) Chauhan, M.; Dean, F. M.; Hindley, K.; Robinson, M. *Journal of the Chemical Society D: Chemical Communications* **1971**, 1141-1142.
(143) Rosenau, T.; Potthast, A.; Hofinger, A.; Kosma, P. *Angewandte Chemie, International Edition* **2002**, *41*, 1171-1173.

(144) Nagaoka, S.; Mukai, K.; Itoh, T.; Katsumata, S. *Journal of Physical Chemistry* **1992**, *96*, 8184-7.
(145) Gregor, W.; Grabner, G.; Adelwöhrer, C.; Rosenau, T.; Gille, L. *Journal of Organic Chemistry* **2005**, *70*, 3472-3483.
(146) Rosenau, T.; Patel, A.; Böhmdorfer, S.; Unpublished Results, 2008.
(147) Rosenau, T.; Netscher, T.; Ebner, G.; Kosma, P. *Synlett* **2005**, *2005*, 243-246.
(148) Rosenau, T.; Habicher, W. D. *Journal für Praktische Chemie/Chemiker-Zeitung* **1996**, *338*, 647-653.
(149) Rosenau, T.; Kosma, P. *European Journal of Organic Chemistry* **2001**, *2001*, 947-955.
(150) Bodanszky, M.; Bodanszky, A. *The Practice of Peptide Synthesis*; 2 ed.; Springer Verlag: Berlin, New York, 1994.
(151) Rosenau, T.; Habicher, W. D. *Tetrahedron Letters* **1997**, *38*, 5959-5960.
(152) Dallacker, F.; Eisbach, R.; Holschbach, M. *Chemiker-Zeitung* **1991**, *115*, 113-16.
(153) Rosenau, T.; Gruner, M.; Habicher, W. D. *Tetrahedron* **1997**, *53*, 3571-3576.
(154) Rosenau, T.; Habicher, W. D.; Potthast, A.; Kosma, P. *Synlett* **1999**, *1999*, 291-294.
(155) Rosenau, T.; Habicher, W. D.; Chen, C.-L. *Heterocycles* **1996**, *43*, 787-798.
(156) Rosenau, T.; Potthast, A.; Ebner, G.; Hofinger, A.; Kosma, P. *Organic Letters* **2002**, *4*, 1257-1258.
(157) Adelwöhrer, C.; Rosenau, T.; Gille, L.; Kosma, P. *Tetrahedron* **2003**, *59*, 2687-2691.
(158) Rosenau, T. PhD Thesis, Technische Universität, 1997.
(159) Lee, C.; Yang, W.; Parr, R. G. *Physical Review B* **1988**, *37*, 785-789.
(160) Miehlich, B.; Savin, A.; Stoll, H.; Preuss, H. *Chemical Physics Letters* **1989**, *157*, 200-206.
(161) Becke, A. D. *Physical Review A* **1988**, *38*, 3098-3100.
(162) Becke, A. D. *The Journal of Chemical Physics* **1993**, *98*, 5648-5652.
(163) Hariharan, P. C.; Pople, J. A. *Theoretica Chimica Acta* **1973**, *28*, 213-222.
(164) Francl, M. M.; Pietro, W. J.; Hehre, W. J.; Binkley, J. S.; Gordon, M. S.; DeFrees, D. J.; Pople, J. A. *The Journal of Chemical Physics* **1982**, *77*, 3654-3665.
(165) Patel, A.; Netscher, T.; Gille, L.; Mereiter, K.; Rosenau, T. *Tetrahedron* **2007**, *63*, 5312-5318.
(166) Wolfe, J. P.; Åhman, J.; Sadighi, J. P.; Singer, R. A.; Buchwald, S. L. *Tetrahedron Letters* **1997**, *38*, 6367-6370.
(167) Ramage, R.; Green, J.; Blake, A. J. *Tetrahedron* **1991**, *47*, 6353-6370.

Curriculum Vitae

Dipl.-Ing. Stefan Böhmdorfer

Born in Vienna on May 22nd, 1980

Address

Meidlinger Hauptstraße 1/13
1120 Wien
Austria

Place of Employment

University of Natural Resources andApplied Life Sciences (Boku), Vienna
Department of Chemistry
Muthgasse 18
1190 Wien
Austria
Tel.: +43 1 47654 6532
stefan.boehmdorfer@boku.ac.at
www.chemie.boku.ac.at/wpf.html

Current Employment

Since X 2006

PhD studies at University of Natural Resources and Applied Life Sciences, Vienna (Boku, Wien), Chair for Wood, Pulp and Fibre Chemistry (Prof. Rosenau), Topic: "Studies into fundamentals of *ortho*-quinone methide chemistry"

Previous Employment

I 2009 – II 2009

Internship at DSM Nutritional Products, Kaiseraugst (Dr. Netscher).

V 2006 – IX 2006

Internship at the *Institute of Applied Synthetic Chemistry* (TU Wien), Research Group for Stereoselective and Solid Phase Syntheses (Prof. Gärtner), continuing the topic of the diploma thesis.

IX 2004

Internship at the *Institute of Chemical Engineering* (TU Wien), Research Group for Process Simulation and Thermal Process Engineering (Prof. Friedl), topic: "Simulation of substance property data for bioethanol plants"

VIII – IX 2003

Internship at the *Institute of Applied Synthetic Chemistry* (TU Wien), Research Group for Stereoselective and Solid Phase Syntheses (Prof. Gärtner) Topic: "*meso*-Hydrobenzoin derivatives as chiral auxiliaries for stereoselective solid phase synthesis"

1998 – 1999

Military Service

Education

IX 1999 – V 2006

Study of Technical Chemistry (Synthesis) at Vienna University of Technology (TU Wien)

V 2006

Master´s Degree in Technical Chemistry with distinction

IV 2005 – III 2006

Thesis at the *Institute of Applied Synthetic Chemistry* (TU Wien), Research Group for Stereoselective and Solid Phase Syntheses (Prof. Gärtner) Topic: "Contributions to the enantioselective synthesis of salmeterol metabolites"

I 2004 – VI 2004

Studies at the Royal Institute of Technology (KTH) Stockholm with Erasmus Exchange Program

1990 – 1998

Secondary School (classical languages) at Bundesgymnasium Wien 13, Fichtnergasse

VI 1998

Matura (passed with distinction)

1986 – 1990

Elementary School in Wien Hietzing

Work-Related Skills

organic synthesis
modern analytics (especially GC-MS, NMR and HPLC)
computer administration
administration of web pages (typo3, html)
computational chemistry

Language Skills

Native speaker: German
Fluent: English
Basic: Swedish, Italian

Interests

juggling bewildering ambidextrous club passing patterns
circus arts
board games
skiing and its biomechanics
skiing instruction (level 1 skiing instructor, training for level 2)
low level platform diving
beer brewing
stop motion animation